Emission, survival and transport of bacterial aerosols associated with infection risk in people with cystic fibrosis

Jessica Angelina Proctor

Submitted in accordance with the requirements for the degree of Doctor of Philosophy

The University of Leeds

EPSRC Centre for Doctoral Training in Fluid Dynamics

September 2021

To Grandad.

Without you I may not have become who I am today. You always believed in me and you would be so proud if you could see all that I have achieved. I will miss you always.

Declaration

The candidate confirms that the work submitted is her own and that appropriate credit has been given within the thesis where reference has been made to the work of others.

This copy has been supplied on the understanding that it is copyright material and that no quotation from the thesis may be published without proper acknowledgement.

Acknowledgements

Firstly, I would like to express my sincere gratitude to my supervisors Prof. Cath Noakes, Prof. Nik Kapur, and Dr. Louise Fletcher for their continued support, invaluable suggestions and enthusiasm for this research project. Their guidance and motivation helped me in completing the most significant academic challenge I have ever had to face. I could not have imagined having better supervisors and mentors during this time. Beside my supervisors, I would like to thank Dr. Ian Clifton, Dr. Marco-Felipe King, Dr. Caroline Williams, Prof. Mike Barer, and Prof. Phil Threlfall-Holmes for their insightful comments, encouragement and immense support on many aspects of this thesis. I am grateful to have had the opportunity to work with Prof. Daniel Peckham, Dr. Helen Chadwick, Lindsey Gillgrass, Lynette Haigh, Anne Wood, and the rest of the team on the cystic fibrosis unit at St James's University Hospital Leeds NHS Trust. Without their support it would not have been possible to complete the cross-sectional study which was such a huge part of this thesis. My gratitude is also due to Dr. David Elliot, Emma Tidswell, and Karen Stevens who never tired of helping out and answering my many questions in the laboratory.

I would like to extend my thanks to all those who are and have been part of the EPSRC Centre for Doctoral Training in Fluid Dynamics. You provided stimulating discussions, companionship when working late nights, and a community to be a part of.

Mum and Dad, I am eternally grateful for the unconditional love and support you have always given me. When I needed it you pushed me in the right direction and gave me the confidence that I could succeed. Although you had to write it down to remember what I was researching, I knew you would always be there for me and help in any way you could. I would also like to thank my brother Josh, for providing the sibling rivalry that pushed me to become Dr. J Proctor first.

Above all, thank you to Charlie for everything you have done for me. This would have been so much harder without you.

Abstract

Cystic fibrosis (CF) is a progressive hereditary disease characterised by persistent pulmonary infections and lung function decline. Inhalation of airborne droplets containing microorganisms has been speculated as a possible transmission pathway for some of these pulmonary infections. Transmission of infectious aerosols is already a well-recognised route of infection for a number of diseases including Tuberculosis and severe acute respiratory syndrome coronavirus 2 (SARS-CoV-2) which is currently causing a world pandemic. Understanding this route of transmission for pathogens associated with CF and how the indoor environment affects this process is essential for developing effective infection control guidelines to further minimise the risk of cross-infection between people with CF.

Droplet size distributions of artificially generated aerosols of *P. aeruginosa* and *M. abscessus* were measured in a sealed constant air flow environment, the bioaerosol characterisation apparatus (BACA). Comparison between the two bacteria found *M. abscessus* decayed at a slower rate . Despite this several strains of both bacteria were found to easily survive in air for up to 4 m without significant decay.

A cross-sectional study measuring cough/exhaled breath aerosols from people with CF in a clinical setting provided clear evidence that *P. aeruginosa* can be aerosolised by people with CF and initial evidence that *M. abscessus* is in exhaled breath. Analysis of the bioaerosol size distributions found that droplets containing culturable bacteria were dominated by sizes within the respirable range (<5 µm).

The clinical data was used to calculate microbial emission rates from people with CF which were used within a mathematical model to determine the probable concentration of bacteria in a room, the exposure and ultimately the risk of infection to a susceptible individual. Analysis highlighted that high emitters were likely to drive the high risks and ventilation and managing the interaction of patients played an important role in reducing the likelihood of infection.

This thesis demonstrates that two pathogens associated with CF are likely to be aerosolised by people with CF and can survive in air and travel up to 4 m in droplets within the respirable size range. Overall, the risk of infection for a person with CF is low but this can significantly increase in the case of high emitters or when considering risk to the whole patient population at a CF unit. These findings strengthen the evidence for airborne transmission as a route of infection and support the need for continued stringent infection control practices for people with CF.

Contents

List of Figures

List of Tables

Chapter 1

Introduction

1.1 Overview

Transmission through infectious aerosols is a well-recognised route of infection for a number of diseases including Tuberculosis (TB), influenza, some hospital acquired infections, severe acute respiratory syndrome (SARS), and severe acute respiratory syndrome coronavirus 2 (SARS-CoV-2) which is currently causing a world pandemic. Understanding this route of transmission and how the indoor environment affects this process is essential for prevention measures against cross infection. Airborne infection was traditionally characterised into two types, large droplet transmission and transmission via droplet nuclei. Large droplet transmission is regarded in clinical practice as particles larger than 5 µm; these particles travel much shorter distances and are assumed to only pose a risk in close proximity to the source (1 m–2 m). Droplet nuclei (<5 µm) remain airborne for long periods of time and hence travel longer distances. However, the current understanding is changing, there is growing recognition that the continuum of droplet sizes matter, that a larger size range can remain in the air over longer distances and that this may vary by disease

(Milton, 2020). In addition, the vocabulary to describe 'droplets' and 'aerosols' is interchangeable and is not standardised across disciplines. For this thesis the word droplet will be used to describe particles of all sizes.

People with cystic fibrosis (CF) are susceptible to persistent pulmonary infections and their lung function decreases over time limiting the ability to breathe. Airborne infection is of particular concern for people with CF as they are both vulnerable to infection and prone to harbouring pathogens in their lungs. There are many pathogens that are associated with CF; this thesis focusses on two: *P. aeruginosa*; the most common pathogen causing chronic infection in people with CF and *M. abscessus*; a newly emerging pathogen which is becoming increasingly recognised as a concern in CF patients. Both pathogens have been shown to increase morbidity and mortality and have been linked to airborne transmission (Emerson et al., 2002; Jones et al., 2003; Esther et al., 2010; Bryant et al., 2013). Therefore, understanding the relationships between the pathogens, aerosolisation and the routes of airborne transmission is essential to improving the lives of those with CF.

Currently CF patients are given strict infection guidelines to prevent against cross-infection (Littlewood et al., 2004) but there is no quantified measure of this risk. For example, there may be a risk associated with sequential outpatient visits in the same room or risk of transmission in a waiting room and this risk may be better understood by evaluating the aerosols produced by patients in these environments.

Despite evidence for airborne transmission, what happens to the pathogen laden droplets in the air once released is poorly understood. The process is a complex multiphase flow problem involving the respiratory system, air in the room, and respiratory fluids containing microorganisms. By bringing a strong fluid dynamics focus to a challenge that is conventionally seen as a medical problem, this thesis aims to bring new insight into the airborne transmission process and hence establish a better understanding of the aerosols people with CF produce, the associated risk, and how best to mitigate against them. The outcomes will be of specific benefit to those tackling infection control in respiratory wards, and have implications for the understanding of other infectious diseases including SARS-CoV-2 and TB.

1.2 What is cystic fibrosis

Cystic fibrosis is a hereditary autosomal recessive condition. The disorder affects a number of organs including the lungs, pancreas, liver, and intestine. Symptoms

include recurrent respiratory infection, elevated sweat chloride levels, and infertility in males, among others. (Davis, 2006; O'Sullivan and Freedman, 2009)

Dorothy Hansine Andersen was the first to recognise CF as its own disease entity when she distinguished it from celiac disease in 1938 (Anderson, 1938). It is now one of the most common life-threatening diseases in the Caucasian population (O'Sullivan and Freedman, 2009), it is theorised that this is because of the European origins of CF (Mateu et al., 2002). In the UK there are just over 10 000 people registered with CF (Charman et al., 2019). Survival in CF has dramatically increased over time, in the UK the median predicted survival age is now 47 years with nearly 60 % of people with CF aged 16 years and over (Charman et al., 2019). There is currently no cure for CF and it is managed through several treatments including antibiotics, physiotherapy, aerosolised medicines, and often lung transplantation is necessary (Davis, 2006; O'Sullivan and Freedman, 2009).

CF is caused by inheriting two mutated copies of the cystic fibrosis transmembrane conductance regulator (CFTR) gene. This gene was first discovered in the 1989 by using cells derived from the sweat duct (Riordan, 1989; Rommens et al., 1989; Kerem, 1989). After the discovery of the gene over 2000 CFTR mutations have been described (Consortium et al., 2005). Different mutations can cause different faults within the CFTR protein, which may affect the severity of the disease (Koch et al., 2001). The mutations can be split into five classes (Zielenski and Tsui, 1995). A class 2 mutation is the most common worldwide (O'Sullivan and Freedman, 2009) and in the UK (Charman et al., 2019), ΔF508, is a deletion of three nucleotides resulting in the absence of a single phenylalanine residue (F) at the 508^{th} position on the protein (Kerem, 1989).

The CFTR is found in epithelial cells of many organs, explaining why CF affects many systems within the body. A normal functioning CFTR acts as a channel protein that controls the flow of water, sodium, and chloride in and out of the epithelial cells. Several theories have been postulated on how the defects in the protein cause the clinical effects of CF. The most current theory suggests the defective CFTR-epithelial sodium channel increases sodium absorption allowing an increased water absorption. Consequently, this results in a dehydrated, viscous airway surface liquid (ASL). This viscous, dehydrated ASL impairs muscoillary function as the cilla cannot move in the thick viscous environment. A product of this is a build up of mucus in the airways which promotes chronic bacterial colonization (Verkman et al., 2003; Clifton, 2009). It is this aspect of the condition that is an important driver for this thesis. Most studies focus on four major bacterial species: *Haemophilus influenzae*, *Staphylococcus aureus*, *Pseudomonas aeruginosa* and *Burkholderia cepacia*

complex, which increase morbidity in CF. However, there are many more bacteria that colonise people with CF's airways and the range of species has widened as life expectancy increases and detection methods improve (Harrison, 2007). This study will focus on two bacteria: *Pseudomonas Aeruginosa* and *Mycobacterium abscessus*.

1.2.1 *Pseudomonas aeruginosa*

P. aeruginosa (Figure 1.1) is a gram-negative, rod shaped, aerobic bacillus that belongs to the family Pseudomonadaceae. The rod roughly measures 1 µm–5 µm long and 0.5 µm–1 µm wide (Kreger et al., 1980; Lederberg et al., 2000).

P. aeruginosa is an opportunistic pathogen and is most commonly associated with causing respiratory tract infection in patients with CF, but is also prevalent among burn victims and the immunocompromised (Bodey et al., 1983; Lederberg et al., 2000). The organism is ubiquitous in the environment and has been detected in soil, plants, and water (Green et al., 1974; Lederberg et al., 2000; Pirnay et al., 2005). *P. aeruginosa* has been isolated from many sources within the home and CF clinics including the wash basin, shower, sink, drain, and bed linen. Moist areas such as the bathroom had the most positive isolates (Jones et al., 2003; Panagea et al., 2005; Schelstraete et al., 2008) which correlates with studies suggesting that *P. aeruginosa* is predominantly found in drains (Purdy-Gibson et al., 2015) and hospital basin U-bends (Moloney et al., 2019). *P. aeruginosa* does not survive well

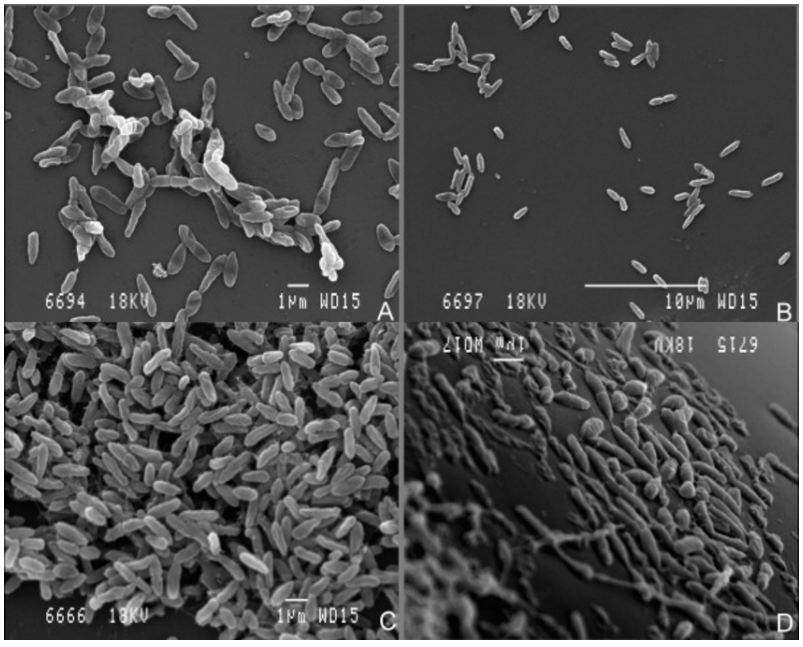

Figure 1.1: Electron microscopy images of *P. aeruginosa* (Deligianni et al., 2010).

in dry environments and has recently been described as a bacterium that is found in environments with intense human activities, although *P. aeruginosa* is ubiquitous in nature many studies to date have found it to be scarce in pristine environments (Crone et al., 2020).

Initially isolates of *P. aeruginosa* express a non-mucoid phenotype which are responsive to anti-pseudomonal antibiotics. It is therefore possible that chronic colonisation can be prevented with early and intensive treatment (Valerius et al., 1991). The definition for chronic infection with *P. aeruginosa* is given by Lee et al. (2003) and described in Table 1.1. A clinically important feature of *P. aeruginosa* is its ability to change to a mucoid phenotype, which is thought to initiate chronic-infection (Lyczak et al., 2002). The mucoid phenotype results from bacterial over production of an alginate, this over production caused by *P. aeruginosa* infection was first isolated from the respiratory tract by Doggett et al. (1964). Later, Lam et al. (1980) described microcolonies of *P. aeruginosa* in the alveoli encased with fibrous matrices. This is what is known to be biofilms, chronic infection of *P. aeruginosa* is caused by biofilm-growing mucoid strains which show a resistance to a wide range of antibiotics (Høiby et al., 2010), and have been found to be more resistant to the host defences than the non-mucoid phenotypes (Hoffmann et al., 2005).

Table 1.1: Criteria for *Pseudomonas aeruginosa* infection (Lee et al., 2003)

Infection	**Criteria**
Chronic infection	When more than 50% of months, when samples had been taken, were *P. aeruginosa* culture positive.
Intermittent infection	When 50% or less of months, when samples had been taken, were *P. aeruginosa* culture positive.
Free of infection	No growth of *P. aeruginosa* during the previous twelve months, having previously been *P. aeruginosa* culture positive.
Never	*P. aeruginosa* never cultured from sputum or cough swab.

1.2.1.1 Infection in people with cystic fibrosis

Infection with *P. aeruginosa* is decreasing but it is still the most common pathogen causing chronic infection in those with CF (Charman et al., 2019). Patients with CF can become infected with *P. aeruginosa* at any time, but studies suggest that 70 %–80 % of patients get it by their teenage years and as people get older infection becomes more likely (Lyczak et al., 2002).

While acquisition of *P. aeruginosa* may occur early in life, the transition from the

non-mucoid to mucoid phenotype can take years. There is a minority set of adults with CF whose infection with *P. aeruginosa* never transitions into the mucoid phenotype, these are long-term non-progressors, it is theorised that this is because of a certain antibody that this set of people with CF have (Pier et al., 1987). CF patients who are not infected with mucoid *P. aeruginosa*, which includes those who only have non-mucoid strains, have a significantly better prognosis and lung function over time than those who have mucoid strains (Henry et al., 1992; Parad et al., 1999).

Those most likely to be at risk of earlier detection of *P. aeruginosa* are females, patients with frequent infection with Staphylococcus aureus, and those of the ΔF508 genotype. Patients who are sicker and spend more time in the hospital were found to be at a greater risk of infection with *P. aeruginosa* (Maselli et al., 2003), suggesting a higher susceptibility to infection and potentially more opportunities for cross-infection.

Prior to modern genomic typing methods patient-patient infection with *P. aeruginosa* was thought to be a rare event, but it is now possible to differentiate between different strains from isolates of *P. aeruginosa*. Since then there has been a multiple outbreaks of several epidemic strains reported within the literature. These epidemic strains have been shown to result in a greater loss of lung function and deterioration in body mass index than infection with unique strains alone (Al-Aloul et al., 2004). Treatment of *P. aeruginosa* infections require intravenous anti-pseudomonal antibiotics which over time can encourage antibiotic resistance, particularly in epidemic strains which exhibit greater antibiotic resistance which develops at a much quicker rate (Ashish et al., 2012). The first reported epidemic strain of *P. aeruginosa* within the UK was from the Liverpool Regional CF centre (Cheng et al., 1996) and was named the Liverpool epidemic strain (LES). Other epidemic outbreaks within the UK have included the Manchester epidemic strain (MES) (Jones et al., 2001) where 14 % of attendees to the Manchester Regional CF centre were infected with this strain and the Midlands epidemic strain (Chambers et al., 2005) with 30 % of patients being infected with this strain. Subsequently, in a multi-centre study these strains were identified in multiple CF centre across England and Wales and the LES strain was isolated from 15 different centres (Scott and Pitt, 2004), emphasising the transmissibility of epidemic strains of *P. aeruginosa* in those with CF.

1.2.2 *Mycobacterium abscessus*

M. abscessus is a rapidly growing, acid-fast, gram-positive bacillus belonging to the genus non-tuberculous mycobacteria (NTM) (Moore and Frerichs, 1953; Malani, 2010). This species is of rod shape and roughly measures 0.2 µm–0.8 µm wide by 1 µm–10 µm (Moore and Frerichs, 1953; Malani, 2010). Recent evidence suggests that *M. abscessus* is a single species that can be divided into three subspecies: *M. abscessus* subsp abscessus, *M. abscessus* subsp massiliense and *M. abscessus* subsp bolletii (Bryant et al., 2013).

Infections caused by non tuberculous mycobacteria (NTM) are mainly found in patients with an underlying medical condition which pre-disposes them to infection (Medjahed et al., 2010). More commonly, NTM affects patients with pulmonary disease such as bronchiolitis and CF (Bange et al., 2001). Patients with compromised lung defences are also at a heightened risk of infection and *M. abscessus* has been described in patients post lung-transplant (Sanguinetti et al., 2001; Chalermskulrat et al., 2006; Taylor and Palmer, 2006) and patients with allergic bronchopulmonary aspergillosis (Mussaffi et al., 2005).

M. abscessus is found worldwide in soil and water (Jordan et al., 2007; Medjahed et al., 2010) and has been isolated from drinking water sources and shower aerosols (Thomson et al., 2013b,a). From data published within the literature it suggests that *M. abscessus* is the most predominant NTM in Europe (Fauroux et al., 1997; Bange et al., 2001; Sermet-Gaudelus et al., 2003; Constantini et al., 2005; Roux et al., 2009), whilst in the American continent it generally comes second place to *M.avium* complex (Olivier et al., 2003; Esther et al., 2005; Prevots et al., 2010).

M. abscessus is a virulent pathogen due to its multi-drug resistance (Sanguinetti

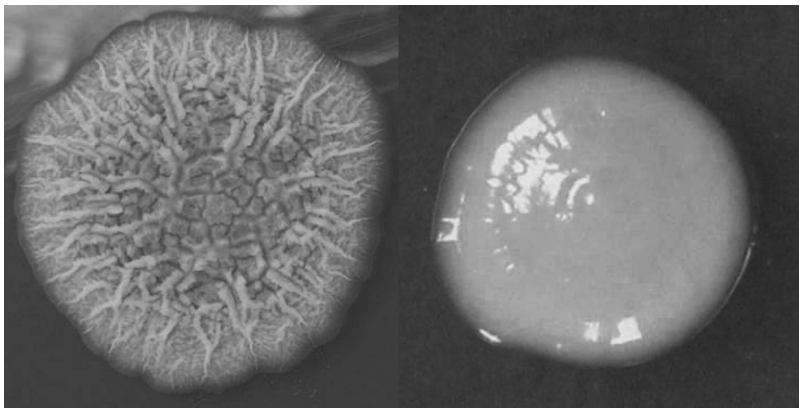

Figure 1.2: Comparison of *M. abscessus* morphotypes. Left: rough. Right: smooth (Rüger et al., 2014).

et al., 2001; Brown, 2010; Nessar et al., 2012). When cultured it can be characterised into two morphotypes, rough (MAR) and smooth (MAS), Figure 1.2 (Rüger et al., 2014). The smooth morphotype has more glycopeptidolipids in the outermost layer of the cell than the rough morphotype (Aulicino et al., 2015). A study conducted by Byrd and Lyons (1999) reported that MAR was able to invade and multiply causing persistent infections within the mice. Whereas, MAS had the ability to form biofilms and colonise but not cause persistent infection, making MAR the more virulent morphotype. Subsequently, Caverly et al. (2015) confirmed the rough morphotype demonstrated a poorer prognosis for the mice than the smooth. Howard et al. (2006) postulated that the cord formation in MAR may be responsible for the ability to cause persistent infection making it more virulent and the lack of cording in MAS is due to the increased amount of glycopeptidolipids. Byrd and Lyons (1999) confirmed that a single clinical isolate of *M. abscessus* had the ability to change from smooth to rough. Which was subsequently found in a study conducted on mice where 21 % of mice inoculated with the smooth morphotype had a change to the rough morphotype (Caverly et al., 2015).

1.2.2.1 Infection in people with cystic fibrosis

Non-tuberculous mycobacterial infections are becoming increasingly recognised in CF (Quittell, 2004), with *M. abscessus* emerging as a major pathogen. *M. abscessus* prevalence has increased from 5.8 % to 6.7 % from 2016 to 2019 and is responsible for more than 41 % of all new reported cases of NTM infection in the UK in 2019 (Charman et al., 2019). *M. abscessus* is becoming a growing concern worldwide, but the prevalence does vary within the literature, the largest studies to date examining 986 (Olivier et al., 2003), 1216 (Esther et al., 2010), and 1582 (Roux et al., 2009) individuals with CF reported prevalence of *M. abscessus* to be 2.08 %, 6.12 %, and 3.16 % respectively.

Symptoms of *M. abscessus* infection are similar to that of other chronic lung infections so often go under diagnosed, it can also be difficult to isolate *M. abscessus* due to overgrowth in culture of other microorganisms such as *P. aeruginosa* (Sanguinetti et al., 2001; Olivier et al., 2003). It is possible that this contributes to an underestimation in the contribution to the decline of lung function in CF. However, with the increased survival of patients with CF and improved methods of identification and detection, colonisation with NTM is on the increase (Lai et al., 2010; Prevots et al., 2010).

It is particularly challenging to diagnose NTM disease in patients with CF because

of the overlap of the clinical and radiographic criteria between disease caused by NTM and late stage CF symptoms. The British Thoracic Society produced clinicial and microbiological guidelines for diagnosing NTM lung disease (Haworth et al., 2017), these are as follows:

- **Clinical (both required)**
    1. Pulmonary symptoms, nodular or cavitary opacities on chest radiograph, or a high-resolution computed tomography scan that shows multifocal bronchiectasis with multiple small nodules;
       and
    2. Appropriate exclusion of other diagnoses.
- **Microbiological**
    1. Positive culture results from at least two separate expectorated sputum samples. If the results are non-diagnostic, consider repeat sputum AFB smears and cultures;
       or
    2. Positive culture result from at least one bronchial wash or lavage;
       or
    3. Transbronchial or other lung biopsy with mycobacterial histopathological features and positive culture for NTM or biopsy showing mycobacterial histopathologic features and one or more sputum or bronchial washings that are culture positive for NTM.

It can be seen from case studies that clinicians find it hard to tell whether isolations of *M. abscessus* from sputum represents colonisation or pulmonary infection and whether colonisation leads to infection (Cullen et al., 2000). It is possible that this is due to the ability of *M. abscessus* to change from a smooth colonising morphotype to the rough more virulent morphotype and whether it does or not. It has been postulated that the ability to switch could have particular relevance in patients with CF, colonisation of the respiratory tract would be favoured by the smooth type, it is then conceivable a change to a rough morphotype may happen which is more virulent and could cause chronic infection (Byrd and Lyons, 1999; Howard et al., 2006).

Within the literature there have been several studies documenting post-transplant fatalities due to infection with *M. abscessus* (Sanguinetti et al., 2001; Chalermskulrat et al., 2006; Taylor and Palmer, 2006). It is important that patients are tested for NTM before lung transplant as it has been shown in patients with end stage

CF pre-transplant culture positive was associated with post-transplant disease and morbidity. However, no genotyping was carried out to confirm whether these were the same strain or a new acquisition due to the fact they were more susceptible to *M. abscessus* infection post transplant (Chalermskulrat et al., 2006). Sanguinetti et al. (2001) theorised that a delayed diagnosis may play a part in the deaths associated with *M. abscessus* infection post transplant and a successful recovery after infection of *M. abscessus* post lung transplant was reported showing that rapid detection and treatment are essential (Morales et al., 2007).

Rough morphotypes occur more frequently in those with CF (Jönsson et al., 2007; Rüger et al., 2014), and is largely believed that NTM infection is more common in older patients (Olivier et al., 2003; Quittell, 2004) with less chronic infection with *P. aeruginosa* (Levy et al., 2008). However, there are several studies within the literature that report the opposite. For example *M. abscessus* was found to be the most prevalent NTM in children and teenagers (Sermet-Gaudelus et al., 2003) and a small paediatric study found 5 out of 6 patients infected had chronic infection with *P. aeruginosa*, but as this was a small study and the statistical results were weak (Mussaffi et al., 2005). The contrast in the studies could be explained by different mycobacterial ecology in the different countries as in general the species isolated were very different.

1.3 Infection transmission routes

Throughout history there has been much controversy over the spread of disease. The 19th century saw the rise of germ theory - the existence of invisible organisms to the naked eye that can cause disease. Work pioneered by Louis Pasteur and Robert Koch saw an end to this debate in western medicine and the 'golden era' of bacteriology began (Carter, 1977).

Today it still remains unclear on how infections are transmitted and there is much debate on how best to tackle them. There must be a source of infectious pathogens, a mode of transmission and a susceptible host. Understanding these pathways is of the utmost importance in tackling infection control. However, transmission routes of many diseases remain poorly understood potentially because transmission of infectious pathogens is a complex process that can involve multiple routes (Nicas and Sun, 2006) and may depend on the microorganism itself (Tang et al., 2006). The CDC in the USA (Kohn et al., 2003) state five main transmission routes of pathogens these are: airborne, droplet, direct and indirect contact, common vehicle,

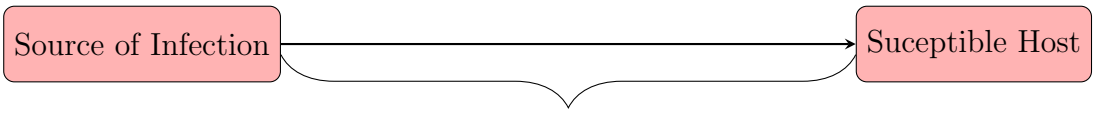

Modes of Infection Transmission.

- Airborne.
- Droplet
- Contact: Indirect and Direct.
- Common Vehicle.
- Vector.

Figure 1.3: Transmission pathways as given by CDC guidelines (Kohn et al., 2003).

and vector, Figure 1.3.

1.3.1 Common vehicle and vector borne transmission

Common vehicle transmission is attributed to a contaminated single source that may infect several susceptible hosts, possibly causing large scale outbreaks (Mangili and Gendreau, 2005). Examples of these include, water, food, medication, intravenous fluid, and equipment. The risk of this transmission route can be mitigated through maintenance of appropriate standards for all sources.

A disease vector is an agent that transmits a pathogen to another living organism, mostly insects or parasites. Mosquitoes are the most common vector transmitting, malaria, dengue, yellow fever, and Japanese encephalitis to name a few. Vector-borne diseases disproportionally affect the poorest populations and this method of transmission is a less frequent in most developed nations (Brenière et al., 2010).

1.3.2 Contact transmission

Direct contact transmission is the direct placement of a pathogen into a susceptible host. Whereas indirect transmission is the transfer of a pathogen to a host via an inanimate object or surface.

Direct contact transmission between health care workers and patients is considered one of primary routes in which an infection may spread within the health care setting. Thus, hand hygiene is considered the most important preventative measure in infection control policies (Beggs et al., 2006). It is not only hands in which direct contact transmission can occur, infection can occur through the use of medical

devices such as: catheters, intravenous feeding lines, and respiratory aids (Loveday et al., 2014).

Contamination onto surfaces and inanimate objects may be from hand contact but deposition of pathogens from respiratory droplets is an issue too. Microorganisms expelled in these droplets can remain viable in droplet form and settle on objects and surfaces in the patients immediate environment. Even those droplets that evaporate into a dry nucleus while falling through the air can survive on surfaces in a dessicated state (Weber et al., 2010) and this can be long enough to be picked up by hands to be deposited elsewhere, including transmission to a host.

1.3.3 Airborne and droplet transmission

An aerosol is defined as a suspension of solid or liquid particles within a gas (Cox and Wathes, 1995). Aerosols can be found in nature or can be artificial. Examples of those found in nature include: fog, clouds, forest exudates, and geyser steam. When we hear the term aerosol we generally think of an aerosol spray - this is an example of an artificial aerosol. Other artificial aerosols include: nebulised medical treatments, dispersal of pesticides, air pollutant, and smoke.

A bioaerosol is defined as:

> An aerosol of biological origin which exerts a biological action in animals and plants by virtue of its viability, infectivity, allergenicity, toxicity, pharmacological or other biological properties, with an aerodynamic diameter in the range 0.5 µm–100 µm. (Cox, 1995).

Bioaerosols are either a suspension of particles that contain living organisms, common sources for this include soil, water, and sewage. Or they have been released from living organism such as humans via breathing, coughing, and sneezing or from plants via spores and pollen (Cox and Wathes, 1995). When we begin to think of common aerosols/bioaerosols found in the indoor environment we think of skin cells, hair, bacteria, and viruses. A representation of sizes of common aerosols is shown in Figure 1.4

Critically microorganisms can be transmitted by droplets, it is these droplets carrying microorganisms which become airborne or droplet transmission. The sizes of these droplets play an important role in how they transmit infections. Bioaerosol droplets can be classified by where they deposit on the respiratory tract into the three ranges inhalable, thoracic, and respiratory and are are described in Table 1.2 (Milton, 2020). Expelled droplets from an infectious host which are larger will

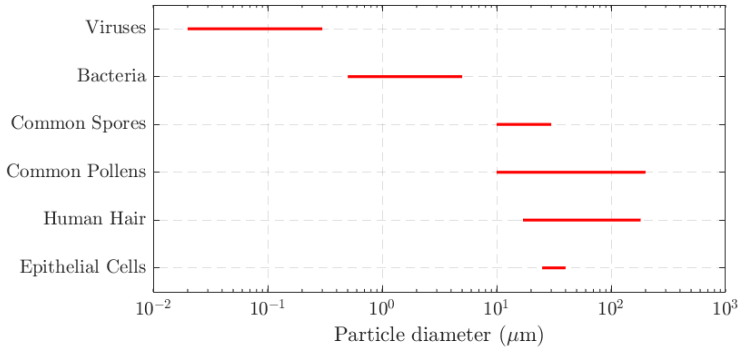

Figure 1.4: Airborne particle sizes and sources from indoor air. Adapted from (Owen et al., 1992).

Table 1.2: Transmission potential of droplets in the inhalable, thoracic and respiratory droplet size ranges (Milton, 2020).

Droplet type	**Droplet diameter**	**Deposition**
Inhalable	$\leq$100 µm	Nose
Thoracic	$\leq$10 to 15 µm	Trachea and large intrathoracic airways
Respirable	$\leq$2.5 to 5 µm	Respiratory bronchioles and alveoli

behave ballistically and fall the the ground quickly or as the aerosolised droplets evaporate they can leave behind a droplet nuclei which may contain an infectious microorganism. The microorganisms can be widely dispersed by air currents and depending on their size can remain airborne for hours (Wells et al., 1934).

Which droplet fraction is most important depends on the microorganism and the target infection site. In the case of *P. aeruginosa* and *M. abscessus* the respirable fraction is most important as the target is the lower respiratory tract. Bioaerosol droplets may be inhaled directly into the respiratory system in any of the droplet size fractions from Table 1.2, which is the process of airborne transmission. Alternatively, ballistic droplets can deposit directly onto nasal mucosa, conjunctiva or open wounds of the susceptible host and would be classified as droplet transmission. Whereas inoculation of these sites via contaminated hands or inanimate objects, following deposition of airborne droplets, is part of indirect contact transmission.

Wells et al. (1934) pioneered the classical study of airborne transmission, where he revealed what is now known as the Wells evaporation-falling curve of droplets. This describes the relationship between droplet size, evaporation, and falling rate. Wells et al. (1934), showed droplets greater than 100 µm rapidly fall to the ground due to

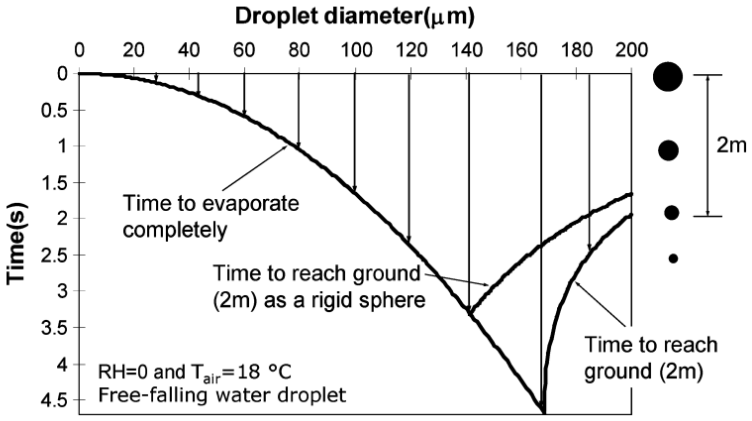

Figure 1.5: Wells' orgional evaporation-falling curve representing particles falling 2 m in quiescent air, adapted by Xie et al. (2007).

gravity and do not travel large distances. He hypothesised that transmission could be split into two forms dependent on the distance from the infectious source to the susceptible host:

Short-range transmission: can be regarded as direct deposition of droplets onto a susceptible hosts nasal mucosa, conjunctiva or open wound by infectious droplets within close proximity to the infected source. Usually this type of transmission is carried out by large infectious droplets and would be considered as droplet transmission.

Long-range transmission: refers to the respiratory droplets being carried by air flows to cause infection many metres away from the infectious source. This type of transmission can only be achieved with small droplets or droplet nuclei and is considered to be airborne transmission.

Xie et al. (2007) subsequently revisited the evaporation-falling curve and came to the same conclusions, that larger droplets evaporate slowly and settle to the ground quickly before totally evaporating. Small droplets evaporate very quickly and can remain in the air for much longer and totally evaporate before falling to the ground. Xie et al. (2007) revised the threshold for droplets between these small and large droplets to droplets between 60 µm–100 µm which would totally evaporate before falling 2 m. However, these studies were based on water droplets and work by Nicas et al. (2005) and Vejerano and Marr (2018) report that respiratory fluids do not evaporate like water, further details can be found in Chapter 3.

It still remains a question whether both transmission routes are equally important or one is more dominant than the other. Traditionally particle size and distance

from the host defined the difference in transmission routes. However, virtually all infectious droplets that can cause infection at long ranges can also cause infection at short range and by direct contact (Tang et al., 2006). Therefore, the term 'long range' describes the potential large distances that these airborne droplets can travel and there has been growing recognition that there is a continuum of droplet sizes that matter and they cannot be placed into distinct categories. There have been studies to suggest airborne is the dominant mode of transmission (Atkinson and Wein, 2008), whereas Nicas and Jones (2009) found airborne equally as important as droplet and indirect/direct contact modes. Comparisons of these two modes of transmission has rarely been reported and in two studies comparing airborne and droplet transmission in close proximity to the source again found differing opinions. Liu et al. (2017a) revealed that transmission occurring in close proximity to the susceptible host included both droplet and short range airborne routes in addition to direct contact. On the other hand Chen et al. (2020) found short range airborne routes dominate transmission in close contact. Although airborne infection may appear to be a simple concept, the literature reveals disagreements and there has not been a general consensus on how infectious respiratory droplets transmit infection.

1.4 Modelling airborne particles

Understanding the role that droplet dynamics, airflow and ventilation play in the dispersion, evaporation, and deposition of infectious particles is paramount in assessing the transmission routes of infection in indoor environments (Noakes et al., 2006). This section explores ways of modelling respiratory infection while considering the fluid dynamics of the problem.

1.4.1 Numerical models

Respiratory particles are comprised of water, inorganic and organic ions, glycoproteins, and pathogens may also be suspended in this medium (Nicas et al., 2005). When droplets are expelled they are released into an environment that will usually have lower relative humidity and temperature; therefore, evaporation of some water will occur resulting in a reduction of the droplet diameter.

Mathematical models using droplet dynamics for single droplets have been used to understand the droplet evaporation and distance droplets can travel, these have included models into quiescent air and droplets as part of a exhaled jet (Xie et al.,

2007). More recently, analytical models have been developed where the effects of respiratory jets, turbulent air, droplet composition, and ambient humidity have been partially considered (Wei and Li, 2015; Liu et al., 2017b; Chen et al., 2020).

1.4.1.1 Computational fluid dynamics

Computational fluid dynamics (CFD) is a numerical modelling approach that can deal with the properties and movements of liquid, gases, and the suspension of droplets. It can be a useful tool to study the movement of infectious particles in fluids especially when considering contaminant dispersal in room air. Many authors have modelled concentrations of bioaerosols in hospitals (King et al., 2013; Hathway et al., 2011; Cho, 2019), aeroplane cabins (Zhang and Chen, 2007) and spacecrafts (Salmela et al., 2018). Empty room models with droplet injection sites have been used determine the fate of infectious expiratory droplets in order to optimize ventilation layouts and provide mitigations for infection in confined spaces (Redrow et al., 2011). These studies have been able to include vapour plumes (Li et al., 2018) and susceptible hosts to determine how effective droplet and airborne transmission are. CFD simulation results can be effectively visualised and allows the user to see clearly how the plume of infectious particles can spread, Figure 1.6. However, air flows are complex to model and assumptions must be made, this leads to uncertainties in the model which must be taken into account when analysing the results.

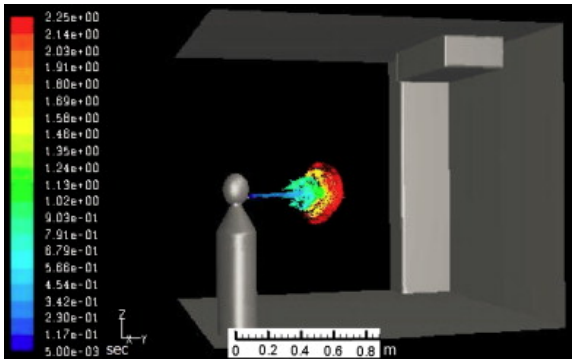

Figure 1.6: Distribution of particles released from the mouth opening, residence time is given by colour, Redrow et al. (2011).

1.4.2 Experimental models

The measurement of airflow patterns can provide insightful information of the potential for droplet and airborne transmission of infectious agents. The use of tracer gas can provide experimental visuals that can be seen in idealised CFD results (Villafru-

ela et al., 2016; Liu et al., 2017a). Mannequins can be used to seek to characterise realistic scenarios where repeatable studies can be performed; these mannequins can be heated and breathe to provide a more realistic environment (Bjørn and Nielsen, 2002; Villafruela et al., 2016; Liu et al., 2017a; Ai et al., 2019), Figure 1.7. Techniques involving non-toxic tracer gases provide ways of tracking a release of infectious particles, but they do not reflect the behaviour of droplet evaporation or deposition.

Schlieren imaging is another way to achieve airflow visualisation, this method relies on the thermal difference at the mouth opening to refract an incident light beam. No seeding particles are needed for Schlieren imaging like those needed for particle image velocimetry (PIV) techniques (Kwon et al., 2012); however, the method only reveals the airflows rather than the behaviour of particles. Tang et al. (2009) used PIV to study the difference in the fluid dynamics mechanisms that spread infections by coughing on patients wearing masks and not, concluding that the rapid turbulent jet produced by coughing was blocked by N95 masks.

Figure 1.7: Use of mennequins for tracer gas experiments Bjørn and Nielsen (2002).

1.4.2.1 Simulating the movement of infectious droplets

Characterising the movement of infectious bioaerosols within the indoor environment can be done by experimentally replicating a release of droplets into a controlled environment. Several studies have developed and investigated the use of cough simulators (Lindsley et al., 2013; Wei and Li, 2017), which may be beneficial when conducting experiments which contain pathogenic materials as this technique can introduce repeatability. Instead of the use of cough simulators which may not accurately replicate human cough profiles, many authors have used nebulisers in test chamber environments to represent the release of infectious particles (Clifton et al., 2008; King et al., 2013; Fletcher et al., 2016). The controlled environments can be idealised replications of hospital isolation rooms where airflows, particle size

distributions, and survival of infectious droplets can be measured.

1.5 Aims and objectives

1.5.1 Research questions

Recurrent chronic pulmonary infections are a major cause of morbidity and mortality in people with CF. Epidemiological studies have demonstrated indistinguishable bacterial strains in unrelated people with CF which has provided compelling evidence of person-person transmission, although the exact mechanisms are not well understood. Despite the implementation of infection control strategies, reports of cross-infection between people with CF has continued and the airborne route has been repeatedly speculated as a transmission pathway. Improving our understanding of the potential for airborne transport of pathogens with relevance to CF, in particular *P. aeruginosa* and *M. abscessus*, will allow for refinement of existing CF infection control guidelines and further minimise the risk of cross-infection between people with CF. Therefore, this thesis aims to address the following research questions:

1. Does the species of bacteria or the rheology of the suspension fluid affect the resulting droplet size distributions of artificially generated aerosols or cough/exhaled breath aerosols from people with CF?
2. Is there a correlation between the overall droplet size distributions produced from aerosolising a bacterial suspension and the culturable droplet size distributions?
3. Can people with CF aerosolise *P. aeruginosa* and *M. abscessus* while coughing/breathing and can the size distributions of these droplets containing viable pathogens be characterised?
4. What is the risk of infection to a person with CF in the indoor environment from airborne bacteria aerosolised by an infectious individual?

1.5.2 Research aim, objectives and methodology

This research uses a multidisciplinary approach to combine experimental techniques and a clinical cross-sectional study with risk modelling to accomplish the overall aim of the thesis:

Gain a deeper understanding of the potential for airborne transmission of *P. aeruginosa* and *M. abscessus* through investigating artificially generated aerosols and cough/exhaled breath aerosols from people with cystic fibrosis and use these data to inform risk models to give quantitative values of risk for airborne pathogens of relevance to cystic fibrosis;

The specific objectives of the study are:

1. Design studies and experiments to test the appropriateness of the methodologies for future investigations into bioaerosols and airborne infection by:
    i Gaining a robust understanding of the factors that influence both droplet and airborne transmission routes;
    ii Literature search evaluating validated methodologies and equipment for investigating bioaerosols and their scope numerically and experimentally in laboratory and hospital settings;
    iii Designing and developing methodologies and equipment to carry out experimental investigations into the airborne transmission of *P. aeruginosa* and *M. abscessus* in the laboratory and hospital setting;
    iv Characterisation of droplets containing microorganisms within a controlled laboratory experiment and use results to determine effectiveness of methodology used;
    v Comparison and evaluation of two differing sampling methods to detect microorganisms in aerosolised droplets from people with CF.
2. Quantify the effect of bacterial strain and suspension fluid properties on droplet size distributions and survival of different microorganisms by:
    i Investigating the rheological properties that can influence droplet size distributions and aerosolisation of fluids;
    ii Investigating the survival of different strains of *P. aeruginosa* and *M. abscessus* between 20 and 80 seconds after aerosolisation and verify the ability of the bacteria to travel and survive up to 4 m from the source;
    iii Comparing droplet size distributions produced by aerosolising microorganisms in different suspension fluids, measured through an aerosol particle technique and size segregation of culturable microorganisms.
3. Measure the presence of *P. aeruginosa* and *M. abscessus* in cough/exhaled breath aerosols from adults with CF by:
    i Gaining a robust understanding of *P. aeruginosa* and *M. abscessus* and their transmission in people with CF within the hospital setting;

   ii Conducting a cross-sectional study on a hospital ward to measure the bacterial load of cough/exhaled breath samples from people with CF;

   iii Comparing number of bacteria and detection of *P. aeruginosa* and *M. abscessus* between participants within the cross-sectional study.

4. Characterise emission rates of bacteria in cough/exhaled breath, in particular *P. aeruginosa* and *M. abscessus*, from adults with CF by:

   i Characterising total bacterial load and bacterial load of *P. aeruginosa* and *M. abscessus* during a cross-sectional study;

   ii Determining the droplet size distributions of all bacteria aerosolised and of *P. aeruginosa* and *M. abscessus*;

   iii Gaining preliminary data to inform future studies on the influence of time and treatment on droplet size distributions and presence of *P. aeruginosa* and *M. abscessus*.

5. Quantify the concentration of airborne bacteria in simulated hospital rooms and the risk of initiating an infection in a person with CF by:

   i Conducting a literature review on microbial aerosol evaporation and dispersion and risk models to quantify airborne infection;

   ii Assessing the similarities and differences between the laboratory experiments on artificially generated aerosols of *P. aeruginosa* and *M. abscessus* and the cough/exhaled breath samples from people with CF;

   iii Comparing steady state calculations of concentration of bacteria within simulated hospital rooms to measurements of the room air taken in the cross-sectional study;

   iv Evaluating the concentration of bacteria within the room and number of bacteria inhaled by a susceptible individual with CF and assessing the risk of initiating an infection with *P. aeruginosa*.

An in depth literature review is carried out in Chapter 2 and 3 to summarise infection transmission in the indoor environment, the role of respiratory droplets in airborne infection, and identify the key gaps in the literature that need to be addressed in this thesis to answer the research questions.

The first part of the research centres on using small and room scale experiments to predict the droplet size distributions and evaporation of aerosolised suspensions containing *P. aeruginosa* and *M. abscessus*. Chapter 4 sets out the experimental methodologies and Chapter 5 describes a series of experiments to be conducted under controlled environmental conditions to determine differences in survival and droplet

distributions produced by varying the bacterial strains and suspension fluids.

The emphasis of the second part of the research is placed on conducting a cross-sectional study to measure cough/exhaled breath aerosols of people with CF. Chapter 6 describes how these samples are taken using a modified cough aerosol sampling system and a non-invasive mask sample, and presents results from both approaches. This study will be particularly useful in measuring total bacterial load of bioaerosols from people with CF and the data will show what size droplets the microorganisms are contained within. Furthermore, the study will determine if *P. aeruginosa* and *M. abscessus* are aerosolised in cough/exhaled breath and provide further evidence that these bacteria can be transmitted via the airborne route.

Finally, the penultimate chapter (Chapter 7) brings together these two elements of the thesis and will use the data measured to infer input parameters, in particular emission rates, into a risk model. This risk model will estimate concentration of bacteria in the room which has been aerosolised by a person with CF. This will allow the number of CFU inhaled by a susceptible person and ultimately the risk of infection to be determined providing quantitative evidence for infection risk in people with CF which may result in suggestions for mitigation measures.

1.5.3 Layout of this thesis

A brief introduction to the chapter layout is given:

Chapter 2: Infection transmission in the indoor environment Here emphasis is made on the investigation of both droplet and airborne transmission in the indoor environment. Background is given on the approaches to measure and model infectious aerosols, experimentally and numerically. This chapter then focusses on transmission routes of pathogens in people with CF in particular the transmission of *P. aeruginosa* and *M. abscessus*. The contents of this chapter covers key points in objectives 1 and 5.

Chapter 3: Respiratory droplets This chapter reviews the relevant literature around respiratory droplets which addresses aspects of objectives 1, 2, 3 and 5. This includes the rheological properties of droplets and how this may affect evaporation and droplet size distributions. Following this is an investigation into published data on droplet size distributions and droplet characteristics produced by healthy and infected volunteers, in particular those with CF. Concluding with exploring the concepts of airborne transmission of evaporating droplets over the last 80 years.

Chapter 4: Experimental methodologies The methodology describes the methods employed to achieve objective 2. Details include how the bacteria and suspension fluids are prepared and characterised. Furthermore, the design and refinement of the aerosol characterisation controlled flow experiments are covered which encompasses points in objective 1.

Chapter 5: Bioaerosol characterisation experiments Here findings to the fluid and aerosol characterisations are presented which covers elements of objective 3. The objectives are to determine the effects of suspension fluid and bacterial strain on aerosolsation, evaporation and survival. Thus, droplet size distributions are measured and multiple bacterial strains are cultured at varying distances in different suspension fluids under controlled conditions.

Chapter 6: Cough aerosol sampling from people with cystic fibrosis: A cross-sectional study This chapter underpins the design, methodology, and analysis in obtaining cough/exhaled breath samples from people with CF in a hospital setting, addressing some of the aspects in objective 1, 3, and 4. Here different sampling methods are used to show that people with CF can produce cough/exhaled breath aerosols that contain microorganisms, including *P. aeruginosa* and *M. abscessus*. Further investigation into the droplet size distributions is conducted and droplets containing microorganisms are shown to be within the respirable size range which could lead to potential exposure to these microorganisms without the proper infection control procedures.

Chapter 7: Evaluation of factors influencing airborne transmission risk Here the results obtained from Chapter 5 and 6 are compared, discussed and form the basis for some of the input parameters, including the bacterial load emitted. The input parameters are adopted in to an infection risk model which focuses on achieving objective 5. The presented findings demonstrate its application by evaluating concentration of bacteria in room air, number of bacteria inhaled by a susceptible individual, and the risk of infection in multiple scenarios, where some include infection control measures such as improved ventilation.

Chapter 9: Conclusions, implications and future work This chapter presents the general conclusions from the study, potential areas for future work and implications of the thesis.

Chapter 2

Infection transmission in the indoor environment

Humans are sources of potentially infectious material which can be released into the air by ordinary human activities such as breathing, talking, coughing, and sneezing. Other activities such as aerosol generating procedures (Thompson et al., 2013) carried out in hospitals and cleaning exercises such as making beds (Shiomori et al., 2002) are known to suspend infectious particles in the air. This chapter analyses the routes of droplet and airborne transmission in the indoor environment and discusses the methodologies that can be applied to understand this complex process. Measurement of respiratory droplets and the microorganisms they carry is discussed in Chapter 3.

2.1 Overview of aerial transmission in the indoor environment

It has long been know that pathogens such as *Influenza*, measles, and chickenpox can be effectively transmitted by the airborne route and there is a case to suggest all pathogens where replication and/or colonisation occurs in the upper respiratory tract could have the potential to be transmitted by large droplets (Xie et al., 2007).

Mycobacterium tuberculosis (TB) is another example of a communicable disease which is well known to be primarily transmitted aerially (CDC, 1977). In the past two decades we have seen the effects of two large pandemics from coronaviruses, SARS and the infamous SARS-CoV-2. Retrospective reports concluded the main pathway of transmission of SARS was the airborne route (Li et al., 2005; Booth et al., 2005; Xiao et al., 2017). While likely SARS-CoV-2 spreads by several transmission routes, droplet and airborne should both be recognised as potential transmission pathways (Morawska and Cao, 2020). Both of these routes are considered to be 'aerial' and are described in section 1.3.3. These transmission routes are graphically presented in Figure 2.1. This section describes the different methods we can employ to sample bioaerosols in the indoor environment and a discussion on the studies sampling indoor air or using large scale models to experimentally interpret the spread of infectious agents indoors.

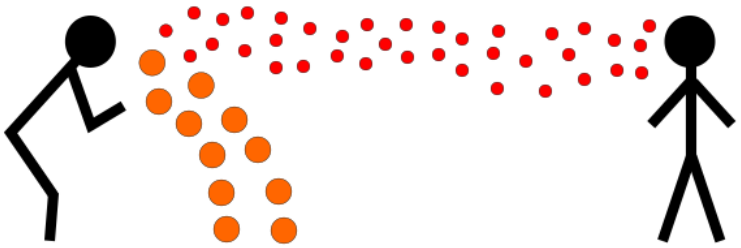

Figure 2.1: Diagram depicting larger droplets depositing close the the emission source (droplet transmission) and smaller droplets travelling long distances (airborne transmission).

2.1.1 Detection of bioaerosols in the indoor environment

2.1.1.1 Methods to detect bioaerosols

There is a wide variety of sampling methods for detecting pathogens in aerosols. Each piece of equipment has its own strengths and weaknesses and the choice of sampler depends on the pathogen aerosolised and location of sampling. Devices include settling plates, impactors, impingers, and centrifugals samplers (Cox and Wathes, 1995).

Settling plates are a simple bioaerosol sampler, they consist of agar plates that face upwards and collect the settling particles. Advantages of this method is that they are very easy to use, quiet, and inexpensive. However, this sampling method

does not provide any information on particle size distributions or quantity of air sampled and it will over represent larger particles due to the gravitational settling as described by Stokes law (Cox and Wathes, 1995).

Centrifugal samplers use a cyclone effect to accelerate the sampled air allowing it to leave the air stream and deposit on liquid or a semi-solid collecting surface (Cox and Wathes, 1995). One of the most common is a hand held and battery powered sampler, the RCS air sampler, which makes it extremely portable and convenient to use in multiple locations; however, this sampler is not good for very small particles ($<2\,\mu m$) (Jensen et al., 1992).

Impingers are glass tubes that sample the bioaerosols by bubbling the sample through an absorbing liquid which force the aerosol particles to leave the air stream. Impingers have been shown to have similar efficiency as the Anderson sampler. With the advantage of not having to account for particles impacting at the same place, yet they cannot provide data for particle sizes (Cox and Wathes, 1995). Many microorganisms can lose viability impacting onto a solid surface so one way to mitigate against this is to collect bioaerosols into liquid using impingers (Lindsley et al., 2017). A common impinger used for bioaerosol sampling is the All-Glass Impinger with the nozzle 30 mm above the base of the collection vessel, called the AGI-30. The inlet tube of the AGI-30 is curved to represent a nasal passage. The BioSampler Swirling Aerosol Collector (SKC) is thought to be an improvement on the AGI-30 through its centrifugal motion design that mimics a human nose (Zheng and Yao, 2017).

Impactors operate on the principle of inertial impaction, the particle will impact on a solid surface and remain there. There are different types of impactors, simple impactors can include spore traps and rotorod samplers, these sample particles of all sizes. Slit-to agar samplers will only sample particles of a certain aerodynamic diameter, these samplers contains slits of a defined diameter. Cascade samplers contain multiple stages with each stage having a decreasing slit size to sample smaller and smaller particles. Some particles will have sufficient inertia and impact on the agar plate while smaller particles will remain entrained in the air stream and move down to the next stage where this process repeats (Cox and Wathes, 1995). The Anderson 6-stage Impactor is a cascade sampler and is the most widely used aerobiological sampler (Cox and Wathes, 1995). One reason for this is because of their multiple stages relating to where the droplet can reach within the human body, see Figure 2.2. Advantages of this sampler is its ability to provide data on particle sizes (Table 2.1) along with samples being collected directly onto culture plates. However, there are several limitations for both low concentration and high

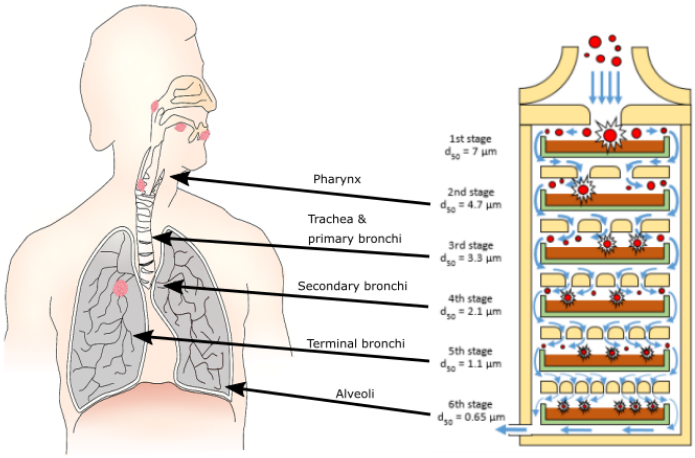

Figure 2.2: Particle sizes for lung delivery with corresponding schematic of the size-stage Andersen impactor, adapted from Lindsley et al. (2017).

Table 2.1: Stages of the Six-stage Andersen impactor and their corresponding droplet diameter range (Andersen, 1958).

Stage	**Droplet diameter**
1	$\geq$7 µm
2	4.7 µm–7 µm
3	3.3 µm–4.7 µm
4	2.1 µm–3.3 µm
5	1.1 µm–2.1 µm
6	0.65 µm–1.1 µm

concentration environments (Lindsley et al., 2017). In low concentrations sampling time is limited to around 20 minutes as to not dry out the agar plates. In higher concentration areas you risk the plates becoming overloaded due to the high flow rate (28.3 L min^{-1}). There is a possibility of more than one particle impacting in the same place on the agar plate and it is necessary to correct for this using 'positive-hole correction' (Macher, 1989). The probability-based correction factor needs to be applied to the results for each impactor stage, the basic formula (2.1) is as follows:

$$P_r = N\left(\frac{1}{N} + \frac{1}{N-1} + \frac{1}{N-2} + \ldots\frac{1}{N-r+1}\right) \tag{2.1}$$

where:

P_r = the estimated culturable droplet count,
N = the total number of holes in the impactor stage,
r = the number of colony forming units observed on the plate.

Due to limitations of commonly used bioaerosol samplers there have been developments into electrostatic samplers which are being increasingly used. These work by using a strong electric field to create a high concentration of unipolar ions. These ions collide and charge airborne particles causing them to be attracted to the collection surface (Lindsley et al., 2017). Many of these new devices have seen improvements in the collection of viruses especially in the sub-micron range (Tan et al., 2011; Ladhani et al., 2017).

2.1.1.2 Sampling bioaerosols in the indoor environment

Pathogenic material being spread through droplets in the air is of great concern for many diseases and there have been many studies focussed on understanding this transmission route through sampling of the indoor environment. Methicillin-resistant *Staphylococcus auresus* (MRSA) has long been a problem in terms of hospital acquired infections (Farrington et al., 1990). MRSA was located in the air on multi-bed wards with absence of any MRSA colonized patients as all MRSA patients were kept in single bed rooms (Wilson et al., 2004; Creamer et al., 2014). Demonstrating the airborne route may be responsible for the transmission of at least some of these infectious droplets.

Other well known airborne bacteria such as TB has been found to be present the air in several locations within a single hospital. There was high concentrations of TB in the negative pressure isolation rooms with TB patients, emergency room, waiting room, and a consulting room of the infectious disease division (Chen and Li, 2008; Sornboot et al., 2019). An explanation for why TB concentrations were so high in the emergency room could be that patients may have been in the early stages of TB disease and not under treatment yet. Hubad and Lapanje (2012) detected TB in the air on a TB ward, a diagnostic laboratory, and inadequately ventilated corridors which had the highest concentrations per unit volume. Based on these results adequate ventilation must be implemented to prevent against airborne infection. Strong evidence supporting the airborne spread of *Acinetobacter* was found in an outbreak in three Dutch hospitals (Bernards et al., 1998). In the two hospitals with outbreaks all source patients were in non-pressurised isolated rooms. Settle plates located both inside and outside the room found the outbreak strain. Whereas, in the third hospital source patients were in a pressurised isolation room

and there was no outbreak.

Aerosolised virus-laden droplets have also been studied. Influenza is a highly contagious repository disease known to be transmitted through the air. Confirmed presence of droplets containing influenza were collected in a hospital emergency department (Blachere et al., 2009). Greater than half of viral particles detected by PCR were characterised to be well within the respirable aerosol fraction (diameter $<4\,\mu m$), supporting the theory that the virus is transmitted through the airborne route. During the pandemic of SARS in 2003 positive air samples were obtained from a room occupied by a patient with SARS, providing experimental confirmation of virus aerosol generation (Booth et al., 2005). After the emergence of SARS-CoV-2 investigations into understanding the nature of transmission began. Airborne routes of tranmission were shown to be possible by Liu et al. (2020) after air sampling was conducted in two Wuhan hospitals and SARS-CoV-2 RNA was detected in aerosols. Concentrations of the virus were very low in well ventilated isolation wards, but they were much higher in less well ventilated areas such a the toilets used by the patients and medical staff areas; however, these levels reduced to undetectable after proper implementation of sanitisation procedures. Highlighting the importance of room ventilation, sanitization of personal protective equipments, and disinfection of less well ventilated areas. The aerosol size distributions showed peaks at $0.25\,\mu m$–$1\,\mu m$ and $>2.5\,\mu m$. Subsequent studies have cultured SARS-CoV-2 from airborne droplets in a hospital (Lednicky et al., 2020) and a car in the size range $0.25\,\mu m$–$0.52\,\mu m$ (Lednicky et al., 2021).

Chadwick and McCann (1994) highlighted other sources of bioaerosols from humans which included vomiting and diarrhoea for particular cases of noroviruses. Nebulisers, tracheostomies, and bronchoscopies have too been shown to contribute to producing pathogen-laden aerosols (Tang et al., 2006), these are known as aerosol generating procedures. Influenza virus has been detected in such procedures at higher rates than the baseline (Thompson et al., 2013). Bronchoscopy produced the highest concentrations of RNA in particles sizes $0.86\,\mu m$–$4\,\mu m$ and $4\,\mu m$–$7.3\,\mu m$.

A positive correlation of increased human activity in the hospital bays with increased concentration of bioaerosols was confirmed by Hathway et al. (2013), concluding one source could have been microorganisms remaining airborne via humans shedding skin squamae. In fact, humans shed approximately 3×10^8 squamae per day, and that each may carry >100 bacteria. This proposes a strong likelihood that susceptible hosts can become infected by inhaling particles from the air (Beggs et al., 2008). Such microorganisms could be spores of *Acinetobacter* and MRSA as these have been known to survive in the air for long periods of time. MRSA can survive on scales of

the skin for up to 80 days (Eames et al., 2009). These high levels of skin shedding leads to the concern of bacterial contamination of the hospital environment during wound dressing, Sergent et al. (2012) found the air was frequently contaminated (38 %) during wound dressing compared to when wounds were not being dressed (14.3 %). It is no surprise that Roberts et al. (2008) reports cleaning activities can cause re-aerosolisation of pathogen laden particles, particularly during bed making. In fact resuspension of infectious particles from bed making has caused concerns since it was first noticed in the 1940's (Thomas and Van den Ende, 1941) and has since had studies dedicated to it. Shiomori et al. (2002) found MRSA-containing particles to be significantly higher 15 minutes after bed making than during the resting period, reiterating the importance of healthcare staff to exercise great care in disinfecting infectious environments.

2.1.1.3 Experimental models of indoor aerial transmission

Understanding bioaerosol dispersion and deposition in mock indoor environments is a powerful tool in understanding and improving our knowledge on exposure. Using artificially generated aerosols and indoor models allow repeatable experimental investigations into the risk of exposure from pathogen-laden droplets.

Room scale models in environmentally controlled chambers have been used to release bioaerosols and monitor their movement using bioaerosol samplers. Hathway et al. (2011) injected *Serratia marcesen* aerosols into an empty room similar in size to a single patient room and sampled the air using an Andersen sampler at twelve locations and monitored deposition using settle plates. The majority of droplets (90 %) were collected on stages 5 and 6 of the Andersen sampler, corresponding to bioaerosols surviving in particle diameters of 0.65 µm–2.1 µm. The study was expanded by King et al. (2013) who used the same chamber to measure bioaerosols in scenarios which mimicked single patient and double patient rooms with the use of heated mannequins. *Staphylococcus aureus* aerosols were released from the patients heads, only settle plates were used in this study and there was no clear correlation between surface concentration and distance from the source. However, using a physical partition to separate the patients was shown to be effective at reducing contamination between the patients.

Duan et al. (2020) explored the use of an in vitro face and airway model with fluorescent droplets as a substitute for pathogens. For all particle sizes from 0.6 µm–5 µm the lips had a greater risk of exposure than the eyes, with and without inhalation, and accounted for more than 80 % of facial mucosa deposition. However, when using

lifelike mannequins as the succeptible host and an infected human source Tang et al. (2014) failed to detect any influenza RNA on or inhaled by the mannequin. It is possible that this may be due to the short exposure times the mannequin had to the source.

Large chambers capable of housing microorganisms are not always readily available; therefore, studies have explored the effects of bioaerosols in reduced-scale room models. Faulkner et al. (2015) gave evidence for a linear trend for decreasing particle concentration with increase in ventilation. However, this was only seen for the small particle sizes, 1.9 µm, and it did not have an effect on the larger particles, 5.4 µm and 7.9 µm. Ventilation plays a role in transporting smaller droplets large distances, Lai et al. (2012) confirms this using a small scale ventilated chamber with common indoor airborne bioaerosols including *Staphylococcus aureus* and *Aspergillus niger*. As expected the results revealed that the larger the droplet the shorter the distance from the inlet.

Knowledge of how long an infectious particle can remain viable while airborne will give us a deeper understanding of aerial transmission. A Goldberg drum (Goldberg et al., 1958) can be used to study the survival of pathogens in small particles by keeping particles with diameters of <6 µm suspended for extended period of time. Thompson et al. (2011) used *Staphylococcus epidermidis* as a surrogate for *Staphylococcus aureus* and gave evidence for staphylocicci's potential airborne dissemination in hospitals. Experiments using the Goldberg drum indicated *S. epidermis* was able to survive for five days at 76 % humidity with the bacterial aerosols found to be in the respirable range (<2.1 µm). Recently Van Doremalen et al. (2020) compared the aerosol survival of SARS and SARS-CoV-2 using the Goldberg drum, aerosols of less than 5 µm were suspended in the drum. Both viruses remained viable for the duration of the experiment, 3 hours, with a similar reduction of a factor of 10 in viral load over the duration. These results demonstrate that the aerosol route of transmission for these viruses is plausible.

2.1.2 Infection transmission and the role of the building

Capturing the parameters involved in the real systems that govern the transmission of pathogens in buildings is particularly important when influencing infection control mitigation strategies. In particular building layout and ventilation play an important role in the dispersal and transport mechanisms for pathogen-laden droplets (Noakes and Sleigh, 2009). Transmission of infectious pathogens is a complex process and transmission through aerial routes is complicated further by adding the role

of building airflows. Despite this, there has been a range of approaches to model the transmission routes in buildings.

2.1.2.1 Ventilation for controlling airborne infection

Ventilation is well recognised as a control for airborne infection (Qian and Zheng, 2018). Ventilation rates are given in terms of air changes per hour, $\mathrm{AC\,h^{-1}}$. Low ventilation rates have conclusively demonstrated higher incidences of *Mycobacterium Tuberculosis* (TB) among health care workers (Menzies et al., 2000) and this evidence was supported by a retrospective study in a Hong Kong Hospital following the SARS outbreak (Li et al., 2005).

Ventilation in UK hospitals can be mechanical or natural depending on the clinical area. Mechanical ventilation uses inlet and exhaust valves to flush out old air ahead of the incoming air. Natural ventilation of fresh outside air into the room from a window can be driven by buoyancy or wind (Li et al., 2007). Windows offer a low cost method of ventilating non-critical areas within a hospital; however, when closed infection risk dramatically increases (Gilkeson et al., 2013).

Heating and ventilation system guidance for UK hospitals is set out in the HTM03-01 (Macintosh et al., 2007). This publication prescribes ventilation strategy for clinical spaces based on need and risk. HTM03-01 indicates the recommended types of ventilation systems for each room type. Details for some examples of health care facilities are set out in Table 2.2.

Table 2.2: Ventilation strategy as described in HTM03-01 for some examples of health care facilities.

Room type	**Ventilation**	**$\mathrm{AC\,h^{-1}}$**	**Pressure (Pa)**	**Temp (°C)**
General ward	S or N	6	-	18–28
Single room	S, E or N	6	0 or -ve	18–28
Operating theatre	S	25	25	18–25
Critical care area	S	10	10	18–25

S= Mechanical supply.
E= Mechanical extract.
N= Natural ventilation.

2.1.2.2 Risk models to quantify airborne infection

Much of the research involved in quantifying infection rates in the indoor environment is based on the work of Wells et al. (1955) and Riley et al. (1978). Together they formed the Wells-Riley equation (2.2) which proposes there is a relationship between infectious (I) and susceptible (S) individuals. The room ventilation rate (Q, $\mathrm{m^3\,s^{-1}}$), breathing rate (p, $\mathrm{m^3\,s^{-1}}$), and the quantity of infectious material in the air predict the number of new cases (N_c) of infection over the exposure time (t, s):

$$N_c = S\left(1 - e^{-Iqpt/Q}\right). \tag{2.2}$$

Here q represents quantum, a concept introduced by Wells et al. (1955). The idea of a quantum is to represent the response of a susceptible individual inhaling an infectious particle. Although some interpret this to be a single particle or a single colony forming unit (CFU), Wells postulated not all inhaled infectious particles will result in infection. Therefore, a quantum was defined as the average dose of infectious particles required to infect $1 - 1/e$ susceptible individuals or equivalently 63 % of the susceptible population know as an infectious dose: ID_{63}.

Numerous researchers have sought to improve the Wells-Riley model. Gammaitoni and Nucci (1997) successfully combined the Wells-Riley model with room ventilation rates to include the effects of non-steady state quanta production and use of personal protective equipment on risk of TB in enclosed spaces. This amendment has been used to predict risk of airborne infection over time in hospital wards (Noakes and Sleigh, 2009) and more recently used to predict infection risk of SARS-CoV-2 based of quanta production (Miller et al., 2020) and inhaled RNA copies (Jones et al., 2021). The rate of change off quanta concentration, C ($\mathrm{quanta\,m^{-3}}$) over time, t, in a space of volume, V ($\mathrm{m^3}$), can be described by a linear differential equation:

$$\frac{dC}{dt} = \frac{E}{V} - \lambda C, \tag{2.3}$$

where emission rate, E ($\mathrm{quanta\,h^{-1}}$), is usually measured retrospectively from disease data. A single removal rate λ ($\mathrm{h^{-1}}$) is used and it is the summed effects of ventilation, deposition, and decay.

Rudnick and Milton (2003) derived an alternative equation. These express infection risk as a function of the fraction of inhaled air that has been exhaled by another individual in the building (rebreathed fraction) using CO_2 concentrations as a marker for exhaled-breath exposure. The authors also derive a non-steady state equation which is particularly useful in poorly ventilated environments. Noakes et al. (2006)

successfully couple the Wells-Riley model with classic epidemic models such as the SEIR model to simulate the long term dynamics of infection while enabling environmental effects such as room ventilation and occupancy. Epidemic models are used to describe outbreaks of disease over time and the SEIR model considers the relationships between the susceptible (S), exposed (E), infected (I), and recovered (R) individuals in a population through a system of coupled non-linear differential equations. Recent studies have attempted to relate quanta to the emission rate of pathogens. Bueno de Mesquita et al. (2020) used data on the emission rate of influenza. While Buonanno et al. (2020) presented a methodology relating droplet size, activity, and viral load in respiratory fluids for SARS-CoV-2.

In hospital settings populations are often small and modelling individual risk may be an important parameter to understand airborne infection. Single-hit dose-response models consider that a single microorganism can initiate an infection (a 'single hit'). The concept of an infectious dose is employed whereby infectious dose is related to the number of microorganisms required to infect an individual, this is where at least one 'hit' causes infection. The quantitative microbial risk assessment (QMRA) framework is used to estimate the risk from exposure to microorganisms by running Monte-Carlo simulations. If a dose-response model is available it can be used to estimate the probability of infection. Researchers have used dose-response models to quantify risk infection for influenza and SARS (Atkinson and Wein, 2008; Cheng et al., 2016; Xiao et al., 2017), but there is a lack of data on dose-response for many respiratory microorganisms.

The simplest case to determine probability of infection is to assume that it is solely dependent on the expected inoculum dosage, D, and that each microorganism exerts an equal and a fixed independent probability to cause an infection, k (Teunis and Havelaar, 2000). This can be expressed as the complement of the probability of absence of infection:

$$\mathrm{P}(\text{infection} \mid D) = 1 - (1 - k)^D \tag{2.4}$$

Typically the expected dose, D, is rarely known exactly and is characterised by the mean of a Poisson random variable, λ and the well-known exponential dose-response relation is give by:

$$\mathrm{P}(\text{infection} \mid \lambda) = 1 - \exp^{-k\lambda} \tag{2.5}$$

2.1.2.3 Computational fluid dynamics approaches

The Wells-Riley model assumes the air is homogeneously mixed. As a consequence this leads to the concentration of bioaerosols to be uniform throughout the space. Therefore, the model does not account for the influence of proximity between the infected host and susceptible individual. This problem can be addressed through computational fluid dynamics (CFD) to simulate the dispersion of infectious particles and revealing the airflow patterns in the indoor environment. However, it must be acknowledged that CFD if not perfect either and has limitations. CFD is still modelling and is good at predicting some air flows, but simulating the dispersal of infectious particles via turbulent exhaled air flows is not straight forward and the predictive capability may not be as accurate.

Computational fluid dynamics enables investigation into ventilation design strategies and has been used to evaluate high risk areas such as operating theatres (Brohus et al., 2006; Abraham et al., 2017; Shirozu et al., 2018) and isolation rooms (Tung et al., 2009; Cho, 2019). Single and multi-bed ward accommodation has been investigated to understand the aerial dispersion of pathogens which may be contributing to the spread of infection on hospital wards (Beggs et al., 2008; King et al., 2013). Retrospective research into outbreaks in hospitals have used CFD to explore the role of air distributions in the transmission of microorganisms (Li et al., 2005; Yu et al., 2005) confirming highest concentrations of pathogen-laden aerosols were consistent with the airborne transmission observed. A small number of studies (Qian et al., 2009; Yan et al., 2017) have directly linked CFD to the Wells-Riley model providing a tool for investigating airborne transmission in enclosed spaces.

2.2 Transmission of pathogens in people with cystic fibrosis

Cystic fibrosis is characterised by consistent bronchial infections, these infections pose a heightened risk to people with CF coming into close contact due to possible human-human transmission. Yet, the source and mechanisms of transmission pathways of airway pathogens in people with CF is still not understood. The primary source of acquisition of these airway microorganisms was considered to be from the natural environment, supported by studies demonstrating the majority of people with CF had unique strains (Römling et al., 1994; Grothues et al., 1988). However, over the years there have been advances in genetic molecular typing techniques

and extensive worldwide studies conducted in CF centres supporting the theory of patient-patient transmission of airway pathogens (Jones et al., 2001; Aitken et al., 2012; Kidd et al., 2013).

2.2.1 Transmission of common cystic fibrosis pathogens in the hospital environment

The microbiology of airway pathogens in people with CF are observed to change during the lifetime of a person with CF (Strausbaugh and Davis, 2007). Common pathogens such as *Haemophilus influenzae* and *Staphylococcus aureus* are found during childhood and *Pseudomonas aeruginosa* infection is the dominant infection in adults with CF (Charman et al., 2019). Other fungi species, gram-negative bacteria and, non-tuberculosis mycobacteria are associated with lung infections in people with CF and are typically observed in older age groups with a more advanced disease (LiPuma, 2010).

Given the possible aerial transmission of pathogens associated with people with CF and the high risk of lung infections, extensive studies in CF units worldwide have been conducted to determine the plausibility of the droplet and airborne transmission route for a variety of microorganisms. Research studies have demonstrated positive air samples of *Burkholderia cepacia* complex (Ensor et al., 1996; Zuckerman et al., 2009) where Zuckerman et al. (2009) additionally detected *S. aureus* including strains of MRSA in the air at CF units. Furthermore, Hansen et al. (2013) postulated airborne as the main transmission route for *Achromobacter* species by ruling out droplet or direct contact due to adherence to infection control procedures.

2.2.1.1 Transmission of *P. aeruginosa* in cystic fibrosis

Many patients with CF acquire *P. aeruginosa* from the environment and hence have their own individual strains (Fothergill et al., 2012). Due to advances in genomic typing methods molecular typing studies have shown that strains are common between siblings (Renders et al., 1997; Grothues et al., 1988), in CF holiday camps (Ojeniyi et al., 2000; Hunfeld et al., 2000), and at clinics (Cheng et al., 1996; Jones et al., 2001; Armstrong et al., 2002) suggesting cross-infection between patients could be happening.

In the landmark study, Cheng et al. (1996) identified the first epidemic strain, the Liverpool epidemic strain (LES) described in section 1.2.2.1. Subsequent studies

have stemmed from these findings with reports emerging of shared strains across their CF populations (Armstrong et al., 2002; Aaron et al., 2010; Kidd et al., 2013). On investigation of the key epidemic strains in the UK Panagea et al. (2005) discovered LES to be isolated from patients hands, clothes, and bed linen. Environmental contamination was only detected in close proximity and short lived. LES was detected in most air samples from inside the cubicles, corridors, and the waiting room. Isolates were found in the air when patients were in the room, but also in their rooms for up to 3 hours prior to testing. On dry surfaces LES survived significantly longer than unique strains but not longer in comparison to other transmissible strains. Hence, the improved environmental survival alone cannot account for the high transmissibility of this strain and airborne routes of transmission must play a significant role in cross-infection of LES. Additionally, a study carried out in Manchester CF unit (Jones et al., 2003) again showed epidemic strains of *P. aeruginosa* being isolated from the air confirming the airborne route possible for cross infection. However, these air samples were only taken when patients were carrying out spirometric tests, nebulisation, and airway clearance which is theorised to produce more aerosolised isolates of *P. aeruginosa* than during normal activities.

2.2.1.2 Transmission of NTM in cystic fibrosis

One of the largest studies on prevalence of non-Tuberculosis mycobacteria (NTM) was conducted by Olivier et al. (2003), providing evidence that almost all strains of NTM were unique indicating person-person transmission is low or non-existent. Furthermore, another study at a single clinic, all patients were shown to have individual strains so it was reported that there was no evidence of person-person transmission (Bange et al., 2001). Again there was evidence for no cross-infection between patients in a french study, with all children having their own unique strains of *M. abscessus* (Sermet-Gaudelus et al., 2003).

However, these studies were conducted nearly 20 years ago and subsequently (Aitken et al., 2012) showed patient-patient transmission for the first time and no *M. abscessus* was found in the environment after. Molecular fingerprinting of *M. abscessus* in a cohort of children with CF found that CF patients could harbour the same strain (Harris et al., 2012). A study in Taiwan showed outbreaks of *M. abscessus* in several hospitals, it was concluded that a tap water source of *M. abscessus* was the source of the outbreak in one hospital. Yet, in another hospital no environmental source had the same strain of *M. abscessus* as those in the patients and it was concluded that patient-patient transmission was the possible source of the outbreak (Huang et al., 2010).

These studies may have been limited by their typing methods, whole genome sequencing can provide a more definitive data on how related the isolates are. Bryant et al. (2013) conducted a study in a adult CF centre using whole genome sequencing and found a strong indication of cross-infection between patients. Patients harbouring the same strain had numerous within hospital opportunities for transmission and there was no detection of and environmental source during the outbreak. Despite this evidence of transmission between patients the exact route remained to be established, direct spread is unlikely due to the strict control guidelines. Therefore, it is possible that transmission can occur by contamination due to *M. abscessus* being resistant to many disinfectants (Wallace Jr et al., 1998) or alternatively via the airborne route. In contrast to this study Harris et al. (2015) conducted a whole-genome sequencing analysis in a paediatric clinic and found no evidence of cross-infection between patients apart from a sibling pair who had intense exposure between each other. This difference could be due to the fact that the children mainly has *M.abscessus* subsp abscessus which was shown to not be as transmissible as *M.abscessus* subsp masiliene in the previous study (Bryant et al., 2013).

2.2.2 Experimental investigations into the transmission of pathogens in people with cystic fibrosis

Repeatable experimental investigations into the spread of *P. aeruginosa* and *M. abscessus* allows deeper understanding of how these pathogens survive and travel within the air. Clifton et al. (2008) demonstrated using a 'laminar flow' model that strains of *P. aeruginosa* were able to travel 4 m providing evidence that *P.aeruginosa* can travel in droplet nuclei, an indication that the airborne route is possible. This study carried out analysis of size distributions and strains, but did not consider evaporation or the influence of the suspension fluid. Subsequently, Clifton et al. (2010) conducted another experiment using artificially generated aerosols in an aerobiological chamber confirming viable counts of *P. aeruginosa* could still be detected 45 minutes after halting aerosol generation. A number of studies have been carried out to measure *P. aeruginosa* in exhaled breath, as discussed in section 3.2.3.1.

Following the work of Clifton et al. (2008) similar scenarios were used to determine survival of *M. abscessus*. In artificially generated aerosols of *M. abscessus*, positive isolates were found in the air 60 minutes after aerosol generation had suspended (Taylor, 2016). Further work by Fletcher et al. (2016) evidenced clinical isolates of *M. abscessus* were found to travel up to 4 m with the majority of isolates found in the respirable size range, less than 2 µm.

2.2.3 Cystic fibrosis infection control guidelines

Consensus documents regarding infection prevention and control are not regularly updated. Infection control guidance has largely focused on avoidance of cross-infection by direct contact through hygiene measures, and large droplet spread of infectious particles, with some guidelines (Saiman et al., 2014) suggesting people with CF to maintain the 1 m–3 m 'bubble' to reduce the risk of infection. With the mounting evidence for transmission of pathogens through the air Jones (2014) believed that future infection control measures will need to consider the need for prevention against airborne pathogens.

The UK CF trust guidelines for infection control stress the great importance of good hygiene measures. Every CF centre and CF clinic should have microbiological surveillance and an infection control policy. There should be segregation of both in-and-out patients according to their microbiological status, which is particularly important for those patients with transmissible strains of harmful pathogens. Away from the hospital, it is recommended that all CF camps and holidays are to be avoided along with spas and other forms of aerated baths. Siblings with CF are also advised to have separate bedrooms and should carry out their physiotherapy treatments separately (Littlewood et al., 2004).

Segregation of patients who have transmissible strains of *P.aeruginosa* is hugely important and out patient clinics should be held on different days for these patients. Clinics should monitor the rate of new acquisition of *P. aeruginosa* and prevalence of multi-resistant strains, as an increase in these suggest the presence of a transmissible strain (Littlewood et al., 2004). The US and European CF society came to a consensus on the recommendations for the management of NTM in those with CF (Floto et al., 2016). The expert panel recognised the potential for cross-infection, particularly for *M. abscessus* and recommended this should be minimised by following national infection control guidelines. The UK CF trust recently updated their NTM guidelines for infection prevention and control following this advice. The document sets out strict guidelines for segregating the patients by their microbiological status similar to the guidelines set out for *P. aeruginosa* with extra measures such as the use of gloves and gowns to be used in patients rooms and for equipment to be single patient use (Jones et al., 2017).

2.2.3.1 Attitudes of people with cystic fibrosis to infection control guidelines

It is a struggle for those within the CF community to balance the risks and benefits of socialisation between each other. In the past patients were encouraged to socialise, go to CF camps, gain a network of support, and a sense of community. Since interaction between CF patients has been linked with transmission of pathogens, socialisation is now discouraged. However, one study reported that the health care workers found this issue complex and found it difficult to discourage socialisation between patients (Miroballi et al., 2012).

Greater adherence to infection prevention guidelines can lower chances of human-human transmission and Masterson et al. (2008) found the majority of people were compliant with infection control guidelines and those who weren't were generally aware of the risk. Those who have established relationships with fellow CF patients may think it is worth the risk of infection to see each other and maintain these relationships, as most participants in the study reported they could benefit from friendships with CF patients. Another study found that of patients who avoided other people with CF, over 60 % did so because of the risk of cross-infection. On the contrary CF patients who did not follow the guidelines felt that segregation would negatively impact their life (Waine et al., 2007). It is commonly found that those who are least likely to adhere to the infection control measures are adolescents rather than any other age group (Somayaji et al., 2015).

2.3 Summary

Analysis of the literature on infection transmission in the indoor environment presents clear evidence that the airborne route of transmission is plausible for many pathogens, including *P. aeruginosa* and *M. abscessus*. This has been repeatedly evidenced through studies sampling indoor air and laboratory based experimental investigations demonstrating pathogens can remain viable in the air and survive long enough to transmit infection. There is some specific evidence for the aerosolisation and survival of *P. aeruginosa* . However, there is a lack of data on effects of different strains and the size distributions of aerosols. Additionally, in comparison there is very little data on *M. abscessus* in aerosols and the comparison of its two morphotypes.

Risk models either in the form of Wells Riley or mass-balance equations have been readily used with dose-response data to determine risk of infection. However, there

is a lack of data on quantitative risk for pathogens associated with CF and it is not known how effective guidelines for infection control are. Models have focused to date on other pathogens, usually communicable diseases that affect the whole population. Ventilation has long been used a source of controlling airborne infection but better data is needed that links the risk of infection with building design. Most infection control guidelines may be outdated and with attitudes to airborne infection likely changing due to the COVID-19 pandemic, now is the time to refine infection control policies.

Chapter 3

Respiratory droplets

Droplets are known to carry pathogenic material through the air which may infect a susceptible individual. Bioaerosols from humans are released through coughing, sneezing, and breathing, which is a complex multiphase process involving a cascade of events leading to respiratory droplet formation. Droplet size distributions produced play an important role in droplet evaporation and aerial transmission. This chapter explores the effects of droplet properties on droplet size distributions, the methods of measuring respiratory droplets and the microorganisms they carry, and investigates the methods of modelling droplet evaporation.

3.1 Fluid dynamics of respiratory droplets

Respiratory droplets are most commonly formed through the momentum caused by inspiration and expiration. This momentum transfer is from air flowing through the lungs to the airway surface liquid which results in wave-like disturbances that lead to droplet creation in a similar manner to Rayleigh capillary instabilities (Fiegel et al., 2006). Experimental results (Basser et al., 1989) and mathematical models (Moriarty and Grotberg, 1999) suggest a critical speed is required to initiate the

wave-like disturbances; this critical speed can vary according to mucus thickness, viscoelastic properties, and surface tension. However, the momentum produced during normal tidal breathing is not sufficient to produce instabilities. A potential mechanism of droplet formation during this process is owed to the reopening of collapsed terminal airways at the onset of inspiration (Wei and Li, 2016).

3.1.1 Rheological Properties

In the study of fluid mechanics there a several important properties to describe the behaviour of a fluid. One of these such properties is dynamic viscosity, the viscosity of a fluid is a measure of its internal resistance to flow at a given rate (Isaacs, 1996). For example fluids with low viscosity, like water, flow easily. The standard unit of dynamic viscosity is the pascal-second (Pa s). Combining the density and dynamic viscosity though equation (3.1), a magnitude of the viscosity can be given by the kinematic viscosity, v:

$$v = \frac{\mu}{\rho}, \tag{3.1}$$

where:
v = kinematic viscosity,
μ = dynamic viscosity,
ρ = density.

Viscosity typically increases with temperature for gases and decreases with temperature for liquids and hence it is important for density, temperature, and viscosity to be measured under the same conditions.

Deformation of a fluid results in viscous stresses which are attributed to the rate of change of deformation (the strain rate). Shearing a fluid causes a deformation, for some fluids the viscosity is constant over a wide range of shear rates; these are Newtonian fluids. Non-Newtonian fluids deviate from this behaviour and can do so in different ways, two examples are (Friedlander and Serre, 2002):

Shear-thickening viscosity increases with the rate of shear strain.

Shear-thinnning viscosity decreases with the rate of shear strain.

Viscosity can be measured with numerous types of viscometers and rheometers. Commonly used varieties are capillary tube and rotational rheometers (Boyes, 2009). A rheometer captures the behaviour of non-Newtonian fluids through measurement of shear stress and shear strain, an example of the typical behaviours of Newtonian and non-Newtonian fluids are given in Figure 3.1.

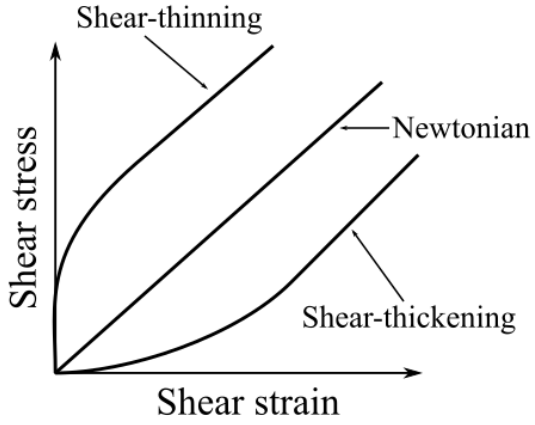

Figure 3.1: Visual representation on how viscosity, the slope of each line, varies among fluids. Fluids are split into three categories Newtonian, shear-thickening, and shear-thinning.

Viscoelasticity is a property of fluids which exhibit both viscous and elastic characteristics. Elastic materials deform when stretched and return to their original configuration when stress is removed (Guedes, 2019). Saliva/mucus is a viscoelastic fluid and when released from the mouth opening this property will cause the adjacent droplets to be joined by a thread, which delays breakup into individual respiratory droplets (Eggers and Villermaux, 2008). Fluid relaxation is an imperative property to measure for a quantitative investigation into the effects of viscoelasticity. Li (2008) defined relaxation time as 'The characteristic time required for the polymer coil to relax from a deformed state to its equilibrium configuration.' While the relaxation time of a Newtonian fluid is instantaneous, a viscoelastic fluid can have relaxation times of the same order. To measure this it must be investigated through dynamic tests, through applying oscillations at constant or changing frequency. Higher relaxation times can be explored through experiments of creep or relaxation (Capurro and Barberis, 2014).

Surface tension is a force which acts along the tangent to the surface of the fluid, it's a term that refers to the interfacial tension between a liquid phase with respect to a gas phase. The attractive force upon the surface molecules of a liquid by the molecules of the bulk phase cause the surface area to be minimised (Eggers and Villermaux, 2008). Surface tension is measured in $\mathrm{N\,m^{-1}}$ and this value strongly depends on the concentration of surfactants which are inherently present or added to the liquid (Eggers and Villermaux, 2008). Surface tension can be measured with an instrument called a tensiometer. Various methods of measurement are employed, direct measurement using a microblance; measurement of capillary pressure; analysis of capillary-gravity forces; gravity distorted drops; and reinforced distortion of drops

(Ebnesajjad, 2010).

Hydrophobicity is a physical property of molecules that 'repel' water, there are no repulsive forces involved; it is an absence of attraction. The 'hydrophobic effect' is an organising force to assemble the lipid bilayer of biological membranes (Atwood, 2017). Hydrophobicity is a concept and can only be measured indirectly and measurements reflect the molecular interactions with water; therefore, various methods may have different meanings. Previous work measuring hydrophobicity of microorganisms has indicated water contact angle is the best method for revealing hydrophobic microorganisms (Mozes and Rouxhet, 1987).

3.1.1.1 Rheological effects on droplet size distributions

Droplet creation through Rayleigh capillary instabilities has been well documented in the literature. The study of how rheology effects resulting droplet size distributions is an important theme in enabling optimal results over many practices. Variation in viscosity and surface tension have both been shown to change droplet size distributions in crop spraying (Carvalho et al., 2017), for nasal sprays (Dayal et al., 2004), and in theoretical models (Dravid et al., 2006). Hence, it is assumed that respiratory droplet creation will be strongly influence by rheological properties of airway fluid. Understanding the mechanisms that govern droplet creation and the effects of liquid properties it may be possible to suppress droplet formation and alter droplet size distributions.

Mathematical modelling has considered the effects of respiratory fluids on airborne transmission. Theoretical studies state that bioaerosol droplet size distributions can be controlled by altering the fluid properties of the airway surface liquid (ASL). Vasudevan and Lange (2005) aimed to suppress pathogenic particles to reduce disease transmission. Rayleigh-Taylor instability analysis was performed on a viscoelastic model and concluded to suppress droplets completely the elasticity of the ASL should increase and the viscosity should decrease. However, if not fully successful this alteration to the ASL can produce smaller droplets and increase transmissibility. Alternatively, it was hypothesised that increasing droplet size may be another solution, in order to achieve this elasticity should be reduced and viscosity increased. Vasudevan and Lange furthered their study by publishing a second paper this time considering the effects of surface tension (Vasudevan and Lange, 2007). Droplet suppression was achieved by increasing elasticity and surface tension and decreasing viscosity. To enlarge droplet size it is the reverse, increase viscosity and decrease elasticity and surface tension. To completely suppress the droplets the viscosity may

be too low for ASL clearance, decreasing the viscosity by the desired amount for CF patients will be a problem as their ASL is naturally more viscous and it may not be possible.

Experimental studies (Hasan et al., 2010) have confirmed that viscoelastic properties had an effect on the droplet size distributions. However, they found a change in surface tension had negligible effects concluding that altering viscoelatic properties not surface tension can control droplet size distributions. Visualisations of sneeze ejecta (Scharfman et al., 2016) revealed that viscoelastic properties delay the fragmentation of droplets. Droplets connected through elongated filaments merge and therefore affect the final droplet size distribution. Inhaled saline solutions alter the physical properties of ASL and administering nebulised isotonic saline resulted in the creation of fewer and larger droplets for at least 2 hours (Edwards et al., 2004; Clarke et al., 2005).

3.2 Droplet size distributions

Given the importance of droplet size in the transmission routes of infectious particles, size profiles of respiratory droplets are important in understanding the fate of these infectious particles. Over the past several decades, different methods have been employed to measure droplet size distributions of respiratory droplets and a disagreement in findings has been reported.

Two early classic studies reporting in a detailed manner the sizes of particles emitted during different activities were Duguid (1946) and Loudon and Roberts (1967b). Both of these studies used a collection media for the droplets followed by microscopy analysis. Duguid (1946) used a dye that was introduced into the subjects mouth and the subject was asked to cough, sneeze, and talk (counting from 1 to 100). A celluloid-surfaced slide was held 6 inches (15.24 cm) from the participants mouth during these expiratory activities and the stain marks on the glass slide were measured by microscopy. It was assumed that particles lost negligible water prior to impact, but would spread when they impacted the slide. To account for this the stain diameters were reduced by one-half to estimate the airborne particle diameters. Less that 1 % of the particles on the slides has airborne diameters $<10\,\mu m$. Therefore, it was assumed these particles had a small mass and were carried past the slide in the deflected air stream. To measure these smaller particles Duguid (1946) used a second technique, where the expiration activity was conducted into a chamber from which the air was collected through a slit sampler onto an oil-coated

slide. Again stained particles were measured through microscopy. However, this time particles appeared spherical and not flattened, it was assumed these particles were completely dessicated and there diameters were increased four fold to account for airborne particle diameter. Duguid (1946) found that all respiratory droplets were between 1 µm–2000 µm.

Loudon and Roberts (1967b) studied three participants who coughed into a chamber of volume 0.057 m^3, bond paper was placed on each section of the chamber floor and walls. Similar to Duguid (1946) a dye was placed in the subjects mouths, and the subjects coughed three times into the chamber. After 30 minutes air was drawn through the chamber at 0.028 $m^3\,min^{-1}$ through a 0.45 µm Millipore filter to collect the suspended particles. Each participant repeated this process five times and then the stain marks were measured by microscopy. Particles with diameters greater than 10 µm were adjusted using a regression equation derived from results in a separate study (Loudon and Roberts, 1967a). The regression equation did not apply to particles less than 10 µm and it was assumed that the stain diameter was the same as the airborne diameter. Again Loudon and Roberts (1967b) found no droplets less than 1 µm but found nearly twice as many droplets in the 1 µm–2 µm range.

Just 50 years after Duguid (1946) reported his finding on droplet size Papineni and Rosenthal (1997) conducted their detailed study using optical particle counters. Each of the five healthy subjects coughed into a funnel connected to an optical particle counter, which was reported to have a lower detection limit of 0.3 µm. No diameter above 2.5 µm was recorded and approximately 85 % of droplets emitted had diameters less than 1 µm. However, particles had the opportunity to evaporate before being measured.

Recent years have seen the rise in the use of optical spectrometers such as the optical particle counter (OPC) and aerodynamic particle counter (APS). Yang et al. (2007) measured 54 healthy subjects cough aerosols using the APS. The size distribution was revealed to be 0.62 µm–15.9 µm with 82 % of droplets in 0.74 µm–2.12 µm. The distribution was multimodal with peaks at 1 µm, 2 µm and 8 µm. APS was used by Morawska et al. (2009) in a wind tunnel like device where participants placed their head within the tunnel. Various speaking manoeuvrers were performed and the majority of particles were seen with diameters below 0.8 µm.

Laser techniques have been employed in a number of studies (Chao et al., 2009; Zayas et al., 2012; Han et al., 2013). Chao et al. (2009) used Interferometric Mie imaging technique with 11 healthy subjects. The geometric mean was 13.5 µm for coughing and 16 µm for speaking. This value is higher than those calculated from most modern

methods and may be explained by the technique only detecting particles larger than 2 µm. Laser diffraction was used by Zayas et al. (2012), their study obtained data on the size distributions of droplets expelled by cough aerosols. Droplets were generated over a wide size range of 0.1 µm–900 µm but with 97 % of droplets less than 1 µm and 99 % of droplets less that 10 µm. Laser diffraction techniques have been used to measure droplet size distrubtutions from sneezes by Han et al. (2013). Within the 44 sneezes measured two types of distributions were observed: unimodal and bimodal. The geometric mean was 360.1 µm for unimodal and 74.4 µm for bimodal, with bimodal peaks at 72 µm and 386.2 µm. Sneeze droplets in this study are shown to be much larger than cough droplets. However, this study uses volume-based size distributions which will skew the data towards larger droplets.

A comparison of the mean diameters of cough droplets is given in Table 3.1. Mean diamter determined by Duguid (1946); Papineni and Rosenthal (1997); and Chao et al. (2009) appear to be in good agreement. However, the techniques used were insensitive to droplets smaller than 1 µm–2 µm which may have resulted in an overestimate in droplet sizes. Yang et al. (2007) bagged samples which allowed significant condensation and droplets were not measured at their expired size. Whereas the methods both using modern optical tehcniques found the mean diamter to be <1 µm, with a large amount of small droplets and smaller fractions of larger droplets. Despite the large amount of droplets <1 µm, these droplets may not be able to contain pathogenic material and it is the droplets >1 µm which can contain bacteria.

There is some debate surrounding the droplet size distributions of healthy vs infected individuals. Using a real time particle spectrometer Hersen et al. (2008) compared the droplet size distributions produced by exhaled breaths of symptomatic and healthy volunteers. The spectrometer was capable of measuring particles in the range of 7×10^{-3} µm–10 µm and demonstrated individuals with symptoms had sta-

Table 3.1: Mean droplet diameters from cough-generated aerosols during experimental investigations.

Reference	**Mean cough droplet diameter (µm)**
Duguid (1946)	14
Loudon and Roberts (1967b)	12
Papineni and Rosenthal (1997)	0.7
Yang et al. (2007)	8.35
Chao et al. (2009)	13.5
Zayas et al. (2012)	<1

tistical similarities and were different from symptomatic individuals. The difference was found in a greater emission of particles, especially particles of the size 0.5 µm and 1 µm, which could contain pathogenic material such as virus or bacteria. Size and amount of aerosols produced by participants infected with influenza during and after illness was studied by Lindsley et al. (2012). Number of particles per cough was significantly greater when participants were infected with influenza but particle sizes did not vary significantly during and after illness. More recently Wurie et al. (2016) studied the effects TB had on bacterial aerosol production during normal tidal breathing. High production aerosols were defined as any 1 µm–5 µm particle count above the median count over all participants. TB was associated with a 3.5 fold increase in high production aerosols, demonstrating TB increases production of respiratory droplets in a size range that could aerially transport bacteria.

3.2.1 Droplet counts and concentrations

Droplet number counts over a given size range are only available from a few studies in the literature (Duguid, 1946; Loudon and Roberts, 1967b; Zhu et al., 2006; Chao et al., 2009) and these references are widely used.

Estimations of total respiratory droplet number during different expiratory activities is important for estimating the amount of pathogens that may be disseminated into the air by an infected patient. Experimental investigations have shown difficulties in characterizing the droplet concentrations within cough jets and values obtained differ between investigations. It is important to note the methodologies used to determine concentrations used in the studies in Table 3.2. Papineni and Rosenthal (1997) acknowledged their methodology was questionable. Concentration was determined by continuously measuring particle count and dividing by the breath volume. This approach would only be accurate if the particle counter captured all of the exhaled breath. Therefore, the similar method used by Chao et al. (2009) who divided total droplet number by the total laser measurement volume is likely more accurate. The results of Yang et al. (2007) are problematic. The process where the authors transferred the sample into a bag created a difference in temperature inside to outside the bag. A dramatic increase in the number of droplets would have been seen, skewing the results. Aerosol dilution and evaporation before sampling may explain the low concentrations by Morawska et al. (2009), but this may provide a reasonable concentration of droplet nuclei.

Respiratory particles from talking have been shown to be smaller than from coughing or sneezing. However, the particles are still large enough to carry communi-

Table 3.2: Average particle concentration per cough obtained from experimental investigations.

Reference	**Number of particles cm^{-3}**
Papineni and Rosenthal (1997)	0.024–0.220
Yang et al. (2007)	881–2355
Morawska et al. (2009)	0.64
Chao et al. (2009)	2.4–5.2

cable respiratory pathogens albeit evidence suggests at much lower concentrations. Morawska et al. (2009) additionally provided data on the concentrations of speech at an average of 0.307 particles cm^{-3}, less than half that reported from coughing. More recently, using APS, Asadi et al. (2019) demonstrated particle concentration from talking varies with loudness (amplitude). Concentrations varied from 0.06 to 3 particles cm^{-3} in low to high amplitudes respectively. These data suggests talking loudly may produce as many droplets as coughing.

3.2.1.1 Super producers

Droplet numbers produced through expiratory activities can vary substantially from subject to subject. Edwards et al. (2004) findings showed two distinct populations: low producers and super producers. The study measured exhaled biaerosol particles from eleven healthy participants and remarkably the super producers (six participants) expired 99 % of the total bioaerosol particles from the entire group. These finding correlate with data from studies measuring culturable isolates from expired bioaerosols, in each group one or more participants produced colony counts much greater than the rest (Fennelly et al., 2004; Wainwright et al., 2009; Fennelly et al., 2012; Lindsley et al., 2012; Jones-López et al., 2013). It is notable that the percentage of high producers in the cohort examined by Williams et al. (2020), 8.3 %, was comparable to that found by Escombe et al. (2008) who reported 8.5 % of patients in their cohort caused 98 % of the secondary animal TB infections. Similar findings have been published for the influenza virus, Milton et al. (2013) reported a significant inter-individual variation and suggested cases with higher viral loads are disproportionality important in the spread of disease. Subsequently, similar cases have been reported in regards to SARS-CoV-2, finding emission rates of several orders of magnitude higher than a normal infected person (Miller et al., 2020) and an estimation of 80 % of infections occur from 10 % of people (Endo et al., 2020). These events have been termed super-spreading events and are caused by an infected per-

son who transmits the pathogen to an abnormally large number of people (Galvani and May, 2005) and have been widely reported in the literature (Shen et al., 2004; Oh et al., 2015; Streeck et al., 2020).

3.2.2 Exhaled flow characteristics

Velocity measurements during expiration activities provide data on how jets from the mouth opening transport bioaerosol droplets through the air. Many studies have used particle imaging velocimetry (PIV) to determine exhaled flow characteristics (Zhu et al., 2006; Chao et al., 2009; VanSciver et al., 2011; Kwon et al., 2012), whereas Tang et al. (2012) made use of shadow imaging. Table 3.3 summarises the velocities obtained from speaking and coughing in these studies. Velocities using the PIV technique are in relatively good agreement with Tang et al. (2012) for male volunteers.

Jets produced by coughing and speaking were found to be complex with varying velocities and entrainment making the jet expand which created vortices. A high velocity core was found in a narrow area of the cough jet (Zhu et al., 2006) about 15 mm in diameter at the mouth exit (Chao et al., 2009). Chao et al. (2009) found the jet produced by coughing was longer than the viewable area of the camera, 45 mm, and the jet produced by speaking was about 40 mm. This correlates well with that found by Tang et al. (2012) who found cough jet propagation to be between 16 mm–55 mm for females and 31 mm–64 mm for males. More recently the potential distance that pathogens can travel within coughs and sneezes is much further than

Table 3.3: Average and range of maximum velocities at the mouth opening when talking and coughing.

Reference	**Measurement technique**	**Talking**	**Coughing**
Zhu et al. (2006)	PIV	-	$11.2\,\mathrm{m\,s^{-1}}$ $6–22\,\mathrm{m\,s^{-1}}$
Chao et al. (2009)	PIV	$3.9\,\mathrm{m\,s^{-1}}$	$11.7\,\mathrm{m\,s^{-1}}$
VanSciver et al. (2011)	PIV	-	$10.2\,\mathrm{m\,s^{-1}}$ $1.15–28.2\,\mathrm{m\,s^{-1}}$
Tang et al. (2012)	Shadow imaging	-	M: $3.2–14\,\mathrm{m\,s^{-1}}$ F: $2.2–5\,\mathrm{m\,s^{-1}}$
Kwon et al. (2012)	PIV	M: $4.07\,\mathrm{m\,s^{-1}}$ F: $2.31\,\mathrm{m\,s^{-1}}$	M: $15.3\,\mathrm{m\,s^{-1}}$ F:$10.6\,\mathrm{m\,s^{-1}}$

previously appreciated, travelling up to 7 m–8 m (Bourouiba, 2020). Owing to the forward momentum of a locally moist and warm turbulent core. This high velocity core which had been previously described (Zhu et al., 2006), allows the droplets to evade evaporation for longer and propels them much further than if they were emitted in isolation.

3.2.3 Measurement of bioaerosol droplets

Understanding the composition of respiratory bioaerosols and the sizes of particles carrying pathogens is important for informing infection control processes. Numerous studies have sought to investigate and measure pathogens within expired aerosols from participants with communicable diseases.

Influenza is well known to transmit via the droplet and airborne route and there are many studies within the literature measuring viral load and size of droplets from infected patients. Lindsley et al. (2010) collected coughs from 47 subjects infected with influenza. Viral influenza RNA was detected in coughs from 38 subjects (81 %) whereas viable influenza virus was only detected in 2 of the 21 subjects cough aerosols. Suggesting a small portion of influenza found is viable. Thirty-five percent of influenza RNA was in particles >4 µm, while 23 % was in particles 1 µm–4 µm and 42 % in particles <1 µm; this was measured using the NIOSH two-stage bioaerosol cyclone sampler. Subsequently, Lindsley et al. (2016) compared viral load in exhalations vs coughing for viable influenza virus. Viable influenza was detected more often in cough aerosol droplets that exhaled aerosol droplets, 53 % vs 42 %. However, the difference in the results was not large and as we breathe more than we cough, exhaling is likely to account for disease transmission. Previously, Stelzer-Braid et al. (2009) came to the same conclusions that breathing may be a source of respirable particles carrying virus. The authors used a novel mask to collect the samples which were analysed using PCR. Of the 25 subjects who had the same virus type detected in nasal mucus and bioaerosol samples, virus was detected in 12 breathing samples, 8 talking samples, and 2 coughing samples. More recently, Yan et al. (2018) confirmed that coughing nor sneezing were necessary for infectious aerosol generation in a large study of 142 influenza patients.

Size of the droplets carrying pathogenic material plays an important role in enhancing our understanding of the spread of airborne infection. Lindsley et al. (2010) demonstrated that the majority of particles containing influenza RNA were found in droplets <4 µm. This finding has been repeatedly seen in numerous studies measuring participants with viral respiratory disease (Gerone et al., 1966; Fabian et al.,

2008; Gralton et al., 2013; Milton et al., 2013). More than 50 years ago Gerone et al. (1966) pioneered the study of measuring bioaerosols with the use of a weather balloon and a 127 L cone shaped chamber for the collection of sneezes and coughs. Particle size distributions from sneezes and coughs produced 50 % and 73 % of particles less than 1 µm respectively. Gralton et al. (2013) used a modified Andersen Impactor to measured the size of particles containing viral RNA. On breathing, 58 % of subjects produced large particles (>5 µm), while 80 % produced fine particles (<5 µm) containing viral RNA. During coughing, 57 % of subjects produced large particles and 82 % produced fine particles containing viral RNA. Similarly to Lindsley et al. (2016), these results demonstrate coughing does not produce a significant amount more viral RNA than breathing. Both Fabian et al. (2008) and Milton et al. (2013) collected exhaled breath samples from their participants. The results from the study by Fabian et al. (2008) demonstrated a huge preferential of influenza RNA to small particles with no particles above 5 µm containing viral RNA and 87 % of particles in exhaled breath under 1 µm. Milton et al. (2013) measure exhaled breath with and without a mask in two size fractions, course (≥5 µm) and fine (<5 µm). Fine particles were found to contain 8.8 fold more viral copies than coarse particles. Surgical masks worn by the participants reduced viral copy numbers in the fine fraction by 2.8 fold, while the coarse fraction viral load reduced by 25 fold. These results highlight the preferential to smaller particles and the importance of wearing a mask in reducing large droplet transmission.

Many of the devices used to detect size fractioned bioaerosols use large custom apparatus; which is not portable for hospital use. A small number of studies have measured bacterial aerosols, and the most successful studies have been carried out using a Cough Aerosol Sampling System (CASS) developed by Fennelly et al. (2004). The CASS consists of a portable drum that houses 2 standard bioaerosol samplers (Anderson Impactor and/or SKC/AGI Impinger) and a tube that participants cough or breathe into. This method has been used to sample Tuberculosis (TB) patients throughout the world (Fennelly et al., 2004, 2012; Jones-López et al., 2013). Cough-generated aerosols cultures were produced by 45 % or less participants in these studies and were associated with new infection and lack of treatment. A non-invasive face mask device developed by the same research group has been shown to detect mycobacterium in TB patients in the UK and South Africa (Williams et al., 2014, 2020). This device offers a less invasive, portable aerosol detection device that could be used more easily in clinical practice for pathogen detection. A novel protocol for diagnosing bacterial infectious at the bedside was developed by Zheng et al. (2018). Exhaled breath condensate and a Lamp Mediated Isothermal Amplification was used to investigate the bacteria in exhaled breath. Pathogens were detected

from 36.5 % of participants and included *H. influenzae*, *P. aeruginosa*, *E. coli*, *S. aureus* and MRSA. However, the face mask and protocol used by Zheng et al. (2018) was not able to provide any data on bacterial droplet distributions.

3.2.3.1 Respiratory droplets of cystic fibrosis pathogens

Studies involving individuals with CF have demonstrated that during coughing, viable aerosols are generated (Wainwright et al., 2009; Knibbs et al., 2014; Wood et al., 2018, 2019; Wood, 2019). Using a CASS similar to that used by Fennelly et al. (2004), Wainwright et al. (2009) were able to find culturable isolates of *P. aeruginosa* in a wide range of particle sizes. In addition, aerosols contained a small number of other gram-negative bacteria including *Burkholderia cepacia* complex, *S. maltophilia* and *A. xylosoxidans*. Wainwright et al. (2009) found the majority of these infectious particles had diameters $\leq$3.3 µm which is within the respirable range. Subsequently, a study by Knibbs et al. (2014) revealed that individuals with CF chronically infected with *P. aeruginosa* generated viable cough aerosols that were able to travel a distance of 4 m and survive in the air for 45 minutes.

Droplet size is key in determining the fate of a viable droplet nuclei. Therefore, to determine the optimum droplet size for pathogen transport Johnson et al. (2016) measured cultured *P. aeruginosa* from aerosols produced by individuals with CF for up to 2700 s. The greatest number of CFU counts were produced by nuclei from droplets in the size range 1.5 µm–5.7 µm, while smaller droplet nuclei despite their large numbers produced few colonies. Healthcare settings are recommended to use face masks as a means of reducing transmission of pathogens. In a study to ascertain if the use of face masks and cough etiquette (covering the mouth when coughing) produced viable *P. aeruginosa* aerosols, Wood et al. (2018) recruited twenty-five adults with CF and chronic *P. aeruginosa*. An Andersen Impactor was placed 2 m from each participant and uncovered a reduction in concentration of *P. aeruginosa* when using a face mask and cough etiquette compared to uncovered coughing. It is possible that some of the viable *P. aeruginosa* aerosols were redirected during covered coughing and adequate ventilation would be needed to reduce viable *P. aeruginosa* concentrations.

P. aeruginosa is the most common pathogen causing chronic infection in people with CF and as a consequence has been extensively studied. However, more recently experiments have began to look into the aerosolisation of common non-*P. aeruginosa* pathogens from people with CF. In a study investigating the cough-generated aerosols of common non-*P. aeruginosa* gram-negative bacteria, Wood et al. (2019)

demonstrated gram-negative bacteria remained viable within droplet nuclei over a distance of 4 m and for up to 45 minutes. The common non-*P. aeruginosa* gram-negative bacteria included *S. aureus*, *Stenotrophomonas maltophilia*, *Achromobacter* species and *Burkholderia cepacia* complex. Wood and collogues furthered their investigation into the aerosolisation of common non-*P. aeruginosa* CF pathogens with an investigation into the feasibility of the aerosolisation of *M. abscessus* in cough-generated aerosols in people with CF (Wood, 2019). The study involved three participants recently infected with *M. abscessus*, one participant produced cough aerosols that were positive for *M. abscessus* at 4 m and after 45 minutes. The remaining two participants did not produce any aerosols with detectable *M. abscessus*.

3.3 Droplet evaporation

Droplets experience evaporation/condensation once they are produced and introduced into the air, leading to a change in size. This change in size will depend on ambient air conditions, size, temperature of the droplet, and relative velocity. Numerous respiratory tract infections are believed to be transmitted through the air and understanding the evaporation and movement of aerosolised respiratory droplets is essential to exploring the fundamental mechanisms that govern the airborne transmission process.

3.3.1 Microbial aerosol evaporation and dispersion

In the last 80 years the concepts of large droplet and airborne transmission have been investigated. Various studies have investigated droplet trajectories and evaporation rates in the indoor environment. Xie et al. (2007) revisited the Wells evaporation-falling curve of droplets to gain insight on how far droplets can move when expelled during different respiratory activities. Xie et al. (2007) analysed the evaporation and movement of pure water and 0.9 % saline droplets. By evaluating effects of droplet size and velocity in an exhaled jet using the fourth order Runge-Kutta numerical method. Results confirmed Wells theory that small droplets evaporate to droplet nuclei rapidly and large droplets fall to the ground quickly. For flows where the droplet was expelled via repiratory activities the critical size for large droplets was found to be between 60 µm and 100 µm dependent on initial air velocity and relative humidity (RH). It was found that large droplets could travel more than 6 m for sneezing at $50\,\mathrm{m\,s^{-1}}$, 2 m for coughing at $10\,\mathrm{m\,s^{-1}}$, and 1 m away for breathing at $1\,\mathrm{m\,s^{-1}}$. These finding correlate with the advised 1 m–3 m bubble advised in infection

control measures for CF patients.

Similar models of exhalation jets have been widely investigated (Wang et al., 2005; Wei and Li, 2015; Chen et al., 2020). Wang et al. (2005) defined large droplets which fell out of the air to be >50 µm at RH >40 %. As RH increased so did the horizontal distance travelled, expanding the area pathogens can spread. When evaluating the the effect of turbulence on a cough jet Wei and Li (2015) demonstrated that small particles (<30 µm) follow the air flow closely and disperse in the whole jet region. The spread of large particles (100 µm) is mainly determined by the initial jet speed, with 1 % of large particles exceeding 2 m. However, these models assume a steady jet flow and the horizontal distance may be over estimated as deceleration of the jet can affect the movement of droplets in the air especially in the horizontal direction.

It remains a question whether large droplets or small airborne droplets dominate airborne transmission. Comparison of these two routes has rarely been reported, Liu et al. (2017a) demonstrated that both of these infection routes can be important within 1.5 m. When using a simple mathematical model which calculated exposure due to inhalation and deposition via expired jets Chen et al. (2020) found short range airborne droplets to dominate exposure during coughing and talking. Large droplet transmission only dominated when subjects were very close, within 0.2 m for talking and 0.5 m for coughing. The debate around large droplet and airborne transmission also considers when we measure droplet size as Li et al. (2018) revealed that due to evaporation some of the large droplets (>100 µm) which would have fallen to the floor now reduce in size and become airborne. These initially larger droplets may potentially have higher concentrations of pathogens, resulting in higher risks of infection. However, de Oliveira et al. (2021) concluded an aerosol cloud of droplets less than 5 µm resulting from 30 s of continued speech was able to reach 2 m in a few seconds and had a viable viral dose higher than that in a short cough. Reiterating the implication that physical distance is not sufficient to stop the transmission of pathogens in the absence of ventilation for long exposure times.

The effects of composition of respiratory fluid and bacteria are not widely addressed. Nicas et al. (2005) considered the dessication of a particle of respiratory fluid and concluded the diameter of a particle would reduce by one-half. This estimation results in particles of 20 µm or less evaporating to their dessicated state in $\leq$0.4 s for RH up to 70 %. However, more recently Liu et al. (2017b) predicted this final droplet size to be 32 % of its original diameter, agreeing with the maximum residue size from the classic Duguid (1946) study, claiming pure water droplets may not accurately predict microbial droplet evaporation. Parienta et al. (2011) examines multi-component droplets. In this model the droplet is assumed to be compromised

of multiple shells, these shells consider the concentrations of water, salts and proteins in the droplet. The multiple shells change how the droplets evaporate, it is a two stage process where the first stage is a rapid decline in diameter, which is similar to that of a uniform droplet, this is followed by a slower decline until evaporation ends. The two stage evaporation process has also been seen by Redrow et al. (2011) when investigating the evaporation of sputum.

3.3.1.1 Environmental factors affecting pathogen viability in droplets

The lifetime of the bacteria within aerosols is dependent upon several factors, environmental, droplet, and bacterial characteristics. Previous studies have shown that temperatures above 24 °C decrease survival for both gram-positive and gram-negative bacteria (Ijaz et al., 2016). In high temperatures and low RH a droplet will evaporate more quickly and bacteria lose viability via dessication and by oxygen toxicity (Cox and Wathes, 1995). Therfore, bacteria survival directly increases with droplet size (Lighthart and Shaffer, 1997). Hess (1965) showed this in an experiment where a rotating drum aerosolised the water containing *Serratia marcescens*, the dehydration of the aerosolised droplet resulted in sensitivity to the lethal effects of oxygen on bacteria. Fernandez et al. (2019) reported a new approach to study bacterial survival in aerosols as a function of environmental conditions. This new technology uses a drop on demand technique captured in an electrodynamic trap and levitated within a controlled chamber. Data showed a 41.5 % decrease in recovered *E. coli* colonies within the first 2 minutes followed by a less pronounced decay.

Relative humidity is know to play a role in survival of pathogens. For viruses viability has a U shaped curve, where viability is highest close to 100 % RH or below 50 % (Yang et al., 2012; Lin and Marr, 2019). Whereas, for bacteria viability decreased with decreasing RH (Lin and Marr, 2019). However, bacterial characteristics such as morphotype may affects this, with gram-negative bacteria surviving best in low temperature and high RH and gram-positive bacteria having the highest death rates at intermediate RH (Ijaz et al., 2016). It is not only these grouped bacterial characteristics that can have an effect on survival but survival can be very different for individual bacterial species (Bolister et al., 1992; Dinter and Müller, 1984). Thus, survival of bacteria will need to be investigated individually as a generalisation may not be accurate.

Droplet characteristics such osmolarity, nutrients and size will effect the evaporation of the droplet (Parienta et al., 2011); hence, the survival of the bacteria. Viability of virus has been shown to dramatically increase in mucus/human saliva (Yang et al.,

2012; Fedorenko et al., 2020). This result may be explained through findings from work completed by Vejerano and Marr (2018). Droplets containing water, salts and mucin upon evaporation presented a protective outer shell morphology, where the mucin separated from other components and became concentrated at the air-liquid interface. These evaporative water losses result in solutes and nutrients becoming more concentrated over time. Lin and Marr (2019) concluded that inactivation of bacteria is influenced by osmotic pressure from elevated concentrations of solutes, while virus inactivation is governed by the product of concentration and time; however, the virus itself has negligible effects on droplet evaporation.

3.4 Summary

Rheological properties have clearly been shown to influence droplet size distributions numerically, artificially, and from cough/exhaled breath samples. Therefore, it is possible to speculate that agents that alter airway surface tension or sputum viscosity can change the droplet size distribution and dissemination of potentially infectious droplets from people with CF. Controlled laboratory studies to investigate the influence of suspension fluids with different rheological properties on aerosolisation and microorganism survival would be beneficial to understand this effect.

Many studies have focussed on measuring overall droplet size distributions during different expiratory activities or culturing biological droplets. This has included demonstrating people with CF are able to produce infectious aerosols from coughs which can contain a variety of pathogens, including *P. aeruginosa* and *M. abscessus*. Although, this has not been shown in the UK climate and *M. abscessus* has only been considered in one study to date with a small number of patients. A further study could provide information regarding whether demographical/clinical factors alter the culturable droplet sizes produced by people with CF. Furthermore, finding if there is a correlation between the overall droplet size distribution produced, the culturable bacteria droplet sizes and the influence of evaporation has not been extensively studied. Thus, more research is required to investigate both the overall droplet size distribution and the culturable droplet size distributions.

Chapter 4

Experimental methodologies

This chapter describes the methodology underpinning an investigation into the impact of bacterial strain and suspension fluid on droplet size and survival. The methods described in this chapter were chosen to enable comparison with those used in previous studies within the literature. Building on the work of Clifton et al. (2008), laboratory based experiments in a controlled flow apparatus were used to determine survival and size distribution of droplets in air, to infer what could happen to respiratory droplets carrying bacteria in the indoor environment. Additionally, details of the microbiological methodologies associated with the cough aerosol sampling study in Chapter 6 are described; further details of the design of this study and experimental protocols are given in Chapter 6.

4.1 Materials

4.1.1 Bacterial Strains

Studies were carried out using two bacteria, *P. aeruginosa* and *M. abscessus*. The environmental strain of *P. aeruginosa* (NCIMB 10848) was obtained from the National Collection of Industrial and Marine Bacteria. All other *P. aeruginosa* strains were obtained and phenotyped from the Centre for Infectious Disease, University of Edinburgh. These strains have been chosen to represent both phenotypes and environmental, unique, and epidemic strains. *P. aeruginosa* strains that were used in these studies are listed in Table 4.1.

Table 4.1: Strains of *P. aeruginosa* used for laboratory experiments

***P. aeruginosa* strain**	**Identification Number**	**Phenotype**
Environmental	NCIMB 10848	Non-mucoid
Unique Patient 1	001PNM	Non-mucoid
Unique Patient 1	002PM	Mucoid
Manchester	003M	Non-mucoid
Newcastle	004N	Mucoid

All strains of *M. abscessus* were obtained from the University of Leicester and were unique clinical strains, so called epidemic strains have not been well documented in the literature as this is a relatively newly emerging pathogen. Morphotype of all strains was determined by sight, Figure 4.1 shows the distinct difference between the two. It is clear from Figure 4.1 why the two morphotypes were given their name. The left image shows the smooth colony which is smooth and almost pimple like in appearance; smooth colonies will shine in light. The rough colony is rough with what look like sharp edges, flatter to the surface and will not reflect any light. *M. abscessus* strains that were used are listed in Table 4.2.

Table 4.2: Strains of *M. abscessus* used for laboratory experiments

***M. abscessus* strain**	**Identification number**	**Morphotype**
Clinical	001S	Smooth
Clincial	002R	Rough

Figure 4.1: Single *M. abscessus* colony grown on 7H10 agar (Cortes et al., 2010). Left smooth morphotype. Right rough morphotype.

4.1.2 Suspension fluids

The bacteria were suspended in a variety of fluids during the experiments. Fluids that are routinely used in microbiological studies have been chosen along with an artificial mucus developed to mimic the mucus of a patient with CF. The suspension fluids used are listed in Table 4.3.

Table 4.3: Suspension fluids used in laboratory experiments.

Fluid	**Rheology**
1/4 Ringers solution	Newtonian
1 % Foetal Bovine Serum (FBS) in 1/4 ringers	Newtonian
Artificial Mucus	Non-Newtonian

Ringers solution was created by adding a single ringers tablet to 500 ml of distilled water. The tablet (Oxoid, UK) is a combination of several salts. The purpose of using ringers solution was to create an isotonic solution relative to the body fluids of an animal. Meaning there is no solute gradient either side of the cell membrane of the bacteria. Therefore, the cell cannot shrink or swell as there is no osmotic pressure gradient to activate diffusion of water across the cell (Lodish et al., 2000).

FBS was used in these studies to try and provide a better representation of human saliva/mucus than 1/4 ringers solution on its own. FBS contains proteins, sodium, potassium, chloride, and lactate (Gstraunthaler and Lindl, 2013) which are found in human mucus (Nicas et al., 2005). This suspension was used in work conducted by Clifton (2009) which provided a comparison. However, Clifton (2009) used a 10 % FBS and preliminary experiments discovered 10 % FBS solution foamed during nebulisation, foam rose to the top of the nebuliser and superfluous fluid was dispensed

(a) 1/4 Ringers solution.

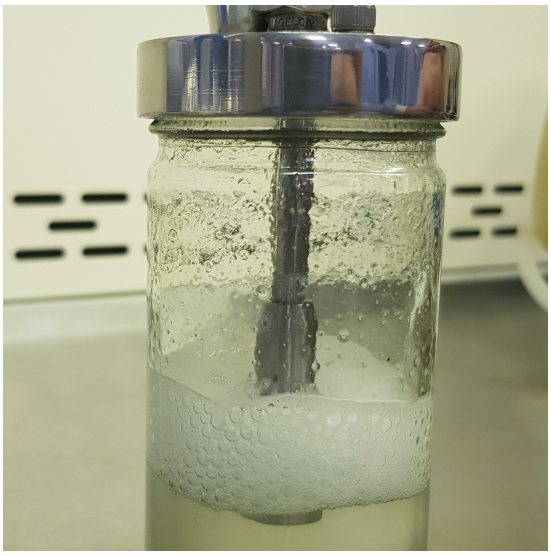

(b) 1 % FBS in 1/4 ringers solution.

Figure 4.2: Suspension fluids in the Collison nebuliser vessel 30 minutes after starting generation.

from the nozzle. The foam disrupted the aerosolisation of the fluid suspension and therefore a high percentage of FBS could not be used. Liquid must not rise above the jets on the Collison nebuliser and in the case of the 10 % FBS solution the foam disrupts these jets. A description of how the Collison nebuliser works is given in section 4.5.4.1. An investigation was undertaken to determine the percentage of FBS solution where the foam would not rise high enough to disrupt the jets and the aerosolisation of the solution, allowing for comparable results to 1/4 ringers solution.

Figure 4.2a shows a representation of the 1/4 ringers solution in the nebuliser; here there is no foam creation and the jets do not hit any fluid. The second figure, Figure 4.2b, shows a 1 % FBS solution 30 minutes after generation began, the longest the nebuliser is operated for. In this case the jets can still be seen and the foam has not risen above these and hindered the nebulisation process. For this reasoning a 1 % FBS solution was used in this study. Other percentages of FBS were also tested during this investigation, these were 2 %, 5 % and the original 10 % FBS solution. During nebulisation of all these solutions the foam rose higher than the jets produced by the Collison 3-jet nebuliser and these solutions were disregarded for use in the study.

A 1 % FBS solution was created by first aliquoting FBS (Merck, UK) into sterile falcon tubes following an aseptic technique. Each falcon tube contained 11 ml of FBS and was frozen at −80 °C until needed. 1 ml of FBS from a falcon tube was dispensed aseptically using sterile pipette tips into 99 ml of 1/4 strength ringers that had been autoclaved at 121 °C for 15 minutes.

A range of mucus simulant gels were used to mimic the viscoelastic properties of real mucus from people with CF. These gels were created using varying amounts of locust bean gum (LBG) solution, sodium tetraborate (ST) solution, and sodium dodecyl sulfate (SDS) surfactant. These ingredients varied the viscoelasticity and surface tension and in total sixty-four samples were created. The gels were prepared by first creating two 100 ml 1 % saline solutions ($NaNO_3$). Each saline solution was split into four 25 ml centrifuge tubes. The surface tension of the samples was varied by mixing in 0 mM, 2 mM, 4 mM and 6 mM of SDS surfactant using a vortex mixer. This resulted in two sets of four 25 ml 1 % saline solutions containing 0 mM–6 mM of SDS surfactant. The solutions were heated and maintained at 80 °C. The required amount of LBG powder was added to each tube incrementally with the first set of four tubes becoming a 0.5 % LBG solution and the second set of four becoming a 1 % LBG solution. Whilst the LBG powder was added, the tubes were stirred using the vortex mixer individually. There were no losses due to evaporation due to the solution being contained in a sealed tube. A 0.1 M ST solution was prepared and volumes of 0 µl, 10 µl, 15 µl, 20 µl, 30 µl, 45 µl, 60 µl and 90 µl of the 0.1 M ST

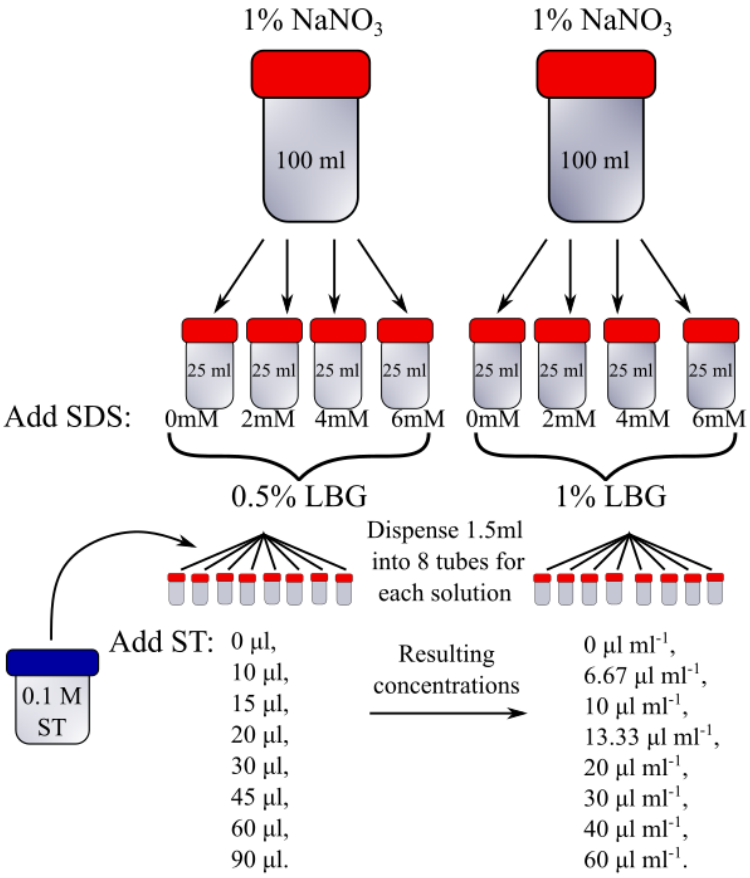

Figure 4.3: Breakdown of the methodology in creating the 64 artificial mucus samples, depicting the range of each ingredient involved.

solution were added to 1.5 ml of each LBG solution and vortexed using a vortex mixer for 2 minutes. The resulting concentrations of ST in the final solutions were 0 µl ml^{-1}, 6.67 µl ml^{-1}, 10 µl ml^{-1}, 13.33 µl ml^{-1}, 20 µl ml^{-1}, 30 µl ml^{-1}, 40 µl ml^{-1} and 60 µl ml^{-1}. A visualisation of this methodology and range of ingredients used is presented in Figure 4.3. Only those mucus gels which were able to nebulise using the Collison nebuliser and behaved more like mucus than water, i.e those which were not too viscous or water like, had their shear viscosity tested. The mucus gel chosen for this study was the best match to that of mucus from people with CF, see Chapter 5 for results.

A larger batch than the 1.5 ml volumes created as described above for the experiments was needed. An initial 150 ml of 1 % saline solution ($NaNO_3$) was created and no SDS surfactant was added to the solution. The solution chosen was 1 % LBG with 6.67 µlml^{-1} of ST. 1.5 g of LBG was added incrementally. To mix the solution a probe sonicator was used and was set to pulse for 10 seconds on and 5 seconds off, 1 minute at a time. This process was repeated until the LBG was mixed. The ST was added afterwards and mixed with the probe sonicator following the same steps.

4.2 Preparation of strain cultures

Each *P. aeruginosa* bacterial culture was delivered on agar slopes. For each strain a sterile loop harvested a single colony from the original slopes which were then inoculated onto sterile 18 ml TSA agar plates using the streak plate method. A sterile loop was used to streak the harvested colony onto the agar plate along one side, a second sterile loop was then used to streak these same colonies across another side; this process is repeated to make a square and was used to isolate single colonies. An illustration of this method and an example is shown in Figure 4.4. This process was completed under aseptic conditions. All inoculated plates were placed into an incubator at 37 °C for a minimum of 12 hours, until colonies were seen to form. Following incubation, a single isolated colony was harvested into 100 ml of nutrient liquid broth. This culture was incubated at 37 °C and shaken at 110 rpm in an orbital incubator (StuartS150), for a minimum of 12 hours, until turbid.

The *M. abscessus* strains were delivered on 90 mm 7H10 agar plates. For each strain a sterile loop harvested a single colony from the original plates which were inoculated onto 18 ml TSA agar plates using the streak plate method. All inoculated plates were placed into an incubator at 37 °C for a minimum of 3 days. Following incubation, a single isolated colony was harvested into a 5 ml solution of 4.5 ml 7H9

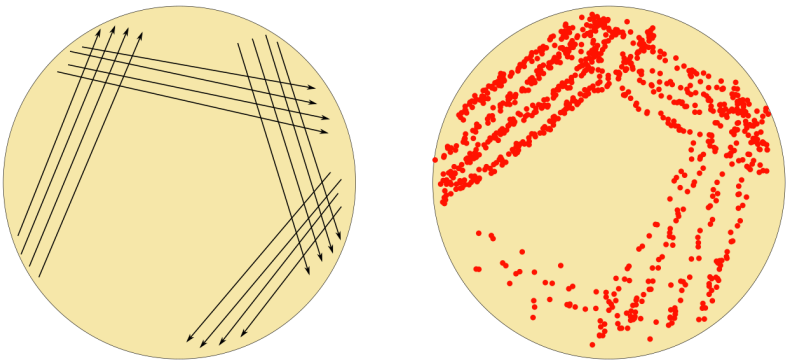

(a) Image illustraing how to perform the streak plate method.

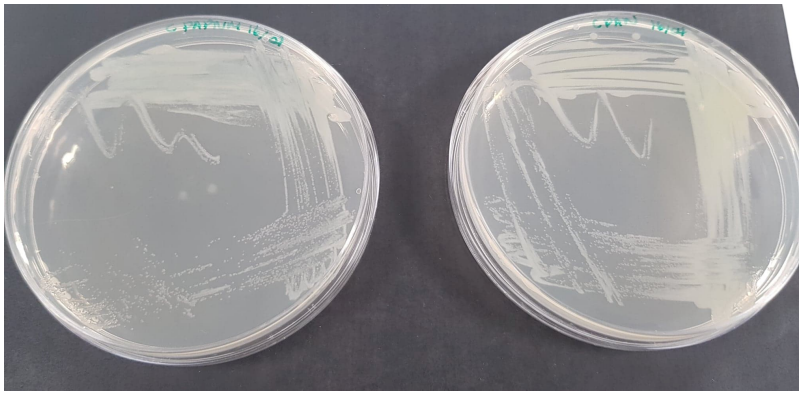

(b) *P. aeruginosa* streak plates on cetrimide agar.

Figure 4.4: Example of the streak plate method for isolating single colonies.

broth and 0.5 ml of acid-dextrose-catalase (ADC). *M. abscessus* can clump due to its exposed lipids on the cell surface that are involved in hydrophobic actions. To overcome this 25 µl–50 µl of Tween 80 was added to the solution along with sterile glass beads with a D50 of 3 mm as advised by Cortes et al. (2010). This solution made a pre-culture liquid stock. Preparation of *M. abscessus* liquid culture involved inoculating 100 µl of the pre-culture into 10 ml of nutrient broth, Tween 80 and glass beads. These cultures were incubated at 37 °C and shaken at 110 rpm in an orbital incubator for a minimum of 3 days for both morphotypes.

4.2.1 Preparation of agar plates

During the laboratory experiments, three different types of agar plates were used: Tryptic soy agar (TSA), cetrimide and RGM agar. TSA agar grows all bacteria and fungi, it is a non-selective agar and does not inhibit bacterial growth. Therefore, TSA agar was used for all experiments conducted in the bioaerosol characterisation rig (section 4.5.1), growing stock cultures, bacterial growth curve experiments, and CFU counts. Cetrimide agar was used for growing cultures of *P. aeruginosa* as this

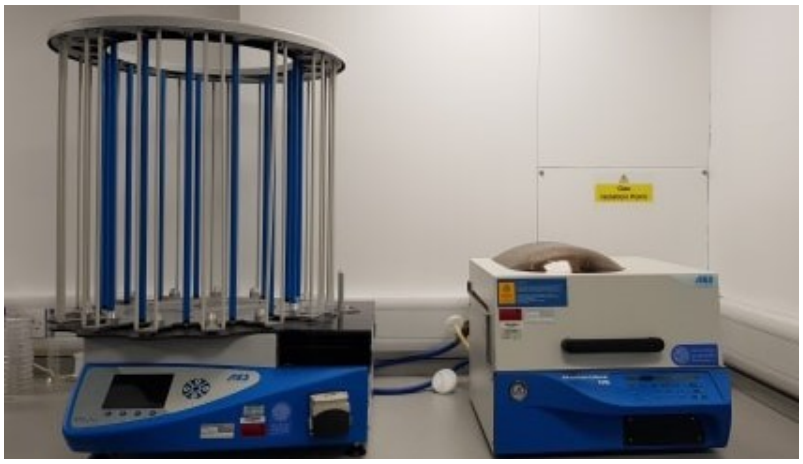

Figure 4.5: Plate pouring apparatus, consisting of the automated pourer stacker (left) and the masterclave 09 (right).

is a selective agar for *P. aeruginosa* bacteria. Colonies harvested from this agar were used to create liquid broth of *P. aeruginosa* strains, using cetrimide reduced the risk of contamination from other bacteria. RGM agar was used to grow cultures of *M. abscessus*, this agar isolates for rapidly growing mycobacteria. Colonies harvested from this agar was used to inoculate pre-culture stock of *M. abscessus* to reduce risk of contamination from other bacteria.

40 g of TSA (Oxoid, UK) per 1 L of distilled water was used to create all TSA agar plates. 45.3 g of Cetrimide (Oxoid, UK) was suspended in 990 ml of distilled water before adding 10 ml of glycerol. RGM agar plates were delivered by courier from Newcastle upon Tyne Hospitals NHS Foundation Trust, these agar plates were 90 mm petri dishes with 25 ml of agar.

Several volumes of agar plates were used in these experiments, a volume of 18 ml and 25 ml were used for spread plates and CFU counts. A volume of 37 ml was used for all Andersen Impactor sampling, this has been shown to yield the correct agar depth for optimum sampling from previous work at the University of Leeds (McDonagh et al., 2013). Agar mixtures were stirred for 5 minutes before being heated up to 121 °C for 15 minutes using the Masterclave 09 (Don Whitley Scientific). After autoclaving the agar was cooled and kept at a constant temperature of 45 °C for pouring. Agar plates were poured in sterile conditions using the automated pourer stacker (APS One) (Don Whitley Scientific) into sterile 90 mm petri dishes. Figure 4.5 shows the plate pouring apparatus, on the right is the Masterclave 09 and on the left is the APS One.

In some cases when only small amount of plates were needed, agar plates were hand poured. The agar was prepared as per the manufacturer's instructions for 500 ml

of medium in duran bottles. The contents were shaken to ensure it was well mixed before autoclaving the agar at 121 °C for 15 minutes. The agar was left to cool to 60 °C and then hand poured into sterile 90 mm petri dishes under aseptic conditions using the correct personal protective equipment. All agar plates were left to cool and solidify before being stored at room temperature until required.

4.2.2 Preparation of liquid broth

To prepare liquid broth for *P. aeruginosa* cultures, 13 g of nutrient broth per 1 L of distilled water was dissolved and 100 ml of the solution was placed into a series of conical flasks. Each flask was loosely plugged with a foam bung, covered in foil, and autoclaved at 121 °C for 15 minutes. Each broth was left to cool and refrigerated at 3 °C until required.

The initial pre-culture stock of *M. abscessus* cultures was grown in 4.5 ml of 7H9 medium with 0.5 ml of ADC and 25 µl–50 µl of Tween 80. This solution was grown in a 150 mm × 16 mm test tube with 3 mm sterile glass beads covering the bottom. 10 ml of sterile nutrient broth (prepared as above) mixed with 25 µl–50 µl of sterile Tween 80 and sterile glass beads covering the bottom was used for liquid *M. abscessus* cultures. Exposed lipids at the cell surface mean that *M. abscessus* has a tendency to create large aggregates in liquid culture. To combat this sterile beads and Tween 80 were used to reduce clumping. Tween 80 also protects against contamination as many other organisms growth are inhibited (Cortes et al., 2010).

4.2.3 Serial dilutions

A serial dilution is a series of sequential dilutions used to dilute a dense culture of bacterial cells to a useable concentration. Using diluted concentrations it is possible to determine the concentration of bacteria ($CFU\,ml^{-1}$) in the stain cultures and bacterial suspensions used in experiments. This section describes the serial dilution method up to 10^{-5}. In this method five McCartney bottles were filled with 9 ml of $^1/_4$ strength ringers solution and autoclaved at 121 °C for 15 minutes. Once cooled the bottles were labelled from 10^{-1} up to the dilution being conducted, in this case 10^{-5}. A 1 ml auto pipette and sterile pipette tip was used to dispense 1 ml of single strain nutrient broth into the 10^{-1} McCartney bottle, the lid was replaced and the bottle agitated for a few seconds to ensure complete mixing. 1 ml of the 10^{-1} ringers and strain solution was then added to the 10^{-2} bottle in the same way. This process was repeated for the rest of the dilutions and all dilutions were completed under

aseptic conditions. The sterile pipette tips were discarded after each dilution. The methodology of this process is depicted in Figure 4.6.

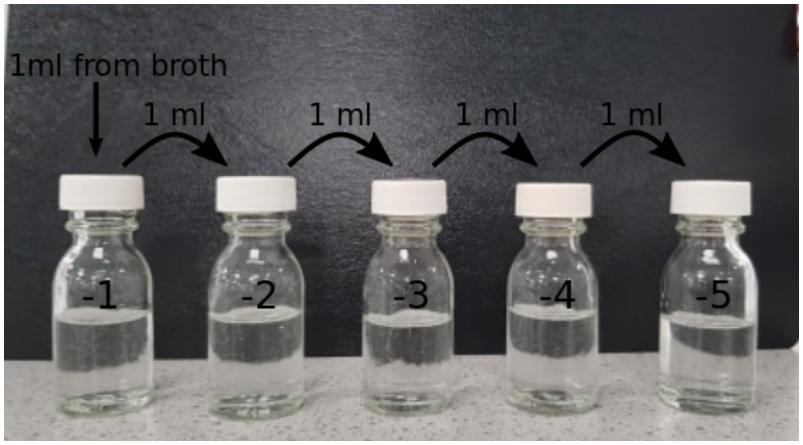

Figure 4.6: Image of the serial dilution method using 9 ml of ¼ ringers solution in McCarthy bottles.

4.3 Growth curves

Growth curves for each bacterial strain were produced to determine the time in which the bacterial strains were in different phases (i.e lag phase (A), exponential phase (B), stationary phase (C) and death phase (D)). A simplified bacterial growth curve is presented in Figure 4.7, showing all phases. The bacterial growth curve represents the number of live cells in a bacterial strain broth over time, the phases are described below:

Lag phase: The initial phase is described by metabolic activity but not growth. No cell division occurs.

Exponential phase: Bacterial cell population grows exponentially. Cells will divide and double after each generation time.

Stationary phase: The population growth experienced in the exponential phase will begin to decline as the available nutrients in the medium decrease. The rate of cell growth matches that of cell death.

Death phase: Nutrients are less available and the number of dying cells continue to rise and population growth experiences a sharp decline.

To ensure clear comparison of bacteria during experiments it is desirable for the bacteria to be in the same growth phase, in particular the exponential phase, as during this phase cells are active and there are no dead/dying cells. This was

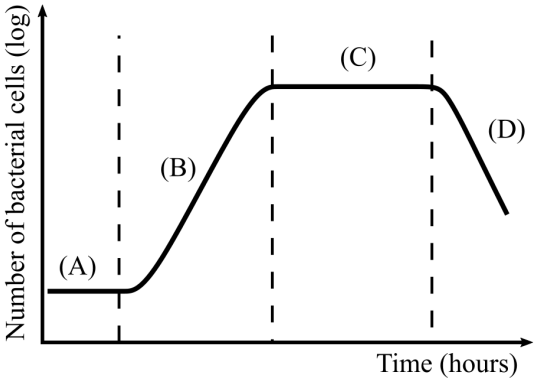

Figure 4.7: Simplified representation of a growth curve of bacteria, indicating the four phases which are part of this process.

not always possible but the bacterial cultures used in the experiments were in the exponential or stationary phase. CFU growth curves for all bacteria were completed; bacteria strains are given in Tables 4.1 and 4.2. All strains were grown in triplicate and for each time point all repeated strains were plated out in triplicate. The concentration of viable bacteria within the liquid broth was expressed as a mean for each strain.

A single colony from cetrimide agar for *P. aeruginosa* strains or 100 µl of *M. abscessus* pre-culture was used to inoculate 10 ml of nutrient broth in 15 ml falcon tubes. Inoculated cultures were incubated using an orbital incubator shaking at 110 rpm at 37 °C. Total Viable counts for *P. aeruginosa* were determined at 3 h, 6 h, 12 h, 24 h and 48 h. Total viable counts of *M. abscessus* were determined at 6 h, 12 h and 24 h, laboratory opening times did not allow for a full investigation into *M. abscessus* growth curves. These counts were used to construct a viable cell concentration growth curve. Appropriate serial dilutions were made and the dilutions were plated out using either the spread plate method or with the Whitley Automatic Spiral Plater (WASP) (Don Whitley Scientific), Figure 4.8, onto 25 ml TSA agar plates.

Once viable cell concentration growth curves had been determined it was possible to determine the time taken for each strain to reach the exponential growth phase in the respective bacterial growth curves. Optical density growth curves were also created; values of optical density were used to determine the doubling time of bacteria in the exponential phase (Dalgaard et al., 1994). Doubling time of bacteria was used to ensure consistent bacterial suspensions between repeat experimental runs. As above, a single colony from cetrimide agar for *P. aeruginosa* strains or 100 µl of *M. abscessus* pre-culture were used to inoculate 10 ml of nutrient broth in 15 ml falcon tubes. Inoculated cultures were incubated in an orbital incubator shaking at 110 rpm at 37 °C. All strains were grown in triplicate and the optical density was

Figure 4.8: The Whitley Automatic Spiral Plater.

expressed as a mean for each strain. Optical densities were taken at 4 h, 5 h, 6 h, 8 h and 10 h for *P. aeruginosa* and 6 h, 12 h, 24 h and 48 h for *M. abscessus*. To measure the optical density of the cultures, 1 ml of each culture was dispensed aseptically using an auto pipette and sterile pipette tips into cuvettes. A spectrophotometer (Thermo Scientific) was used to determine optical density at path lengths of 600 nm.

Optical density calibration curves for each strain were used to determine approximate concentrations quickly rather than having to undertake serial dilutions, plating, and incubation. The spectrophotometer measured optical density at path lengths of 600 nm for a series of dilutions to measure the relationship between optical density and bacterial concentration (CFU ml^{-1}).

4.4 Fluid characterisation model

These experiments aimed to characterise the effects that the bacteria may have on the fluid properties of the suspension. This was considered important as these properties in turn can affect the droplet size distribution once the fluid is aerosolised. Bench-scale experiments were carried out to measure the surface tension with and without bacteria. In addition, generation rates of the suspension fluids were investigated to allow for accurate comparisons between survival rates of the bacteria in the different suspensions.

4.4.1 Surface tension measurements

All surface tension measurements were taken using a Torsion balance (Whites Electrical Inst.), Figure 4.9, using 5 ml of liquid. Measurements were taken according to the user's manual. The platform holding the vessel of liquid was raised until the platinum 40 mm DuNuoy ring touched the surface of the liquid. The ring was slowly raised using the mechanism of the Torsion balance and the platform holding the vessel of liquid was lowered to keep the balance zeroed. When the meniscus of the fluid broke all motion stopped and the surface tension was read off the torsion balance.

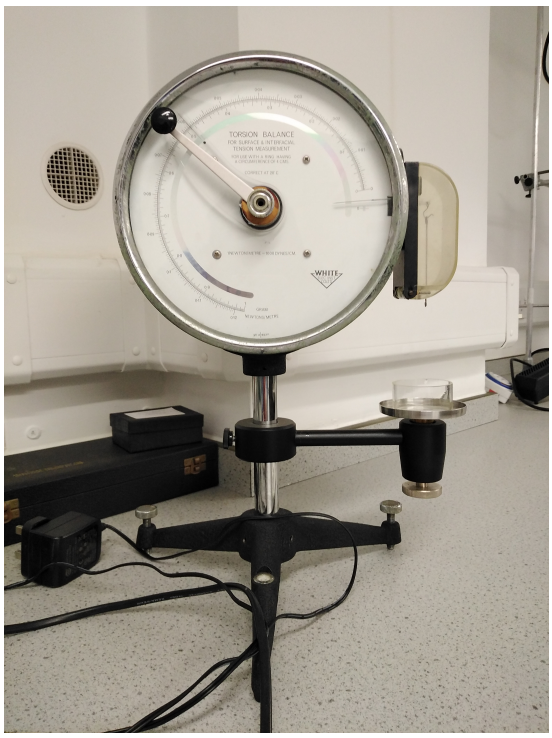

Figure 4.9: The torsion balance.

4.4.2 Aerosol generation of suspension fluids

Generation of aerosols from the Collison 3-jet nebuliser using two suspensions, 1/4 ringers solution and 1 % FBS in 1/4 ringers solution, were analysed over a period of 60 minutes. 100 ml of each suspension was added to a sterile nebuliser vessel and weighed pre-nebulisation on a mass balance with readability of 0.01 g. Each 100 ml suspension was nebulised for a total of 60 minutes using the Collison 3-jet nebuliser at 6 L min^{-1}. At the intervals of 15, 30 and 60 minutes nebulisation came to a halt and the nebuliser vessel with the remaining suspension was weighed, all

measurements were taken in triplicate. For each suspension this experiment was ran in triplicate.

4.5 Aerosol characterisation models

In the course of these experiments droplet size distributions and bioaerosol viability counts of *P. aeruginosa* and *M. abscessus* were measured along different lengths of pipe. A set up based on the idea of the 'laminar flow' model used by Clifton et al. (2008) was constructed. In addition to the similar geometry used by Clifton et al. (2008), Figure 4.10, a particle size instrument Spraytec (Malvern Instruments, UK) was used to measure droplet size distributions. Several experimental scenarios were explored and are detailed below.

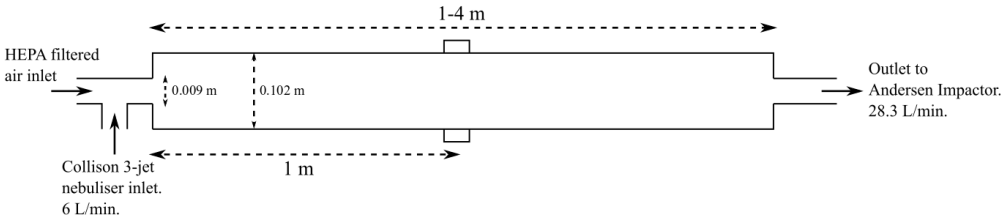

Figure 4.10: Original geometry of the 'laminar flow' model used by Clifton et al. (2008).

4.5.1 Bioaerosol Characterisation Apparatus (BACA)

The experimental apparatus was constructed from 0.5 m or 1 m lengths of 110 mm diameter polyvinyl chloride (PVC) piping. The length of the apparatus varied from 1 m–4 m; the maximum length of 4 m was chosen due the size of the class II aerobiological chamber where the experiments were carried out. Lengths of pipe were joined together by PVC air tight double socket coverings, and the ends were sealed with PVC air tight end caps. Holes were drilled through the end caps to allow for delivery of the aerosol and for the bioaerosol sampling. The inlet for the nebuliser was a pipe of diameter 0.013 m and the air inlet and outlet for air sampling were pipes of diameter 0.0284 m. The inlet was designed to reduce recirculation; the results of this can be seen in the CFD model (section 4.5.2). A window for the Spraytec device was created in the last 0.5 m section of the pipe, the window measured 69 mm by 50 mm, and is at the centre of the last 0.5 m section. Spraytec was made airtight to the pipe with two cones attached to the transmitter and receiver mounted onto the pipe and sealed with silicone, Figure 4.11 is an image of this attachment. HEPA

filters were used at either end of the apparatus to ensure the air at both the intake and the exhaust was free from bacterial contamination. Figure 4.12 shows images of the Bioaerosol Characterisation Apparatus (BACA) and Figure 4.13 is a schematic of the BACA design.

(a) Top view. (b) Side view.

Figure 4.11: Airtight attachment onto Spraytec from the Bioaerosol Characterisation Apparatus.

(a) Inlet. (b) Top view. (c) Outlet.

Figure 4.12: Bioaerosol Characterisation Apparatus set-up in the class II microbiology chamber.

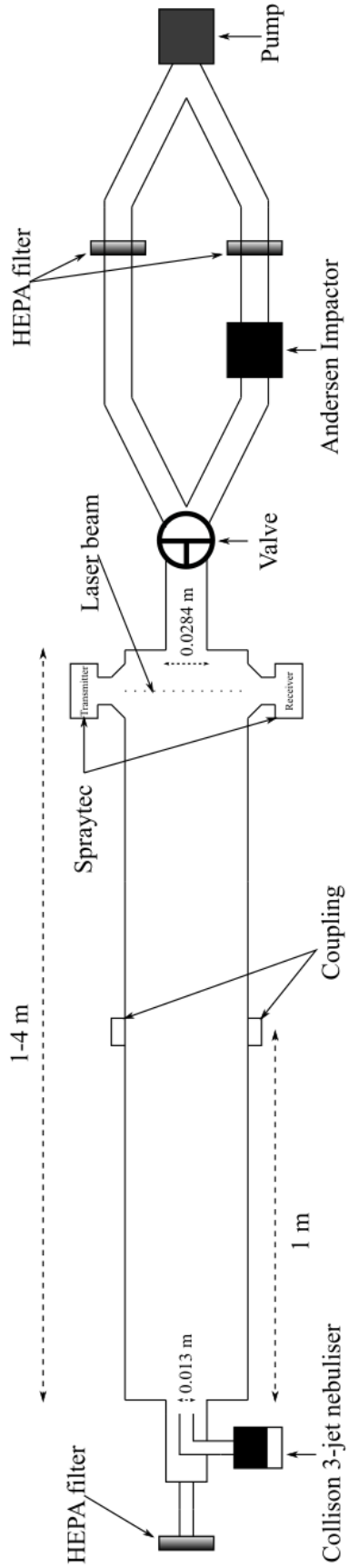

Figure 4.13: Schematic of the Bioaerosol Characterisation Apparatus (BACA).

4.5.2 Refining rig design

Previous research did not consider the airflow within the BACA during experiments and analysis. It was hypothesised that there are re-circulation zones within the BACA that could affect the air sampling, particularly at the beginning of the BACA where the nebuliser is connected. Therefore, this project turned to CFD to evaluate and refine the design of the BACA to provide confidence in using a customised inlet, details can be found in Appendix A. The customised inlet balanced the velocities of air coming into the BACA through a difference in pipe sizes. This inlet was a 'pipe within a pipe' design and the size of the pipes used are shown in Figure 4.13.

4.5.3 Experimental set up considered

The experimental apparatus was located within the environmentally controlled, negatively pressured, class II aerobiological chamber at the University of Leeds to safely aerosolise the bacteria and ensure that environmental conditions were constant. Dimensions of the chamber were 4.26 m (L) × 3.36 m (W) × 2.26 m (H). All walls were well insulated and can be considered to be adiabatic. External air was supplied to the chamber through a HEPA filter and was then conditioned by a humidifier and heater. Air was supplied to the chamber though a high level diffuser and extracted through a low level and diagonally opposite diffuser of the same design. The extraction of air within the chamber was at 12 air changes per hour. This air exchange ensures the room was well mixed and the temperature and humidity were assumed to be constant throughout. Temperature within the chamber was 22 °C ± 2 °C. Relative humidity in the chamber was 50 % ± 5 %.

4.5.4 Aerosol generation

Generation of all aerosols was under controlled conditions of relative humidity and temperature. Aerosols were generated using a Collison 3-jet nebuliser (BGI, USA) operating at $6\,\mathrm{L\,min^{-1}}$. Suspension in the nebuliser vessel was from 1 ml of $10^7\,\mathrm{CFU\,ml^{-1}}$ *P. aeruginosa* or $10^6\,\mathrm{CFU\,ml^{-1}}$ *M. abscessus* culture dispensed into 100 ml of sterilised suspension fluid. Each experiment required the preparation of two sterile Collison nebuliser vessels, one vessel was connected to the Collison 3-jet nebuliser head and used for nebulisation and the other was placed in the chamber under the same environmental conditions for the duration of the experiment. Concentrations of each vessel were compared pre and post experimental runs to

determine if there was any die off of bacteria due to the stress of nebulisation.

Serial dilutions were performed on nebuliser spray suspensions pre and post nebulisation. Measurements were made on two suspensions in two vessels, the vessel that was used to aerosolise the bacterial suspensions and a second vessel that was kept in the microbiological chamber under the same conditions but the suspension was not aersolised. There was no change in the magnitude of CFU ml^{-1} pre or post nebulision for either vessel and no difference between the aerosolised and non-aerosolised suspension. As a result this suggests there was no die off of the bacteria in the suspension over the course of the experiment or due to pressure on the bacteria through the aerosolisation process. The meant that the initial nebuliser concentration could be used with confidence to compare between experiments. However, the serial dilution method to measure the CFU ml^{-1} of the bacteria is not precise and it was only assumed to be accurate to the order of one log CFU ml^{-1}.

For all experiments the number of bacteria in the nebuliser was of the same order of magnitude. To decide on what number this should be preliminary studies were conducted. Clifton et al. (2008) determined the ideal concentration was 10^7 CFU ml^{-1}, equating to 10^5 CFU ml^{-1} in the nebuliser vessel, with a sample time of 2 minutes. These conditions were chosen for *P. aeruginosa* in the current study with sampling carried out over the 1 m–4 m pipe length range. This concentration of bacteria was also chosen for the shorter 1 minute samples when only sampling for the 1 m–2 m range. A preliminary study was conducted for each *M. abscessus* strain in 1/4 ringers and the concentration of 10^6 CFU ml^{-1}, equating to 10^4 CFU ml^{-1} in the nebuliser vessel, was most appropriate. This study gave 'countable' CFU counts which were not heavily loaded. Andersen (1958) claimed that observed counts of up to 380 CFU were reliable, to ensure this limit was not reached and that there would be observed colonies on the agar plates all colony counts were roughly greater than 50 CFU but less than 200 CFU.

When conducting the *P. aeruginosa* experiments a suspension was made up the day before and its concentration was checked before starting the experiments. This was adjusted using the optical density relationship if necessary. Experiments using strains of *M. abscessus* a slightly different approach was used. The growth time of this bacteria was at least 3 days and by the time the counts in the concentration test sample had grown some of the bacteria in the main suspension would have died and the CFU ml^{-1} would not be the same. Therefore, during the preliminary experiments concentration and optical density values were both measured. The optical density of 0.01 for both rough and smooth was chosen for experiments in the preliminary studies, this optical desnsity was measured to be 10^6 CFU ml^{-1} for

both strains.

4.5.4.1 Collison nebuliser

The Collison 3-jet nebuliser is a pneumatic apparatus for aerosol generation and is widely used to produce fine aerosols from a liquid supply. The device is designed to use compressed air to break up fluid into droplets (John, 1993). When compressed air passes through a narrow hole, the pressure reduces, and the air velocity increases. This fall in pressure sucks fluid up the tube and the fluid is then broken up by the air jet into a large distribution of droplet sizes. The larger droplets hit the internal wall of the spray vessel with the smallest droplets escaping out the nebuliser as a fine aerosol with droplet size distribution of 0.5 µm–20 µm (May, 1973). Figure 4.14a represents the British Standard of the Collison nebuliser where the spray bottle was originally a 'Kilner' jar. In this image a baffle is used instead of an internal wall for the spray of larger droplets to hit. The only essential difference in design from Figure 4.14a and that used in experiments (Figure 4.14b) is the shape and volume of the spray bottle.

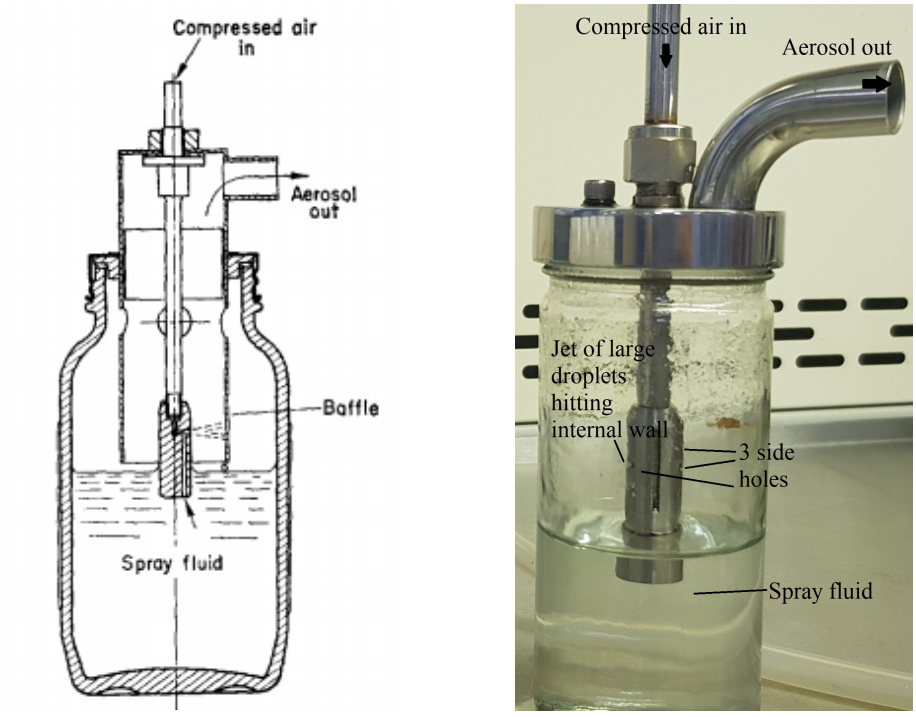

(a) Bristish standard specification of the Collison nebuliser.

(b) Collison 3-jet nebuliser used in experiments.

Figure 4.14: Collison nebuliser.

4.5.5 Measurements of droplet size distribution

The size distribution of the droplets within the experimental apparatus was measured using a laser diffraction based particle sizer, Spraytec (Malvern, UK). Aerosolised droplets passed through the laser beam generated by a 632.8 nm, 5 mW helium-neon laser. When droplets pass through the laser they scattered the light; smaller droplets scatter the light at larger angles than the bigger droplets. Spraytec measures the scattered light by using a series of photodetectors placed at different angles which is known as the diffraction pattern. The instruments software uses this diffraction pattern to calculate the droplet sizes. Spraytec is capable of measuring droplets in the range of 0.1 µm–2000 µm. During this study all measurements were performed using the 300 mm lens on the rapid setting set to record for 10 seconds.

4.5.6 Bioaerosol sampling

Bioaerosol sampling was conducted in both the controlled flow laboratory experiments using the BACA and the cross-sectional hospital study (as described in Chapter 6). During the controlled flow experiments air was drawn through an Andersen 6-Stage Impactor (Anderson Inc.) at 28.3 L min^{-1}. The Andersen impactor contained TSA agar plates at either stages 5 and 6 or at each stage. Once sampled all agar plates were incubated at 37 °C for at least 12 hours for *P. aeruginosa* and 3 days for *M. abscessus*, or until colonies formed. The number of colonies on each plate was counted using the Gallenkamp colony counter, these were then corrected using the positive-hole correction tables (Macher, 1989). Description of the Andersen Impactor, how it works, and the need for positive hole correction is described in section 2.1.1.1.

4.5.7 Overview of experimental scenarios

4.5.7.1 Nebuliser droplet size distribution

In order to determine the initial droplet size distributions produced by the Collison 3-jet nebuliser and what happens at short distances from the aerosol generation droplets were first sized under a microscope. To do this the fluid in the nebuliser was dyed with 500 µl of black food colouring. The nebuliser flow meter and pump were set up in a microbiological class II cabinet (Figure 4.15). The cabinet used a controlled air flow to protect the user from what was inside; when the bacteria was

sprayed inside the cabinet the airflow prevents it from exiting. Inside the cabinet the nebuliser was turned on, microscope slides were placed in front of the nebuliser individually at distances of 0 mm, 50 mm and 100 mm. At each distance the bacteria suspensions were sprayed onto three microscope slides. Microscope slides were covered until reaching the desired position, uncovered for 10 seconds in which they moved from side to side and then covered again before removing and placing in a slide box. Pictures of the dyed droplets on the slides were taken on a Axiolab microscope at a magnification of $\times 50$. Sizing of the droplets was done through image analysis using MATLAB (vR2019b).

In addition, droplet size distributions of the combinations of bacteria and suspension used in the BACA experiments were measured at 0 mm, 50 mm and 100 mm. The Spraytec transmitter and receiver were placed 300 mm apart and the outlet of the Collison 3-jet nebuliser was placed in the centre at 150 mm, Figure 4.16. The experiments were conducted in the class II aerobiological chamber, and the nebuliser was operated remotely from outside the chamber for safety. All experiments were performed for 10 seconds in triplicate and droplet size distributions were measured by Spraytec using the methodology described in section 4.5.5.

Figure 4.15: Class II microbiology cabinet.

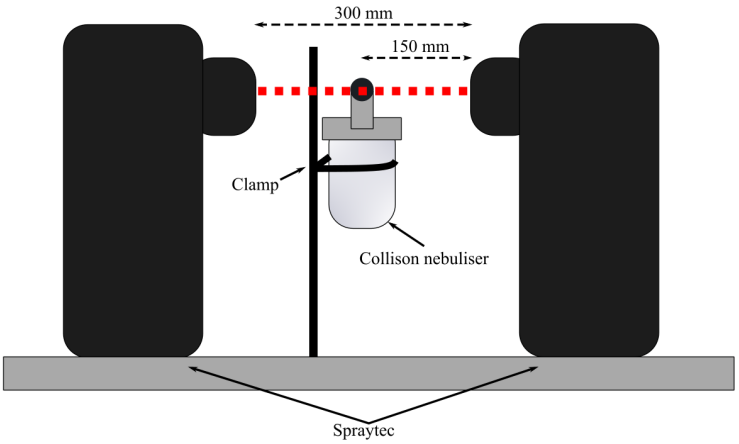

Figure 4.16: Schematic of the apparatus used in measuring short range bioaerosol distributions.

Sensitivity analysis The image analysis toolbox on MATLAB (vR2019b) was used to detect the circles on the microscope images. The original microscope images were not clear so the images was blurred using the Gaussian blur method. Removing background noise and allowing the circle detector to find the boundaries at higher levels of sensitivity.

A sensitivity analysis was performed to determine the appropriate sensitivity and edge threshold levels in the circle detection tool on MATLAB. The sensitivity level is a value between 0 and 1 with 1 being the highest level of sensitivity. Edge threshold controls how high the gradient on the pixel edges must be before it is considered a pixel edge. A value close to 1 will have strong edges whereas a value closer to 0 will have weaker edges. The analysis was performed on the images of the aerosols produced by *P. aeruginosa* Manchester strain in 1/4 ringers solution at 0 mm, 50 mm and 100 mm. After an initial analysis by eye a sensitivity level of 0.87 and edge threshold of 0.09 was determined to be a good fit.

Analysis was based on how close the model predicted the number of droplets on the image with a preference of under prediction rather than over prediction. The model did not have to pick up all droplets and it would be deemed unfit if it was identifying a large amounts of droplets that were not there. Initially the edge threshold was changed between 0.8 to 0.95 in increments of 0.1. In the second round of analysis the sensitivity was set to at 0.87 and 0.88 while changing the edge threshold from 0.05 to 0.15 in increments of 0.01. The values of 0.87 and 0.88 were chosen as these were ranked the highest over all lengths.

Ranking was in ascending order of absolute value of number of droplets counted by eye on the image minus the number of droplets the model predicted. The intersection

between the top ranked variables at each length was calculated and these were checked that they were not over predicting the number of droplets by more than 10 droplets. After the second round of analysis the intersection produced three separate cases which had a rank of 7 or below at each length. Overall the sensitivity of 0.88 and edge threshold of 0.09 performed the best over all three lengths and this choice of variable values produced the smallest value of over predictions. Therefore, these values where chosen for the image analysis on all future runs of the model. An example of the image used in the analysis are given in Figure 4.17.

If an image was not clear the model could over predict droplets in a way that almost filled the image with predicted droplets. To exclude such calculations from any data analysis, if the model counted more that 100 droplets this image was automatically removed from the droplet size distribution due to unreliability. However, there were some cases where there was a large over prediction of droplets but this count was still below 100 and such images were caught by eye and removed from any data analysis.

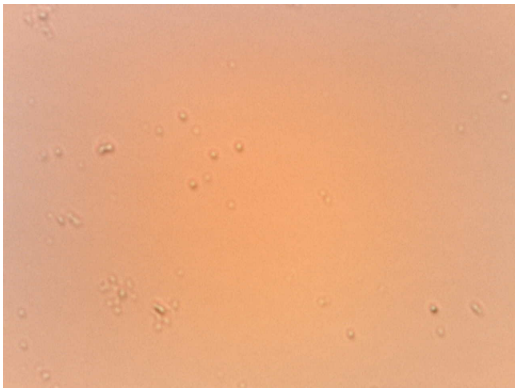

(a) Original image.

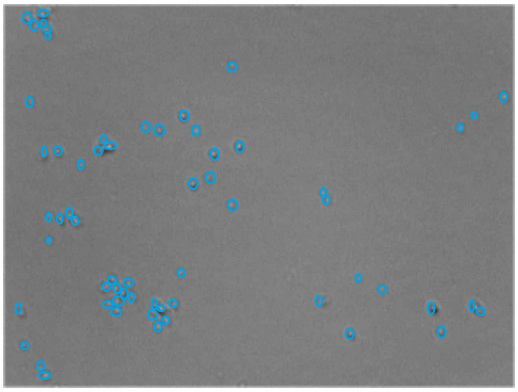

(b) Gray scale image with number of droplets drawn on by eye as blue ovals.

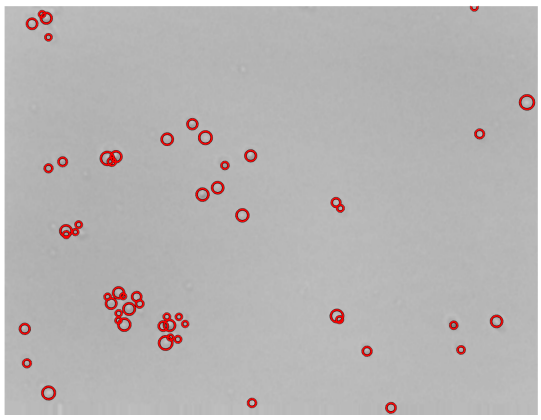

(c) Image after analysis with prediction of droplet boundaries given by red circles.

Figure 4.17: Example of the microscope image analysis of droplets produced by *P. aeruginosa* Manchester strain at 0 mm.

4.5.7.2 Effect of bacterial strain

In order to assess the influence of bacterial strain on survival, aerosols were generated using 100 ml of ¼ strength ringers containing 10^5 CFU ml^{-1} or 10^4 CFU ml^{-1} of each strain of *P. aeruginosa* and *M. abscessus* respectively. Aerosols were released into the BACA with samples taken at distances of 1 m–4 m. Agar plates were only used at stages 5 and 6 of the Anderson sampler for this series of experiments, as done by Clifton et al. (2008). This resulted in the capture of particle sizes of 0.65 µm–1.1 µm and 1.1 µm–2.1 µm respectively. Sampling time using the Andersen Impactor was 2 minutes. The environmental, Manchester, and Newcastle strains of *P. aeruginosa* were used to compare environmental vs epidemic strains and mucoid vs non-mucoid. Only the smooth strain for *M. abscessus* was used. Droplet size distributions were measured by Spraytec using the methodology described in section 4.5.5.

4.5.7.3 Effect of suspension fluid

To assess the influence of suspension, aerosols were generated into the BACA and sampled at distances of 1 m and 2 m. These lengths were selected as they had the highest survival of bacteria and it was possible to determine what happens over a unit distance. Due to the higher CFU counts on 1 m and 2 m the sampling time with the Andersen Impactor was reduced to 1 minute. Two fluid suspensions, ¼ ringers and 1 % FBS, and all stages of the Andersen Impactor were used in these experiments. 1 ml of bacterial culture was added in 100 ml of the suspensions resulting in 10^5 CFU ml^{-1} or 10^4 CFU ml^{-1} of *P. aeruginosa* and *M. abscessus* respectively in the nebuliser vessel. The unique patient *P. aeruginosa* CF strains were used to compare the difference between mucoid and non-mucoid phenotypes. Both rough and smooth strains of *M. abscessus* were used. Droplet size distributions were measured by Spraytec using the methodology described in section 4.5.5.

4.6 Summary

The methodologies presented in this chapter described how the experiments in Chapter 5 were carried out along with some of the microbiological methodologies associated with the cross-sectional study in Chapter 6. In particular this chapter detailed the materials used in the laboratory experiments; how to carry out growth curve experiments, which allowed for better comparison between bacteria and a more accurate prediction of bacterial concentrations; characterisation of the suspension fluids,

this determined effects of surface tensions and volume of fluid dispensed through nebulisation; and aerosol characterisation of bioaerosols which built on the work of (Clifton et al., 2008). Furthermore, through building on the work by (Clifton et al., 2008) and utilising additional methods to detect droplet size distribution allowed for a comparison between size segregated culturable bacteria and the overall droplet size distribution to determine the appropriateness of these methodologies.

Chapter 5

Bioaerosol characterisation experiments

This chapter examines the survival and droplet size distributions of *P. aeruginosa* and *M. abscessus* in air under experimental conditions following the methodologies described in Chapter 4. Given the importance of droplet size distributions in the transmission of airborne particles, this series of experiments sought to find if there was any relationship between suspension fluid, bacterial strain, and droplet size distributions. First, initial investigations into the effect of suspension fluid were considered to establish if rheological properties had an influence of droplet size distributions and culturable droplet size. Droplet size distributions were further investigated at short ranges ($\leq$100 mm) and were compared to distributions of evaporated droplets. Finally, survival and droplet size distributions of bioaerosols were measured in an experimental environment similar to that of Clifton et al. (2008) to determine the behaviour of both microorganisms suspended in air over time.

5.1 Bacteria and suspension fluid characterisation

Prior to the aerosolisation experiments a series of measurements were carried out to characterize the growth of bacteria and the fluid properties of the suspensions. These experiments were completed in order to have good baseline data to be able to accurately analyse the aerosolisation experiments.

5.1.1 Growth curves

Understanding the behaviour of each strain through growth curves gave better insight into if all the bacterial strains behaved in similar ways. Furthermore, the growth curves and bacteria doubling time allowed for prediction of incubation times for the bacterial cultures used in experiments to ensure they were in the exponential or stationary phase.

Growth curve measurements were conducted for five strains of *P. aeruginosa* and are displayed in Figure 5.1 following the methodology described in section 4.3. These data suggested that by 12 hours all had entered the stationary phase, depiction of a simplified representation of the stationary phase is given in Figure 4.7. The patient mucoid strain grew at a faster rate and entered the death phase before other strains, estimated to be around 24 hours.

The time it took for bacterial cells in the nutrient broth to double (divide) was

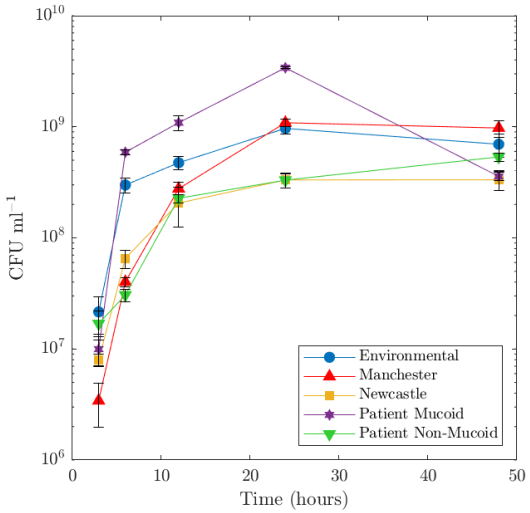

Figure 5.1: Growth curve for all *P. aeruginosa* strains in 10 ml of nutrient broth.

determined by measuring turbidity of bacterial cultures using a spectrophotometer; the wavelength chosen for these experiments was 600 nm. Increase in number of cells (N) over time (t) was proportional to the number of cells:

$$\frac{dN}{dt} = \mu N, \tag{5.1}$$

where the proportionality factor μ is the growth rate. Solving this differential equation gives the growth equation in its well known form:

$$\ln N = \mu t + \ln N_0 \tag{5.2}$$

$$\implies N = N_0 e^{\mu t}. \tag{5.3}$$

Two further important assumptions were: first, the time passed was exactly the doubling time, $t = t_d$. Then within this time the initial number of cells N_0 has become $2N_0$ such that (5.2) yields:

$$\ln \frac{2N_0}{N_0} = \mu t_d, \tag{5.4}$$

and hence,

$$\mu = \frac{\ln 2}{t_d}. \tag{5.5}$$

The second assumption considered that the turbidity or the optical density (OD) was proportional to the cell density. Utilising that relationship and choosing two OD values, OD_1 and OD_2, and their corresponding time points t_1 and t_2 (as shown in the Figure 5.2a). The relationship in (5.2) can be expressed as:

$$\ln OD_2 - \ln OD_1 = \mu(t_2 - t_1) \tag{5.6}$$

$$\implies \mu = \frac{\ln OD_2 - \ln OD_1}{t_2 - t_1}. \tag{5.7}$$

The equation (5.7) allowed data from optical density readings to determine the growth rate μ and hence the doubling time. Growth rates and doubling times for the bacteria used in the laboratory experiments are summarised in Table 5.1. These data were determined from Figures 5.2 and 5.3 for *P. aeruginosa* and *M. abscessus* respectively. Comparing the data from the *P. aeruginosa* growth curves (Figure 5.1) and the OD_{600} growth curves (Figure 5.2), by hour 10 the environmental, patient mucoid and patient non-mucoid had left the exponential phase. Hence, these points were excluded from the line of best fit and the doubling time calculations.

Due to lab opening hours is was not possible to collect data for a full growth curve on *M. abscessus*. Thus, all OD_{600} data points were joined to create a growth curve from

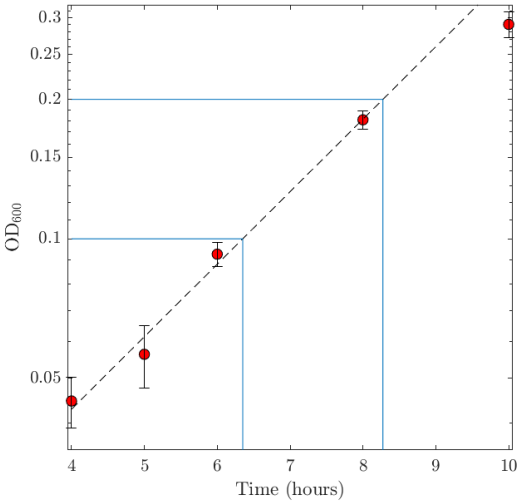

(a) Environmental

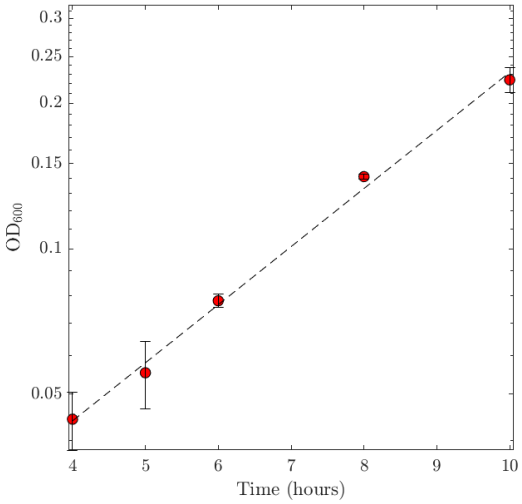

(b) Manchester

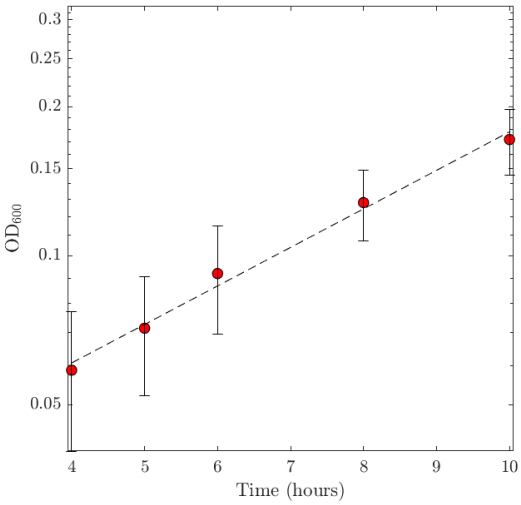

(c) Newcastle

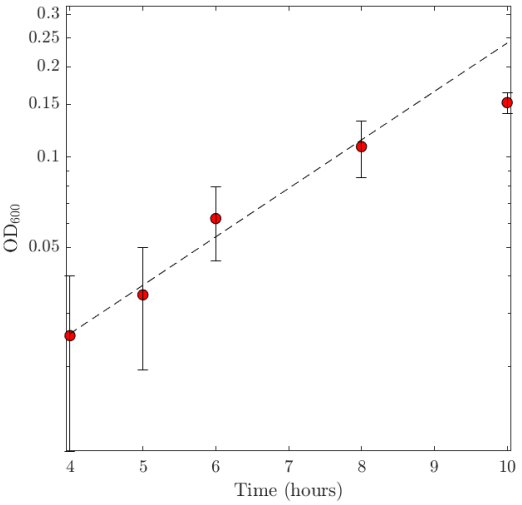

(d) Patient mucoid

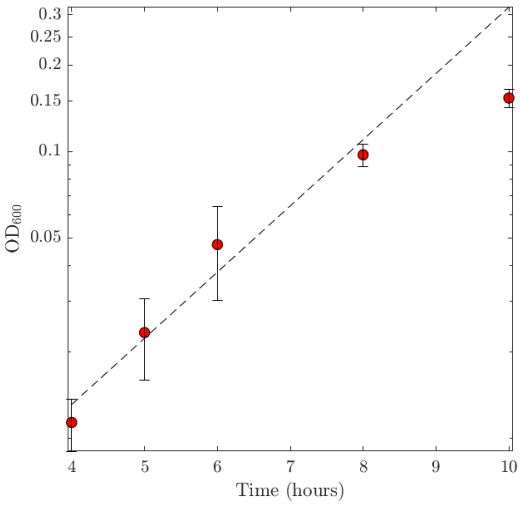

(e) Patient non-mucoid

Figure 5.2: Optical density-incubation time plot for the growth of multiple strains of *P. aeruginosa* at 37 °C, 110 rpm in 10 ml of nutrient liquid broth.

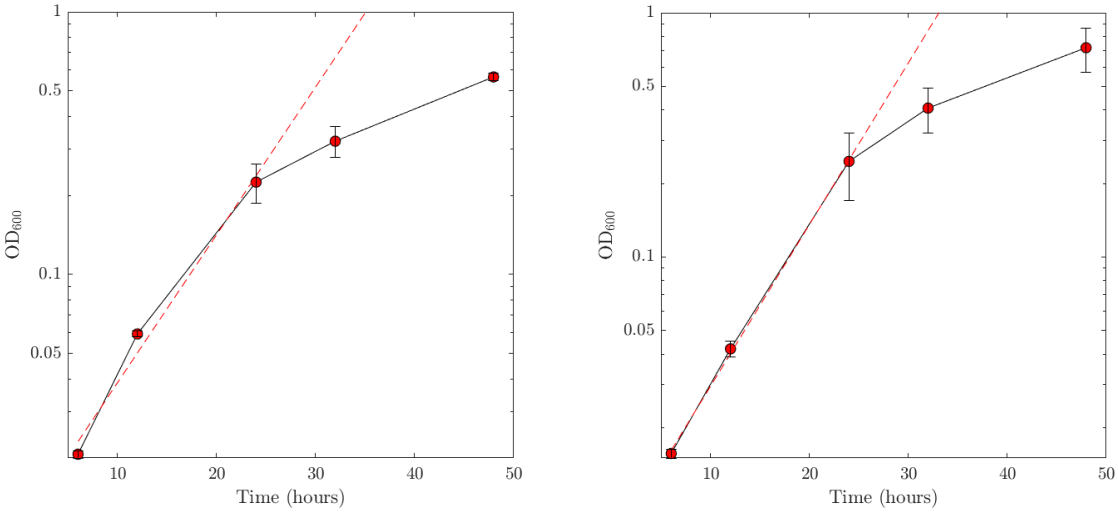

(a) Smooth (b) Rough

Figure 5.3: Optical density-incubation time plot for the growth of both morphologies of *M. abscessus* at 37 °C, 110 rpm in 10 ml of nutrient liquid broth.

Table 5.1: Growth rates and doubling time (hours) of bacteria from optical density data.

Strain	**Growth Rate μ**	**Doubling time t_d**
P. aeruginosa		
Environmental	0.36	1.92
Manchester	0.28	2.50
Newcastle	0.18	3.87
Patient mucoid	0.37	1.86
Patient non-mucoid	0.53	1.30
M. abscessus		
Smooth	0.13	5.35
Rough	0.15	4.55

the optical density data, as seen in Figure 5.3. Inspection of these values suggested the first three data points formed the exponential section of the *M. abscessus* growth curves. Data were collected for a subset of the *M. abscessus* CFU growth curves at 6, 12, and 24 hours. The values were compared to the exponential growth rate calculated from Figure 5.3 and displayed in Figure 5.4. As expected, much like the predicted growth rates from Table 5.1 the *M. abscessus* rough strain grew at a faster rate than the smooth strain and the predicted growth rates loosely fit the measured values.

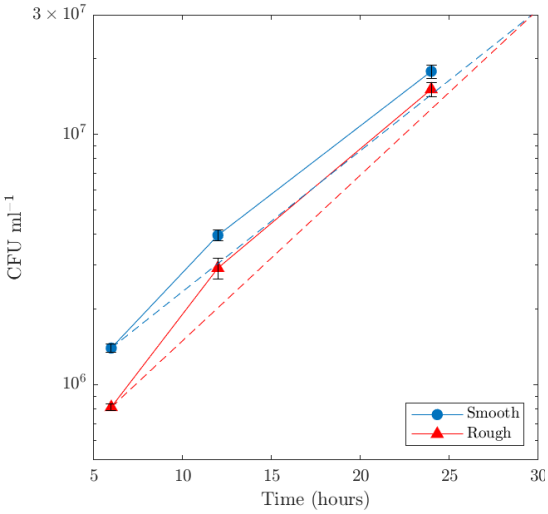

Figure 5.4: Subset of the growth curve for *M. abscessus* strains in 10 ml of nutrient broth, compared with exponential growth rate from OD_{600} data.

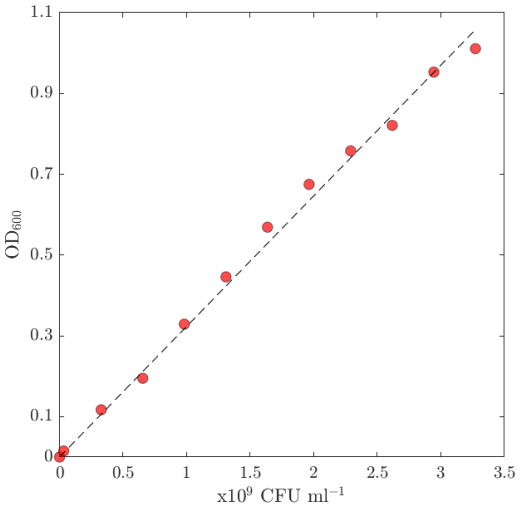

(a) *P. aeruginosa* environmental

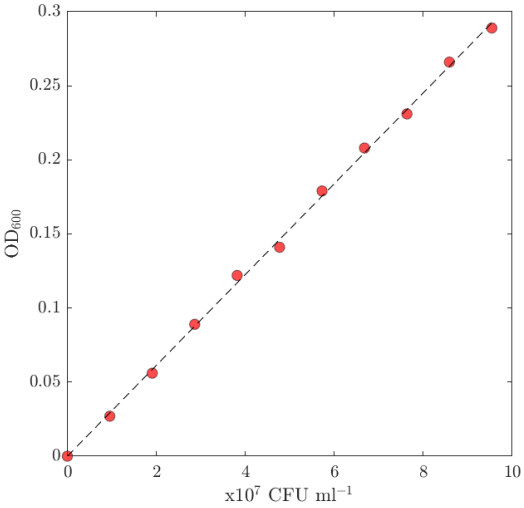

(b) *M. abscessus* smooth.

Figure 5.5: Examples of optical density calibration curves, optical density vs CFU ml^{-1}.

Optical density measurements were made at a series of dilutions to determine the relationship between OD and CFU ml^{-1} creating an optical density calibration curve. This allowed CFU ml^{-1} concentrations to be determine for each bacterial strain from OD values. Figure 5.5 gives an example of these plots for *P. aeruginosa* environmental and *M. abscessus* smooth. The line of best fit passes through (0,0) as 0 CFU ml^{-1} in the suspension gives a value of 0 OD. Hence, all lines of best fit are of the form $y = mx$. Gradients of the lines of best fit for all bacteria used in the laboratory experiments to determine CFU ml^{-1} from OD values are given in Table 5.2.

Table 5.2: Gradient (m) from the line of best fit ($y = mx$) for optical density calibration curves.

Strain	Gradient (m)
P. aeruginosa	
Environmental	0.323
Manchester	1.033
Newcastle	1.113
Patient mucoid	0.215
Patient non-mucoid	0.324
M. abscessus	
Smooth	0.031
Rough	0.034

5.1.2 Surface tension measurements

Surface tension has been theoretically shown to change droplet size distributions (Vasudevan and Lange, 2007). Considering the hydrophobicity of both *P. aeruginosa* (Van Loosdrecht et al., 1987) and *M. abscessus* (Cortes et al., 2010) it was hypothesised these bacteria had the potential to change the surface tension of the suspension fluid. Due to SARS-CoV-2 and lab closures not all measurements could be completed and it is acknowledged that further investigation is needed.

Surface tensions measurements taken of suspensions and bacteria in ¼ ringers solutions at different concentrations are outlined in Table 5.3. The results in the table show that all measured surface tensions were very similar and that the suspension fluids tested and the addition of bacteria did not influence the surface tension significantly. The largest difference from ¼ ringers alone was a 3.6 % difference from the non-mucoid strain. However, this could attributed to human error in measurement accuracy. In addition, the increase in concentration, to higher than used in the aerosolisation experiments, did not alter the surface tension more than lower concentrations of bacteria. With the small differences measured, key non-dimensional number such as the Weber and Ohnesorge number did not change by any significant value and it was assumed that the size distributions of droplets were not affected by a change in surface tension caused by *P. aeruginosa*.

Table 5.3: Surface tension measurements of suspensions and bacteria in 1/4 ringers solution.

Fluid	**Surface Tension ($\mathbf{N\,m^{-1}}$) (SD)**
Suspensions	
Ringers	0.0524 (0.0004)
Ringers and nutrient broth	0.0518 (0.0003)
Ringers, nutrient broth and black dye	0.0542 (0.0003)
Bacteria in 1/4 ringers ringers	
P. aeruginosa environmental strain 10^6 CFUml^{-1}	0.0539 (0.0016)
P. aeruginosa environmental strain 10^7 CFUml^{-1}	0.0536 (0.0013)
P. aeruginosa environmental strain 10^9 CFUml^{-1}	0.0520 (0.003)
P. aeruginosa patient mucoid strain 10^6 CFUml^{-1}	0.0536 (0.0006)
P. aeruginosa patient non-mucoid strain 10^6 CFUml^{-1}	0.0543 (0.001)

SD is the standard deviation

5.1.3 Aerosol generation of suspension fluids

Additional knowledge surrounding the generation rates of the suspension fluids allowed accurate comparisons between survival rates of the bacteria in the different suspensions.

Mass loss via aerosol generation from the Collison 3-jet nebuliser for the duration of 1 hour is presented in Table 5.4 and graphically in Figure 5.6. An initial volume of 100 ml was placed into the vessel and the mass of the fluid over 60 minutes was measured using a mass balance while the nebuliser was operated. Plotted lines of best fit, Figure 5.6, gave a strong negative relationship with both the 1/4 ringers and 1 % FBS solution, with the 1/4 ringers solution losing a smaller volume of liquid over the time period. However, note that the axis only spans between 94 g–100 g so this difference is small, where 1/4 ringers loses approximately 0.054 g per minute and 1 % FBS looses 0.081 g per minute under these conditions. In conclusion, it was assumed that the suspension fluid did not have a dramatic affect on the amount of liquid dispensed from the nebuliser as the 1 % FBS loss is slightly higher, but they

Table 5.4: Average mass loss from the Collison 3-jet nebuliser over the period of 1 hour for each suspension fluid.

	Mass lost (g)		
Suspension	**15 min**	**30 min**	**60 min**
1/4 Ringers	-0.840	-1.671	-3.270
1 % FBS	-1.027	-2.410	-4.777

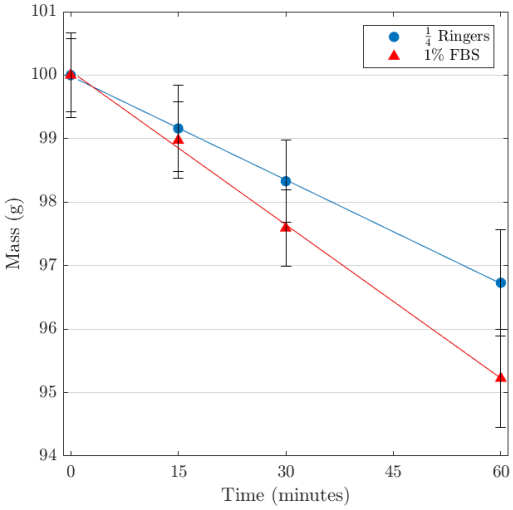

Figure 5.6: Mass of the fluid in the Collison 3-jet nebuliser over the period of 1 hour for each suspension fluid.

are a similar order of magnitude. Therefore, any difference in number of culturable colonies was due to survival in the suspension fluid.

All samples taken with the Andersen Impactor during the aerosolisation experiments in the BACA (section 5.3) were 1 or 2 minutes. Hypothetically, in this time if no fluid were to evaporate 0.054 ml of 1/4 ringers and 0.081 ml of 1 % FBS aerosolised droplets would pass through the sampler in 1 minute and for 2 minutes these values are doubled. After inoculation, the aerosolised suspension containing *P. aeruginosa* had 10^5 CFU ml^{-1} bacteria present and 10^4 CFU ml^{-1} bacteria present for *M. abscessus*. Assuming the bacteria were homogeneously mixed during each sample, the order of 10^3 *P. aeruginosa* were released during a 1 minute sample and the order of 10^4 in a two minute sample. For *M. abscessus*, the order of 10^2 were released in a 1 minute sample with the order of 10^3 was released during a 2 minute sample. These predicted numbers of released bacteria are compared to the raw counts of colonies on the agar places from the Andersen Impactor samples in sections 5.3.1 and 5.3.2.

5.1.4 Evaporation of aerosol particles

After aerosolisation of the suspension fluid the resulting droplets will undergo evaporation. Maximum evaporation will occur when the droplet loses all its water and retains all its nonvolatile solutes (e.g. proteins, surfactants, salts and the bacteria). The resulting evaporated droplet has an equilibrium droplet diameter, d_{eq}, which is a fraction of the initial droplet diameter, d_0. When a droplet loses all its water, the mass of the nonvolatile species in the dried droplet must be the same as in the aerosolised droplet:

$$\frac{\pi}{6} d_{eq}^3 \rho_{nonvolatile} = \frac{\pi}{6} d_0^3 C_{nonvolatile}. \tag{5.8}$$

where $\rho_{nonvolatile}$ is the density of the suspension containing its non-volatile solutes and $C_{nonvolitie}$ is the mass concetration of each of the components, these both have the same units $\mathrm{g\,L^{-1}}$. By rearrangement of (5.8), the equilibrium diameter of the droplet is related to the initial diameter by the following equation:

$$d_{eq} = \left(\frac{C_{nonvolatile}}{\rho_{nonvolatile}} \right)^{1/3} d_0. \tag{5.9}$$

An estimate for $\rho_{nonvolatile}$ is $\rho_{nacl} = 2200\,\mathrm{g\,L^{-1}}$, the density of sodium chloride. Nicas et al. (2005) used this estimate when excluding proteins and only considering the ions in a respiratory fluid. The 1/4 ringers suspension fluid components are summarised in Table 5.5. Following the methodology of (Nicas et al., 2005) the mass concentration of each of the components are totalled to give $C_{nonvolatile} = 2.525\,\mathrm{g\,L^{-1}}$. Now the equilibrium diameter can be calculated as $d_{eq} = 0.10 \times d_0$; hence, the equilibrium diameter is one tenth of its initial diameter. All major components in the composition of FBS (Gstraunthaler and Lindl, 2013) are small concentrations ($\mathrm{mg\,ml^{-1}}$ or less), which are further diluted as it is a 1 % solution. Therefore, these slight changes in composition will not have a great effect on the equilibrium diameter and it was assumed that the equilibrium diameter was the same for both the 1/4 ringers and 1 % FBS solutions. In reality some water will be retained in the droplet when at equilibrium diameter. Following the same method described by Nicas et al. (2005) the adjustment to account for some water being retained would be $d_{eq} = (1.19) \times 0.1 d_0 = 0.12 d_0$, at 50 % relative humidity which were the conditions in the class II microbiological chamber where the aeosol experiments were conducted. Under the same conditions Nicas et al. (2005) predicted the equilibrium diameters for respiratory fluids with and without proteins over a standard indoor air relative humidity range, these predictions and the equilibrium diameter prediction for 1/4 ringers solution are displayed in Figure 5.7.

Table 5.5: Components of Oxide 1/4 ringers solution as per the manufactures product literature.

Species	**Concentration g L^{-1}**
Sodium chloride	2.25
Potassium chloride	0.105
Calcium chloride $6H_2O$	0.12
Sodium bicarbonate	0.05

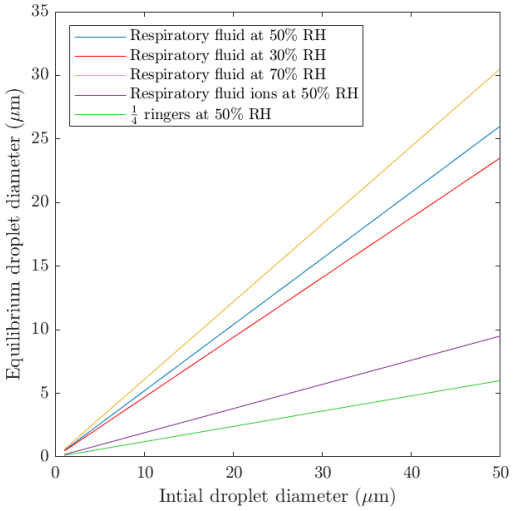

Figure 5.7: Initial droplet diameter vs equilibrium droplet diameter for fluids of varying components as described by Nicas et al. (2005).

5.2 Nebuliser aerosol size characterisation

The following experiments were completed to determine the initial droplet size distributions produced by the Collison 3-jet nebuliser. The first measured dried droplets aerosolised onto surfaces and the other measured the droplet size distribution in the air with Spraytec. These experiments were important for analysing the size distributions in the aerosolisation experiments using the BACA.

5.2.1 Bioaerosol droplet size distributions on glass slides

Droplets containing black dye were sprayed onto glass microscope slides to provide a preliminary data set for evaluating the droplet size distributions of the Collison nebuliser following the methodology described in section 4.5.7.1. It is important to note that these droplet size distributions were for dried droplets on microscope

slides as the during the time from aerosolisation to measurement the droplets had fully evaporated.

Droplet diameters were calculated by the method described in section 4.5.7.1. Previous studies which determined droplet sizes in a similar manner (Duguid, 1946; Loudon and Roberts, 1967b), estimated the airborne particle diameter in several ways. Duguid (1946) reduced the size of 'large' droplets by half as these droplets seemed flattened. In another method for detecting 'small' droplets the diameters were increased four fold to account for evaporation, no reasoning was provided for either of these calculations. Loudon and Roberts (1967b) referenced a previous paper (Loudon and Roberts, 1967a) and used the regression equation to adjust the size of the droplets. However, this was only applied to droplets larger than 10 µm. This experiment did not aim to determine the un-evaporated volume of the droplets so any increase in diameter was unnecessary. Additionally, no reasoning was given by Duguid (1946) for the droplet size reduction and both studies did not reduce the size of droplet in the size range of data measured in this experiment; therefore, no adjustment to the droplet size was made.

Figures 5.8–5.10 and Figures B.1–B.3 in the appendix display number fraction histograms of droplet size distributions measured on the microscope slides. These figures show a bimodal pattern. The first mode has a diameter in the range 0.8 µm–1 µm. The second mode of the droplet size distribution was less distinct and has a diameter around 1.5 µm. All distributions showed a similar range with the vast majority of droplets between 0.8 µm–2 µm which was expected for aerosolised droplets with a Collison nebuliser. Additionally, the distributions given by each of the suspensions, ¼ ringers and 1 % FBS, do not show stark differences and for droplets in this size range it was assumed there was no difference to the distributions made by the suspensions. The majority of droplets sizes given by these data would have been large enough to contain a *P. aeruginosa* or *M. abscessus* microorganism, with the exception of those in the first size bin. The maximum droplet size found by this method was 2.22 µm, this would have allowed a maximum number of two bacteria to fit in these droplets. Yet, for the majority of the droplets is was expected there was only one bacteria present. Therefore, it was assumed that each CFU in the survival experiments was from one droplet.

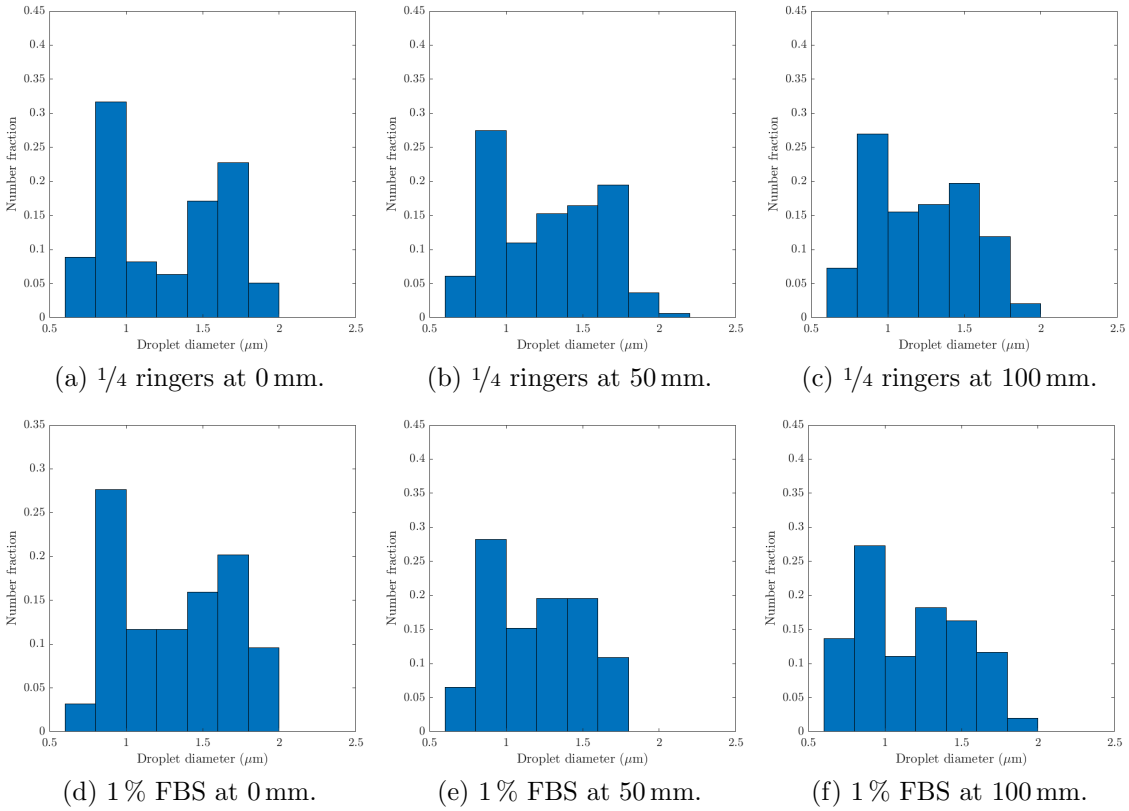

(a) 1/4 ringers at 0 mm. (b) 1/4 ringers at 50 mm. (c) 1/4 ringers at 100 mm.

(d) 1 % FBS at 0 mm. (e) 1 % FBS at 50 mm. (f) 1 % FBS at 100 mm.

Figure 5.8: Number fraction droplet size distributions from aerosolising *P. aeruginosa* patient mucoid strain in different suspensions onto microscope slides in the class II microbiology cabinet.

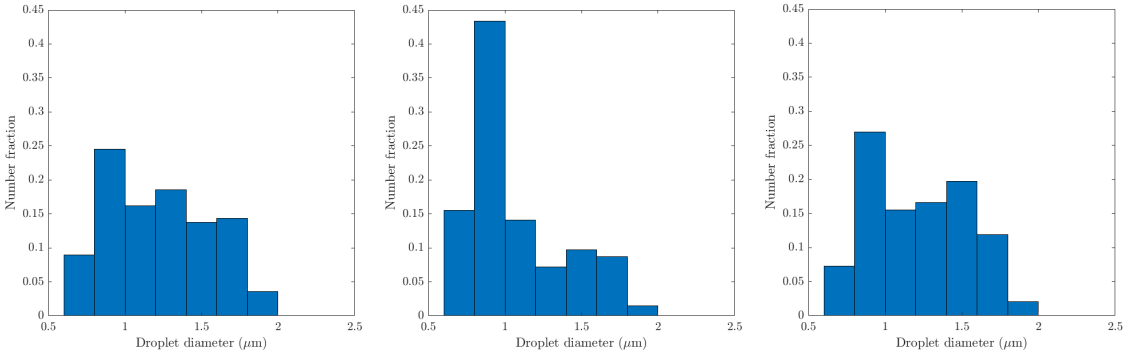

(a) 1/4 ringers at 0 mm. (b) 1/4 ringers at 50 mm. (c) 1/4 ringers at 100 mm.

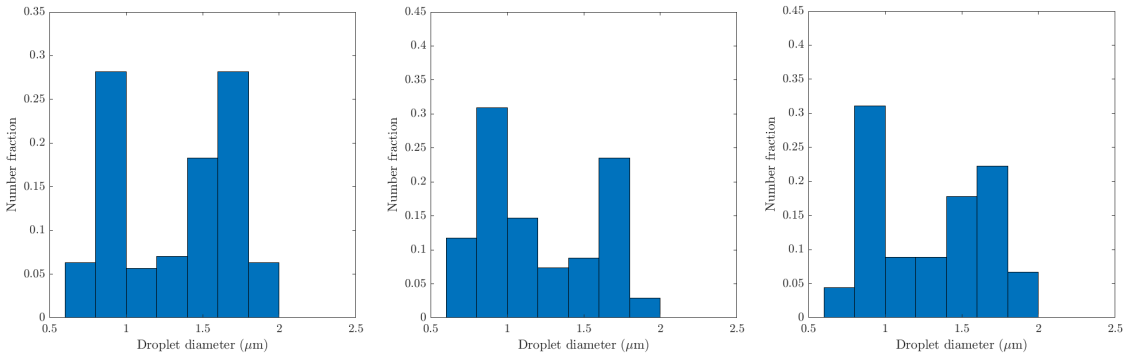

(d) 1 % FBS at 0 mm. (e) 1 % FBS at 50 mm. (f) 1 % FBS at 100 mm.

Figure 5.9: Number fraction droplet size distributions from aerosolising *P. aeruginosa* patient non-mucoid strain in different suspensions onto microscope slides in the class II microbiology cabinet.

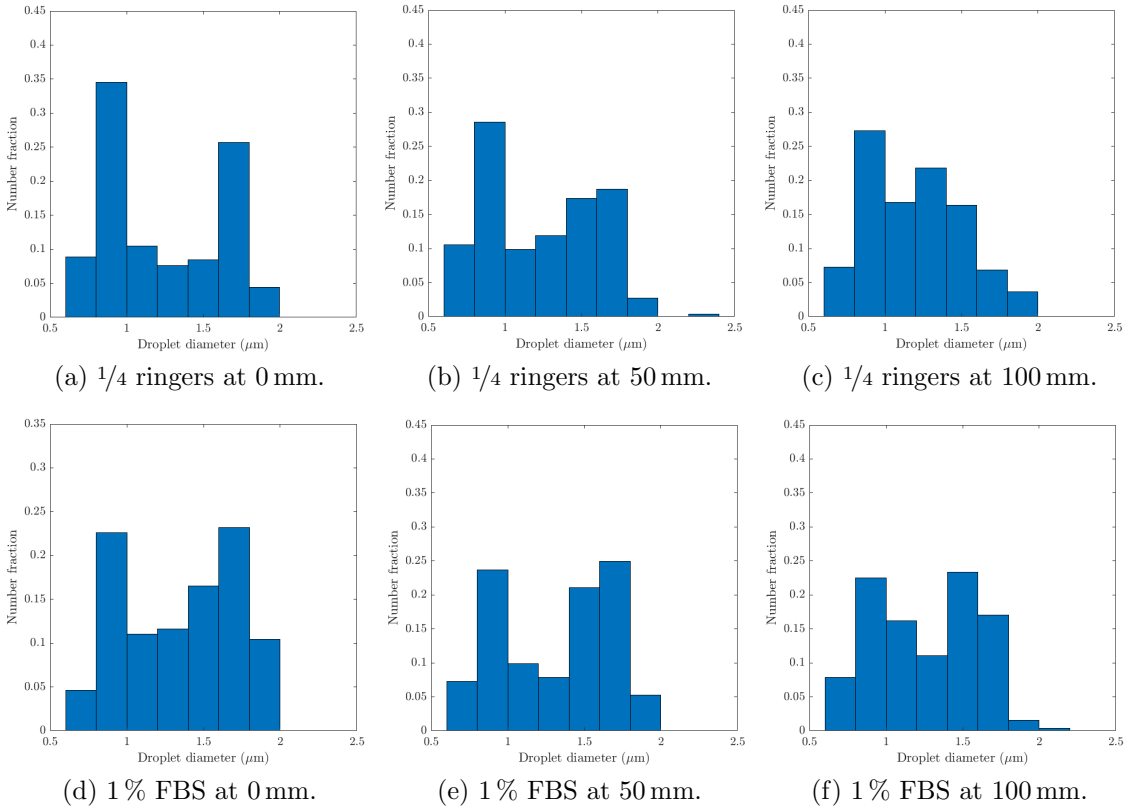

(a) 1/4 ringers at 0 mm. (b) 1/4 ringers at 50 mm. (c) 1/4 ringers at 100 mm.

(d) 1 % FBS at 0 mm. (e) 1 % FBS at 50 mm. (f) 1 % FBS at 100 mm.

Figure 5.10: Number fraction droplet size distributions from aerosolising *M. abscessus* smooth strain in different suspensions onto microscope slides in the class II microbiology cabinet.

Time taken for the droplet to reach 50 mm and 100 mm was approximated through a simple droplet momentum equation (7.9). Initial droplet diameter was approximated as the mean droplet diameter, $d_0 = 1.27\,\mu\text{m}$ and the flow rate from the nebuliser was calculated to be $\mathbf{u_d} = 1.2\,\text{m}\,\text{s}^{-1}$. Ambient air in the class II microbiology cabinet where the experiments took place had an average speed of $0.39\,\text{m}\,\text{s}^{-1}$, measured with a Airflow LCA501 anemometer (BSRIA), in the same direction as the droplets were sprayed (Figure 4.15). Figure 5.11 displays the reduction in speed for the droplet over time. The model estimates the time taken for the droplet to lose all initial momentum and move with the airflow within the microbiology cabinet was 0.04 s. Therefore, for simplicity droplet speed was assumed to be that of the ambient air and the time taken to reach 50 mm and 100 mm is 0.128 s and 0.256 s respectively.

Evaporation of a stationary droplet in air entails computing the diffusion of water vapour through the boundary layer surrounding the droplet. This diffusion is driven by the difference in partial pressure between the water vapour immediately above the droplet and that of the ambient air. Nicas et al. (2005) gives the time-dependant,

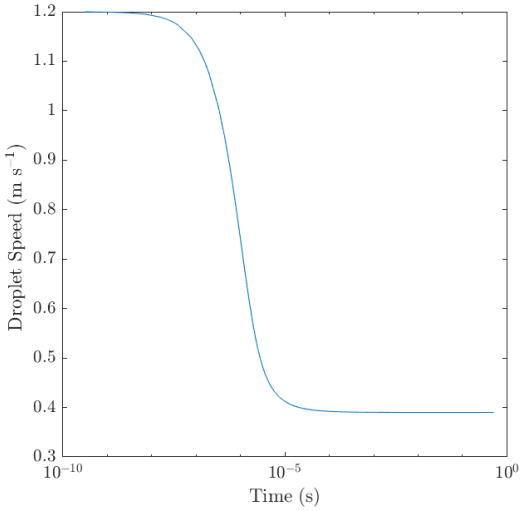

Figure 5.11: Horizontal velocity of a droplet being released into the class II microbiology cabinet from the Collison 3-jet nebuliser at $6\,\mathrm{L\,min^{-1}}$.

t, equation to determine the droplet diameter, d (m), from its initial diameter, d_0:

$$d(t) = \sqrt{d_0^2 - 8 \times v_m \times D \times \left(\frac{P_{\mathrm{sat}} - P_{\mathrm{H2O}}}{k \times T}\right) \times t} \tag{5.10}$$

where:

v_m = condensed-phase volume occupied by a single water molecule ($3 \times 10^{-29}\,\mathrm{m^3}$) ,
D = molecular diffusivity of water vapour in air ($1.8 \times 10^{-5}\,\mathrm{m^2\,s^{-1}}$),
P_{sat} = partial pressure of water vapour (Pa),
P_{H2O} = partial pressure of water vapour in ambient air (Pa),
k = Boltzmann's constant ($1.38 \times 10^{-23}\,\mathrm{J\,K^{-1}}$),
T = ambient temperature ($293\,\mathrm{K}$).

For simplicity the decrease in P_{sat} due to solutes is neglected and $P_{\mathrm{H2O}} = (\mathrm{RH}/100) \times P_{\mathrm{sat}}$. This equation is used for further analysis on droplet evaporation in section 7.1.1, but for this analysis (5.10) was rearranged to estimate the time for a particle to reach is equilibrium state ($d_{eq} = 0.12 \times d_0$) as per section 5.1.3, the equation used was:

$$t_{eq} = \frac{\epsilon}{P_{\mathrm{sat}} - P_{\mathrm{H2O}}} \left(d_0^2 - d_{eq}^2\right) \tag{5.11}$$

where ϵ is a combination of all the constants and had the value $9.35 \times 10^8\,\mathrm{kg(m^3 s)^{-1}}$. At 50 % RH the estimated time for a droplet with d_0 =1.27 µm, the mean droplet diameter, to attain d_{eq} =0.1524 µm was 0.0013 s. This demonstrates that within

a fraction of a second the droplets nebulised will have reached their equilibrium state. Therefore, this prediction meant there was evaporation expected between the measurements at 0 mm and 50 mm with those at 100 mm fully evaporated. However, since the time to reach equilibrium diameter was very short timescales human error in how 'close' 0 mm was could potentially have led to no evaporation being seen.

Box plots for the droplet size distributions are given by Figures 5.13–5.15. In all strains apart from *M. abscessus* smooth there was a reduction in the median droplet size from 0 mm to 50 mm. *P. aeruginosa* mucoid in 1 % FBS and *P. aeruginosa* non-mucoid in 1/4 ringers and 1 % FBS had a statistically significant difference in their medians at the 5 % level (Wilcoxon signed rank test $p = 0.00$, $p = 0.03$, and $p = 0.01$ respectively). One of the mucoid strains, *P. aeruginosa* Newcastle, had the largest medium droplet size and the medium droplet size from the patient mucoid strain was bigger than the patient non-mucoid strain. Mucoid phenotypes could influence droplet size distributions to produce larger droplets on average; however, further study would be needed to confirm this.

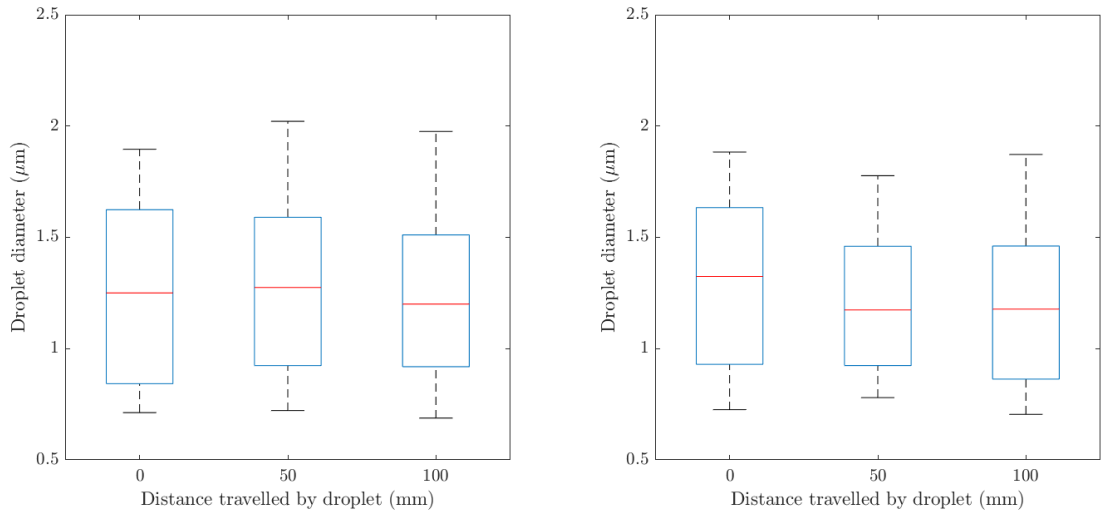

(a) 1/4 ringers.

(b) 1 % FBS.

Figure 5.12: Box plot of the droplet distribution produced by aerosolising *P. aeruginosa* patient mucoid strain in different suspensions onto microscope slides in the class II microbiology cabinet.

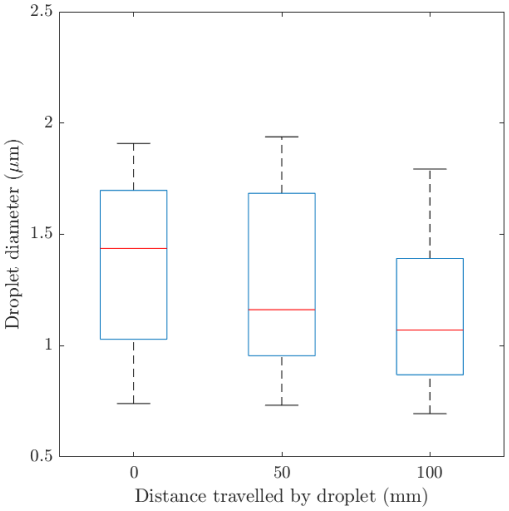

(a) *P. aeruginosa* Environmental.

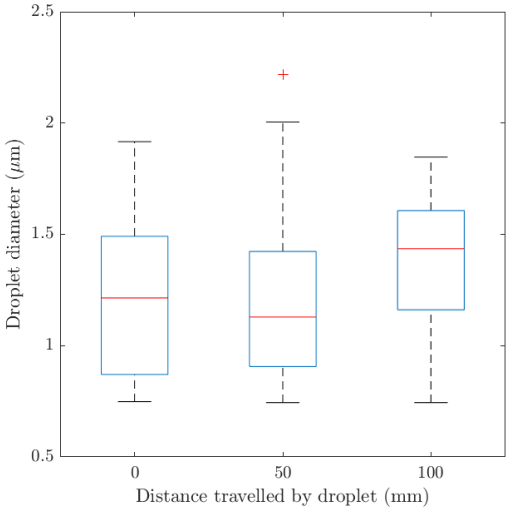

(b) *P. aeruginosa* Manchester.

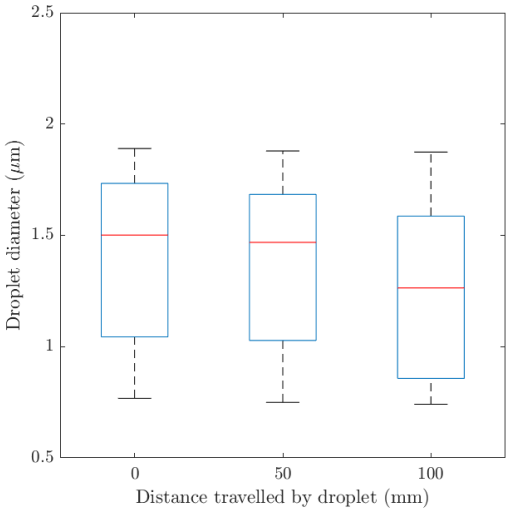

(c) *P. aeruginosa* Newcastle.

Figure 5.13: Box plot of the droplet distribution produced by aerosolising *P. aeruginosa* bacterial suspension onto microscope slides in the class II microbiology cabinet.

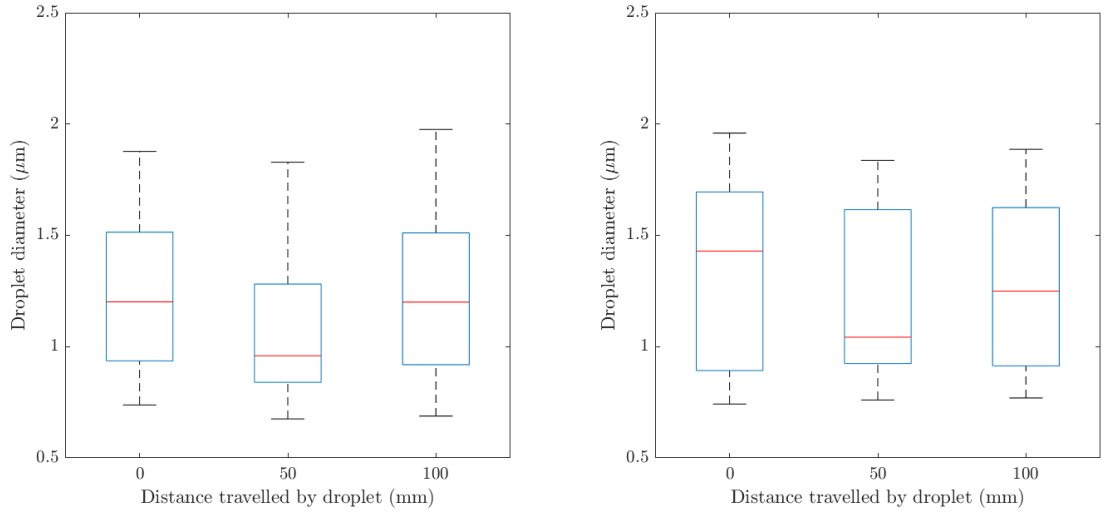

(a) 1/4 ringers. (b) 1 % FBS.

Figure 5.14: Box plot of the droplet distribution produced by aerosolising *P. aeruginosa* patient non-mucoid strain in different suspensions onto microscope slides in the class II microbiology cabinet.

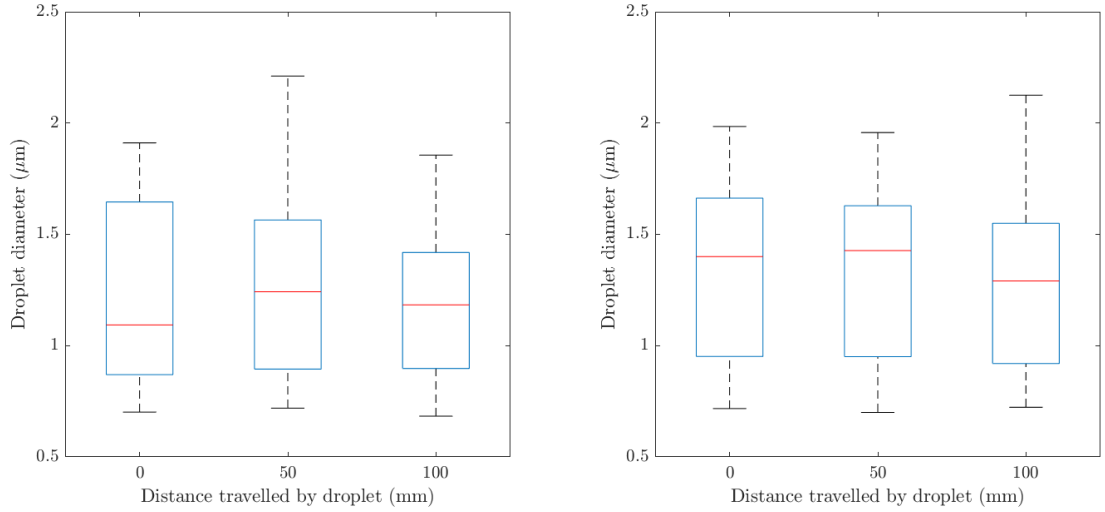

(a) 1/4 ringers. (b) 1 % FBS.

Figure 5.15: Box plot of the droplet distribution produced by aerosolising *M. abscessus* smooth strain in different suspensions onto microscope slides in the class II microbiology cabinets.

5.2.2 Spraytec measurements of short range bioaerosol distributions

Short range droplet size distributions in air were measured by the Spraytec device following the methodology described in section 4.5.7.1. This second method of measuring droplet size distributions assisted in analysing the data from the BACA and provided an initial droplet size distribution for the Collison 3-jet nebuliser.

The resulting droplet size distributions from aerosolising bacterial suspensions through the Spraytec laser are given in Figure 5.16, Figure 5.17, and Figures B.4–B.8, an appendix is used because of the number and similarity in the figures.

The volume frequency data reveal a clear pattern of two distinct peaks around 1 µm and 10 µm followed by a less significant peak between 100 µm–1000 µm. It is important to note that these figures are volume frequency rather than particle frequency like the droplets on slides and hence a very small number of particles in a higher size fraction can dominate the volume. In addition, it is possible some of these larger droplets in these experiments could be entrainment of background particles. The experiments were conducted in a HEPA protected environment but they were not contained like the BACA. Comparing the volume frequency data for ¼ ringers and 1 % FBS there is a difference in the overall pattern, the 1 % FBS suspension has less significant peaks and higher percentage volume at larger droplet sizes. This pattern is visible for all distances measured (0 mm–100 mm) and using the overall volume frequency plots it was not possible to distinguish between the different distances.

There did not appear to be any significant difference between the distributions from each bacterial strain. All strains followed the same patters for both ¼ ringers and 1 % FBS. In conclusion, the different strains of *P. aeruginosa* and *M. abscessus* are not believed to alter the droplet size distribution of the Collison 3-jet nebuliser.

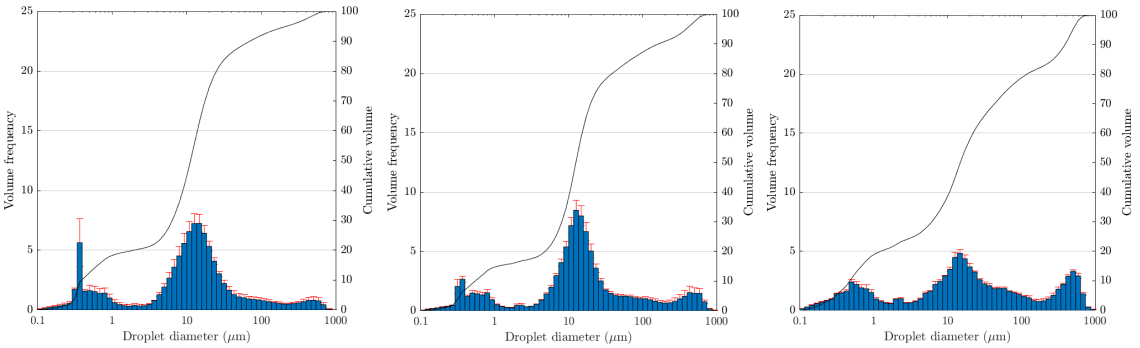

(a) 0 mm. (b) 50 mm. (c) 100 mm.

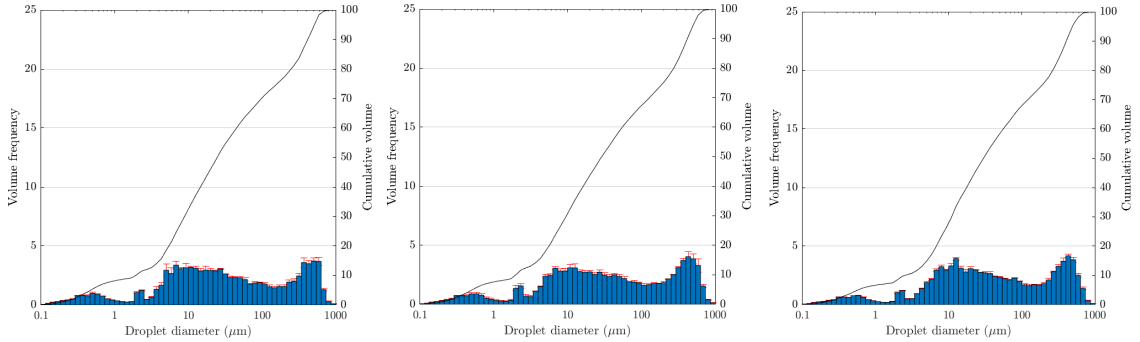

(d) 0 mm. (e) 50 mm. (f) 100 mm.

Figure 5.16: Cumulative volume and volume frequency of aerosolised *P. aeruginosa* patient mucoid in ¼ ringers ((a)–(c)) and 1 % FBS ((d)–(f)) into room air at a distance of 0 mm–100 mm from the Spraytec device.

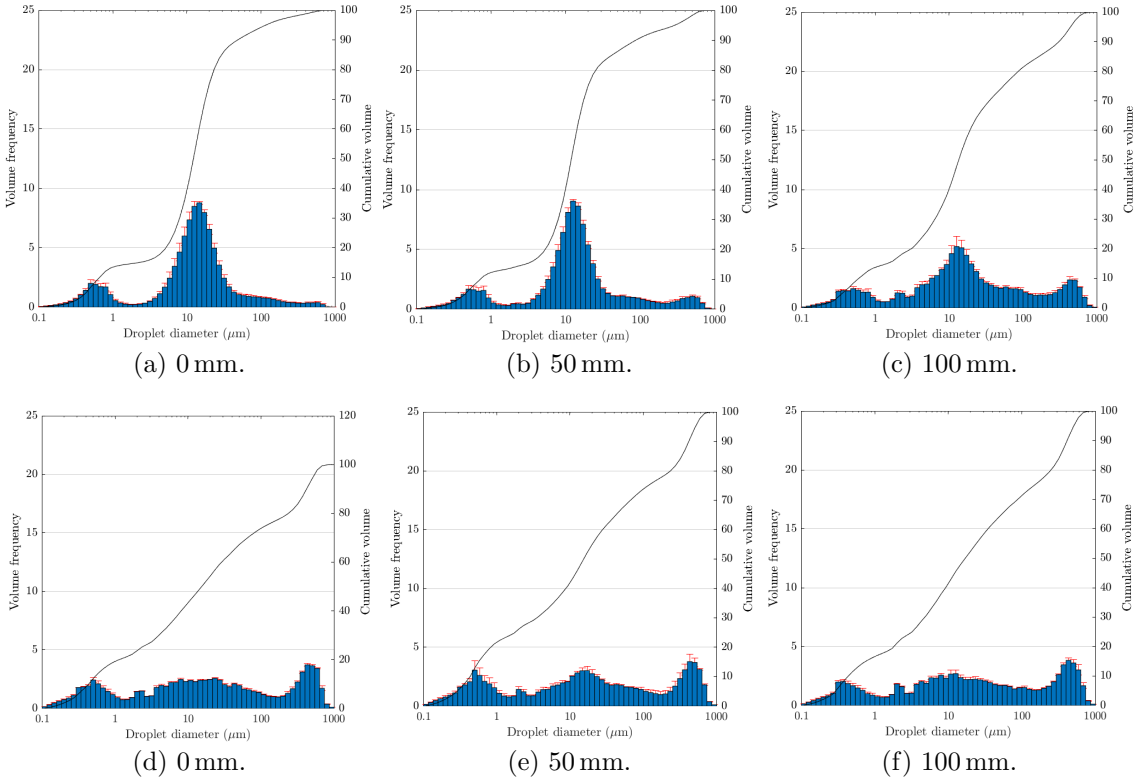

(a) 0 mm. (b) 50 mm. (c) 100 mm.

(d) 0 mm. (e) 50 mm. (f) 100 mm.

Figure 5.17: Cumulative volume and volume frequency of aerosolised *M. abscessus* smooth in ¼ ringers ((a)–(c)) and 1 % FBS ((d)–(f)) into room air at a distance of 0 mm–100 mm from the Spraytec device.

Droplet size distributions of volume frequency and number fraction (volume frequency divided by droplet volume) were plotted over the size range of the Andersen Impactor. The size range of the Andersen Impactor was investigated to determine if there was any correlation to the culturable droplet size distributions. Size bins closest to those for each stage of the Andersen Impactor (Table 2.1) were chosen, the size bin edges were as follows 0.6 µm, 1.2 µm, 2.2 µm, 3.4 µm, 4.6 µm, 7.4 µm and 10 µm. The figures presenting these data are Figure 5.18, Figure 5.19, and Figures B.9–B.13, an appendix is used because of the number and similarity in the figures. The figures do not appear to present a difference between the droplet size distribu-

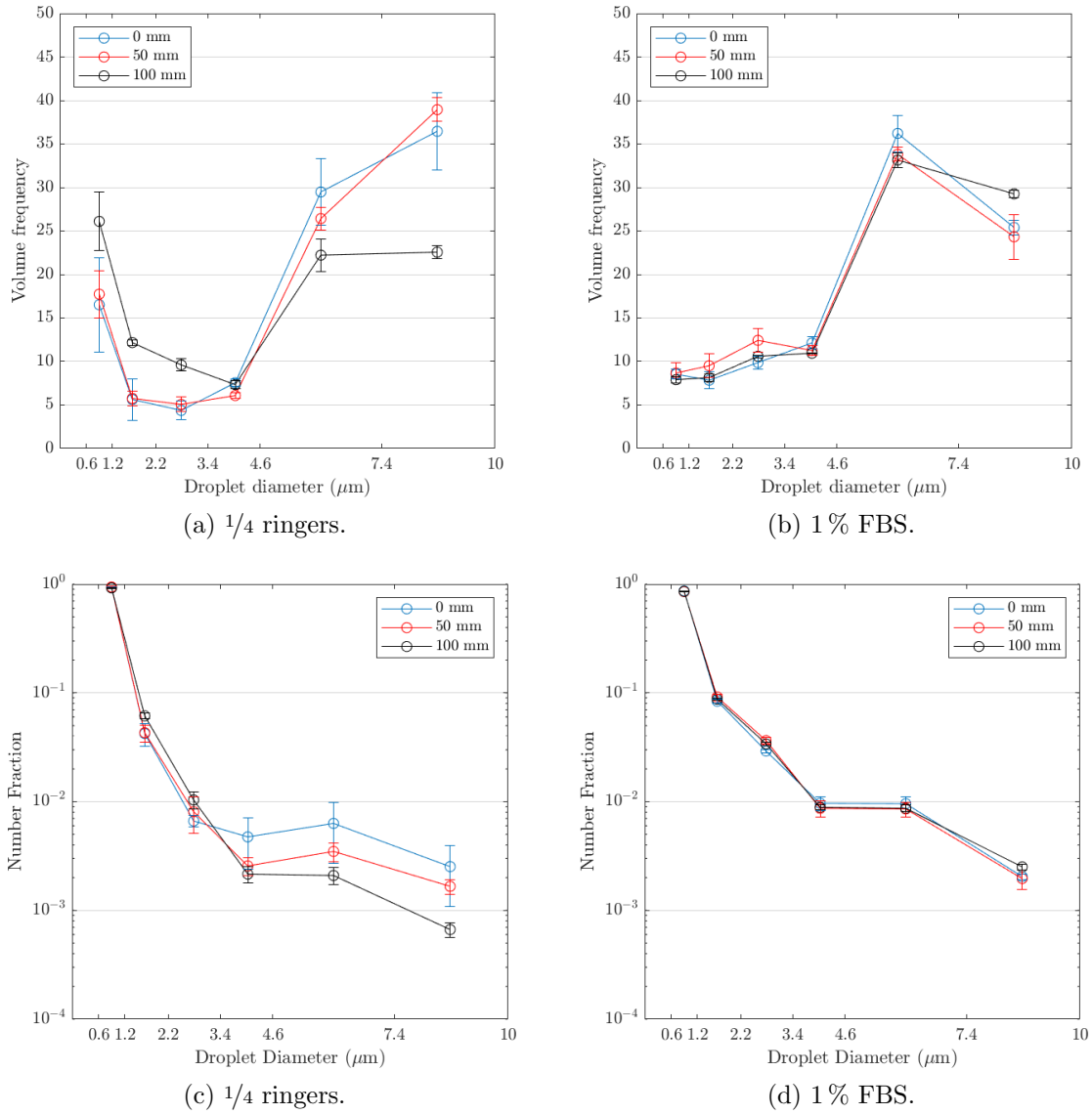

(a) 1/4 ringers.

(b) 1 % FBS.

(c) 1/4 ringers.

(d) 1 % FBS.

Figure 5.18: Volume frequency ((a)–(b)) and number fraction ((c)–(d)) droplet size distribution truncated for the Andersen Impactor size range produced by aerosolising *P. aeruginosa* patient mucoid strain in different suspensions into room air at a distance of 0 mm–100 mm from the Spraytec device.

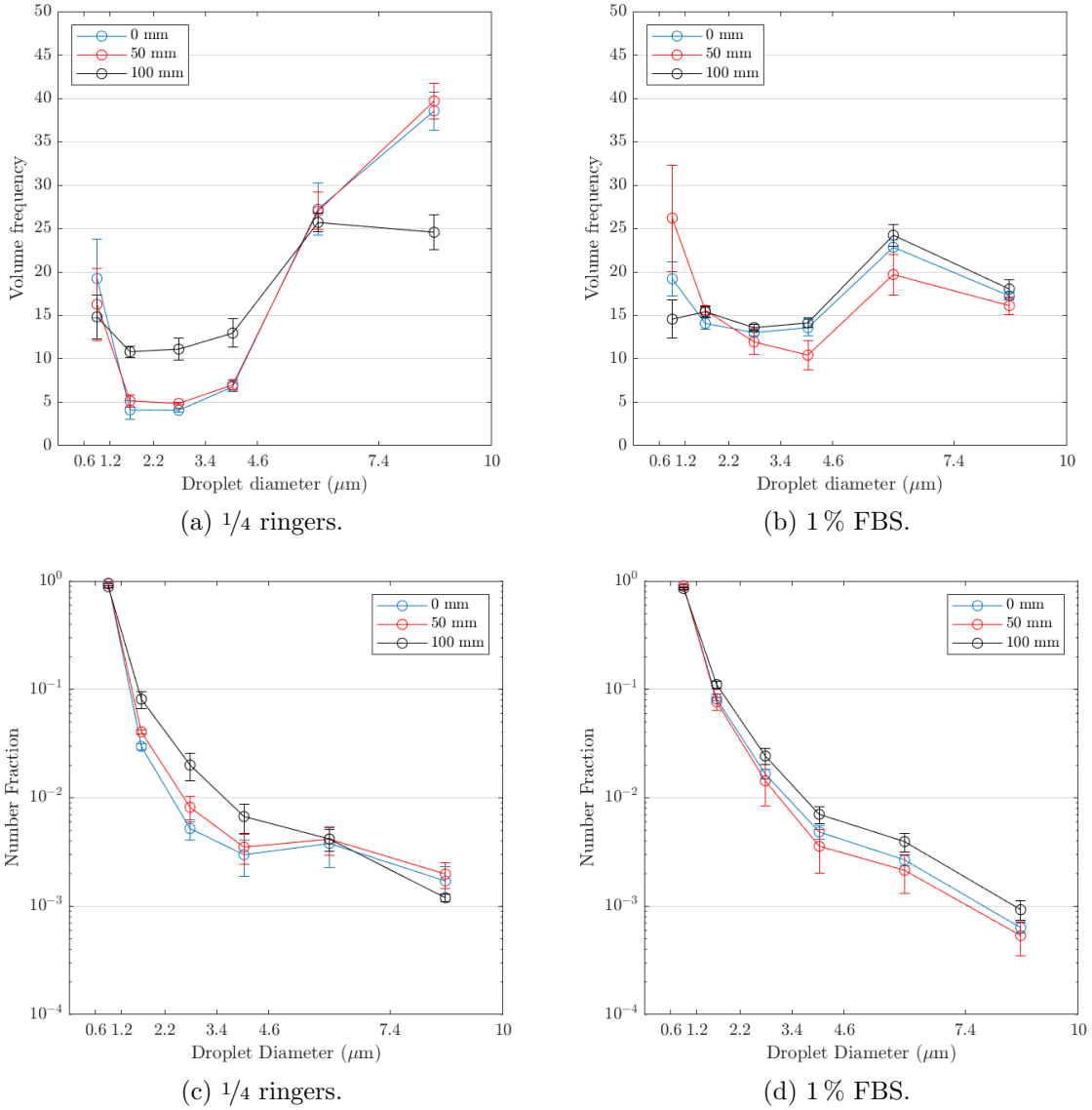

(a) 1/4 ringers.

(b) 1 % FBS.

(c) 1/4 ringers.

(d) 1 % FBS.

Figure 5.19: Volume frequency ((a)–(b)) and number fraction ((c)–(d)) droplet size distribution truncated for the Andersen Impactor size range produced by aerosolising *M. abscessus* smooth strain in different suspensions into room air at a distance of 0 mm–100 mm from the Spraytec device.

tions for 1/4 ringers and 1 % FBS over the Andersen Impactor range. As a trend for both suspensions the volume frequency plots are heavily affected by droplets greater than 4.6 µm. Potentially there was a larger volume of droplets >4.6 µm due to smaller droplets not reaching the sensor and being driven in a different direction by the room air. For both suspensions the number fraction of small droplets dominate the distribution and the Collison nebuliser produces a significant amount of droplets <1.2 µm which are less likely to contain *P. aeruginosa* or *M. abscessus*. The distributions on the Andersen Impactor size range are in agreement with the overall distributions and conclude that there was no observed difference in the droplet

Table 5.6: Droplet size distribution averages (µm) for short range bioaerosol number distributions from Spraytec data.

		0 mm		50 mm		100 mm	
Strain	**Suspension**	$\mathbf{D_{n50}}$	$\mathbf{D_{32}}$	$\mathbf{D_{n50}}$	$\mathbf{D_{32}}$	$\mathbf{D_{n50}}$	$\mathbf{D_{32}}$
P. aeruginosa							
Environmental	1/4 ringers	6.74	12.28	7.77	12.22	6.37	17.51
Manchester	1/4 ringers	0.28	0.79	1.76	3.41	1.86	3.47
Newcastle	1/4 ringers	5.41	9.88	6.09	10.70	8.16	11.88
Patient mucoid	1/4 ringers	5.80	11.20	7.09	12.05	9.31	13.51
	1 % FBS	4.71	30.18	5.03	32.57	4.74	34.79
Patient	1/4 ringers	9.58	23.23	7.01	12.99	8.98	19.75
non-mucoid	1 % FBS	4.05	8.92	8.24	25.62	5.31	35.04
Mean	1/4 ringers	2.17	5.02	1.67	2.75	2.26	4.44
(SD)		(3.02)	(7.15)	(2.16)	(3.51)	(2.73)	(5.62)
	1 % FBS	4.38	19.55	6.64	29.10	5.03	34.92
		(0.33)	(10.63)	(1.61)	(3.48)	(0.29)	(0.13)
M. abscessus							
Smooth	1/4 ringers	5.63	11.61	6.55	11.56	6.20	12.48
	1 % FBS	4.38	11.99	7.44	17.88	0.21	5.36
Rough	1 % FBS	2.96	25.33	7.41	21.52	1.35	12.63
Mean	1 % FBS	3.67	18.66	7.43	19.70	0.78	9.00
(SD)		(0.71)	(6.67)	(0.02)	(1.82)	(0.57)	(3.64)

SD is the standard deviation.

size distributions for the bacterial strain measured by Spraytec over the distances 0 mm–100 mm. Although one deviation from the pattern was observed in volume frequency of the *M. abscessus* strains in 1 % FBS, these data showed similar volume frequencies observed across all the Andersen Impactor sizes suggesting these bacterial suspensions were less affected by the larger droplets.

The Spraytec software allows outputs of the arithmetic mean diameter of the number distribution, D_{n50} and the Sauter mean diameter, D_{32}, after a conversion to a number frequency distribution. These statistics are summarised in Table 5.6. The Sauter mean diameter is commonly used in spray applications to express an average droplet size. In the literature Sauter mean diameter is known as average ratio of volume to surface area of the droplets, and defined by (Pacek et al., 1998):

$$d_{32}\frac{\int_{d_{min}}^{d_{max}} d^3\mathrm{q}(d)\mathrm{d}d}{\int_{d_{min}}^{d_{max}} d^2\mathrm{q}(d)\mathrm{d}d}, \tag{5.12}$$

where d_{min} and d_{max} are the minimum and maximum values of diameter of the histogram q(d). The droplet size distributions average values suggest that there could be a difference between ¼ ringers and 1 % FBS for *P. aeruginosa* strains, but this could be a greater variability within the 1 % FBS suspension. Conversely, this does not appear to be the case for the *M. abscessus* strains and both suspensions have similar averages. There is not any distinguishable variability between the strains of *P. aeruginosa* or *M. abscessus*. There is one exception to this, the *P. aeruginosa* Manchester strain, the averages are much lower than the rest, there is nothing to explain this and it is likely unreliable data. Furthermore, the statistics demonstrate that the average value of droplet size is large enough to carry bacteria at all distances, but no droplet evaporation is observed.

5.2.3 Summary of droplet measurement results

Comparing the results from the dried droplets aerosolised onto glass slides and the distributions measured in air by Spraytec did not find many similarities. The sized droplets on the glass slides were only able to record a small subset of the droplet size distribution and this could potentially be a reason why the distributions were not observed to be comparable. The Spraytec device was able to record many more small droplets which dominated the number fraction results and this was not seen with the droplets on slides; these were either not recorded or not picked up in the measurement technique. However, one of the peaks on the droplets on glass slides was <1 µm suggesting that these small droplets were there. In addition, the droplets on glass slides did not record droplets larger than 2.25 µm and the volume frequency distributions produced by Spraytec found a significant peak around 10 µm, but it must be noted that this is volume frequency so size of the droplets can skew the results. Although there was differences observed between the two measurement techniques there were similarities in the average droplet sizes, both techniques found average droplet sizes to be large enough to carry microorganisms and small enough to be transported large distances in air.

5.3 Controlled flow aerosol characterisation experiments

The controlled flow experiments comprised of two experiments using the BACA to determine if there was a correlation between the measured droplet size distributions with Spraytec and the culturable droplet size distributions. In addition, the first experiment explored the effect of bacterial strain and the second the effects of suspension fluid on the droplet size distributions and survival of bacteria.

5.3.1 Effect of bacterial strain

The first set of experiments considered a range of *P. aeruginosa* and *M. abscessus* strains aerosolised in most cases from a 1/4 ringers suspension. Samples were taken at distances of 1 m–4 m, representing residency times from 20 s–80 s, and the experiment was conducted following the methodology described in 4.5. It is worth noting that all droplets measured at these lengths were assumed to have evaporated to their minimum diameter. All samples taken using the Andersen Impactor were on stages 5 and 6. Colony counts are presented in CFU m^{-3} following a positive hole correction as described by section 4.5.6 and herein will be referred to as colony counts. The strains used were: *P. aeruginosa* environmental, *P. aeruginosa* Manchester (M), *P. aeruginosa* Newcastle (N), and *M. abscessus* smooth (S). When conducting the *P. aeruginosa* environmental experiments the colony counts were lower than expected (1×10^4 CFU m^{-3}) and the experiment was repeated to ensure better comparison between the strains. Therefore, the following survival analysis uses data from two repeated environmental strain experiments, the environmental stain at reduced concentration (E) and the repeated environmental strain (E2).

Survival with distance Figure 5.20 displays the logarithmic colony counts in CFU m^{-3} for four *P. aeruginosa* strains. As expected, the change in starting concentration between the repeated environmental strain experiments made a large difference in number of colony counts found at each measurement. Although the strains could not be directly compared, all four follow similar trends with distance, and are easily able to survive to 4 m without much decay. The environmental strain (E2) had the highest colony counts over all of the lengths and hence it had the best survival. Mucoid phenotypes of *P. aeruginosa* have shown greater resistance to antibiotics and the hosts immune system (Hoffmann et al., 2005; Høiby et al., 2010).

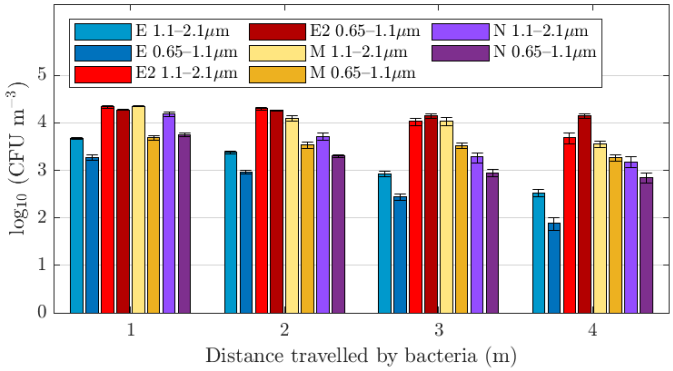

Figure 5.20: Distribution of logarithmic colony counts (CFU m^{-3}) for multiple strains of *P. aeruginosa* in 1/4 ringers using the BACA over 1 m–4 m. Environmental strain at reduced concentration (E), environmental strain (E2), Manchester strain (M), and Newcastle strain (N).

Therefore, it was expected a mucoid strain, the Newcastle strain, would show greater colony counts than a non-mucoid strain, the Manchester strain, but this was not the case. The Manchester strain appeared to have higher concentrations of bacteria on the Andersen Impactor stages and this was likely down to the improved survivability of the epidemic Manchester strain not the differences in the mucoid/non-mucoid phenotype.

The logarithmic colony counts for the *M. abscessus* smooth strain are displayed in Figure 5.21. Like the *P. aeruginosa* strains the *M. abscessus* strain followed a similar trend over distance and showed high levels of survival at 4 m. Overall, the majority of cases for *P. aeruginosa* and *M. abscessus* had higher concentrations on stage 5, stage 5 measures droplets of size 1.1 µm–2.1 µm. Whereas stage 6 has the size range of 0.65 µm–1.1 µm and it is likely that the bacteria were too big for many droplets in the stage 6 size range and the reason why the majority of colony counts were found on stage 5. The exception was the repeated environmental strain (E2) which has comparable colony counts on both stages. Inspection of the raw colony counts with number of predicted bacteria released into the BACA by the Collison nebuliser (section 5.1.3), determined that raw colony counts were of the order 10^2 for both *P. aeruginosa* and *M. abscessus* at all lengths compared to the prediction of 10^4 and 10^3 for *P. aeruginosa* and *M. abscessus* respectively. As a consequence this could imply that *M. abscessus* had better survivability within aerosolised droplets.

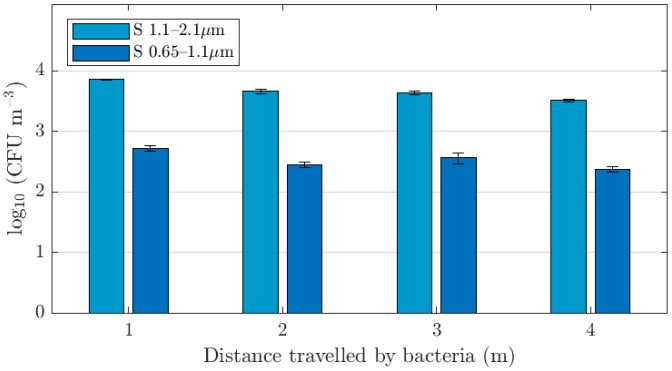

Figure 5.21: Distribution of logarithmic colony counts (CFU m^{-3}) for *M. abscessus* smooth (S) in 1/4 ringers using the BACA over 1 m–4 m.

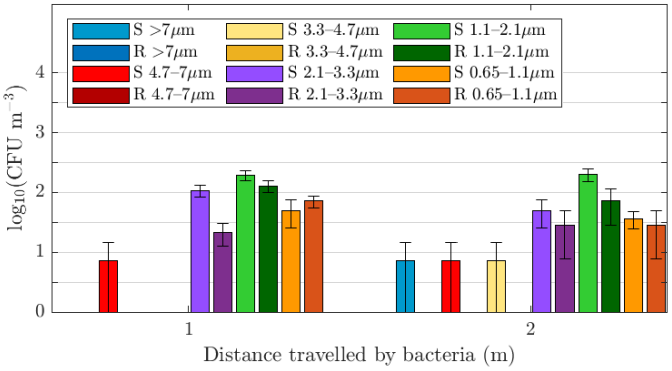

Figure 5.22: Distribution of logarithmic colony counts (CFU m^{-3}) for *M. abscessus* smooth (S) and rough (R) in 1 % FBS using the BACA over 1 m and 2 m.

Figure 5.22 compares the colony counts of culturable *M. abscessus* in this case measured at all stages of the Andersen Impactor in 1 % FBS at 1 m and 2 m using the BACA. These experiments present results for 1 % FBS as it was not possible to conduct the experiments for 1/4 ringers due to COVID-19 lab closures. Similar to what was found in the *P. aeruginosa* strains and *M. abscessus* smooth in 1/4 ringers solution for lengths 1 m–4 m, in 1 % FBS both *M. abscessus* rough and smooth did not show much decay over the 1 m unit distance. Stage 5 showed the highest colony counts and was found to be the dominant stage for both strains. Survival of *M. abscessus* was poor in the larger droplets, stages 1–3. The *M. abscessus* smooth strain had higher concentrations in all but one measurement, stage 6 at 1 m, and in conclusion it is likely that the *M. abscessus* smooth morphotype survives better in artificially generated aerosols into air than the rough morphotype. However, the

reliability of these results is unclear as the *M. abscessus* did not survive well overall in 1 % FBS and the colony counts were low. This is discussed further in section 5.3.2.

Decay rates Survival of *P. aeruginosa* and *M. abscessus* over time is presented in Figure 5.23 and the generalised survival of *P. aeruginosa* is given in Figure 5.24. Average velocity of the air inside the BACA was calculated to be $0.05\,\mathrm{m\,s^{-1}}$, representing a residency time of 20 s for each 1 m of the BACA. Total number of colony forming units per metre cubed, n, was normalised with the initial $\mathrm{CFU\,m^{-3}}$ of the bacteria in the suspension. This value was calculated from the initial concentration of bacteria within the suspension ($\mathrm{CFU\,ml^{-1}}$), mass of fluid dispensed in the measurement time, and the volume of air measured. Initial concentration of bacteria was calculated from OD_{600} or from serial dilutions. Section 5.1.3 calculates the fluid dispensed from the nebuliser during the measurement time. The initial $\mathrm{CFU\,ml^{-1}}$ is divided by 10 to account for the 0.01 ml of fluid dispensed during the measurement time of 2 minutes. This calculation gave the approximation of the initial number of bacteria released, CFU_0, during the measurement time, t. Flow rate was Q =28.3 $\mathrm{L\,min^{-1}}$ and initial number of bacteria per m^3, n_0 was calculated using the following equation:

$$n_0 = 1000 \times \frac{\mathrm{CFU}_0}{(t \times Q)}. \tag{5.13}$$

In addition, the colony forming units were normalised by their value at 1 m. The normalised number of colony forming units per metre cubed with respect to initial concentration are displayed in Figure 5.23a and detail that while the *P. aeruginosa* environmental strain (E2) had the highest colony counts it had the greatest reduction in concentration over the first metre, including the *P. aeruginosa* environmental strain with a lower initial concentration (E). This suggests that potentially the initial concentration plays an important role in the decay of bacteria at short timescales. However, when normalised by colony counts at 1 m (Figure 5.23b) the environmental strain (E2) shows the least decay over time and does experience the same decay rate for the reduced environmental strain (E2) after the first 1 m. Suggesting that the *P. aeruginosa* environmental strain has reached a less dramatic die off rate at around 5 % of the initial concentration. Furthermore, this is supported by all the *P. aeruginosa* strains reducing to around 5 % of their initial value by 80 s residency time and the decay appears to slow down. Survival of the Newcastle strain has a greater drop off than seen with Manchester strain again showing the enhanced survivability of this epidemic strain. *M. abscessus* smooth demonstrates a slower

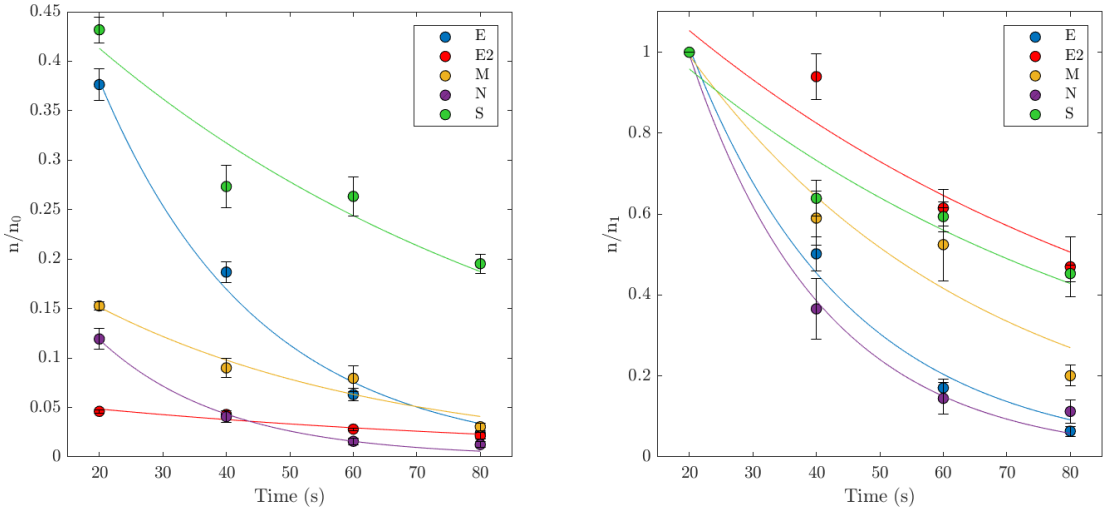

(a) Normalised with respect to initial concentration.

(b) Normalised with respect to colony counts at 1 m.

Figure 5.23: Survival of *P. aeruginosa* and *M. abscessus* strains over residency time 20 s–80 s after aerosolisation into the BACA in 1/4 ringers suspension. *P. aeruginosa* strains: environmental strain at reduced concentration (E), environmental strain (E2), Manchester strain (M), and Newcastle strain (N). *M. abscessus* smooth strain (S).

decay in aerosolised droplets than the *P. aeruginosa* strains. When normalised by their initial concentrations there is a 6 % difference in the initial survival at 20 seconds between *M. abscessus* smooth (S) and the *P. aeruginosa* environmental strain at reduced concentration (E) and by 80 seconds the increase in survivability is eightfold. Difference in the cell structure of each bacteria could be playing a part in the survivability of these microorganisms, with the outer lipid present in mycobacteria possibly providing some protection.

Combining the results for the *P. aeruginosa* strains allowed a generalised decay curve for *P. aeruginosa* to be created, Figure 5.24. A first order exponential decay is a good fit for the measured values and is of the form $N_0 e^{-kx}$ where N_0 is the initial concentration and k is the decay rate. The decay rate for *P. aeruginosa* was equal to $k = 0.03\,\mathrm{s}^{-1}$ and for *M. abscessus* the decay rate was $k = 0.01\,\mathrm{s}^{-1}$, this equates to a half life of 23 s and 69 s respectively. These decay rates are rapid when compared with artificially generated aerosols of *P. aeruginosa* into an environmentally controlled chamber (Clifton et al., 2010) and cough generated aerosols of *P. aeruginosa* from people with CF (Knibbs et al., 2014). However, the timescales to calculate this decay were short (80 s) and it is likely both bacteria experienced rapid initial die off possibly as a result of the experimental conditions. Clifton et al. (2008) conducted a similar experiment and the data suggested a similar rapid die off concluding that

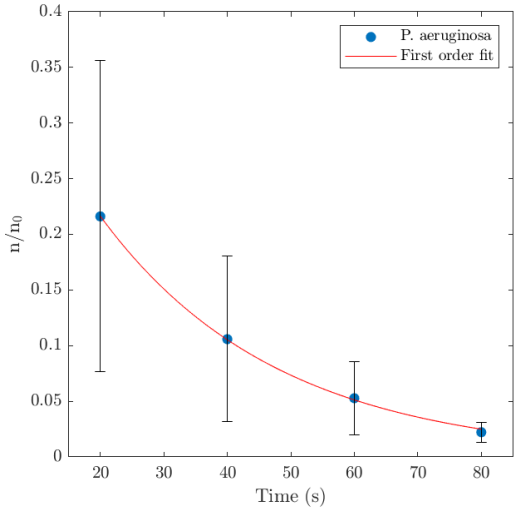

(a) Normalised with respect to initial concentration.

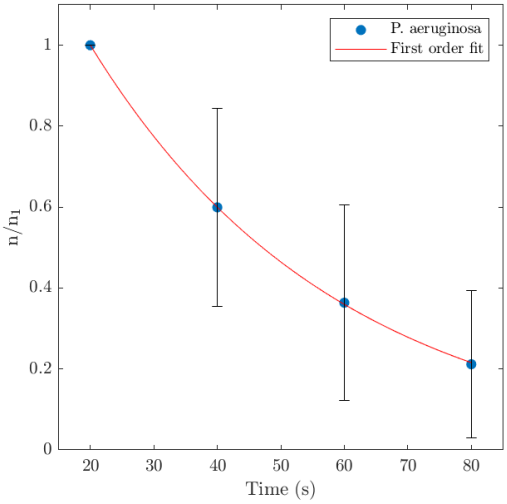

(b) Normalised with respect to colony counts at 1 m.

Figure 5.24: Survival of the combination of four *P. aeruginosa* strains over time after aerosolisation into the BACA in ¼ ringers suspension.The strains used were environmental strain at reduced concentration (E), environmental strain (E2), Manchester strain (M), and Newcastle strain (N).

P. aeruginosa may experience rapid die off at short timescales, but this requires further investigation and whether it is a feature of the pathogen, the suspension fluid or the aerosolisation technique (Brouwer et al., 2017).

Spraytec droplet size distributions Results of the cumulative volume and volume frequency measured using the Spraytec device, over 1 m–4 m for each strain of bacteria in ¼ ringers suspension are displayed in Figures 5.25, Figure 5.26, and Figures B.14–B.15, an appendix is used because of the number and similarity of the figures. The different bacteria do not seem to affect the volume frequency distribution which is in agreement with the droplet size distributions measured at short ranges. Results suggest no clear pattern emerging from the change in distance, which could be expected as all of these aerosol distributions will be fully evaporated. There are four peaks in all measurements these are: less than 1 µm, just above 1 µm, around 10 µm and between 100 µm–1000 µm. The majority of the size bins have volume frequency less than 5 %. Yet, there are several anomalies to the general pattern with much greater volume frequency. It is possible that at larger droplet sizes these are noise, error bars are much greater indicating that this is not repeated. The peaks found in these results do not demonstrate as clear of a pattern as those observed in the short range measurements by Spraytec. Although, the split peak around 1 µm was found when measuring droplets on glass slides.

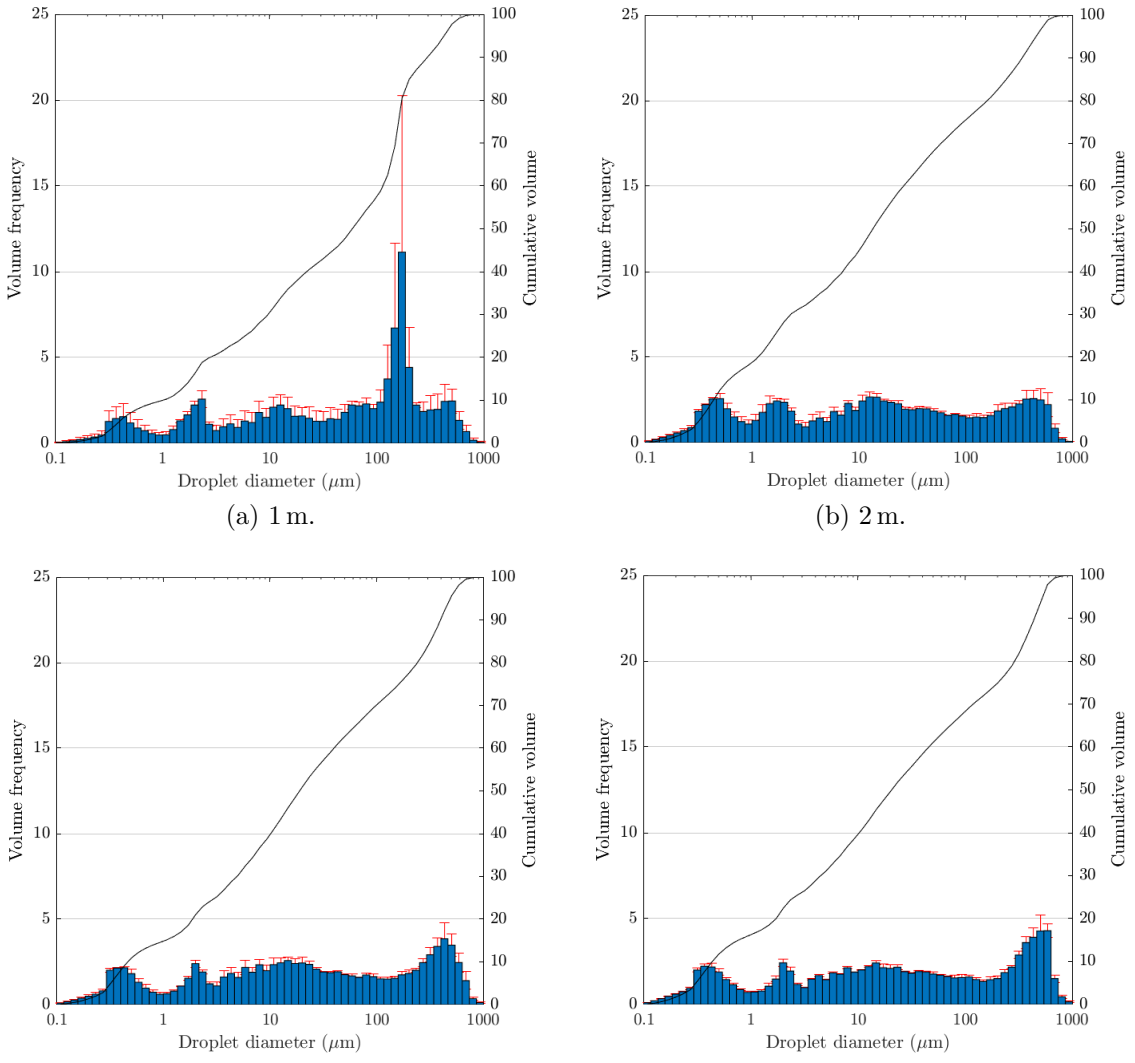

(a) 1 m. (b) 2 m.

(c) 3 m. (d) 4 m.

Figure 5.25: Cumulative volume and volume frequency of aerosolised *P. aeruginosa* environmental in 1/4 ringers solution using the BACA over 1 m–4 m.

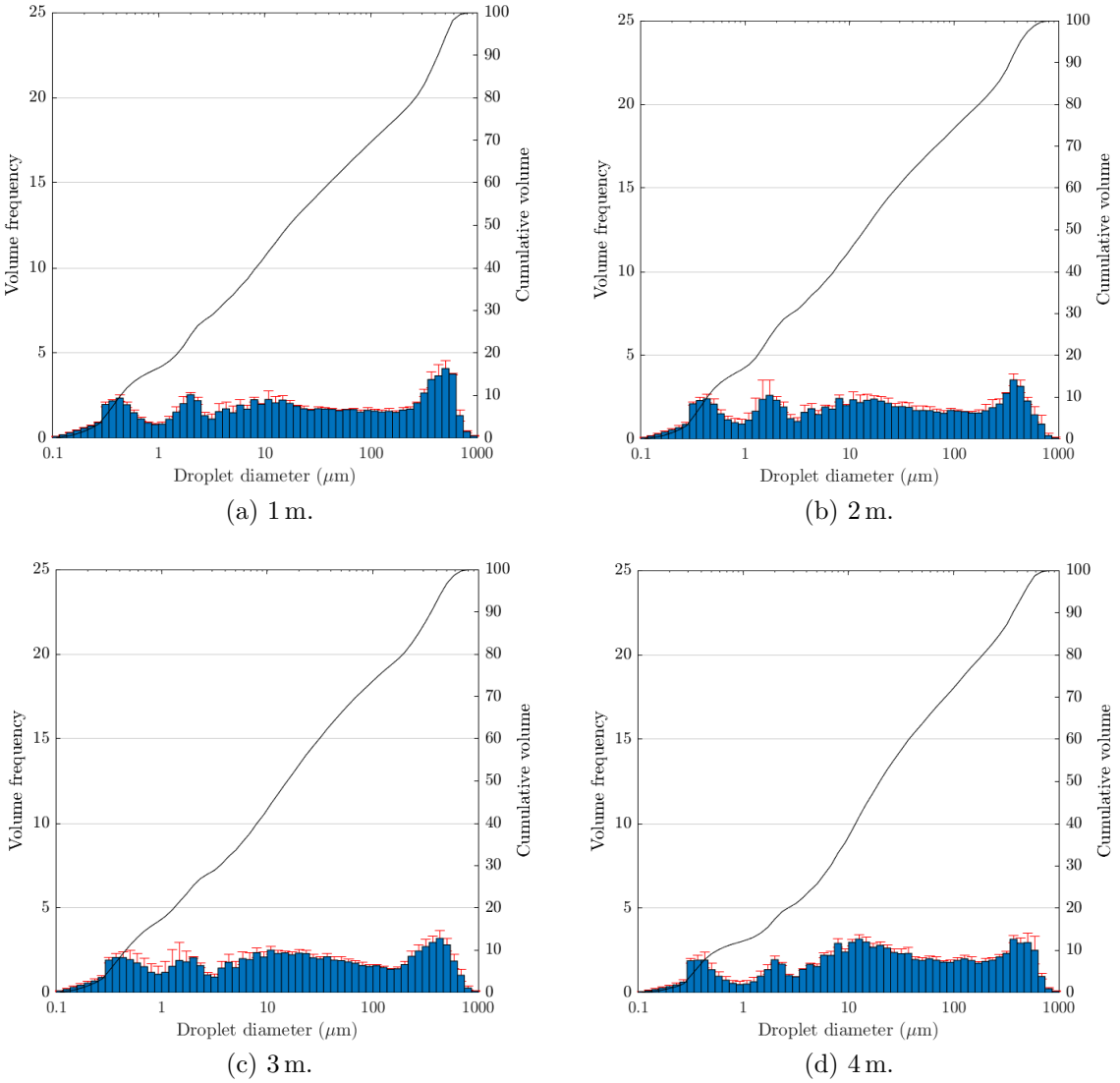

(a) 1 m. (b) 2 m.

(c) 3 m. (d) 4 m.

Figure 5.26: Cumulative volume and volume frequency of aerosolised *M. abscessus* smooth in 1/4 ringers solution using the BACA over 1 m–4 m.

Droplet size distributions of volume frequency and number fraction (volume frequency divided by droplet volume) were plotted over the size range of the Andersen Impactor, Figure 5.27. The size range of the Andersen Impactor was investigated to determine if there was any correlation to the culturable droplet size distributions. At this size range there does not appear to be a difference in the distributions between the aerosolised *P. aeruginosa* and *M. abscessus*. The number fraction distributions are dominated by the smaller droplets, but these droplets will not carry the majority of the bacteria. The volume frequency distributions show the peak droplet size recorded is in the range 1.2 µm–2.2 µm which is at stage 5 of the Andersen Impactor. This result correlates to the culturable distributions measured by the Andersen Impactor (Figures 5.20 and 5.21). At the stage 5 droplet size there is a drop in volume

frequency from the 1 m and 2 m to the 3 m and 4 m measurements. It can be theorised this reduction in overall volume at these sizes could be down to a reduction in the number of bacteria and hence droplet nuclei containing these bacteria reaching these lengths. However, this is not seen on the number fraction figures and the total number of bacteria released compared to the number of droplets is small so it may not be possible to see this affect. In addition, the current data set it small and would need more work so it is not possible to be confident in this conclusion.

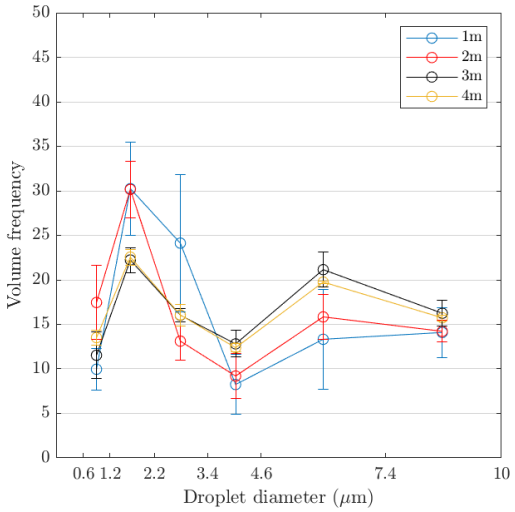

(a) *P. aeruginosa* environmental volume frequency.

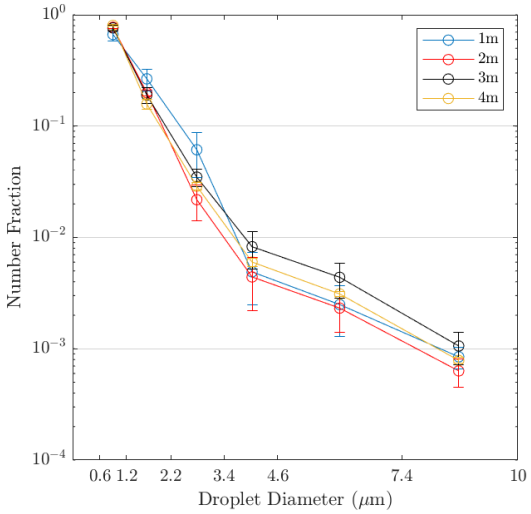

(b) *P. aeruginosa* environmental number fraction.

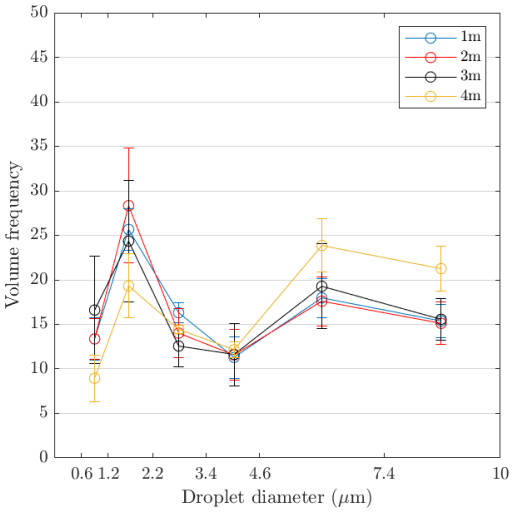

(c) *M. abscessus* smooth volume frequency.

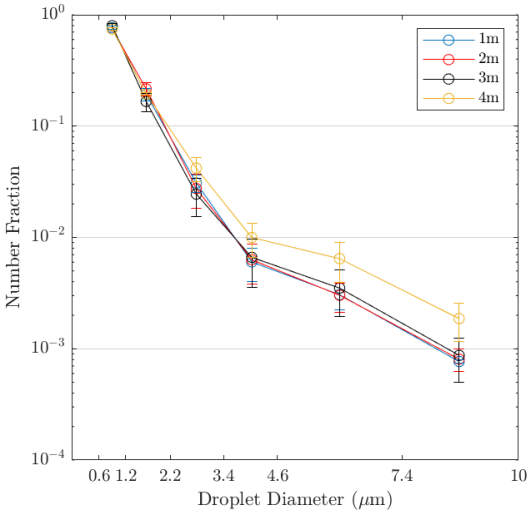

(d) *M. abscessus* smooth number fraction.

Figure 5.27: Droplet size distribution truncated for the Andersen Impactor size range produced by aerosolising bacterial suspensions in 1/4 ringers using the BACA over 1 m–4 m.

Averages of the number droplet size distributions are summarised in Table 5.7. The averages of the number distribution is similar for both bacteria at all lengths. The arithmetic mean, D_{n50}, is less than 1 µm and demonstrates that the majority of the droplets measured are very small and would not contain any bacteria. The Sauter mean is larger than D_{n50} for these distributions and has a range of 3.86 µm–6.48 µm and would easily contain a microorganisms. Although this covers stages 1–3 of the Andersen Impactor which did not measure high concentration of bacteria compared to stages 4–6 and the droplets on glass slides did not measure droplets of this size. Therefore, this calculation of the mean could be influenced by the recording of some larger droplets.

Table 5.7: Droplet size distribution averages for controlled flow experiments in the BACA over lengths 1 m–4 m using ¼ ringers solution.

	1 m		**2 m**		**3 m**		**4 m**	
Strain	$\mathbf{D_{n50}}$	$\mathbf{D_{32}}$	$\mathbf{D_{n50}}$	$\mathbf{D_{32}}$	$\mathbf{D_{n50}}$	$\mathbf{D_{32}}$	$\mathbf{D_{n50}}$	$\mathbf{D_{32}}$
P. aeruginosa								
Environmental	1.25	10.73	0.17	3.29	0.16	3.78	0.17	5.08
Manchester	0.11	3.53	0.19	5.52	0.20	3.83	0.17	3.13
Newcastle	0.91	3.56	0.16	3.93	0.16	4.91	0.16	3.36
Mean	0.76	5.94	0.17	4.25	0.17	4.17	0.17	3.86
(SD)	(0.478)	(3.39)	(0.12)	(0.94)	(0.02)	(0.64)	(0)	(0.87)
M. abscessus								
Smooth	0.16	4.41	0.44	2.83	0.21	6.48	0.17	3.45

SD is the standard deviation.

5.3.2 Effect of suspension fluid

Aerosols generated in ¼ ringers and 1 % FBS suspensions were measured at 1 m and 2 m and it was assumed at these lengths that all droplets had evaporated to their minimum size. Measurements were made using all stages of the Andersen to get a full description of the droplet size distributions in different suspensions following the methodology described in section 4.5. Colony counts are presented in CFU m^{-3} following a positive hole correction as described by section 4.5.6 and herein will be referred to as colony counts. In this case four bacterial strains were used, *P. aeruginosa* patient mucoid, *P. aeruginosa* patient non-mucoid, *M. abscessus* smooth, and *M. abscessus* rough. The *P. aeruginosa* strains used were not the same as those used in the previous experiments in the BACA testing the effect on bacterial strain. This

was because the experiments sought to determine if the mucoid/non-mucoid phenotype affected the distribution and the difference observed between the mucoid and non-mucoid strains in the previous experiments was overshadowed by the improved survivability of the Manchester strain. Due to circumstances surround SARS-CoV-2 and lab closures there was not the opportunity to gather a full data set for the *M. abscessus* rough strain in 1/4 ringers and data presented for this strain is in 1 % FBS only.

Bioaerosol size distributions Comparing 1/4 ringers solution to 1 % FBS in Figure 5.28 and 5.29 demonstrates that 1 % FBS gave a better survival for both *P. aeruginosa* patient mucoid and patient non-mucoid strains at stages 5 and 6, which is consistent with what Clifton et al. (2008) found who only took measurements on these stages. However, at 1 m the *P. aeruginosa* patient mucoid strain results (Figure 5.28) show 1 % FBS improving survivability at all stages, but by 2 m this protection from 1 % FBS is only at stages 5 and 6. *P. aeruginosa* patient non-mucoid does not follow the same pattern and there is only improved survivability in the 1 % FBS suspension at stages 5 and 6 for both lengths. At 2 m on stages 1 and 2 there is not enough colony forming units of bacteria to draw full conclusions. The extra proteins in the 1 % FBS solution may only form protection to the bacteria when the droplets are very small, similar to the protective outer shell morphology seen by Vejerano and Marr (2018) and it appears to have a greater affect on the *P. aeruginosa* patient mucoid strain. Evaluation of the colony counts of bacteria show that the patient mucoid strain of *P. aeruginosa* had greater colony counts than *P. aeruginosa* non-mucoid strain at all stages apart from stage 1 in 1/4 ringers, demonstrating a greater survivability of the mucoid phenotype. Furthermore, stage

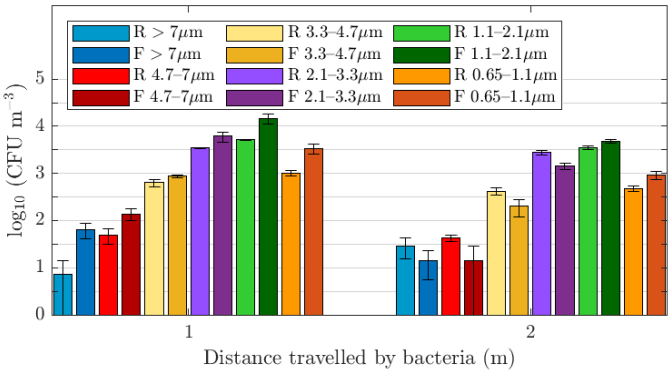

Figure 5.28: Distribution of logarithmic colony counts (CFU m^{-3}) for *P. aeruginosa* patient mucoid in 1/4 ringers (R) and 1 % FBS (F) using the BACA over 1 m and 2 m.

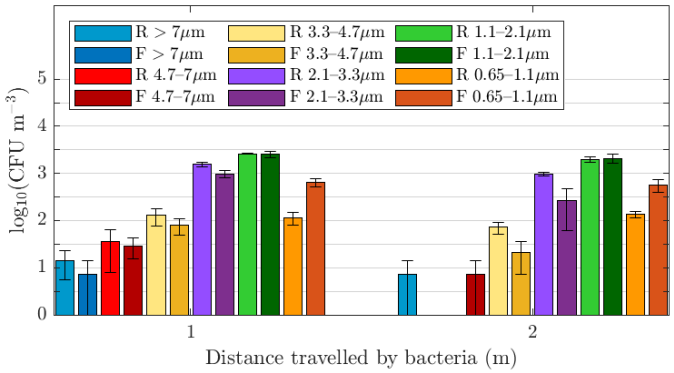

Figure 5.29: Distribution of logarithmic colony counts (CFU m^{-3}) for *P. aeruginosa* patient non-mucoid in ¼ ringers (R) and 1 % FBS (F) using the BACA over 1 m and 2 m.

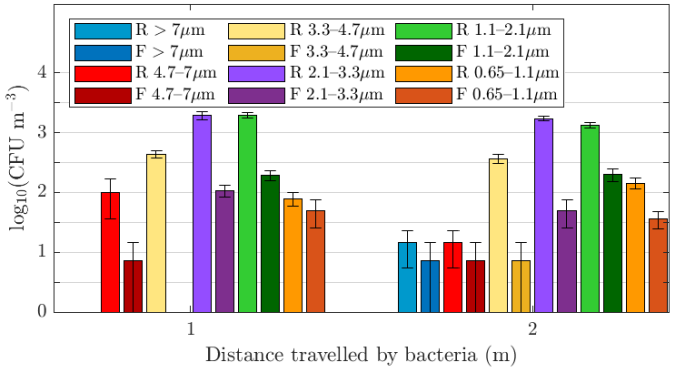

Figure 5.30: Distribution of logarithmic colony counts (CFU m^{-3}) for *M. abscessus* smooth in ¼ ringers (R) and 1 % FBS (F) using the BACA over 1 m and 2 m.

5 was the dominant stage for both *P. aeruginosa* strains and this correlates to the results from the previous section for other *P. aeruginosa* strains. This leads to the conclusion that *P. aeruginosa* has a higher prevalence in evaporated droplets of the size 1.1 µm–2.1 µm for artificially generated aerosols.

The culturable droplet size distributions produced by *M. abscessus* smooth, Figure 5.30, found that the 1 % FBS solution did not improve survivability in *M. abscessus* but in fact reduced the concentration of bacteria found at each Andersen Impactor stage at both 1 m and 2 m. This result was unexpected and it could likely be due to the hydrophobicity of *M. abscessus* (Cortes et al., 2010) interacting with the foaming of the 1 % FBS solution and in a foam fractionation like event not being aerosolised by the Collison nebuliser. However, this was not assumed to be the case for *P. aeruginosa* which is reported to be hydrophobic too (Van Loosdrecht et al.,

1987), but potentially the impacts were greater for *M. abscessus* . Despite the low colony counts for *M. abscessus* smooth in 1 % FBS stage 5 was clearly the preferred droplet size, but in ¼ ringers stage 4 and 5 showed comparable results.

Comparing the *M. abscessus* smooth distribution to the *P. aeruginosa* strains the larger droplets, stage 1 and 2, had higher concentrations in the ¼ ringers solution for *M. abscessus* than *P. aeruginosa* at 1 m, but by 2 m and in 1 % FBS the results are comparable, despite the lower starting concentration. Inspection of the raw colony counts compared with number of predicted bacteria released into the BACA by the Collison nebuliser (section 5.1.3), determined that total raw colony counts were of the order 10^2 for *P. aeruginosa* in both suspensions compared to the prediction of 10^3, demonstrating suspension fluid did not have a significant effect on *P. aeruginosa* strains. For *M. abscessus* in ¼ ringers it was of the order 10 and or the order 1 in 1 % FBS and compared to the prediction of 10^2. As a consequence this could imply that *M. abscessus* had better survivability within aerosolised droplets of ¼ ringers than 1 % FBS, but the reliability of the results in the 1 % FBS solution are unclear.

Spraytec droplet size distributions Characterisation of the droplet size distributions in both ¼ ringers and 1 % FBS suspensions are given in Figure 5.31, Figure 5.32, and Figures B.17–B.18, an appendix was used because of the number and similarity of the figures. The difference in distributions between ¼ ringers and 1 % FBS is much less prominent that what was seen in the short range bioaerosols (section 5.2.2). In fact, these distributions do not appear to show a difference based on the suspension fluid. The pattern of the same four peaks are seen again: less than 1 µm, just above 1 µm, around 10 µm and between 100 µm–1000 µm, albeit with more noise than the previous data. The majority of the volume frequency recordings for the size bins measure at less than 5 %, and the few outliers are in larger droplets which is likely attributed to noise. The results do not show a difference in their distributions that can be attributed to either distance or bacteria.

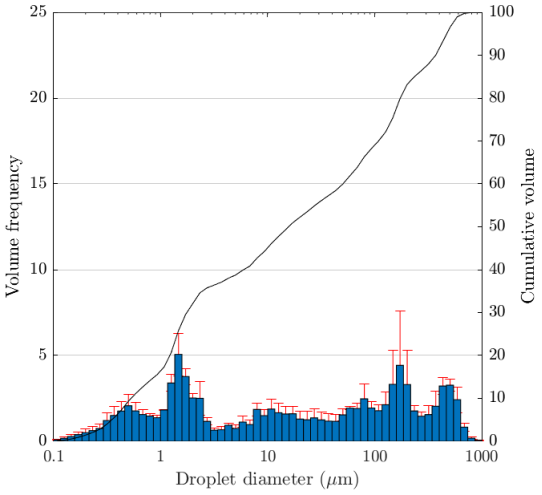

(a) 1/4 ringers at 1 m.

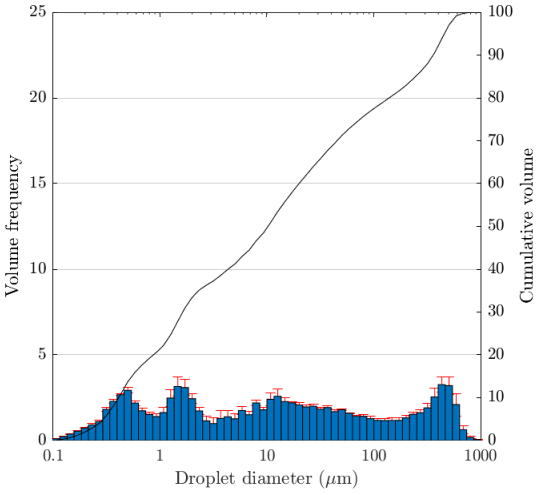

(b) 1/4 ringers at 2 m.

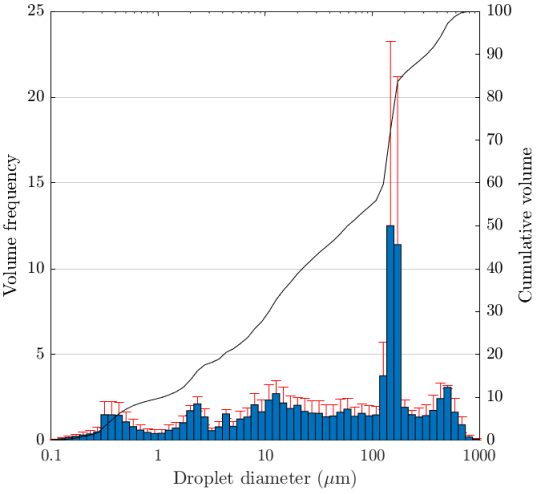

(c) 1 % FBS at 1 m.

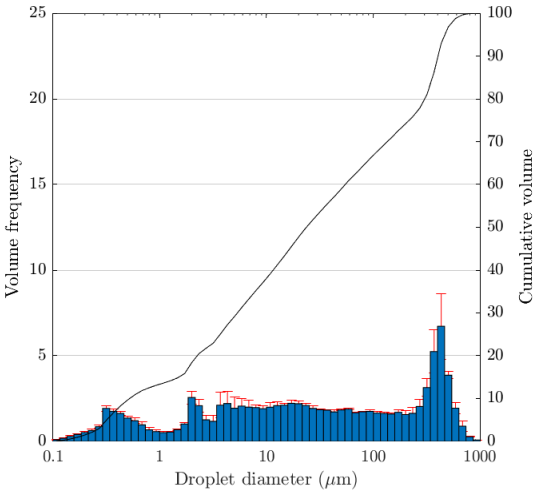

(d) 1 % FBS at 2 m.

Figure 5.31: Cumulative volume and volume frequency of aerosolised *P. aeruginosa* patient mucoid in two suspensions using the BACA at 1 m and 2 m.

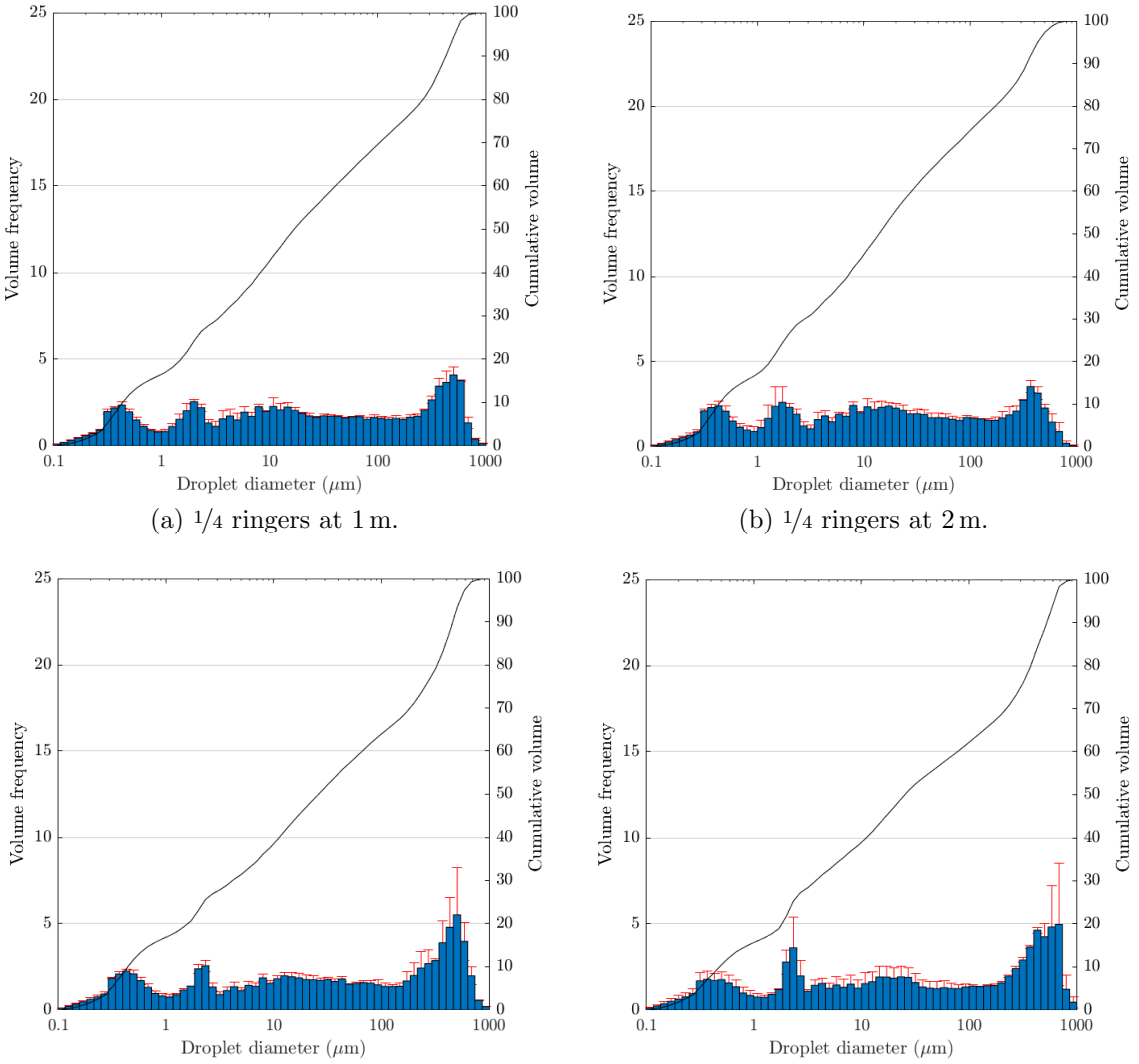

(a) 1/4 ringers at 1 m.

(b) 1/4 ringers at 2 m.

(c) 1 % FBS at 1 m.

(d) 1 % FBS at 2 m.

Figure 5.32: Cumulative volume and volume frequency of aerosolised *M. abscessus* smooth in two suspensions using the BACA at 1 m and 2 m.

The size range was reduced to the Andersen Impactor size range and the resulting data for volume frequency and number fraction distributions is displayed in Figures 5.33 and 5.34 and Figures B.19 and B.20 in an appendix. In these droplet size distributions it could be argued that there is a possible effect due to the suspension fluid for the *P. aeruginosa* strains but *M. abscessus* is not affect by this. The aerosolised droplets in 1/4 ringers solution clearly have a peak at 1.2 µm–2.2 µm representing stage 5 on the Andersen Impactor, which was observed in the previous section. Whereas aerosolised droplets in 1 % FBS have a much less defined distribution of volume frequency and do not have a clear peak in their data. However, differences are not observed in the number fraction data and these are dominated by the small droplets representing stage 6 of the Andersen Impactor. Stage 6 does contain some

culturable bacteria but it is not the stage with the highest concentrations, indicating that there are high proportions of small droplets being produced by the Collison nebuliser but many of these droplets do not contain bacteria.

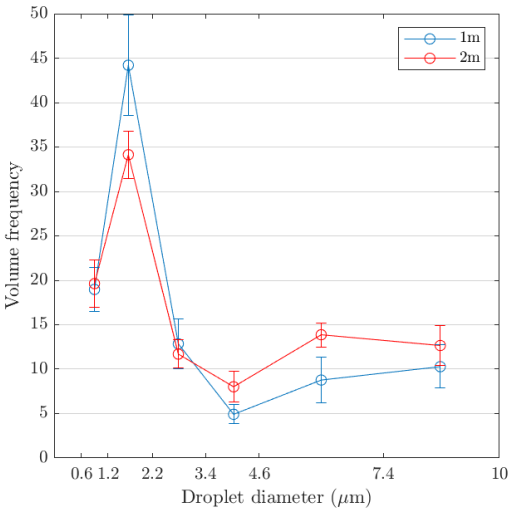

(a) 1/4 ringers volume frequency.

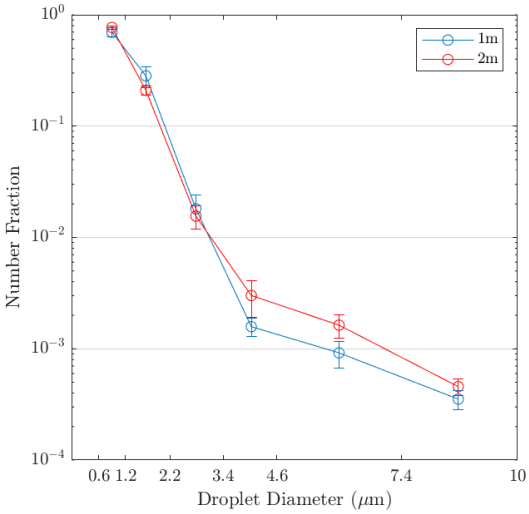

(b) 1/4 ringers number fraction.

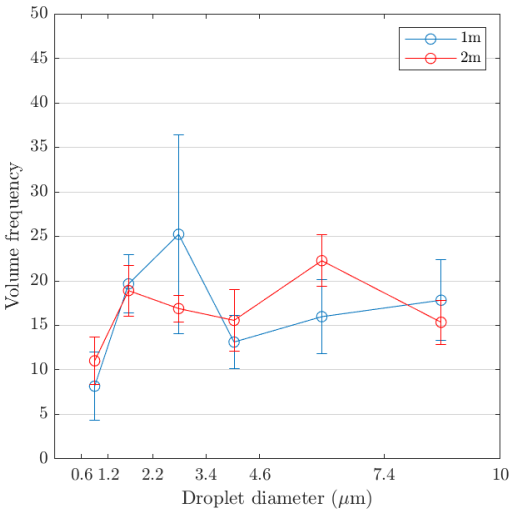

(c) 1 % FBS volume frequency.

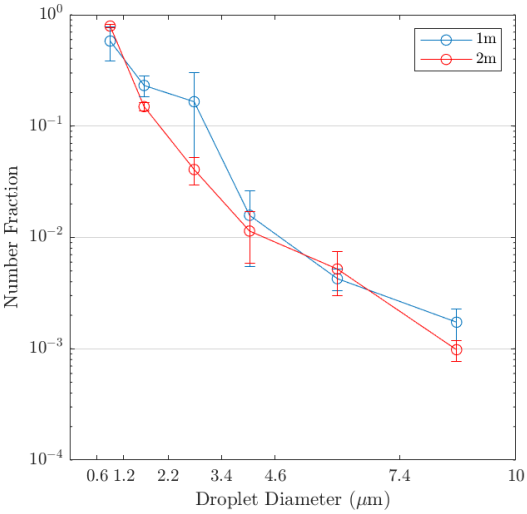

(d) 1 % FBS ringers number fraction.

Figure 5.33: Droplet size distribution truncated for the Andersen Impactor size range produced by aerosolising *P. aeruginosa* patient mucoid in two suspensions using the BACA at 1 m and 2 m.

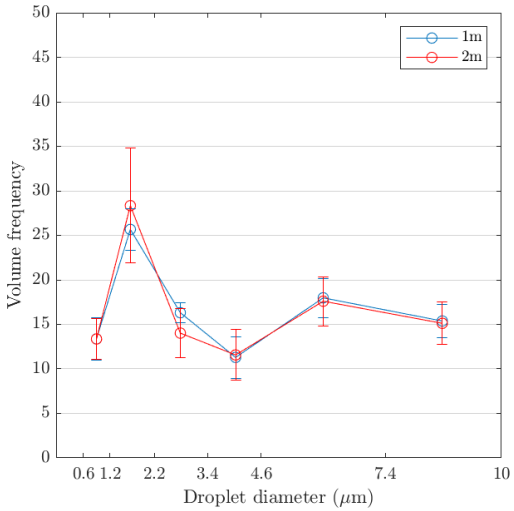

(a) ¼ ringers volume frequency.

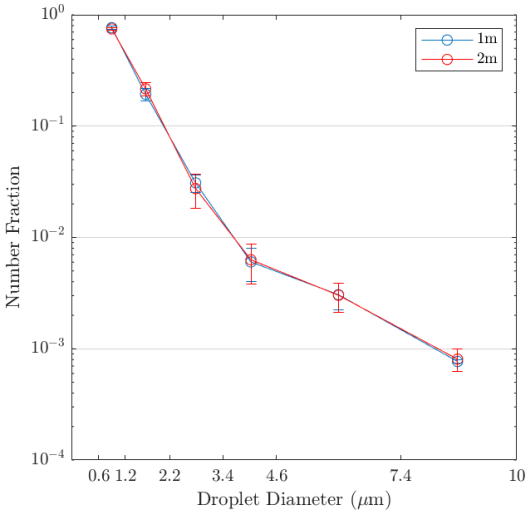

(b) ¼ ringers number fraction.

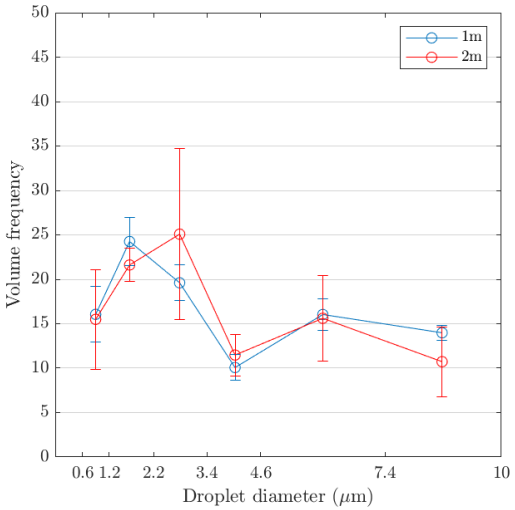

(c) 1 % FBS volume frequency.

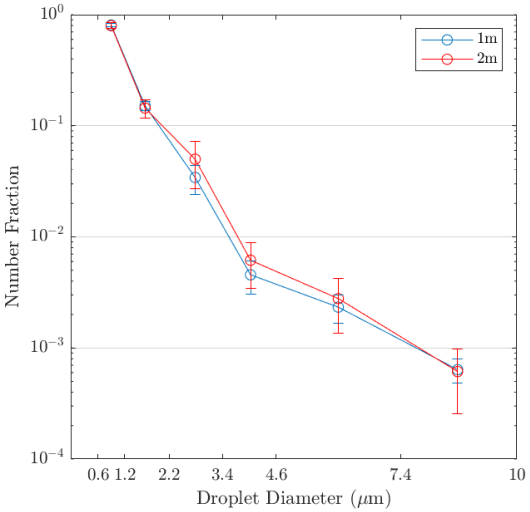

(d) 1 % FBS ringers number fraction.

Figure 5.34: Volume frequency droplet size distribution truncated for the Andersen Impactor size range produced by aerosolising *M. abscessus* smooth in two suspensions using the BACA at 1 m and 2 m.

Averages of the droplet number distribution are summarised in Table 5.8. These data suggest that there is no significant difference between the averages of the measured distributions in the ¼ ringers solutions and the 1 % FBS solution. A small value for D_{n50} (<1 µm) highlights the large number of small droplets aerosolised by the Collison nebuliser that will not contain microorganisms. The Sauter mean is larger than the D_{n50} and has the range of 2.97 µm–7.02 µm which is stages 1–3 of the Andersen Impactor. It is possible this average value is influence by a few large droplets which may not be realistic of the spray as these stages did not measure the largest numbers of culturable bacteria.

Table 5.8: Droplet size distribution averages for controlled flow experiments in the BACA over lengths 1 m and 2 m using ¼ ringers and 1 % FBS solutions.

		1 m		**2 m**	
Strain	**Suspension**	$\mathbf{D_{n50}}$	$\mathbf{D_{32}}$	$\mathbf{D_{n50}}$	$\mathbf{D_{32}}$
P. aeruginosa					
Patient mucoid	¼ ringers	0.17	3.58	0.10	2.58
	1 % FBS	0.16	3.67	1.12	9.72
Patient non-mucoid	¼ ringers	0.17	3.85	0.16	3.35
	1 % FBS	0.20	4.30	1.12	9.72
Mean (SD)	¼ ringers	0.17 (0)	3.72 (0.14)	0.13 (0.03)	2.97 (0.39)
	1 % FBS	0.18 (0.02)	3.99 (0.32)	0.64 (0.48)	7.02 (2.7)
M. abscessus					
Smooth	¼ ringers	0.16	4.41	0.44	2.83
	1 % FBS	0.16	4.15	0.17	3.44
Rough	1 % FBS	0.16	3.57	0.19	6.19
Mean (SD)	1 % FBS	0.16 (0)	3.86 (0.29)	0.18 (0.01)	4.82 (1.38)

SD is the standard deviation.

5.3.2.1 Artificial mucus

The effect of rheological properties of artificial mucus simulant samples on the size distribution and volume concentration of artificially generated droplets of *P. aeruginosa* was investigated. Number and size distribution have been theorised to be controlled through rheological properties and people with CF regularly take mucolytic agents which break down the gel structure of mucus and therefore decrease its elasticity and viscosity. Hence, it is important to gain a deeper understanding of how rheological properties affect droplet size distributions.

Initially sixty-four mucus simulant gels were created to mimic the viscoelastic prop-

erties of real mucus from people with CF. Only those mucus simulant gels that were able to nebulise in the Collison 3-jet neubliser had their shear viscosity tested. Other artificial mucus samples were excluded from the shear viscosity testing as they behaved like water and did not present a significant enough difference from the 1/4 ringers or 1 % FBS solutions. After exclusions a total of 10 artificial mucus samples had their shear viscosity measured by the Kinexus rheometer (Malvern, UK). Shear stress was set to range between 0.1 Pa–100 Pa, for comparison to the real human airway mucus samples from people with CF (Shah et al., 2005), and temperature was maintained at 20 °C.

Data on the shear viscosities of human airway mucus samples from CF patients (Shah et al., 2005) are presented in Figure 5.35. The profiles of shear stress and shear rate are complicated and hard to mimic, this can include an increase in viscosity followed by a dramatic decrease in viscosity with increased shear (Girod et al., 1992). It must be noted that this is a small sample and the airway mucus from people with CF has great variability as mucus rheological properties are tightly associated with lung function and disease status (Ma et al., 2018).

Comparing Figures 5.35 and 5.36 it is clear the complexities of the CF mucus were not replicated. The higher viscosities could have potentially been achieved by some of the artificial mucus simulant samples, as done by Hasan et al. (2010), but these would not have been able to aerosolise with the Collison nebuliser. After the turning points at around 10 Pa the CF airways mucus experience a sharp decline in viscosity and the values are comparable to the artificial mucus samples. It is these higher shear rates that that are experienced on the airway surface liquid during coughing

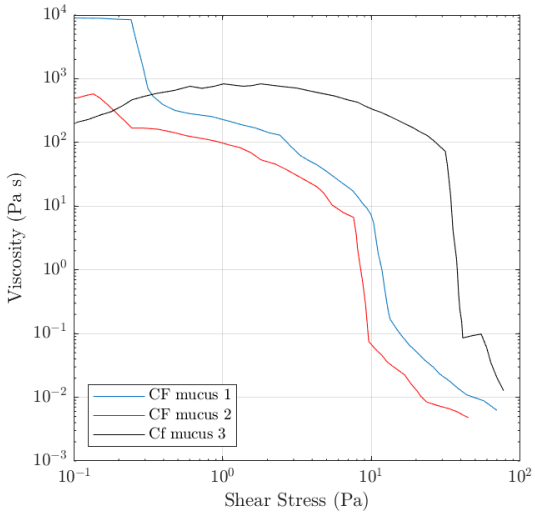

Figure 5.35: Rheological properties for real human airway mucus from people with CF. Data obtained from Shah et al. (2005)

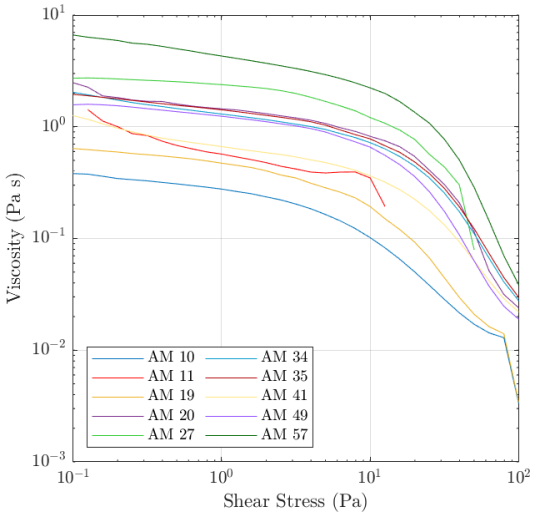

Figure 5.36: Rheological properties of multiple artificial mucus suspensions measured with the rheometer. Displayed here are the 10/64 artificial mucus (AM) samples which had their viscosity tested over varying shear stress.

(Tarran et al., 2005) and the Collison nebuliser is well known to induce shear forces (Zhen et al., 2014). The group of artificial mucus samples that all gave similar measurements followed the tail end of the CF mucus measurements the best overall. Out of these samples AM 35 was chosen as visually this was the most viscous and had 0 SDS, with no addition of SDS there was no foaming which is desirable when working with the Collison nebuliser.

Due to SARS-CoV-2 only initial experiments with the artificial mucus suspension were completed. The conditions for these experiments were not the same as those in the main series of experiments. The artificial mucus solution was inoculated with 1 ml of *P. aeruginosa* Manchester strain which had a concentration of 1×10^8 CFU ml^{-1}, resulting in a concentration of 1×10^6 CFU ml^{-1} in the suspension. *P. aeruginosa* Manchester strain was inoculated into 1/4 ringers suspension with the same concentration for comparison. Both suspensions were nebulised and measured in the BACA at 1 m and 4 m. Temperature in the chamber was 28 °C ± 2 °C. Relative humidity had a greater variation between the two experiments, during the 1/4 ringers measurements humidity was 54 % ± 2 % and for artificial mucus it was 44 % ± 1 %.

Measurements taken by the Andersen Impactor on stages 5 and 6 were close to filling all 400 holes for both experiments. When the number of colonies on the agar plate collected from the Andersen Impactor is near the maximum of 400 holes the data gathered may not be completely reliable as the air sampled may have been

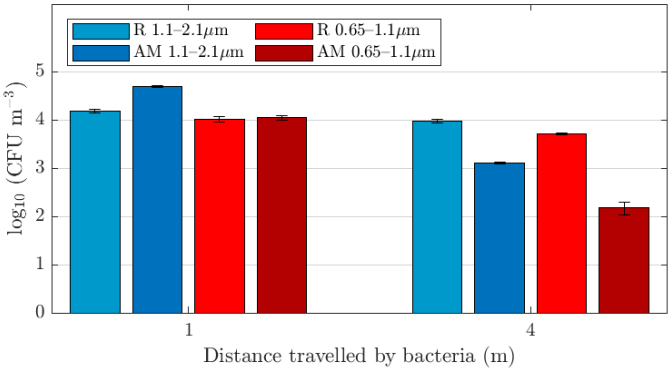

Figure 5.37: Distribution of logarithmic colony counts (CFU m^{-3}) for *P. aeruginosa* Manchester strain in 1/4 ringers and artificial mucus using the BACA at 1 m and 4 m.

able to fill more than 400 holes but was restricted by the measurement sample (Andersen, 1958). In the 1/4 ringers suspension, Figure 5.37 displays a smaller reduction in colony counts to that seen previously in section 5.3.1. Interestingly, while the artificial mucus suspension seems to have comparable colony counts at 1 m to the 1/4 ringers suspension, by 4 m there was a much more significant drop in the colony counts for the artificial mucus suspension. This difference could be due to the sampling being close to the maximum concentration possible, and therefore restricting the concentrations measured at 1 m. It is also a possibility that something in the make up of the artificial mucus solution is decreasing the microorganism survivability over time at a much faster rate compare to the 1/4 ringers solution. In both cases it is noticeable that stage 5 has the most culturable bacteria at both lengths, with a more significant difference by 4 m.

The cumulative frequency and volume frequency, Figure 5.38, are dominated by the large proportion of volume allocated to droplets greater than 100 µm. As discussed previously droplets of this size with high volume frequencies are most likely noise and reducing the volume frequency for other droplet sizes. The pattern of peaks seen throughout this series of experiments, less than 1 µm, just above 1 µm, around 10 µm and between 100 µm–1000 µm, is there but it is not as clear as previous data. Visually there is no observed difference between the artificial mucus and the 1/4 ringers solution for the overall volume frequency distributions. In addition, the distance does not affect the droplet size distributions, but large droplets which are likely not from the aerosolised bacterial suspension are not as dominant at the 4 m measurements.

Inspecting the data set on the Andersen Impactor range Figure 5.39 displays a

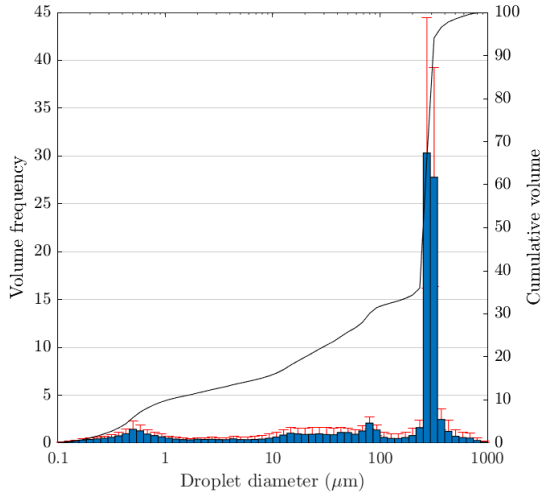

(a) 1/4 ringers at 1 m.

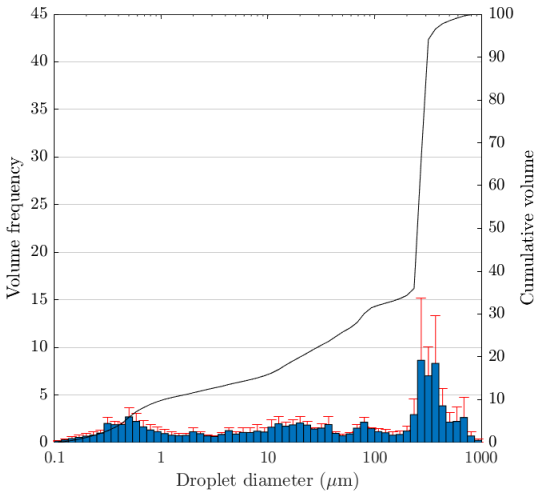

(b) 1/4 ringers at 4 m.

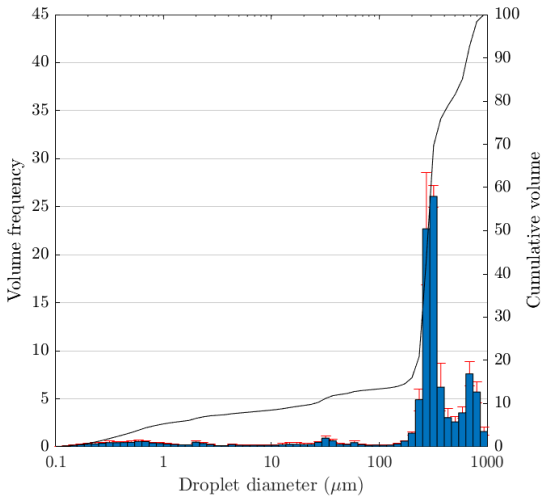

(c) Artificial mucus at 1 m.

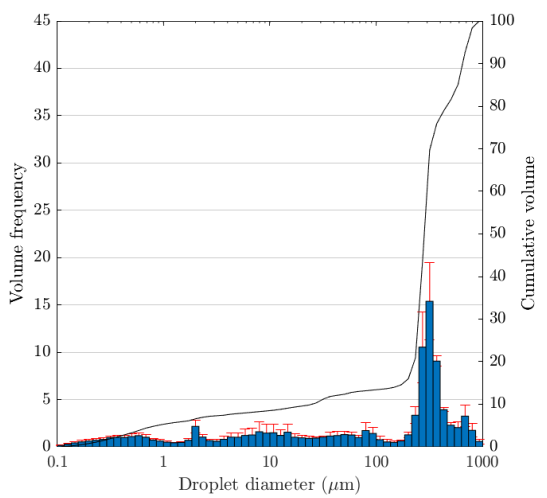

(d) Artificial mucus at 4 m.

Figure 5.38: Cumulative volume and volume frequency of aerosolised *P. aeruginosa* Manchester strain in 1/4 ringers (R) and artificial mucus (AM) using the BACA at 1 m and 4 m.

similar pattern for both the 1/4 ringers and artificial mucus suspensions in the volume frequency and number fraction distributions. Stages 5 and 6 have the largest volume frequencies, but these plots do not show the peak at stage 5 like the measured data in sections 5.3.1 and 5.3.2. Number fraction plots are dominated by the smaller droplets and this is observed for both suspensions. Therefore, the Spraytec device was not able to detect a difference between 1/4 ringers and the artificial mucus sample for aerosolised droplets of *P. aeruginosa* Manchester strain using the Collison nebuliser.

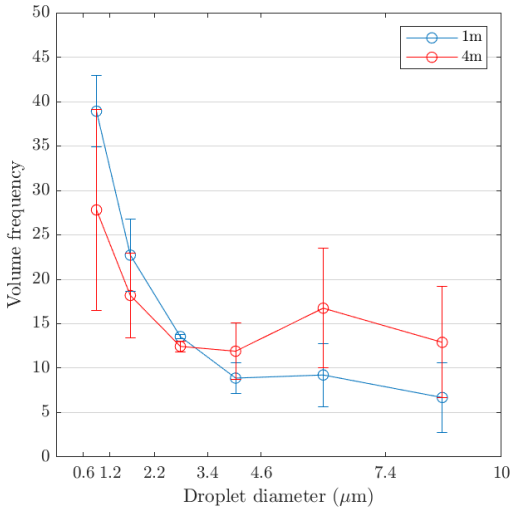

(a) 1/4 ringers volume frequency.

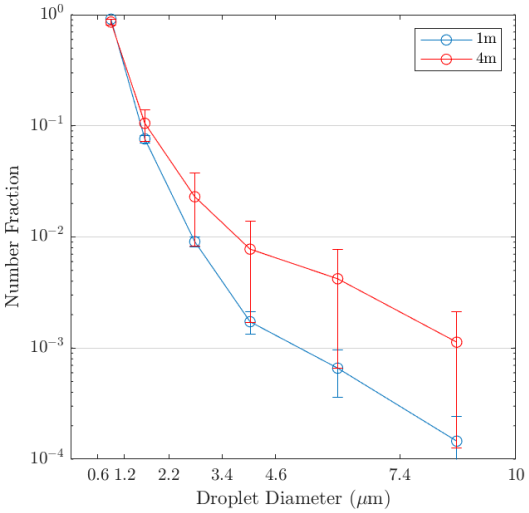

(b) 1/4 ringers number fraction.

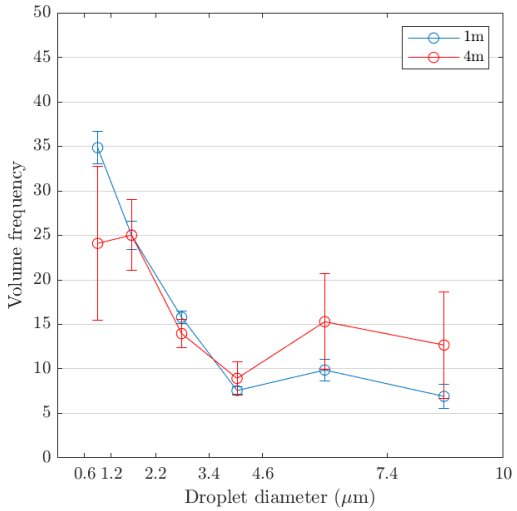

(c) Artificial mucus volume frequency.

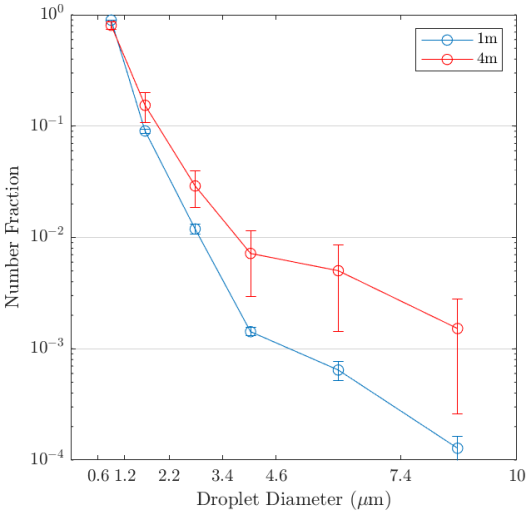

(d) Artificial mucus number fraction.

Figure 5.39: Droplet size distribution truncated for the Andersen Impactor size range produced by aerosolising *P. aeruginosa* Manchester strain in 1/4 ringers and artificial mucus using the BACA at 1 m and 4 m.

5.4 Evaporation analysis

Evaporation analysis on the droplet size distributions measured by Spraytec allowed a predicted evaporated droplet size distribution to be compared to measured evaporated distributions. This analysis also provided an evaporated total volume of the bacterial suspension that passed through the Spraytec laser on measurement. This allowed a calculation of the number of droplets size distributions at evaporated lengths.

Distributions measured at 0 m into the air (section 5.2.2) were assumed to be an un-evaporated distribution. These 0 m distributions were taken with the nozzle of the Collison nebuliser at 0 m from the Spaytec laser, the humidity inside the nebuliser and the nozzle was assumed to be 100 % and therefore the aerosolised droplets leaving the nozzle at 0 m were not evaporated.

The output of data measured by Spraytec was a log histogram. The geometric mean diameter was found for each size bin and was used to determine a representative droplet volume, v, for each bin. The un-evaporated volume (ml) for each suspension was calculated as described by section 5.1.3 and transformed to μm^3, the same units as the droplet volumes. Knowledge of the un-evaporated total volume allowed a proportion of this volume to be allocated to each size bin based on the bins volume frequency, this was called the bin volume, V_{bin}. Next, the number of droplets, N, in each bin was determined by the following:

$$N = \frac{V_{bin}}{v}. \tag{5.14}$$

Number of droplets, N, was used to calculate a total evaporated volume for each suspension. First, the evaporated geometric mean diameter of each bin was calculated using equation (5.9). Secondly, this value was used to calculate the new evaporated droplet volumes, v_{evap} and the predicted total evaporated volume was calculated by,

$$V_{tot} = \sum \left(N \times v_{evap} \right). \tag{5.15}$$

This value was calculated for two suspension, 1/4 ringers and 1 % FBS.

After finding the evaporated droplet volume the aims for this section of analysis were as followed:

1. Compare the volume frequency distributions of the predicted evaporated distribution to a measured evaporated distribution.

2. Interpret the number of droplets from the volume frequency distributions.

To compare the prediction to the measured evaporated distributions volume fraction for each bin, VF, was found for each suspension by,

$$\mathrm{VF} = \left(\frac{N \times v}{V_{tot}}\right) \times 100. \tag{5.16}$$

The values of volume frequency were assigned to an original bin size for comparison with the measured distribution. Anything less then 0.1 µm was ignored as this was the lower limit of Spaytec and would not have been recorded and so the volume distribution was adjusted over the new size range. Figure 5.40 displays the original 0 m distribution with a volume distribution following full evaporation of the droplets. As highlighted in section 5.1.4, this evaporation happens within a fraction of a second for the droplet size ranges of interest, and hence measurements in the BACA at 1 m and beyond are assumed to be fully evaporated.

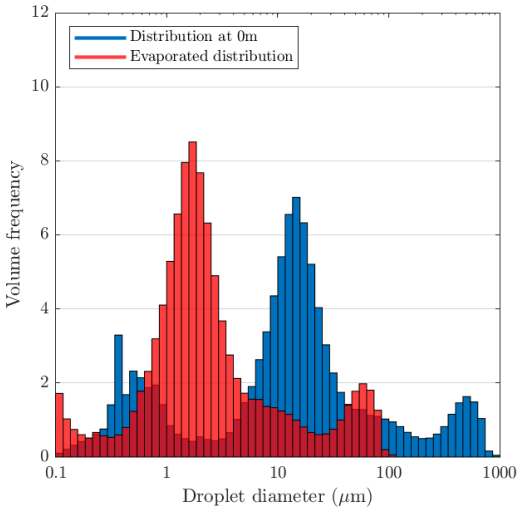

Figure 5.40: Comparison of a typical volume frequency droplet size distribution at the un-evaporated length of 0 m and the corresponding predicted volume distribution following evaporation to the minimum size (determined by the non-volatile concentration).

The total evaporated volume, V_{tot}, of each suspension was used to calculate a number frequency distribution from the measured Spraytec data. Number of droplets, N, within each bin size range were computed by the following equation,

$$N = \frac{\mathrm{VF} \times V_{tot}}{100 \times v}. \tag{5.17}$$

5.4.1 Evaporated vs measured distributions

The first aim was to compare predicted evaporated distributions to the volume frequency distributions at their minimum size. Figure 5.41 displays the comparisons for two strains of *P. aeruginosa*, environmental and Manchester, the other strains Figures B.21–B.25 are in the appendix due to the number of plots and their similarity. The evaporated distributions in blue show a prominent peak at around 1 µm, in droplet size distributions of *P. aeruginosa* and *M. abscessus*, this could be expected due to the size of the microorganisms the droplets could be carrying. The red distribution is the evaporated distribution measured at 1 m, in the Manchester strain this fits relatively well, both distributions follow similar peaks and troughs; excluding what is above 100 µm. There is a split peak around 1 µm that is not observed in the predicted evaporated distributions, it is a possibility that some droplets containing microorganisms are not evaporating and splitting the peak, but the number of droplets measured is much larger than the of bacteria released and questions the likelihood. Furthermore, the other distributions do not match as well and look like they have been shifted to the left. This implies the 0 m distribution which was evaporated may have already evaporated for some distributions as it happens in a fraction of a second and the Spraytec device was not able to measure an un-evaporated distribution.

The size range was reduced to the Andersen Impactor size range and the resulting data for volume frequency for *P. aeruginosa* environmental and Manchester strains

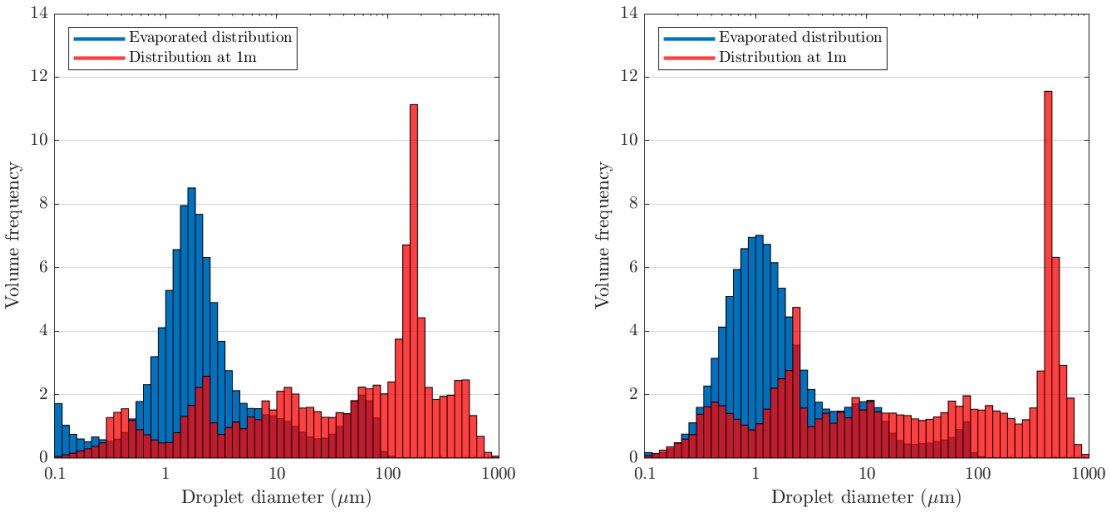

(a) Environmental (b) Manchester

Figure 5.41: Comparison of predicted evaporated volume frequency droplet size distribution and droplet size distribution of aerosolised *P. aeruginosa* strains in 1/4 ringers at 1 m in the BACA.

is displayed in Figure 5.42. The other strains of *P. aeruginosa* and *M. abscessus* are displayed in Figures B.26–B.30 in an appendix. Focussing on this truncated droplet size range shows a different picture and the predicted evaporated distributions and the volume frequency distributions are comparable over all bacterial strains.

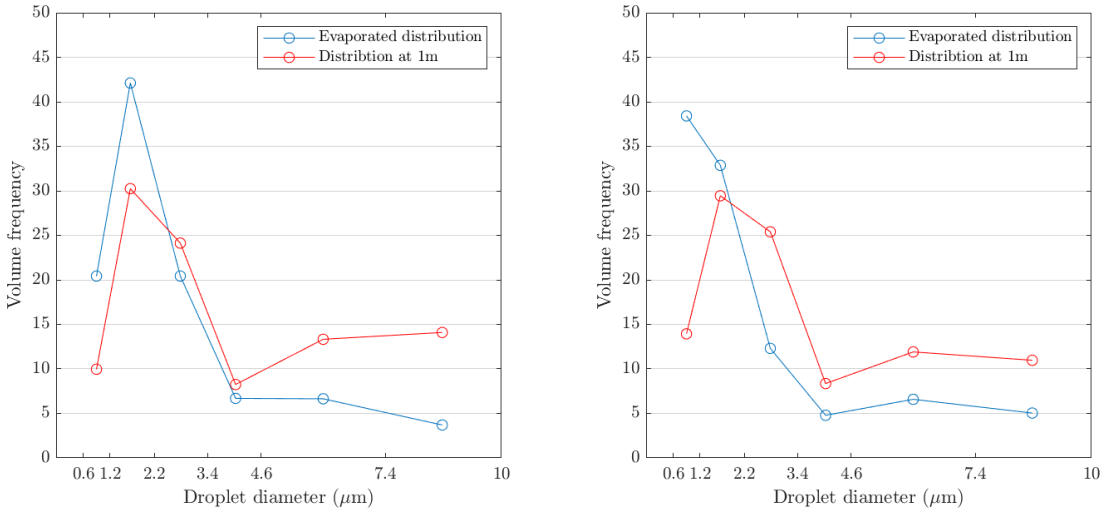

(a) Environmental (b) Manchester

Figure 5.42: Comparison of predicted evaporated volume frequency droplet size distribution and droplet size distribution of aerosolised *P. aeruginosa* strains in 1/4 ringers at 1 m in the BACA truncated to the Andersen Impactor size range.

5.4.2 Number of droplets

The second aim was to use the data from the evaporated distribution in air to interpret the number of droplets measured by the Spraytec device. Figure 5.43 gives an example of the number of droplets distributions measured by Spraytec of artificially generated aerosols of *P. aeruginosa* and *M. abscessus*. The figure is displayed on a log scale because of the number of droplets less than 1 µm dominated the overall distributions. There are a greater number of droplets at 0 m than 1 m but this is also a consequence of the calculation. Importantly there is a shift to the left in the distrubtions from 0 m to 1 m, this is a shift to smaller droplets. This implies that the droplets have undergone evaporation. The bacteria do not appear to have any effect on the number distribution, but the number of bacteria released was 10^4 for *P. aeruginosa* and 10^3 for *M. abscessus* and comparing these values to the number of droplets measured it is unlikely that they will have a significant impact on the number distribution.

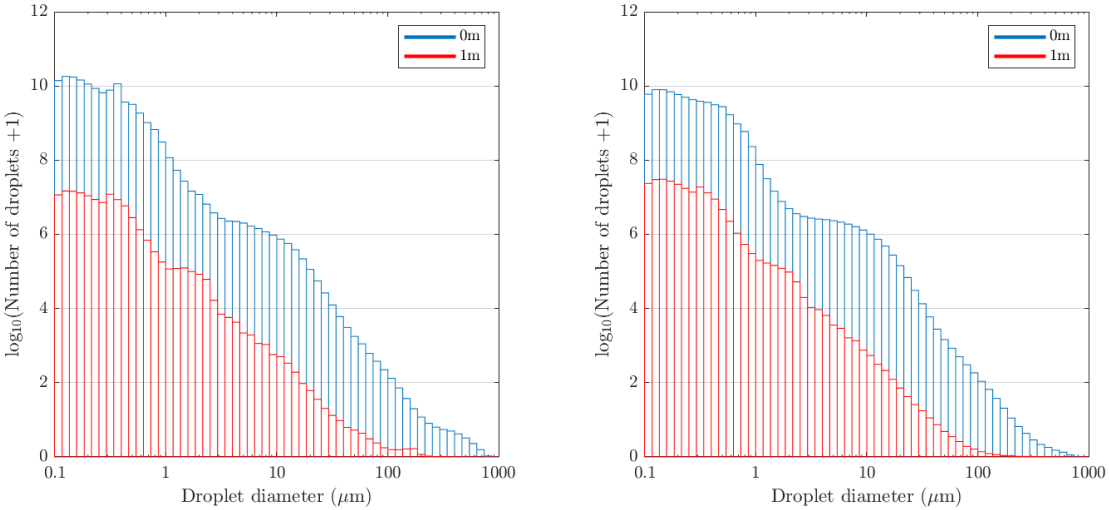

(a) *P. aeruginosa* environmental (b) *M. abscessus* smooth

Figure 5.43: Comparison of logarithmic droplet size distribution produced by aerosolising bacterial strains in ¼ ringers using the BACA at 1 m and 2 m

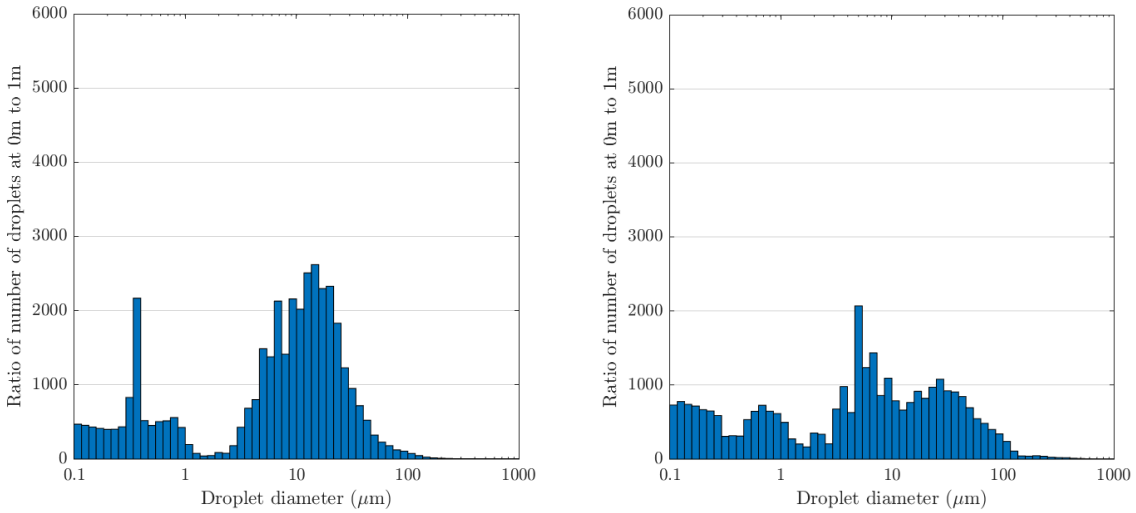

(a) ¼ ringers. (b) 1 % FBS.

Figure 5.44: Ratio of one droplet at 1 m using the BACA to number of droplets at 0 m in air after aerosolisation of *P. aeruginosa* patient mucoid in two suspensions.

Figure 5.44 presents the ratios for *P. aeruginosa* patient mucoid strain and Figure 5.45 presents the data for the *M. abscessus* smooth strain, for the other bacterial strains their data is in Figures B.31–B.33 in an appendix. The ratio is between 1 droplet at 1 m to the number of droplets at 0 m. There appears to be a difference in the ratios between the ¼ ringers and the 1 % FBS suspensions, this could be a consequence of the difference in their volume frequency distributions from the measurements of the nebulised aerosols in air (section 5.2.2). The main differences

in number of droplets are found at around 10 µm and just below 1 µm which correlate to the peaks observed in section 5.2.2. There is a trough in the ratio number just above 1 µm and these are the size droplets that are most likely carrying bacteria and potentially be influencing this lack of change. However, the likelihood of this comes into question when examining the difference between total number of droplets and number of bacteria released.

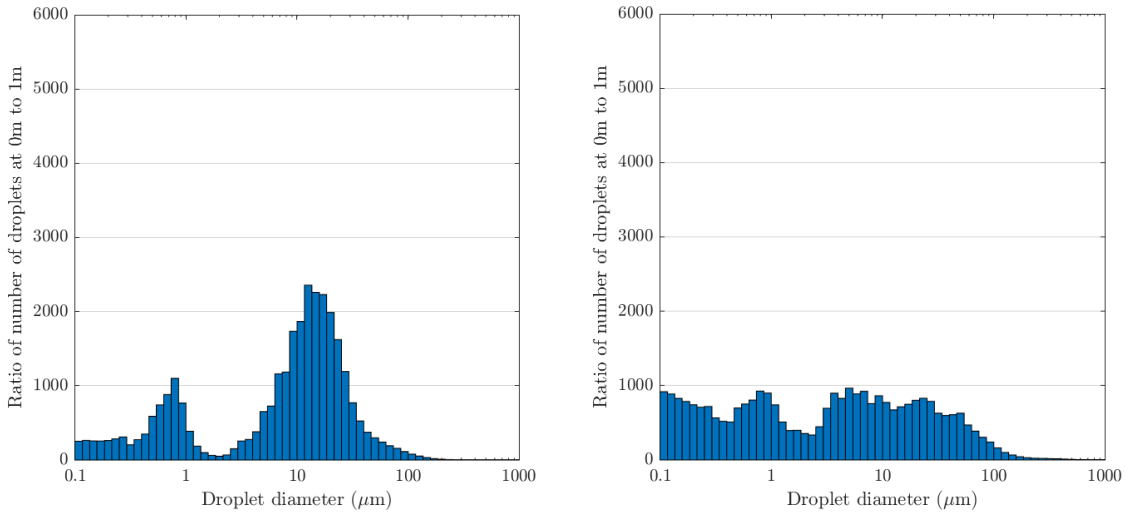

(a) 1/4 ringers.

(b) 1 % FBS.

Figure 5.45: Ratio of one droplet at 1 m using the BACA to number of droplets at 0 m in air after aerosolisation of *M. abscessus* smooth in two suspensions.

5.5 Summary

Measurements of fluid properties showed that the presence of bacteria did not have a noticeable influence. Investigation into whether *P. aeruginosa* could influence surface tensions found the presence of the microorganisms did not significantly impact on the properties of the suspension fluid at the concentrations measured. Key non-dimensional numbers such as the Weber and Ohnesorge number would not have altered with the small changes measured and it was therefore assumed in subsequent experiments that droplet size distributions were not affected by a change in surface tension caused by *P. aeruginosa*.

The culturable droplet size distributions showed a difference between the different strains of *P. aeruginosa*; the environmental strain had the best survival. The Manchester epidemic strain (non-mucoid) showed greater survivability than the Newcastle epidemic strain (mucoid) and the difference in their morphotypes did not appear

to make a difference, but the patient mucoid strain had higher colony counts than the non-mucoid morphotype. Comparing the normalised decay curves of *P. aeruginosa* strains and *M. abscessus* smooth demonstrated that *M. abscessus* decayed at a slower rate than *P. aeruginosa*, this was backed up by the predicted number of bacteria released into the BACA and the raw colony counts. Despite this all bacteria were easily able to survive for up to 4 m without much decay and the majority of droplets were of the size 1.1 µm–2.1 µm. The smooth morphotype of *M. abscessus* had higher concentrations of bacteria measured by the Andersen Impactor than the rough morphotype, although the results for *M. abscessus* in the 1 % FBS are less certain as there were very low colony counts which could be due to the hydrophobicity of *M. abscessus* and foam fractionation.

The decay rate measured for both *P. aeruginosa* and *M. abscessus* was rapid when compared with artificially generated aerosols of *P. aeruginosa* into an environmentally controlled chamber (Clifton et al., 2010) and cough generated aerosols of *P. aeruginosa* from people with CF (Knibbs et al., 2014). However, the timescales to calculate the decay in these experiments were short (80 s) and it is likely the bacteria experienced rapid initial die off possibly as a result of the experimental conditions. Clifton et al. (2008) conducted a similar experiment and the data suggested a similar rapid die off concluding that *P. aeruginosa* may experience rapid die off at short timescales, but this requires further investigation.

Neither the short range nebuliser aerosol characterisation experiments or the controlled flow aerosol characterisation experiments were able to detect a difference in the droplet size distributions for *P. aeruginosa* and *M. abscessus*. This was likely because the number of bacteria released had a maximum of the order of 10^4 for *P. aeruginosa* and the order of 10^3 for *M. abscessus* and comparing these values to the number of droplets measured it is unlikely that they would have had a significant impact on the number distribution. In conclusion bacterial strain did not affect the droplet size distribution for these experiments.

Measurement of culturable droplet size distributions with the Andersen Impactor demonstrated that for *P. aeruginosa* 1 % FBS improved the survivability particularly for small droplets on stages 5 and 6 (0.65 µm–2.1 µm). However, this was not the case for *M. abscessus* and 1 % FBS resulted in lower colony counts on all stages. The low number of colonies implied that it was possible that the hydrophobicity of *M. abscessus* played a role in foam fractionation and *M. abscessus* was not aerosolised homogeneously in 1 % FBS. The artificial mucus sample that was tested had comparable colony counts at 1 m to the ¼ ringers suspension, but at 4 m there was a significant drop in the colony counts for the artificial mucus compared to the

¼ ringers suspension. This difference could be due to the sampling being close to the maximum concentration possible, and therefore restricting the concentrations measured at 1 m.

The nebuliser aerosol characterisation of droplets on glass slides found no difference between the ¼ ringers and 1 % FBS suspensions. However, the volume frequency distributions measured by Spraytec in the air at short ranges presented a different pattern in the volume frequency. Overall volume frequency distributions did not appear to be affected by suspension fluid, but a difference was observed between ¼ ringers and 1 % FBS when truncated to the Andersen Impactor size range. The Spraytec device was not able to detect a difference between ¼ ringers and the artificial mucus sample for aerosolised droplets of *P. aeruginosa* Manchester strain using the Collison nebuliser. All number fraction plots were dominated by the small droplets and therefore no difference were observed in the distributions. These data suggest it is possible that suspension alters the droplet size distributions; however, the inconsistencies and small sample size conclude that there needs to be further investigation to determine if this is the case.

Correlations can be drawn between the Andersen Impactor samples and the Spraytec data. The majority of the volume frequency plots, in particular those for ¼ ringers suspension, over the Andersen Impactor range demonstrated a clear peak at stage 5. Stage 5 was found to be the stage with the greatest concentration of bacteria for all experiments ran using the BACA for both bacteria. However, this series of experiments has shown that droplet size distribution data alone does not give sufficient information on microbial droplets and it is important to measure the culturable distributions too. The overall distributions in these experiments were not representative of the culturable data.

Droplet size distributions measured on the glass slides found bimodal distributions with peaks at 0.8 µm–1 µm and roughly 1.5 µm. This split peak was observed in evaporated distributions measured by Spraytec using the BACA. Other similarities with the distributions found average droplet sizes to be large enough to carry microorganisms but small enough to remain suspended in air. The D_{n50} for the Spraytec data using the BACA was less than 1 µm and confirmed that the majority of droplets measured were too small to carry either *P. aeruginosa* or *M. abscessus*. The Sauter mean was larger than D_{n50} and represented an average size of droplets in the Andersen Impactor range. This was larger than stage 5, the dominant stage, but was potentially influenced by larger droplets that were measured but not realistic for the aerosolised bacteria.

Predicted evaporated distributions compared to the measured evaporated distributions at 1 m in the BACA showed some similarities, in particular over the Andersen Impactor size range, but there was also many differences. Some of the distributions looked shifted and what was used as the un-evaporated distributions may have been in fact evaporated in some cases as evaporation of droplets of this size occurs in a fraction of a second. Although, predicting the number distributions demonstrated a shift to the left representing an evaporation towards smaller droplets from 0 m to 1 m.

In conclusion, it is a challenge to measure the droplet size distributions of artificially generated aerosols of small droplet sizes, many of the droplets measured may not be realistic of the generated aerosol and it is difficult to distinguish between what is real and what is noise. To observe any evaporation the distance needed to be extremely small, which could incur error, as evaporation of small droplets happens in a fraction of a second. In addition, Spraytec does not provide data on the number of droplets and this does not make it easy to get accurate numbers. Furthermore, when measuring microorganisms Spraytec and optical particle counters in general cannot be relied on alone as there was large difference between the number of bacteria released versus the total droplet count and the nuances between the different bacteria will not be observed with overall droplet size distributions. Therefore, the Spraytec device is not recommended for use alone when measuring droplet size distributions of bioaerosols.

Chapter 6

Cough aerosol sampling: A cross-sectional study

Many papers have highlighted evidence for the potential of bacteria to be released in respiratory droplets and to be transmitted via the airborne route. Chapter 5 gave further evidence to support this potential transmission route, and *P. aeruginosa* has been shown in respiratory aerosols in a clinical Australian study. However, there is no robust evidence for *P. aeruginosa* and *M. abscessus* in respiratory droplets in a climate similar to the United Kingdom. The cross-sectional study obtained cough/exhaled breath bioaerosol data from people with CF, to seek to determine if these bacteria are aerosolised in respiratory droplets. The use of a cross sectional study is important in providing an evidence base from a representative subset of the CF population to determine behaviours of respiratory droplets outside the laboratory environment.

6.1 Overview

A cross sectional study was conducted which quantified bacterial load and measured droplet size distributions and viability of *P. aeruginosa* and *M. abscessus* in cough/exhaled breath samples from people with CF in an inpatient and outpatient hospital setting. These samples were measured using a modified cough aerosol sampling system (CASS) that had been developed for measuring cough generated aerosols of *Mycobacterium tuberculosis* (Fennelly et al., 2004) and a non-invasive Mask sample (Williams et al., 2014). These approaches have aided in determining that it is possible to detect *P. aeruginosa* and *M. abscessus* within aerosols generated by people with CF and the droplet size distributions of these aerosols within the UK climate and hospital setting. Thus, providing evidence for the possibility of airborne transmission. Background data on the patients and the study groups have provided preliminary information to evaluate how time of day, exacerbation, and medication can have an effect on the droplet characteristics.

6.2 Objectives

The study was conducted on the CF unit at St James University Hospital Leeds Teaching Hospitals Trust (LTHT) during 2019/2020, which is under the management of Leeds Centre for Respiratory Medicine. This study was managed under the clinical supervision of Dr. Ian Clifton at LTHT and in collaboration with Prof. Michael Barer and Dr. Caroline Williams at the University of Leicester.

The primary aim for this study was:

1. To measure the presence of *Pseudomonas aeruginosa* and *Mycobacterium abscessus* in cough/exhaled breath aerosols from adults with CF.

The three secondary aims of this study were:

2. To characterise total bacterial load and the particle size distribution of cough and exhaled breath aerosols from adults with CF.
3. To compare the number of bacteria containing aerosols and detection of *Pseudomonas aeruginosa* and *Mycobacterium abscessus* with a CASS and mask sampling approach.
4. To gain preliminary data to inform future studies on the influence of time and treatment on droplet size distributions and presence of *Pseudomonas aerug-*

inosa and *Mycobacterium abscessus* in cough/exhaled breath aerosols from adults with CF.

6.2.1 Rationale

Rationale for aim 1: There are several pathogens that concern people with CF; this study focussed on detecting two which are selected due to their clinical importance. *P. aeruginosa* is the most common pathogen causing chronic infection in those with CF. *M. abscessus* is a newly emerging pathogen which is becoming increasingly recognised as a concern in people with CF. It has been shown that people with CF produce viable *P. aeruginosa* bacterial aerosols while coughing or through exhaled breath in an Australian study (Wainwright et al., 2009) and it is hypothesised that this is the same for *M. abscessus*. Detecting these pathogens in aerosols would provide clear evidence to support the need for enhanced airborne infection control precautions in a UK setting.

Rationale for aim 2: Particle size distribution is a key factor in determining where a droplet can deposit within the respiratory tract and its ability to remain airborne in a room. The study measured size distributions of the viable bacterial count in cough/exhaled breath. Outcomes of the patient sampling study were compared to the laboratory experiments (Chapter 5) in section 7.1 and can provide valuable input data for mathematical models to enable a more realistic assessment of airborne transmission risk. This will be of specific benefit to understanding how to change infection control strategies on respiratory wards.

Rationale for aim 3: Easily detecting whether a patient is producing an infectious aerosol is beneficial for determining appropriate infection control precautions. The CASS is a proven method for detecting bacterial aerosols in breath, but is cumbersome to use and not appropriate for widespread use in a clinical setting. A mask however presents a very straightforward method for easily taking an aerosol sample. By verifying the application of this approach, the study will provide data to support whether this is a viable future method as part of an infection control strategy. This will have benefits for the clinical team and people with CF. Currently people with CF are restricted in their close personal interactions with each other for infection control reasons. Having greater certainty about whether a person is infectious or not will enable decisions around such interactions to be evidence based.

Rationale for aim 4: Changes to the rheology of a liquid has been shown to change the droplet size distributions. In particular, reducing the viscosity reduces droplet

sizes (Hasan et al., 2010). People with CF take medication that alters the viscosity of their sputum and it is hypothesised that this may reduce the size of the droplets in cough aerosols making them more likely to remain airborne. Determining whether medication affects the generation of bioaerosols or the droplet size distributions could impact when patients take their medication in hospital to reduce the risk of airborne transmission. Furthermore, it is likely that the aerosol produced by a participant will change over the duration of their treatment and possibly through the day. For resource reasons and participant comfort, it was not feasible to take numerous samples from each participant. However, four samples per person with *P. aeruginosa* in were taken over two sessions and four samples were taken per person with *M. abscessus*, this gave preliminary data on whether total bacterial aerosol load or size distribution changed with time and treatment.

6.3 Study methodology

6.3.1 Study location

The study was conducted on the CF unit at St James University Hospital LTHT. The unit consists of twelve inpatient single bed rooms with en-suite facilities and four single patient side rooms for outpatient clinics. All patients on the unit are part of the LTHT adult CF clinic. Many of the patients have chronic respiratory infections due to the nature of CF and there are strict infection control policies in place, the patients stay in their own rooms and do not interact with each other. Recruitment, background data, and aerosol samples were all taken in the single patient rooms on site where each participant was located.

6.3.2 Consent and recruitment

Participants were recruited from adults with CF who had chronic infection with *P. aeruginosa* and/or *M. abscessus* and are treated by the CF unit in Leeds Teaching Hospitals NHS Trust. For ease convenience sampling was used; all adults with CF at the clinic during the study period were potentially eligible for the study. During the study period a clinical member of the research team invited individuals to participate in the study and provided a participant information sheet, Appendix C.2. The participant information sheet provided described the nature and objectives of the study and any potential risks involved. If a participant wished to participate

in the study a clinical member of the research team assessed for eligibility. Once eligibility was confirmed participants were able to ask further questions to members of the research team and a clinical member of the research team sought consent. All potential participants were given sufficient time to give written informed consent to take part in the study. Following informed consent, each study participant was randomly issued with a study ID from numbers 01–99 to allow for anonymisation of the study data and were allocated to a group (section 6.3.3). A letter to the participants GP was sent to inform them of their participation in the study, this letter and the consent form were recorded in the study master file and the participants medical records. The identity of each study ID was recorded in the study master file and was stored according to Good Clinical Practice Guidelines, the study master file was only accessed by clinical members of the research team. Ethical approval (Ref: 18/SC/0654, Appendix C.1) was granted by the Research Ethics Committee, Health Research Authority and LTHT.

6.3.2.1 Inclusion/exclusion Criteria

During the design of the study the following were decided upon for inclusion and exclusion criteria in conjunction with the clinical lead.

The following gives the list of inclusion criteria:

- Adult (≥18 years).
- Ability to provide informed consent.
- Diagnosis of CF as defined by ECFS guidelines.
- One or both of:
    - Chronic *P. aeruginosa* infection as defined by Lee et al. (2003).
    - Chronic *M. abscessus* infection as defined by recent BTS NTM guidelines (Haworth et al., 2017) .
- A patient of the Leeds Regional Adult CF unit at the time of sampling.

The following gives the list of the exclusion criteria:

- Was involved in a interventional medical trial at the time of sampling.
- Forced expiratory volume in 1 s (FEV_1) <30%.
- Known infection with MRSA, *Mycobacterium tuberculosis*, influenza or *Burkholderia cepacia* complex.

- Known pregnancy.
- Previous history of cough syncope or vomiting associated with coughing.

6.3.3 Groups

During the study each participant was allocated into one of the three even groups, group A, B or C. Definitions of the groups including timings and samples taken are provided in Table 6.1.

Participants infected with chronic *P. aeruginosa* and not *M. abscessus* were randomly allocated to group A or B. Random allocation was completed through block randomisation with a block size of two, this method was designed to randomise participants into two groups of equal size.

6.3.3.1 Withdrawal from the study

A participant was able to withdraw from the study at any time due to medical/personal reasons or if they were no longer eligible. Each participant was asked before commencing the second sampling session if they give their consent to continue. Data from partial samples was still used in the study unless consent was withdrawn, with the analysis adjusted as appropriate to deal with reduced time or replicates.

A flow chart describing the study process from recruitment to processing and analysis of data is given in Figure 6.1.

Table 6.1: Definition of the three groups used in the cross-sectional study.

Group	**Chronically infected with**	**Timings of samples**	**Samples taken in session 1**	**Samples taken in session 2**
A	*P. aeruginosa* and not *M. abscessus*	Start (first two days) and end (last two days) of hospital stay/IV treatment.	Three samples. Mask, CASS with Andersen Impactor and sputum.	One sample. CASS with Andersen Impactor.
B	*P. aeruginosa* and not *M. abscessus*	During one day, morning and afternoon, any time during hospital stay/IV treatment. Ensured physio/medication was taken in between.	Three samples. Mask, CASS with Andersen Impactor and sputum.	One sample. CASS with Andersen Impactor.
C	*M. abscessus* not excluding those also infected with *P. aeruginosa*	Any time the participant attended the cystic fibrosis unit.	Four samples. Mask, CASS with Andersen Impactor and AGI-30 and sputum.	N/A

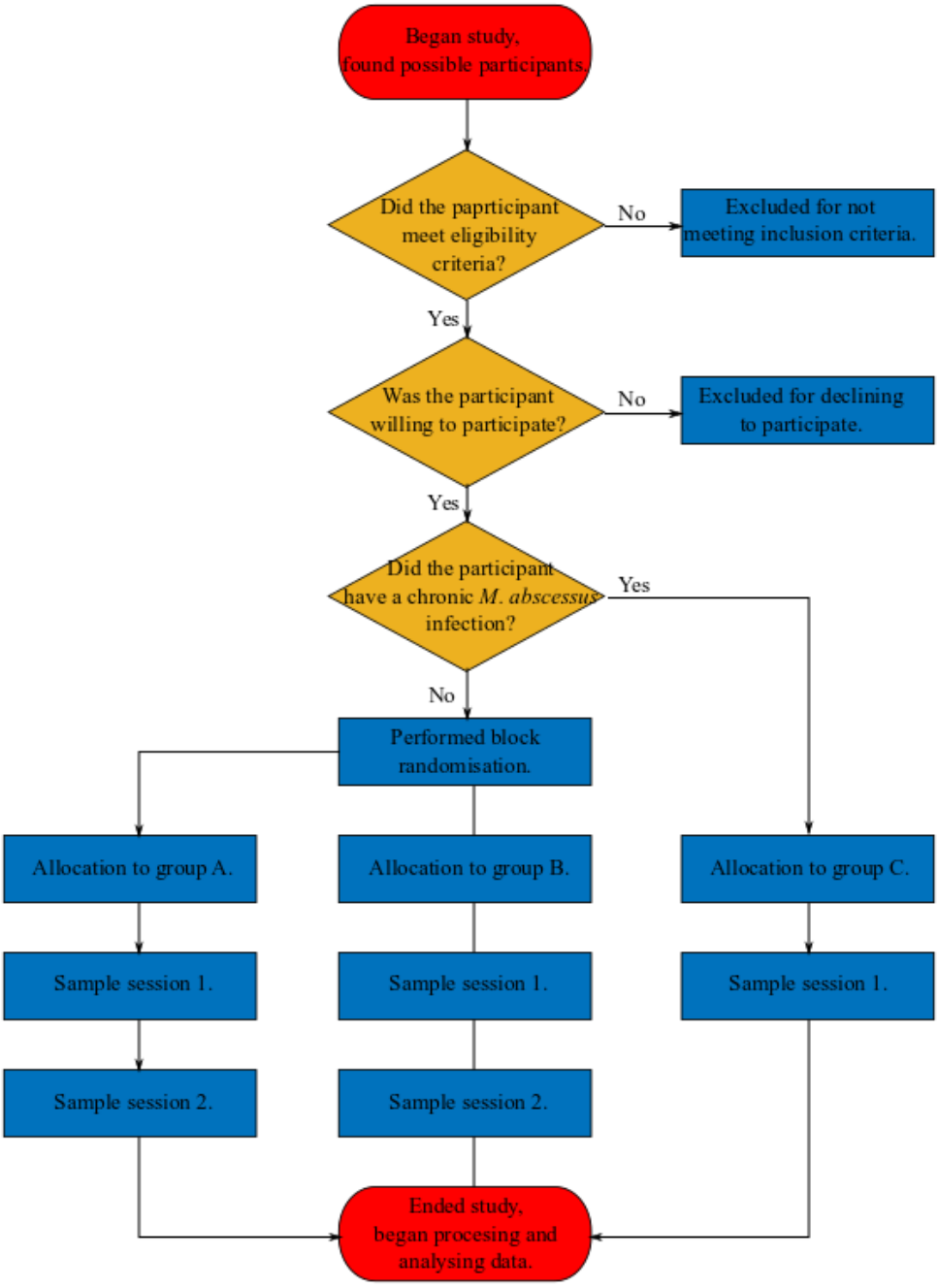

Figure 6.1: Flow chart describing the steps taken in the study from recruitment to processing and analysis of data.

6.3.4 Sampling methods

6.3.4.1 Sample size

In a review on calculating sample sizes in medical research Charan and Biswas (2013) stated the sample size, n, in a study estimating the prevalence parameter within a population is given by:

$$n = \frac{\left(Z^2_{1-\alpha/2} p(1-p)\right)}{\beta^2} \tag{6.1}$$

where:

α = probability of a type I error,
$Z^2_{1-\alpha/2}$ = standard normal variate,
p = expected proportion from previous studies,
$1-\beta$ = power,
β = probability of the type II error.

In the case of this study the statistical significance level was chosen to be 95%; hence, $\alpha = 0.05$ and $Z^2_{1-\alpha/2} = 1.96$. Power was chosen as $1-\beta = 0.9$, which gave a statistical probability of a 90% chance of detecting the presence of *P. aeruginosa* or *M. abscessus* in cough aerosols. The value p was calculated using data from previous studies. Wainwright et al. (2009) conducted a study which found *P. aeruginosa* in cough aerosols in 25 out of 26 patients infected with chronic *P. aeruginosa*. This gave evidence to assume $p = 0.96$ for the *P. aeruginosa* case. Sample size was calculated using (6.1),

$$n = \left((1.96)^2 \cdot 0.96(1-0.96)\right)/(0.1)^2 \approx 15.$$

At the point of designing the cross-sectional study there was no data on capturing *M. abscessus* in cough aerosols and it was not possible to use this calculation for sample size. However, it was expected for *M. abscessus* to be as prevalent in cultures as *P. aeruginosa* due to laboratory experiments showing both *P. aeruginosa* and *M. abscessus* can be aerosolised, survive in air for up to 45 minutes, travel up to 4 m (Clifton et al., 2008; Clifton, 2009; Fletcher et al., 2016; Taylor, 2016), and can be cultured in a laboratory with a similar ease. Therefore, the decision was made to recruit fifteen patients to each group with chronic *P. aeruginosa* and fifteen patients with chronic *M. abscessus*.

6.3.4.2 Sampling order

During a sample session participants were randomly allocated a sampling sequence, CASS (section 6.3.4.5) or mask (section 6.3.4.6) first. This was completed using the random study ID for each participant, if the first number was even (including 0 in this case) participants would sample with the mask first, if the number was odd the participant would sample with the CASS first. When CASS sampling, if participants sampled with the AGI-30 impinger this was the first CASS sample. This was followed by a second CASS sample using the Andersen Impactor. The following list describes the order of how a sample session was conducted in this study.

1. Began recording environmental air quality data in participants room, this was recorded throughout the sampling session.
2. Room air biological sampling.
3. Asked participant to provide sputum sample when possible.
4. First cough/exhaled breath sample in sampling sequence, mask or CASS.
5. Second cough/exhaled breath sample in sampling sequence, mask or CASS.
6. A clinical team member and the research team filled in source data.

Participants in groups A and B took part in two sampling sessions. In the second sampling session only CASS sampling using an Andersen Impactor took place, there were no extra sputum or mask samples. Only group A had data sets from each sampling session on the total viable count of background room air, as those sampling sessions were on different days.

6.3.4.3 Room air quality and environmental data

Air quality in participant rooms on the CF unit was taken; each participant was in a single room. This was measured using a stand-alone data logger (AirVisual) that recorded CO_2, temperature, humidity, $PM_{2.5}$ and PM_{10}. The data logger was placed in the participants room for up to one working day on the day of sampling. Data from the loggers were collected at 10 second intervals for the first 10 minutes followed by 5 minute intervals thereafter and stored electronically.

Prior to the start of the study all patient rooms on the CF unit were accessed and dimensions of the rooms were recorded. There are three main layouts of patient rooms on the unit, see Figure 6.2 for plan of the ward. South-east facing rooms have windows which face the front of the building, these rooms get direct sunlight

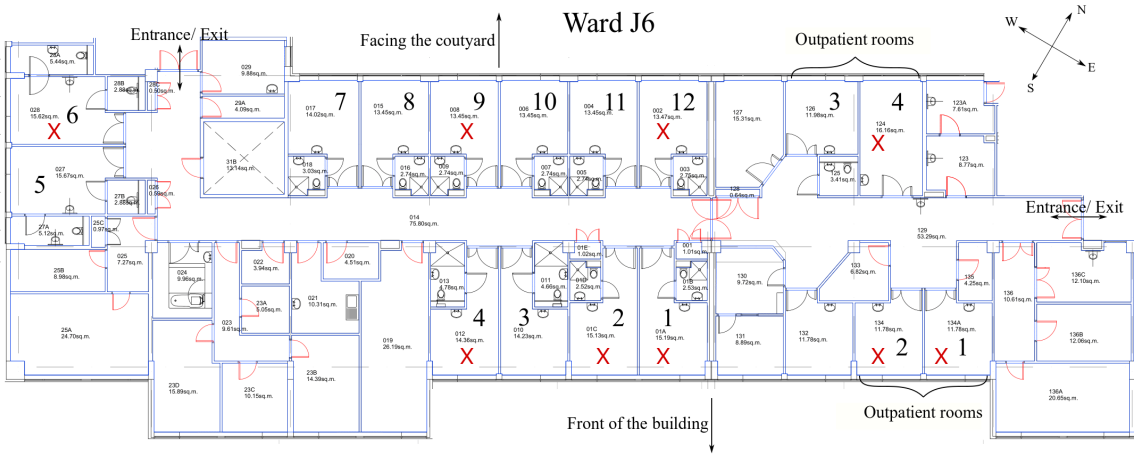

Figure 6.2: Plan of the cystic fibrosis unit, ward J6, at St James University Hospital. Numbers represent the room numbers of the inpatient and outpatient rooms and crosses indicate rooms where sampling took place.

and are in general warmer and windows are open more frequently. The north-west facing rooms are the mirror of those on the opposite side of the corridor and the windows face a courtyard; these rooms are generally cooler. Rooms at the end of the corridor (5, 6) have a window which faces another wing of the hospital. These rooms are bigger than both the south-east and north-west facing rooms, and direct sunlight reaches these rooms in the late afternoon. Ventilation on the unit is mainly natural ventilation via opening windows. Portable fans are used to improve thermal comfort. Make and model of fans were recorded if they were in use, along with if the window was open. Weather conditions on the day of sampling were recorded, particularly wind and rain as the data loggers gave information on temperature and humidity. Appendix C.3 gives a blank source data sheet for the principal investigator, paper copies were stored in the source data folder, and data was inputted on to an excel spread sheet and stored electronically for further analysis.

6.3.4.4 Room air sampling

Total viable count of bacteria of the room air in participant rooms was collected via a MicroBio MB2 single stage impactor (Cantium Scientific), Figure 6.3. Air samples were collected using a 90 mm petri dish filled with 37 ml of TSA agar, with 1 ml of cycloheximide added to 500 ml of agar to prevent any fungal growth. If the participant was in group A or B, participants infected with *P. aeruginosa*, an extra room air sample was taken using cetrimide agar; this agar is selective for *P. aeruginosa*. All agar was prepared according to section 4.2.1 in Chapter 4 for small volumes of plates. Instead of hand pouring plates 37 ml of agar was dispensed using

Figure 6.3: Microbio MB2 used for room air sampling in cross sectional study.

50 ml stripettes with a pipette controller (Satorius) under aseptic conditions.

It is advisable for air samples that bacterial load is not too high (approximately <200 CFU) or too low (approximately >50 CFU). Therefore, when conducting the first sample the user took three samples at both 5 minutes and 10 minutes at 100 $\mathrm{L\,min^{-1}}$ to determine the best sampling time. Using this data, it was found that 5 minutes was an appropriate sampling time.

Room air was sampled for 5 minutes at 100 $\mathrm{L\,min^{-1}}$ and taken in triplicate. A delayed start of 30 s was used so the user could move away from the sampler. All room air samples were taken at least 1 m away from any windows and doors as these can affect the airflow in the room and possibly the sample. If there were any fans on in the rooms these were allowed to stay on to keep the room well mixed but they were turned away from the sampler. Bathrooms and sinks are well known sources of bacteria and could affect the samples and therefore all samples were completed with the bathroom door closed and 1 m away from sinks. The sample was taken at least 1 m away from the patient and at least 1 m in height but no higher than the patients breathing height. The patients breathing height was chosen based on whether they were in their chair or bed the majority of the time.

6.3.4.5 Cough aerosol sampling system (CASS)

The CASS chamber provided a small defined environment to enable sampling of cough/exhaled breath. The idea was to create sterile chamber that effectively captured bacteria particles from cough/exhaled breath with no outside contaminants. Coughing/breathing directly into the sampler would cause an imbalance in the flow rate as there would have been no Spirosafe filter to balance the flow, leading to possible outside contamination. Furthermore, the CASS provides a sealed environment in which it would be possible to sample for higher biosafety level pathogens such as TB and keep all equipment contained inside the chamber before opening in the safety of an appropriate laboratory.

A modification of the CASS previously used by Fennelly et al. (2004) was used for this study. The modifications included adding ports on the drum so the CASS could be used with both and AGI-30 Impinger and an Andersen Impactor located either inside or outside the chamber. In addition, extra ports were added for a future study on the CASS and the airflow within it. The CASS used in this study is pictured in Figure 6.4 and CAD drawings are provided in Appendix C.4. For this study both the AGI-30 impinger and six-stage Andersen Impactor were used on the outside of the chamber using the bottom port, as seen in Figure 6.4a. This configuration was chosen for ease of use in setting up the equipment and keeping the bioaerosol samplers outside the chamber.

When using the CASS each subject coughed through a disposable mouthpiece (Vitalograph SafeTway Mouthpice) connected to 32 mm inside diameter flexible tub-

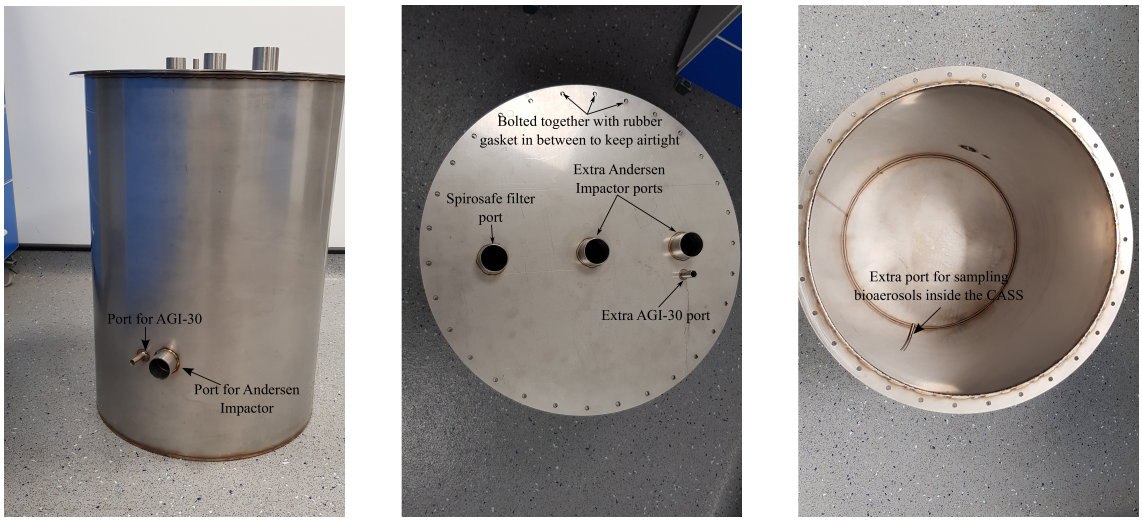

(a) (b) (c)

Figure 6.4: Cough aerosol sampling system used in this cross-sectional study.

ing (RS Components UK). This tubing connected to the chamber of the CASS drum whereupon a pump drew cough/exhaled breath containing respiratory droplets though either the Andersen Impactor or the AGI-30 impinger which sat outside the chamber. Air was drawn through the chamber at a faster rate than that of coughing/tidal breathing. To balance the flow, a small amount of room air was drawn into the chamber through a Spirosafe filter to ensure that the only bacteria present in the chamber was that of the participants cough/exhaled breath.

When the Andersen Impactor was used 32 mm flexible tubing (RS Components UK) connected the CASS chamber to the Andersen Impactor. The Andersen Impactor was loaded with six 90 mm petri dishes filled with 37 ml of TSA agar with cycloheximide added. Air was drawn through the chamber and Andersen Impactor at 28.3 L min^{-1}, the pump was connected to the Andersen Impactor via 8 mm flexible tubing. A HEPA filter was used to ensure no bacteria entered the exhaust air.

On the occasions when the AGI-30 impinger was used it was connected to the chamber with 10 mm flexible tubing. Each impinger was filled with 30 ml of ¼ ringers solution and autoclaved for 15 minutes at 121 °C prior to sampling. Air was drawn through the chamber and AGI-30 at 12.5 L min^{-1} and respiratory droplets in the air were entrained into the liquid within the sampler. A HEPA filter was used to ensure no bacteria entered the exhaust air. The configuration of the CASS during sampling is shown in Figure 6.5

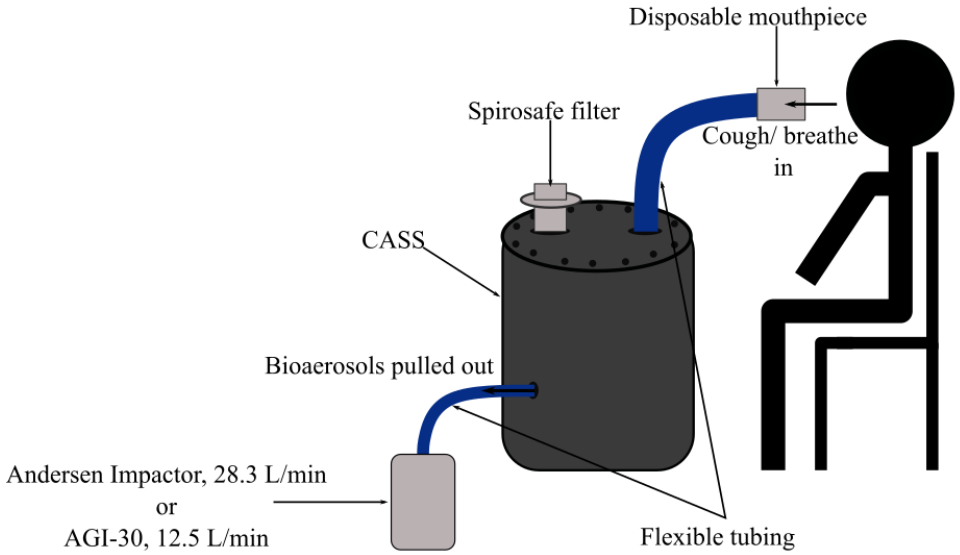

Figure 6.5: Configuration of the CASS when participants were sampled. Not to scale.

CASS protocol The Andersen Impactor was loaded with the agar plates at room temperature in the participant rooms. The AGI-30 was prepared prior to sampling. All ports on the CASS not in use were occluded with foil and tape. Subjects were instructed to cough at least once every 30 s for 15 minutes. At the onset of coughing the timer was set for 15 minutes and the pump was started. These timings were chosen after a change in protocol. Initially the protocol required coughing into the CASS as strongly and frequently as possible for 5 minutes, as used by Wainwright et al. (2009). Sampling for only 5 minutes resulted in low CFU counts and hence an increase in sampling time was decided upon, for more details on this change in protocol see section 6.3.9. The participant was able take a break at any point during sampling, if a break was signaled the timer was paused and the participant placed the palm of their hand over the mouthpiece to ensure no room air entered the CASS chamber until sampling and the timer resumed. After 15 minutes of sampling participants were asked to place the palm of their hand over the mouthpiece for a further two minutes to entrain any remaining bacteria from the drum; this time was calculated using the total volume of the drum and the flow rate. Cough frequency was assessed quantitatively and recorded on the principal investigator source data sheet (Appendix C.3). Between samples participants were given time to rest if needed, and they could withdraw from the study at any time if they felt unable to continue.

6.3.4.6 Mask aerosol sampling system (MASS)

The masks used in this study were developed and manufactured by the University of Leicester. Studies using previous and current designs of the mask have been completed (Williams et al., 2014; Kennedy et al., 2018; Williams et al., 2020). Each mask used was a modified duck billed face mask (Integrity®) containing strips of capture material at the centre, Figure 6.6. The capture material was created from Polyvinyl Alcohol (PVA) filaments which were 3D printed in house into a PVA matrix. All masks were assembled in a class II biological chamber and sterilised under UV light. Each mask was stored in a sterile plastic bag along with a small sterile spray bottle of molecular grade water, Figure 6.7.

MASS protocol Each participant was asked to wear the modified duck billed face mask for 30 minutes. Subjects were given no instructions on vocal manoeuvrers and were allowed to talk, breathe or cough as they wished. If participants needed to expectorate sputum the mask was lifted and the sputum collected in a pot. All participants were observed to ensure the mask was worn for 30 minutes of sampling

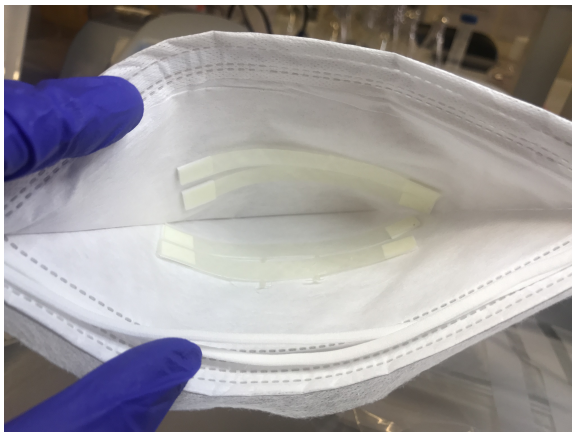

Figure 6.6: Duck billed face mask adapted with capture material at the centre.

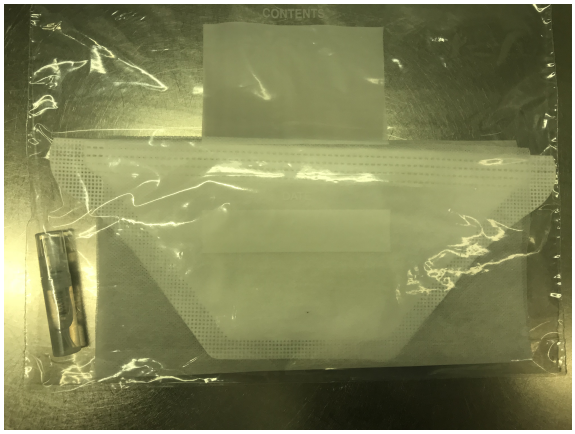

Figure 6.7: Sterile bag, mask and molecular grade water.

and to assist with lifting or removal if it was needed by the participant. Total time wearing the mask and any activities such as cough count, eating, and time the mask was removed were recorded on the principal investigator source data sheet (Appendix C.3). The researcher wore gloves at all times when handling the mask. The mask was removed from its sterile bag and the mask and bag were labelled with the date, study ID, and group. The mask was opened carefully without touching the capture material and using the provided molecular grade water the capture material was sprayed six times, three times on each set of filter strips. When complete the researcher assisted in putting on the mask, the participant was asked to hold the bottom of the mask on their chin while the researcher lifted the straps over their head. When the participant had the mask in a comfortable position the researcher smoothed the metal bar at the top of the mask onto the participants face to reduce possible contamination from room air. At the end of the 30 minutes the mask was carefully removed and placed back into its sterile bag without flattening.

6.3.4.7 Sputum samples

All participants at the start of sampling were asked to provide a sputum sample. If a participant needed to expectorate sputum during sampling, sampling would halt and a 50 ml screw cap falcon tube was be provided. If no sputum was provided during sampling, participants were encouraged to provide a sample at the end of sampling. If that was not possible the participant was given the option of providing a sputum sample at a later date and it was given to a clinical member of the research team. Date when the sputum was provided was recorded and each 50 ml screw cap falcon tube was labelled with the date, study ID, and group.

6.3.4.8 Clinical parameters

The following data were recorded from the participants clinical record under their study ID on the clinical source data sheet. These data were recorded by a clinical member of the research team,

- Demographics:
  - Age.
  - Gender.
- Lung function:
  - Forced expiratory volume in 1 s ($FEV_1\%$) and date obtained according to standard guidelines (Miller et al., 2005).
- Sputum microbiology:
  - Presence of Chronic *Pseudomonas aeruginosa* (Y/N) (According Lee et al. (2003)).
  - Presence of Chronic *Mycobacterium abcessus* (Y/N) (According to Haworth et al. (2017)).
  - Bacteria present in sputum in last 6 months.
  - If presence of chronic *M. abscessus* had sputum ever tested positive for other non-tuberculosis mycobacterium, plus which.
- Antibiotic treatment:
  - IV antibiotics (Y/N) plus which.
  - Nebulised antibiotics (Y/N) plus which.
  - Long-term oral antibiotics (Y/N) plus which.
- Mucolytic treatment:

- Hypertonic saline (Y/N).
- DNAase (Y/N).
- Modulated treatment (Y/N), plus which.

Other data such as relative health, presence of exacerbation, date of admission, and if participant was on home IV's were recorded. If any antibiotic, mucolytic or physiotherapy treatment was conducted before each sampling session this was recorded along with the participants $FEV_1\%$ with the date closest to the start of the sampling session. A blank source data for the clinical team is shown in Appendix C.3.

6.3.5 Data and sample storage

All paper copies of source data were stored in the source data folder. This was kept on the CF unit at St James University Hospital and stored according to good clinical practice guidelines. Once complete, these data were transcribed into an excel data sheet and stored electronically for analysis.

At the end of each sampling session all agar plates were put into a sealed bag in a sealed container with an EU standard biohazard label on and were transported to the University of Leeds on the same day. On arrival at the University of Leeds all agar plates were incubated, two days for *P. aeruginosa* and five days for *M. abscessus*, and after analysis all samples were safely destroyed.

Under aseptic conditions AGI-30 samples were split into two 10 ml samples in sterile 15 ml falcon tubes. These samples were centrifuged for 35 minutes at 3000 g (Eppendorf). It is important for the centrifuge to be balanced while on, this was done by filling two 15 ml falcon tubes with water until they weighed the same as the samples. Once the centrifuge was complete the supernatant was removed and discarded from both the 15 ml falcon tubes. The resulting pellet was small, so for consistency around 500 µl was left at the bottom of the tube. Next, 10 ml of sterile 10 % glycerol was added to one falcon tube (Wolkers and Oldenhof, 2015). This sample was frozen in a −80 °C freezer prior to being transported to the University of Leicester where they underwent bacterial quantification and extraction. The second sample was transported to the LTHT Infection Control Lab at Leeds General Infirmary via standard pathology transport to be tested for presence of *P. aeruginosa* or *M. abscessus*. Once analysed the anonymised results were transported back to the ward under standard paper results protocol and were filed with the study master file. This sample could not be transported to the LTHT pathology labs after sampling

and analysed the same day. Therefore, once the supernatant had been removed and discarded 500 µl of double strength nutrient broth was added. Creating a 1 ml nutrient broth solution with the collected bacteria. This sample was incubated via an orbital incubator (Stuart) at 37 °C and 110 rpm overnight and was transported the following morning. Allowing the sample to experience no die off of bacteria from being stored in ¼ ringers solution; the test was only for presence/absence and it did not matter if the number of bacteria increased.

Mask samples were stored in their individual sterile bags in a specified box at room temperature prior to transport to the University of Leicester.

Sputum samples were stored in a locked freezer at −80 °C prior to being double bagged and transported to the University of Leicester. Where the samples underwent bacterial culture, extraction examination, and quantification.

6.3.6 Management of risk

Risk of cross infection: To prevent cross-infection a maximum of one participant was sampled each day. There were two modified CASS samplers, one for participants infected with *P. aeruginosa* and not *M. abscessus* and another for participants infected with *M. abscessus*, resulting in a low to no risk of cross infection between participants bacteria. All equipment was cleaned with chlorine wipes before sampling and left in the participants room between samples if they were on the same day. When sampling participants the researcher adhered to the infection control protocol of the ward including wearing disposable gloves and aprons when needed. All tubing, mouth pieces, and SpiroSafe filters were disposed after each use. The CASS, Andersen Impactor, and AGI-30 were autoclaved at 121 °C for 15 minutes between participants/samples on different days. All mask samples were conducted using a single use disposable mask.

Discomfort during sampling: There was a risk of coughing becoming uncomfortable during the sampling. Participants were told to try and cough at least once every 30 seconds and breathe normally during this time. Participants were told they can take as many breaks as needed and the sampling time can be split up. If a participant needed a break during sampling the timer stopped and the researcher discussed with them if they wanted to continue. If they were ready to continue the timer and sampling resumed. During this time the participant covered the mouth piece to ensure no room air entered the CASS chamber. The mask sampling may have caused participants to feel warm and could become uncomfortable. Partici-

pants were allowed to try the mask on prior to enrolment. It was possible for the mask to be lifted or removed for a short period if it became too hot or the subject could have withdrawn from the sampling at any time.

Safeguarding: The researcher had all required DBS and health checks prior to the study. If the researcher was aware of any safeguarding issue, this was to be reported to the healthcare team immediately.

6.3.7 Microbiology analysis

6.3.7.1 Agar plates

Quantitative colony forming unit (CFU) counts were performed and recorded for all agar plates from both the Andersen Impactor and the MicroBio MB2. Agar plates from group A and B were incubated for 24 hours and a CFU count was performed. These plates were then incubated for a further 24 hours, totalling 48 hours of incubation to monitor and record any new growth. Agar plates from group C were initially incubated for 24 hours and CFU counts were performed. These plates were then monitored and recorded each day for new growth for the next four days as it can take up to five days for *M. abscessus* to grow. The number of colonies on each plate were counted and these counts were then corrected using the positive-hole correction tables (Macher, 1989) according to the methods described in section 4.5.6. Following presumptive screening (characteristic colonial appearance), the identity of both *P. aeruginosa* and *M. abscessus* were confirmed via the use of cetrimide agar and RGM medium respectively. CFU counts of both bacteria at each stage were recorded along with any positive isolates in the room air samples.

Cetrimide agar is a well established method of isolation of *P. aeruginosa* and is advised as the primary isolation media by Public Health England (Cowling et al., 2015); it has been used many times for detection in those with CF. When cetrimide agar was tested for growth of other species of gram-negative rods most failed to grow on this medium and those that did gave scanty growth (Brown and Lowbury, 1965). Positive *P. aeruginosa* colonies were counted when there was heavy growth on cetrimide agar and a characteristic appearance of *P. aeruginosa*. Figure 6.8 displays the difference between scanty and heavy growth. Agar plates which had greater than twenty colonies with the characteristic appearance of *P. aeruginosa* and same morphology, had a random selection of eight colonies tested using cetrimide agar. If all these colonies came back as positive isolates for *P. aeruginosa* it was assumed that all colonies with this morphology were colonies of *P. aeruginosa*.

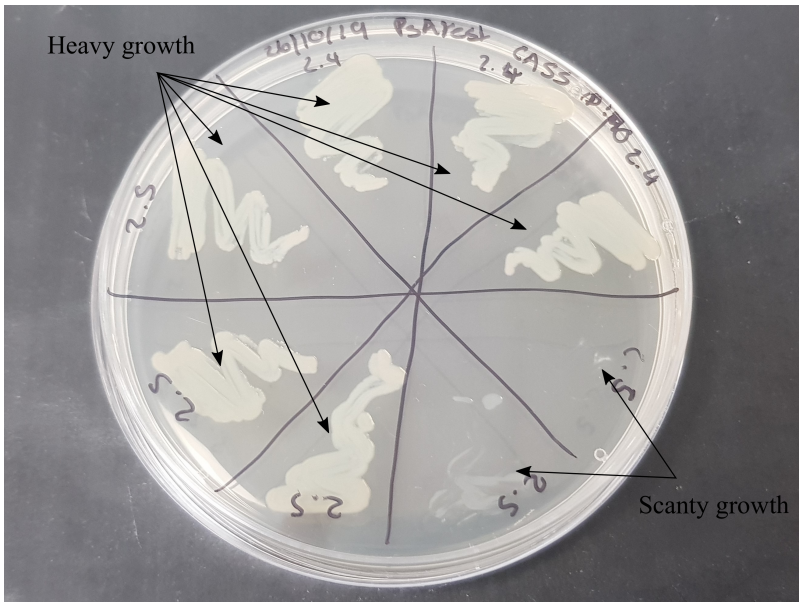

Figure 6.8: Picture of a test for positive *P. aeruginosa* colonies on a cetrmide agar plate showing the difference between heavy and scanty growth.

Recently, a new selective medium (RGM medium) has been shown to have high performance in the recovery of rapidly growing non-tuberculosis mycobacteria (NTM) from respiratory specimens from people with CF (Preece et al., 2016; Rotcheewaphan et al., 2019). Respiratory specimens included sputum samples and broncoalveolar lavage fluids. This new medium showed great resistance to the growth of non-mycobacterial strains of bacteria and fungi, with studies reporting 94 % or better inhibition rates (Preece et al., 2016; Rotcheewaphan et al., 2019). Preece et al. (2016) included a range of species that that are commonly recovered from the sputa of patients with CF, such as: *P. aeruginosa*, Staphlococcus, Bacillus and Aspergillus. Hence, if there was growth on RGM medium from a colony collected in the study it was assumed to be a positive NTM colony. To be confident that growth on the RGM agar plates was *M. abscessus* and not a different NTM, participants infection history of NTM's were recorded. All participants who had an infection with *M. abscessus* were checked for infections with other NTM's, if the participant had shown no growth of other NTM's in their sputa in the last 6 months and there was growth on the RGM agar plates the isolate was recorded as positive for *M. abscessus*.

6.3.7.2 AGI-30 impinger

The samples sent to the pathology labs at LTHT were analysed using selective media used in standard protocols for confirming presence of bacteria in people with CF's sptuta. These media were Columbia chocolate media with Bacitracin for *P.*

aeruginosa and RGM for *M. abscessus*. Columbia chocolate agar is recommended by Public Health England (Cowling et al., 2015) to isolate Pseudomonas species from clinical specimens, the media then used the antibiotic Bacitracin which inhibits gram-positive bacterial growth. Each sample was incubated at 37 °C. *P. aeruginosa* samples were incubated for 48 hours and examined for growth at two days. *M. abscessus* samples were incubated for twenty one days and examined for growth twice a week.

6.3.7.3 Mask

All samples sent to the University of Leicester were sent anonymously under the participants study ID. Each strip of PVA was placed in a stomacher bag (Seward, UK) with 5 ml of molecular grade water (Hyclone™, UK). The PVA was dissolved by manual manipulation of the matrix. To dissolve any microscopic PVA clumps that were missed by manual manipulation the liquid was vortexed on a flat vortex platform for 5 minutes. The dissolved PVA matrix was centrifuged at 13 400 g for 10 minutes, the supernatant was removed and the pellet was overlaid with 100 µl of TE buffer. Cells in the bacterial pellets were disrupted by bead-beating with 0.3 g glass beads (Sigma-Aldrich USA) and DNA extraction based on the methods of Reddy et al. (2007). Copy numbers of each sample were quantified using real-time q-PCR run in Rotor-gene software (Qiagen, UK).

6.3.8 Analysis of data

Aerobic colony counts (CFU m^{-3}) for Andersen Impactor stages were logarithmically transformed before analysis to correct for skewness and outliers in the data (Changyong et al., 2014). Outliers were included in the analysis as these data points were not measurement errors but were a phenomenon of the so called 'super producers' (section 3.2.1.1).

Homogeneity of variances was tested using the Brown-Forsythe test which uses deviations from the groups medians and is therefore less sensitive to outliers. Analysis was mainly performed on small data sets (<20 measurements), the test for normality may not be accurate in small data sets as they have little power to reject the null hypothesis (Ghasemi and Zahediasl, 2012) and due to the presence of outliers non-parametric tests were used. For larger data sets the Sharpiro-Wilk test was used to test for normality and the assumption of normality was violated in all cases.

Continuous variables from two independent groups of equal variance were analysed with the Mann-Whitney U test, the non-parametric equivalent of the t-test. Paired measurements with equal variance were taken for participants in group A and B (section 6.4.5), the Wilcoxon signed-rank test which is non-parametric equivalent of the paired t-test was used to infer statistical difference between the two measurements taken from each group. Both tests do not assume normality and compare the medians of the samples and test against the null hypothesis that all samples are drawn from the same population (i.e they have the same median). When the assumption of equal variance could not be met, the case when deriving if there was a difference between droplet size distributions produced by participants from group A and B and from participants in group C, the Welch's t-test was used regardless of whether or not the assumption of normality was met.

Measured aerobic colony counts were grouped by droplet size into six groups corresponding to each stage of the Andersen Impactor. The Kruskal-Wallis test is the non-parametric equivalent of the one-way ANOVA and was used to ascertain statistical difference between aerobic colony counts on the stages of the Andersen Impactor. The test assumed inter-group independent observations, but not normality. The medians of the samples were compared and tested against the null hypothesis that all samples are drawn from the same population (i.e the medians are equal). On rejection of the null hypothesis post-hoc analysis was performed using Dunn's multi comparison test which does not assume normality of the data. Pairwise comparisons between the groups were tested against the null hypothesis that there is no difference between the groups.

Fishers exact test was used to test the association between positive isolates of *P. aeruginosa* or *M. abscessus* in cough/exhaled breath samples or ambient air room samples and categorical data. The Fishers exact test was used for this study because for data with small number of measurements it is more accurate than the chi-square test or G-test. When an ordinal variable had k categories such as droplet sizes on the Andersen Impactor (stage 1–stage 6) and a two variable response, the data was assessed for an association with the presence/absence of bacteria with the Cochran-Armitage test for trend.

Spearman's rank correlation coefficients and the corresponding p-values were estimated between logarithmically transformed aerobic colony counts and clinical and demographic factors where available for all participants. In addition, factors associated with room conditions were correlated to logarithmically transformed ambient air colony counts and the Spearman's rank correlation coefficients and corresponding p-values were reported. This ranks data and provides a measure of relationship

between two continuous random variables and is robust to outliers. Spearman's rank correlation coefficient ranges from -1 where strong negative correlation is observed to $+1$ where strong positive correlation is apparent.

All reported p-values were two-sided and tested at the 5 % ($p < 0.05$) and 10 % ($p < 0.10$) significance level. All analysis were performed using MATLAB (vR2019b).

6.3.9 Protocol amendments

Amendments were only made when conducting the study or analysing the data if it could not be seen that it was possible to do it in a better way or the method described in the protocol was not working. The principal investigator was responsible for reporting amendments to the protocol. The decision to amend the protocol, and the determination as to whether it is a substantial or non-substantial amendment was made by the sponsor. During the study there were two amendments made to the protocol, both of these were determined to be substantial amendments by the sponsor, the University of Leeds.

Amendment 1: Before the study began one of the initial exclusion criteria was forced expiatory volume in 1s (FEV_1%) of less than 40 %. Several weeks into commencing the study no participants had been recruited. Many patients coming onto the CF unit were on the borderline of this criteria, greatly reducing the number of possible participants. After discussion with the clinical team it was concluded that decreasing the exclusion criteria to FEV_1% <30 % was acceptable and presented no risk to the participants.

Amendment 2: After several negative *P. aeruginosa* AGI-30 samples from LTHT, but positive colonies of *P. aeruginosa* found on the Andersen Impactor samples, albeit low CFU counts, the research study team came to the decision that the CASS sample timing of 5 minutes should increase. The new suggested timing was a total of 30 minutes for all CASS samples over all sessions. Participants in group A and B would now only take part in Andersen Impactor samples with the CASS, reducing their total number of samples using the CASS to two. This meant the total time for each CASS sample for all groups would be 15 minutes. Participants were now told to cough at least once every 30 seconds instead of as often and as hard as they feel comfortable, reducing the strain on the participant. After discussion with the clinical team this amendment was deemed clinically acceptable. The participants that had taken part until this point had no trouble coughing frequently for 5 minutes. Therefore, experience told the clinical team this would be well tolerated by the

patients by reducing the cough frequency but sampling for longer. Hence, this increase was justifiable and if participants felt any discomfort they were able to take a break or stop sampling altogether.

6.3.10 Impacts of SARS-CoV-2

The COVID-19 pandemic hit during the middle of the study and it was not possible to recruit or sample any more patients. The study had planned to recruit 45 participants and when the pandemic hit only 14 out of the 45 participants had been recruited and sampled. Analysis of data that was to be completed by the University of Leicester was greatly affected by the pandemic and most of the mask samples were not able to be analysed. Two Andersen Impactor samples were not tested for presence of *M. abscessus* as laboratories were forced to close. The following presentation of the analysis is based on the data from those patients that the study was able to recruit and sample. Interpretation of the findings account for the enforced cancellation of the study.

6.4 Results and discussion

6.4.1 Detection of *P. aeruginosa* and *M. abscessus* in cough/exhaled breath

The following analysis considers all of the data collected in the study to determine whether *P. aeruginosa* or *M. abscessus* could be found in aerosols from cough/exhaled breath, addressing the primary aim of the study:

> To measure the presence of *Pseudomonas aeruginosa* and *Mycobacterium abscessus* in cough/exhaled breath aerosols from adults with CF.

Fourteen subjects were recruited and completed the voluntary coughing, mask and sputum samples over a period of 6 months. Participants in group A and B (four and five participants respectively) completed two sampling session while participants in group C (five participants) completed one sampling session, totalling twenty three sessions. A breakdown of the demographics for each participant over each session is given in Table 6.2. Most subjects had chronic *P. aeruginosa* (86 %) infections as per the Leeds definition (Lee et al., 2003), only 39.1 % were exacerbating at the time of sampling and there was an even split between those who were inpatients

and outpatients at the clinic (Table 6.2). Forced expiratory volume data was not obtained for participant 26 as they were unable to complete spirometry tests due to health issues. Participant 16 was the only participant to use oxygen in the study.

Table 6.3 shows the demographics of the study population. The table splits the population into aerosol negative and aerosol positive. Aerosol positive is defined by at least one colony on an agar plate used in CASS sampling with the Andersen Impactor to test positive for *P. aeruginosa* or *M. abscessus*. *M. abscessus* was not detected in any cough/exhaled breath aerosols measured with the Andersen Impactor CASS samples.

There was a non-random association between chronic infection with *M. abscessus* and aerosol negative ($p = 0.00$ Fishers exact test). While this was the only statistically significant p-value at the 5 % level, at the 10 % level there was a non-random association with being an inpatient and an aerosol positive result ($p = 0.10$ Fishers exact test). However, this result was likely swayed by the ratio of outpatient aerosol negative *M. abscessus* participants. Additionally, there was a strong association between chronic infection with *P. aeruginosa* and aerosol positive, but this was not statistically significant ($p = 0.16$ Fishers exact test).

Table 6.2: All participant demographics at enrolment to each session.

No.	Study ID	Group	Session	Age	Gender	Chronic *P. aeruginosa*[*]	Chronic *M. abscessus*[†]	Exacerbating	FEV_1[‡]	(In/Out)patient[§]
1	60	C	1	24	M	N	Y	N	53	Inpatient
2	85	B	1	28	F	Y	N	N	42	Inpatient
			2					N	42	
3	41	C	1	37	M	Y	Y	N	84	Outpatient
4	7	A	1	49	M	Y	N	Y	45	Outpatient
			2					N	58	
5	91	A	1	27	F	Y	N	Y	57	Inpatient
			2					N	64	
6	70	A	1	32	F	Y	N	Y	31	Outpatient
			2					N	35	
7	32	B	1	22	M	Y	N	Y	43	Inpatient
			2					Y	43	

8	90	B	1	31	F	Y	N	N	34	Inpatient
			2					N	34	
9	69	C	1	33	F	N	Y	N	53	Outpatient
10	48	B	1	29	F	Y	N	Y	38	Inpatient
			2					Y	38	
11	54	C	1	21	F	Y	Y	N	38	Outpatient
12	94	A	1	38	M	Y	N	Y	31	Outpatient
			2					N	34	
13	26	C	1	19	F	Y	Y	N	NULL	Outpatient
14	16	B	1	39	F	Y	N	N	53	Inpatient
			2					N	53	

* As defined by the Leeds criteria (Lee et al., 2003).
† As defined by BTS NTM guidelines (Haworth et al., 2017).
‡ Forced expiratory volume.
§ Inpatient defined as patients who lived at the hospital while receiving their care. Outpatient defined as patients who attended the hospital for treatment without staying there overnight.

Table 6.3: Characteristics of participants at enrolment to each session according to cough aerosol sampling system results.

	All (n = 14, sessions = 23)	**Aerosol Negative*** **(n = 6, sessions = 8)**	**Aerosol Positive (n = 8, sessions = 15)**	***P*-value†**
Median (range) age (years)	30 (19-49)	28.5 (19-38) 29.63 (19-38)‡	30 (22-49) 32.47 (22-49)‡	$p = 0.57$M $p = 0.46$M‡
Gender				$p = 0.58$F
Male	5	3	2	
Female	9	3	6	
Chronic *P. aeruginosa*	12	4	8	$p = 0.16$F
Chronic *M. abscessus*	5	5	0	$p = 0.003$F
Current exacerbation (%)‡	9 (39.1)	2 (25)	7 (46.7)	$p = 0.40$F
Mean (SD) FEV_1‡	45.09 (12.68)	49.43 (19.08)	43.07 (8.65)	$p = 0.80$M
Patient Status				$p = 0.10$F
Inpatient	7	1	6	
Outpatient	7	5	2	

* Results show absence of any *P. aeruginosa* or *M. abscessus* in Andersen Impactor CASS samples.
† Categorical variables compared using Fishers exact Test (F) and continuous variables from two independent groups using Mann-Whitney U Test (M).
‡ Calculated over all sessions.

6.4.2 Cough aerosol microbiology

This section discusses total viable count and detection of *P. aeruginosa* and *M. abscessus* aerosols in the sampling approaches, covering two secondary aims. This consists of the second aim,

> To characterise total bacterial load and the particle size distribution of cough and exhaled breath aerosols from adults with CF.

and the third aim of the study,

> To compare the number of bacteria containing aerosols and detection of *Pseudomonas aeruginosa* and *Mycobacterium abscessus* with a CASS and mask sampling approach.

All participants took part in Andersen Impactor CASS sampling. Only three *P. aeruginosa* participants took part in AGI-30 CASS sampling along with all five *M. abscessus* participants, see section 6.3.9 for details. Resulting in a total of thirty one samples taken with the CASS across the three study groups. Table 6.4 summarises the isolated bacteria from the CASS sampling method. All participants infected with chronic *P. aeruginosa*, including those also infected with *M. abscessus*, had their Andersen Impactor CASS samples tested for presence of *P. aeruginosa*. Unfortunately, two *M. abscessus* AGI-30 samples sent to the LTHT microbiology lab had to be discarded and were not tested. In addition, due to circumstances surrounding SARS-CoV-19 and lab closures it was not possible to complete the test for presence of *M. abscessus* for two Andersen Impactor CASS samples.

P. aeruginosa was isolated from Andersen Impactor CASS samples in fifteen different sessions. All but one participant with *P. aeruginosa* only (participants from

Table 6.4: Summary of bacteria isolated during the study with CASS sampling methods.

	CASS Andersen*	**CASS AGI-30 Impinger†**
P. aeruginosa isolated	15/21	1/3
P. aeruginosa not isolated	6/21	2/3
M. abscessus isolated	0/3	0/3
M. abscessus not isolated	3/3	3/3

* Tested for *P. aeruginosa* n = 21. Tested for *M. abscessus* n = 3. Due to circumstances surrounding SARS-CoV-19 and lab closure it was not possible to complete testing for two *M. abscessus* samples.

† See amendments (§6.3.9) for low testing numbers. Tested for *P. aeruginosa* n = 3. Tested for *M. abscessus* n = 3, two samples untested by the lab.

group A or B), participant 94 in group A, had *P. aeruginosa* isolated from at least one out of the two sessions. Another participant from group A or B only isolated *P. aeruginosa* during a one session, this was participant 91 in group A who isolated *P. aeruginosa* from session one only. The other sessions with no isolation of *P. aeruginosa* were all sessions from participants in group C who was also infected with chronic *M. abscessus*. No *M. abscessus* was isolated from any of the tested samples from the Andersen Impactor CASS samples, nor the AGI-30 CASS samples. *P. aeruginosa* was isolated from one of the three tested AGI-30 CASS samples, this positive sample came from participant 85 in group B who was an outlier for total CFU counts (Table 6.6).

6.4.2.1 Comparison of CASS and mask sampling approach

All participants had a single mask sample taken. However, due to circumstances surrounding SARS-CoV-19 and lab closures it was only possible to have three masks tested for presence of *M. abscessus* and none for presence of *P. aeruginosa*. Therefore, there was not sufficient data to draw conclusions, but it is clear that the masks appear to be more efficient at detecting *M. abscessus* than both CASS sampling approaches. Table 6.5 compares the isolated bacteria from CASS and mask sampling methods for participants infected with chronic *M. abscessus*. Mask samples which were tested by the University of Leicester all came back positive for *M. abscessus* compared with zero CASS samples testing positive for *M. abscessus*. This demonstrates the expected distinction between the sensitivity in the analysis of the sampling methods for *M. abscessus*. In addition, it is worth considering that the masks were able to capture more aerosol droplets, including the larger droplets that the Andersen Impactor could not measure and this may have influenced the ability

Table 6.5: Comparison of bacteria isolated during the study with CASS and mask sampling methods for participants infected with chronic *M. abscessus*.

	CASS Andersen*	**CASS AGI-30 Impinger†**	**Mask‡**
M. abscessus isolated	0/3	0/3	3/3
M. abscessus not isolated	3/3	3/3	0/3

* Tested for *M. abscessus* n = 3. Due to circumstances surrounding SARS-CoV-19 and lab closure it was not possible to complete testing for 2 *M. abscessus* samples.
† Tested for *M. abscessus* n = 3. Two samples untested by the lab.
‡ Due to circumstances surrounding SARS-CoV-19 and lab closure it was only possible to have 3 masks tested by the University of Leicester.

for the masks to detect *M. abscessus* in cough/exhaled breath from people with CF.

6.4.2.2 Variation between participants

The main method of detection for presence of *P. aeruginosa* and *M. abscessus* was through the Andersen Impactor CASS samples. Cough counts, aerobic colony counts (ACC), and positive colony counts (PCC) for this method of sampling are given in Table 6.6. Corrections were made to measured CFU to account for the possibility of multiple hits as per Macher (1989) (section 2.1.1.1), all ACC were corrected and will now only be referred to as ACC. ACC varied widely among the participants in the study (21 CFU m^{-3}–3208.1 CFU m^{-3}, Table 6.6). Participant 85 in session 1 was shown to be an outlier (1.5 times the IQR above the third quartile). While participants 48 in session 1, 69 in session 1 and 70 in both session were extreme outliers (3 times the IQR above the third quartile). These outliers or high producers which produced much greater colony counts have been seen in a previous studies on people with CF (Wainwright et al., 2009) and have been named 'super producers' within the literature (Edwards et al., 2004). Difference in the colony counts from the agar plates from the higher producers can easily be seen when compared a participant with the median (56.3 CFU m^{-3}) colony counts, participant 91, in Figure 6.9. The agar plates from participant 91 show 6 CFU, whereas you can distinctly see the pattern of the holes from the Andersen Impactor on the plates from participant 48 with 204 CFU; just over half of the total 400 holes. These so called 'super producers' sway the mean of the data set to a much larger value than the median. It is possible to compare the aerobic colony counts seen in this study to those measured by Wainwright et al. (2009) who reported a range of 0–13 485 corrected CFU; the maximum nearly filling all 400 holes on each agar plate. Examining these results tell us that there were some participants who did not measure any ACC in their

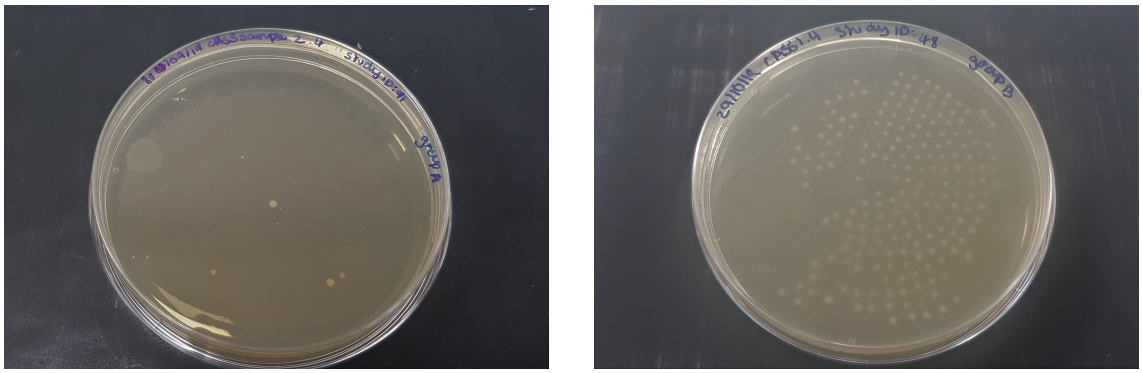

(a) Participant 91, session 2.

(b) Participant 48, session 1.

Figure 6.9: TSA agar plates from Andersen Impactor CASS samples at stage 4 (2.1 µm–3.3 µm).

Table 6.6: Summary of cough frequency and microbiology data from the Andersen Impactor CASS samples.

Participant	**Session**	**Cough count Andersen Impactor**	**ACC (CFU m^{-3})**	**PCC (CFU m^{-3})***
7	1	42	197.2	15
	2	77	27.3	8.4
16	1	116	21	4.2
	2	98	37.8	4.2
26	1	30	108.5	0
32	1	42	42.3	10.5
	2	54	21	4.2
41	1	55	24	0
48	1	123	1437.9	1427.1†
	2	43	81.3	66.4
54	1	92	197.3	0
60	1	93	61.5	0
69	1	58	1084.6	0
70	1	117	1163.7	1124.5†
	2	102	3208.1	2256.2†
85	1	81	354.5	240.7
	2	71	92.5	30.7
90	1	57	21.1	2.1
	2	46	42.2	21.1
91	1	83	56.3	10.2
	2	85	53	0
94	1	32	27.4	0
	2	30	25.3	0
Mean/Median		70.7/71	364.6/56.3	348.4/15
IQR		50	170	236.5

Highlighted shows those which are extreme outliers (3 times the IQR above the third quartile) for aerobic CFU counts.
The lighter highlight shows those which are outliers (1.5 times the IQR above the third quartile) for aerobic CFU counts.

* Positive colony counts (PCC) was defined by positive colonies of either *P. aeruginosa* or *M. abscessus*. However, there was no positive *M. abscessus* colnies and hence all PCC are positive for *P. aeruginosa*.

† Outliers for positive CFU counts (3 times the IQR above the third quartile).

cough samples. Although, in contrast to this study the agar used by Wainwright et al. (2009) was selective for gram negative bacteria. Secondly and perhaps more importantly a total of 6 'super producers' were also seen by Wainwright et al. (2009) and some had higher ACC than those measured in this study.

Positive colony counts (PCC) are shown in addition to ACC in Table 6.6. PCC was defined by positive colonies of either *P. aeruginosa* or *M. abscessus*. However, all PCC displayed are positive *P. aeruginosa* as there was no presence of *M. abscessus* in any Andersen Impactor CASS samples. As shown by the dagger (Table 6.6) the same high producers were again extreme outliers for PCC. This did not include participant 69 who did not have chronic *P. aeruginosa* and no *M. abscessus* was isolated. Again these high producing participants increased the size of the mean compared to the median.

A scatter plot correlating the ACC and the PCC is given in Figure 6.10. These data were used to determine if participants who produce more of everything produce more positive *P. aeruginosa* or *M. abscessus* colonies. The figure shows a strong positive correlation between ACC and PCC counts, with the exclusion of participants with chronic infection with *M. abscessus* (marked with +) as these participants produced no positive isolates. When considering participants with chronic infections with *P. aeruginosa* only, the Spearman's rank correlation coefficient is $r_s = 0.82$ and $p = 0.00$, resulting in a statically significant correlation between aerobic and positive

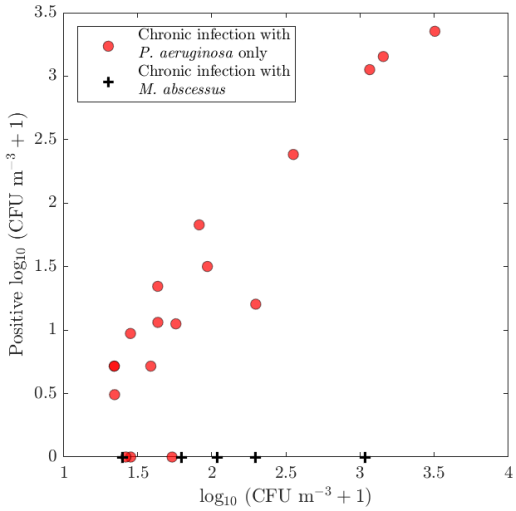

Figure 6.10: Correlation of logarithmic aerobic colony counts ($\mathrm{CFU\,m^{-3}}$) with positive logarithmic aerobic colony counts ($\mathrm{CFU\,m^{-3}}$) from Andersen Impactor CASS samples. Positive aerobic colony counts is defined by positive colonies for either *P. aeruginosa* or *M. abscessus*.

colony counts. If all participants are included, the Spearman's rank correlation coefficient is $r_s = 0.46$ and $p = 0.03$, producing a statically significant result. The CASS did not measure *M. abscessus* colonies and hence including participants chronically infected with *M. abscessus* affected the correlation and reduced the significance of the p-value.

Distributions of the logarithmic ACC and the logarithmic ACC of *P. aeruginosa* in CFU m^{-3} are displayed in Figure 6.11 and Figure 6.12 respectively. In these figures the participant and session are given in ascending order of ACC. The bars for the extreme outliers (final 4 bars) or 'super producers' were clearly higher than the other session totals for all ACC and ACC of *P. aeruginosa*. These outliers were a factor of 10 higher than 70 % of all other session totals for ACC and a factor of 10 higher than all other ACC of *P. aeruginosa* apart from participant 85 session 1. On the agar plates used in the Andersen Impactor CASS samples this was on average equivalent to less than 10 CFU for the majority of participants and greater than 100 CFU for the high producers.

Comparisons between the ACC and ACC of *P. aeruginosa* can be made with Figure 6.13. These plots only compare those participants infected with chronic *P. aeruginosa*. The highest four ACC had much higher proportions of *P. aeruginosa* compared to other microorganisms. *P. aeruginosa* made up more than 67 % of the ACC from these four sessions, with a maximum for participant 48 session 1 at 99 %. These high percentages of *P. aeruginosa* in the top sessions were not seen in the remaining sessions apart from one. The session proportions of *P. aeruginosa* similar

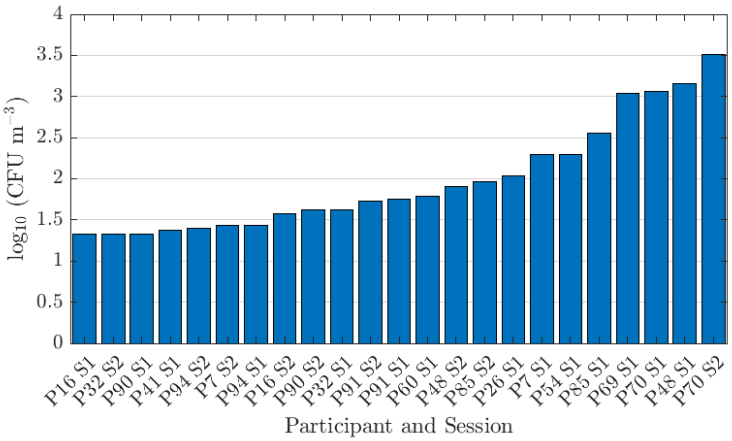

Figure 6.11: Distribution of logarithmic aerobic colony counts (CFU m^{-3}) for each participant and session of Andersen Impactor CASS samples.

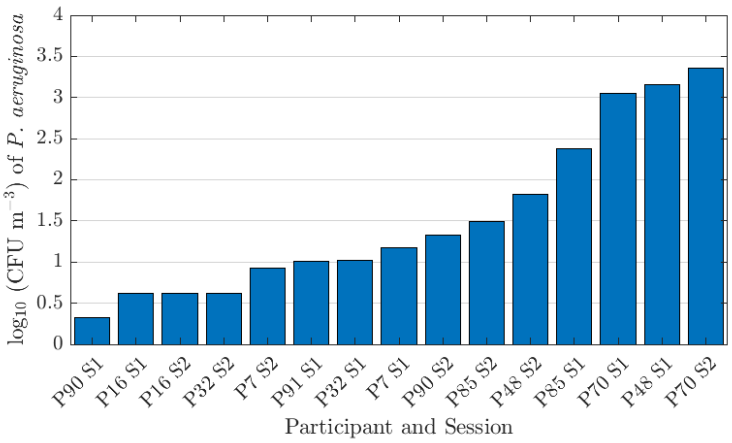

Figure 6.12: Distribution of logarithmic aerobic colony counts ($\mathrm{CFU\,m^{-3}}$) of *P. aeruginosa* for each participant and session with viable *P. aeruginosa* colonies from Andersen Impactor CASS samples.

to the four outliers was participant 48 session 2 with a percentage of 82 %. However, participant 48 in session 1 had the highest percentage of *P. aeruginosa* out of their ACC; therefore, it was expected that participant 48 in session 2 would also have a high percentage of *P. aeruginosa*.

Examining Figure 6.13 the six sessions which did not isolate *P. aeruginosa* can be clearly identified. It is compelling that no *P. aeruginosa* was isolated from the agar plates of participants infected chronic *P. aeruginosa* and *M. abscessus*. Especially since the majority of participants with chronic *P. aeruginosa* had *P. aeruginosa* isolated from their Andersen Impactor CASS samples. Therefore, it was significant that no participant infected with chronic *P. aeruginosa* and *M. abscessus* had *P. aeruginosa* isolated. Evidence in the literature concludes co-colonisation with two microorganisms in people with CF can have an effect on clinical outcomes (Hubert et al., 2013) and antibiotic efficiency (Orazi and O'Toole, 2017). Hence, it was possible to speculate that infection with *M. abscessus* may block the aerosolisation of *P. aeruginosa*. Yet, this was a small sample size; therefore, it was difficult to draw conclusions and further work is needed.

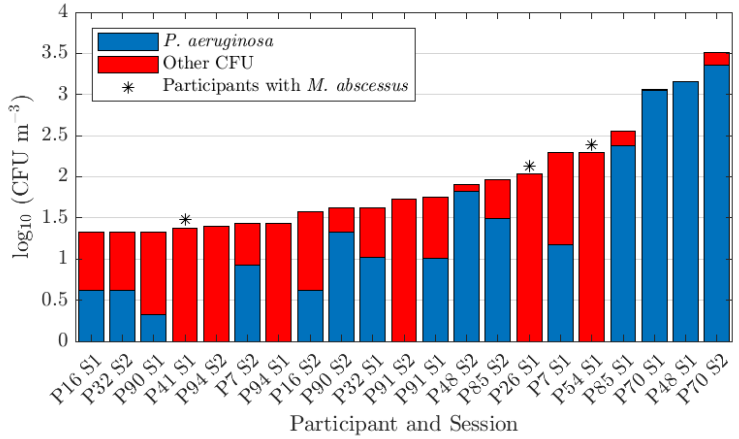

(a) Distribution of all aerobic and positive *P. aeruginosa* colony counts.

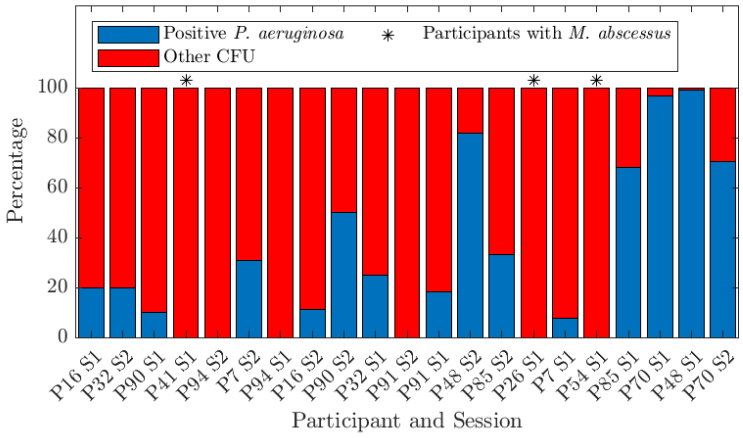

(b) Percentage of aerobic colony counts for *P. aeruginosa* and other CFU.

Figure 6.13: Comparison of all aerobic and positive *P. aeruginosa* colony counts ($\mathrm{CFU\,m^{-3}}$) from Andersen Impactor CASS samples for participants with chronic *P. aeruginosa*.

6.4.2.3 Factors associated with cough aerosol microbiology

Total viable count of all aerobic colony counts (ACC) and colony counts of *P. aeruginosa* were associated with measured variables within the study. The Mann-Whitney U test was performed on male and female ACC, the result gave a statistically significant p-value at the 5 % level ($p = 0.04$). Hence, the null hypothesis *H_0:* there is no difference between the ACC for male and female participants, was rejected. However, all of the high producing participants or 'super producers' were female for this study and in turn increased the colony counts for the female group. This begs the question, 'Were the participants super producers because they were female, or

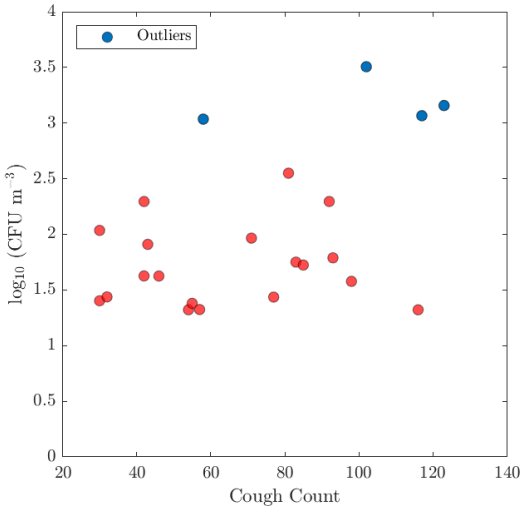

Figure 6.14: Correlation of cough count with logarithmic aerobic colony counts (CFU m^{-3}) from Andersen Impactor CASS samples. Blue dots represent the outliers from Table 6.6.

did measuring only female high producers skew the results?' Previous studies within the literature have not gendered their high producing participants and as this is a small data set and more investigation into these 'super producers' is needed.

At the start of each session a recording of if the participant was undergoing an exacerbation was taken. Participants were split into two groups, participants undergoing an exacerbation and those who were not. After splitting the participants into these groups the effect of exacerbation on ACC was analysed and it was determined there was no significant difference between ACC for participants in these two groups ($p = 0.31$ Mann-Whitney U test). Additionally, participants were split into another two groups, those with positive ACC for *P. aeruginosa* (as no participants had positive *M. abscessus* ACC) or participants with no *P. aeruginosa* or *M. abscessus* found in their Andersen CASS samples. A statistical test was performed to determine if their cough count differed based on their aerosol microbiology. Cough count was found to have no difference on the participant isolating *P. aeruginosa* in their cough/exhaled breath ($p = 0.23$ Mann-Whitney U test). However, when correlating these values against each other as shown by Figure 6.14 it could be argued there was a weak positive correlation. This result was backed up with the low but not statistically significant p-value on Table 6.7. Yet, when ignoring the high producing participant marked in blue the correlation is random. The high producing participants had a cough during sampling and were exacerbating; hence, they coughed more. Another question from this data was raised from the results surrounding high producing participants, 'Were these participants always going to produce more ACC because they were high producers or was it because they were

exacerbating and coughing more frequently?' An interesting case to look at is participant 48, this participant coughed at a higher frequency during their first session and was one of the outliers (Table 6.6), but during their second session they coughed significantly less (cough count dropped by more than one half) and this session was not an outlier. However, there are other cases such as participant 16 who coughed more than the average and was not a high producing participant. There is debate around this area and it may need more investigation, but similar studies have found no correlation between cough count and ACC and even found during sleep microorganism output was not affected (Williams et al., 2020).

Table 6.7 displays the Spearman's rank correlation coefficients and p-value for continuous recoded variables vs logarithmic ACC. There is one statistically significant correlation, FEV vs logarithmic ACC of *P. aeruginosa* , with a negative correlation shown in Figure 6.15. Recent work has identified that sputum rheology is correlated with lung function and disease status (Ma et al., 2018) and considering this evidence it could be assumed lung function has an affect of ACC of *P. aeruginosa* and even ACC. If the participants are split by FEV_1 greater than or less than 50 %, there is a clear divide in the ACC of *P. aeruginosa*. Demonstrating further evidence that lung function may play part in bacterial aerosol production, likely caused by changes in sputum rheology or even sputum volume. However, it appear the outliers in blue drive the correlation, Wainwright et al. (2009) found a statistically significant positive correlation with FEV_1 and ACC. After investigating their data it was concluded that their high producing participants had high FEV_1 which resulted in the posi-

Table 6.7: Spearman's rank correlation coefficients and p-values for continuous recorded variables vs logarithmic aerobic colony counts.

Factor	r_s	***P*-value**
Cough count	0.335	0.119
Count count*	0.267	0.336
Cough count†	0.292	0.176
FEV	-0.227	0.309
FEV*	-0.513	0.051
FEV†	-0.189	0.400
Age	-0.226	0.300
Age*	-0.083	0.769
Age†	-0.236	0.278

Where highlighted represents a statistically significant value at the 10 % level.

* For positive *P. aeruginosa* counts only

† For small droplets only, counts on stages 3, 4 and 5 (0.65 µm–4.7 µm).

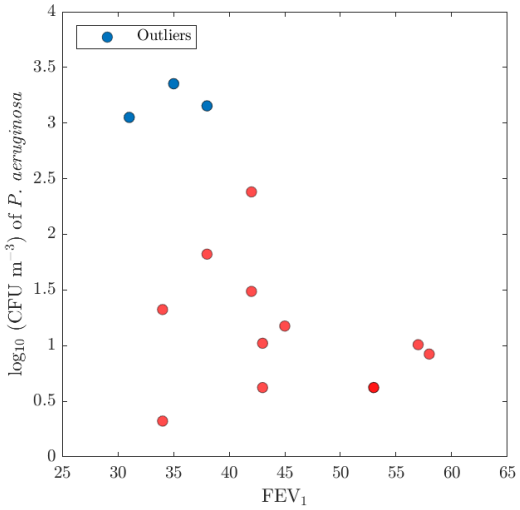

Figure 6.15: Correlation of FEV_1 with logarithmic aerobic colony count of positive *P. aeruginosa* (CFU m^{-3}) from Andersen Impactor CASS samples. Blue dots represent the outliers from Table 6.6.

tive correlation found. The difference in these two studies suggests that while lung function may have some effect on ACC, it is the high producing participants that will determine the positive or negative correlations, or if there is any correlation at all.

6.4.3 Aerosol droplet size distributions

Droplet size distributions of aerosolised microorganisms play an important role in understanding the infection transmission routes of these microorganisms. Therefore, this section analyses all the data from the study and investigates the droplet size distributions of aerobic colony counts for all microorganisms and for *P. aeruginosa*. The themes of the following analysis cover the second aim,

> To characterise total bacterial load and the particle size distribution of cough and exhaled breath aerosols from adults with CF.

and the third aim of the study,

> To compare the number of bacteria containing aerosols and detection of *Pseudomonas aeruginosa* and *Mycobacterium abscessus* with a CASS and mask sampling approach.

6.4.3.1 Droplet size distributions

Total viable count for a range of droplet sizes (Table 2.1) was collected by the Andersen Impactor and is presented in Figure 6.16a. The majority of the culturable bacteria was present on stage 4 (2.1 µm–3.3 µm). Droplet size distributions given by the Andersen Impactor did not follow the same pattern for aerobic colony counts (ACC) and ACC of *P. aeruginosa*. From highest to lowest ACC are as follows: stage 4, stage 3, stage 2, stage 5, stage 1, and stage 6. Whereas, for ACC of *P. aeruginosa* from highest to lowest are: stage 4, stage 3, stage 5, stage 2, stage 1, and stage 6. The least amount of viable bacterial colonies were present on stage 6 (0.60 µm–1.1 µm) for both ACC and ACC of *P. aeruginosa*, stage 6 also has the smallest percentage of *P. aeruginosa* in the overall ACC at just 8 %. This result was expected as *P. aeruginosa* is roughly 0.5 µm–1 µm wide and 1 µm–5 µm in length (Lederberg et al., 2000) and a droplet containing a bacteria of this size would frequently be outside of the size range for stage 6. After stage 6, stage 1 has the lowest ACC, ACC of *P. aeruginosa* and percentage of *P. aeruginosa* at 33 %. The low percentage of *P. aeruginosa* in the overall ACC was interesting as these droplets could contain more than one bacteria. Examining the plates from stages 1, Figure 6.17, it is not possible to see if a colony has come from a single or multiple viable bacteria. However, the colonies formed have a uniform morphology, so it was possible that a single large droplet contained more than one of the same bacteria. Hence, colony counts from stage 1 could be under represented from having multiple bacteria per droplet, or

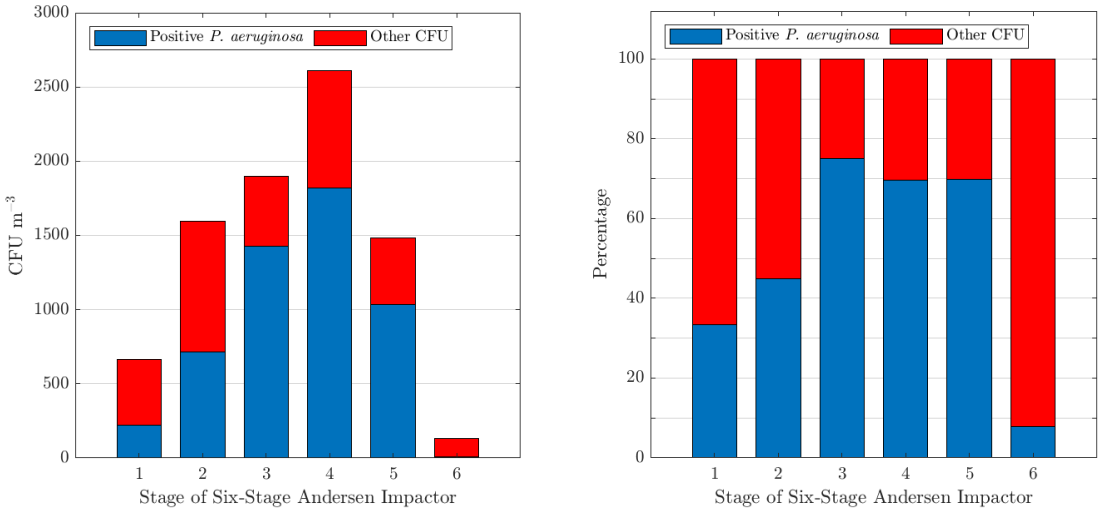

(a) Results expressed as CFU m^{-3}.

(b) Results expressed as a percentage of the CFU m^{-3}.

Figure 6.16: Comparison of the droplet size distributions of aerobic colony counts for all bacteria and *P. aeruginosa* (CFU m^{-3}) from Andersen Impactor CASS samples.

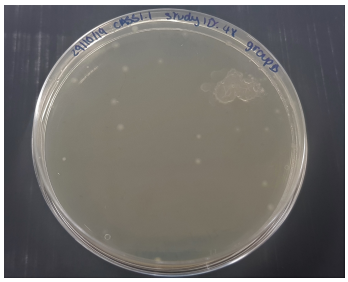

(a) Participant 48 session 1.

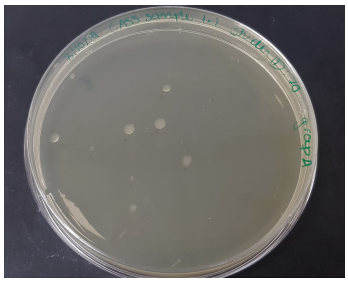

(b) Participant 70 session 1.

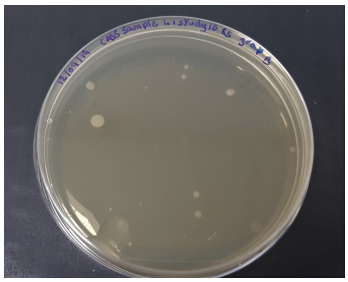

(c) Participant 85 session 1.

Figure 6.17: TSA agar plates from Andersen Impactor CASS samples at stage 1 (7.0 µm and above).

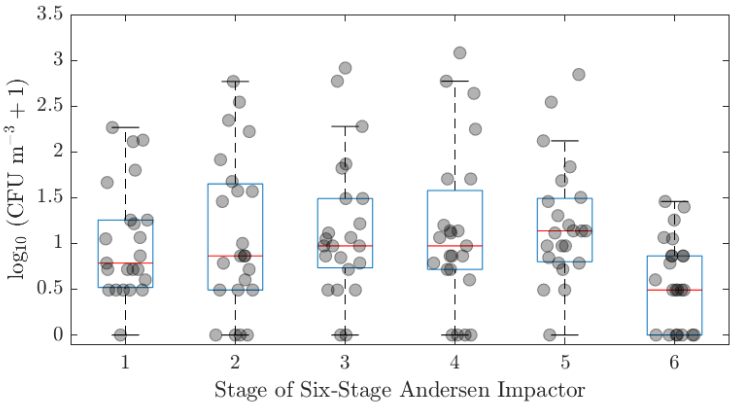

Figure 6.18: Box plot of the logarithmic aerobic colony counts (CFU m^{-3}) droplet size distributions produced by each participant and session for Andersen Impactor CASS samples.

microorganisms may have a preference for droplets smaller than stage 1, especially *P. aeruginosa*. Another point of interest in Figure 6.16 is that while stage 4 displays the highest total counts for ACC and ACC of *P. aeruginosa* , it is stage 3 that has the highest percentage of *P. aeruginosa* in the ACC, with stage 4 displaying the same percentage of ACC of *P. aeruginosa* as stage 5. The differences in these percentages is not large (5 %); thus, the results are interpreted as as *P. aeruginosa* having a preference for droplets within the size range 1.1 µm–4.7 µm (size range of these stages). The other microorganisms measured had a different preference but still within the respirable range.

A scatter plot of all measured data on each Andersen Impactor stage is given in Figure 6.18 along with the corresponding box plot for the data at each stage. Results on Table 6.6 recorded five outliers (ACC 1.5 times the IQR above the third quartile). However, in Figure 6.18 only stages 3, 4 and 5 have outliers for their respective data sets. Stage 4 was shown to have the highest ACC counts in Figure 6.13a. Yet, the

median is highest for stage 5 and this result was caused by the median being less affected by outliers; therefore, in this data set the median was a better average. Performing the Kruskal-Wallis test the null hypothesis was rejected *H_0:* There is no difference between the groups at the 5 % level ($p = 0.03$). After post-hoc analysis using Dunn's multiple comparison test the medians of stage 5 and 6 were found to be significantly different ($p = 0.01$). Values of 0 CFU m^{-3} are represented by their scatter points in Figure 6.18. Stage 1 and stage 5 have one data point each (0.04 %), the smallest measured, which recorded no colony counts. Concluding that while these stages may not have the highest colony counts it is very likely that a droplet of that size containing microorganisms will be aerosolised. To determine if there was any significance in droplet size on presence of any bacteria in the droplet a Cochran Armitage test was performed with null hypothesis, *H_0:* No significant association between ordered droplet size and culturable bacterial colonies in cough/exhaled breath aerosols. Results gave a p-value of $p = 0.01$ which rejected the null hypothesis at the 5 % level. In conclusion, there was a significant relationship between droplet size and culturable bacteria in this study.

A box plot for each session containing positive colonies of *P. aeruginosa* and the corresponding data points on each Andersen Impactor stage is given in Figure 6.19. Out of the three outliers identified in Table 6.6, there was outliers present on stages 3, 4 and 5. To determine if there was a difference in ACC of *P. aeruginosa* between the stages the Kruskal-Wallis test was performed, the null hypothesis was rejected *H_0:* There is no difference between the groups at the 5 % level ($p = 0.02$). After post-hoc analysis using Dunn's multiple comparison test the medians of both stage

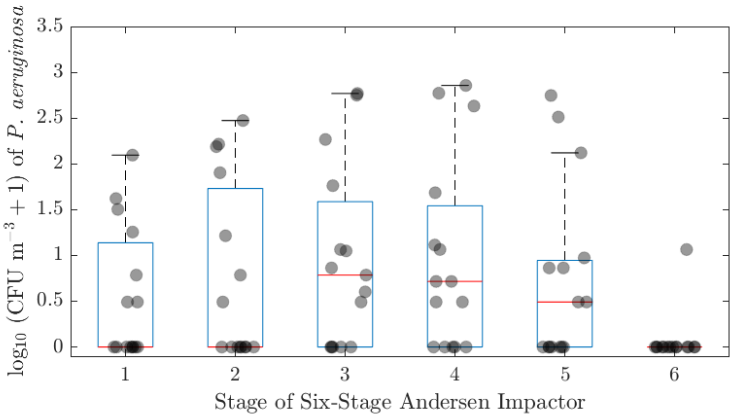

Figure 6.19: Box plot of the logarithmic aerobic colony counts of *P. aeruginosa* (CFU m^{-3}) droplet size distributions produced by each participant and session for Andersen Impactor CASS samples.

3 and 4 were found to be significantly different to stage 6 with $p = 0.01$ and $p = 0.01$ respectively.

If positive colonies of *P. aeruginosa* were isolated during a session, not all stages of the Andersen Impactor would have positive colonies. This is evidenced by the many data points at 0 CFU m^{-3} on Figure 6.19. Stages 3 and 4 each show five data points which had no positive isolates of *P. aeruginosa*, the lowest out of all stages, and it was possible that *P. aeruginosa* had a preferential for these size droplets. The Cochran Armitage test was used to determine if droplet size had any effect on if *P. aeruginosa* was isolated, the results give a p-value of $p = 0.09$ accepting the null hypothesis, H_0: There is no significant association between ordered droplet size and positive *P. aeruginosa* colonies in cough/exhaled breath aerosols, at the 5 % level but rejecting the null hypothesis at the 10 % level. Providing evidence that *P. aeruginosa* may have had a preference droplet size within the respirable range for this data set.

6.4.3.2 Fraction of small and large droplets

The traditional definitions of small and large droplets were used in the following analysis. A small droplet was defined as <5 µm and a large droplet as ≥5 µm. The Andersen Impactor stages were split into small and large droplets that were most representative of their defined sizes. The split was as follows: stage 1 and 2 for large droplets (4.7 µm–7.0 µm and above); and stage 3, 4, 5 and 6 for small droplets (0.65 µm–4.7 µm). Out of all the aerobic colony counts (ACC) in this study 73 % of droplets containing culturable bacteria were found in small droplets. Moreover, 82 % of droplets containing *P. aeruginosa* were found in small droplets. Figure 6.20a displays the distribution of ACC of large and small droplets. Small droplets had higher ACC for both *P. aeruginosa* and other bacteria combined. Furthermore, not only did small droplets have higher ACC, but out of the overall ACC there was a higher percentage of *P. aeruginosa* in small droplets than large droplets, 70 % vs 41 %.

Figure 6.21 presents the box plots for large and small droplets from Andersen Impactor CASS samples for ACC from each participant and session (Figure 6.21a) and for ACC of *P. aeruginosa* from each participant and session which had at least one stage with *P. aeruginosa* isolated (Figure 6.21b). It is observed that outliers were only present in small droplets in Figure 6.21a and the median was higher for smaller droplets in both figures. When droplet size is grouped as large and small Figure 6.21 demonstrates that only the large droplet size has data points with 0 CFU m^{-3}

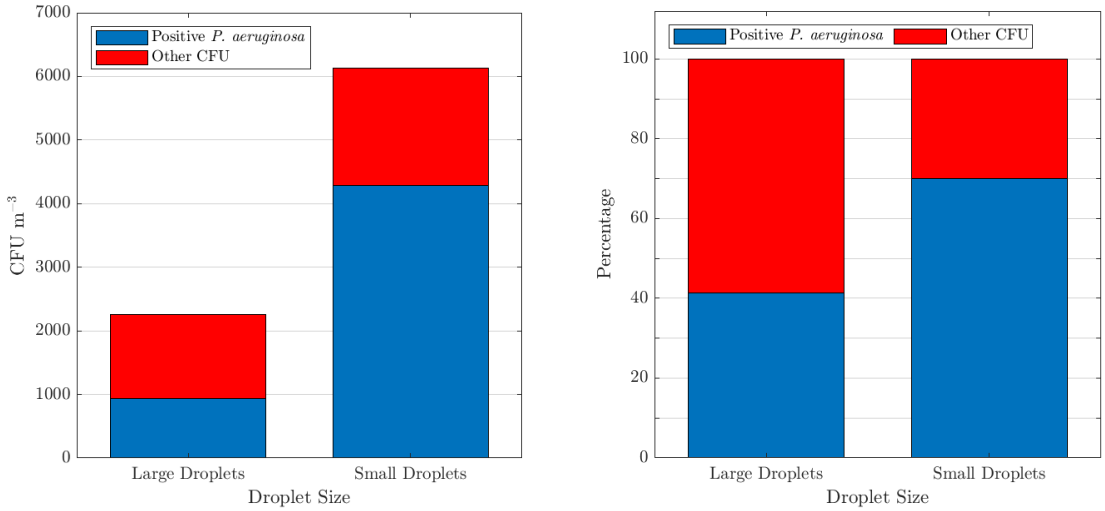

(a) Results expressed as CFU m^{-3}.

(b) Results expressed as a percentage of the CFU m^{-3}.

Figure 6.20: Comparison of large (≥5 µm) and small (<5 µm) droplet aerobic colony counts from all bacteria and *P. aeruginosa* (CFU m^{-3}) from Andersen Impactor CASS samples.

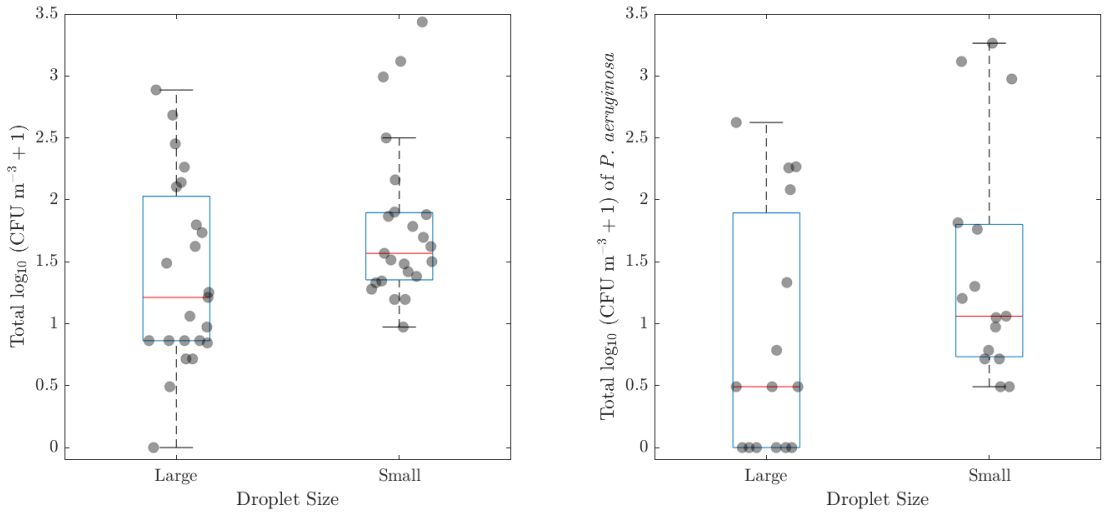

(a) Large and small droplets of all bacteria.

(b) Large and small droplets of *P. aeruginosa*.

Figure 6.21: Box plot of the logarithmic aerobic colony counts for all bactera and *P. aeruginosa* (CFU m^{-3}) in large (≥5 µm) and small droplets (<5 µm) from Andersen Impactor CASS samples.

and data points for large droplets had a greater range, as shown by the larger IQR. The Mann-Whitney U test was used to ascertain if there was a significant difference between the ACC for the two droplets sizes, large and small. The test resulted in a p-value of $p = 0.04$; therefore, the null hypothesis was rejected and it was concluded there was a significant difference between the two groups. The Mann-Whitney U test was repeated for positive *P. aeruginosa* ACC. The resulting p-value was $p = 0.05$

and the null hypothesis was rejected at the 5 % level. This result was significant as this data presents evidence that participants are clearly producing droplets that are within the repairable range (Table 1.2) and at greater quantities than larger droplets.

6.4.3.3 Variation between participants

Variation between the participants droplet sizes was analysed. Figure 6.22 displays the droplet size distribution results for each session measured during the study and the results were ordered in ascending order of aerobic colony counts (ACC).

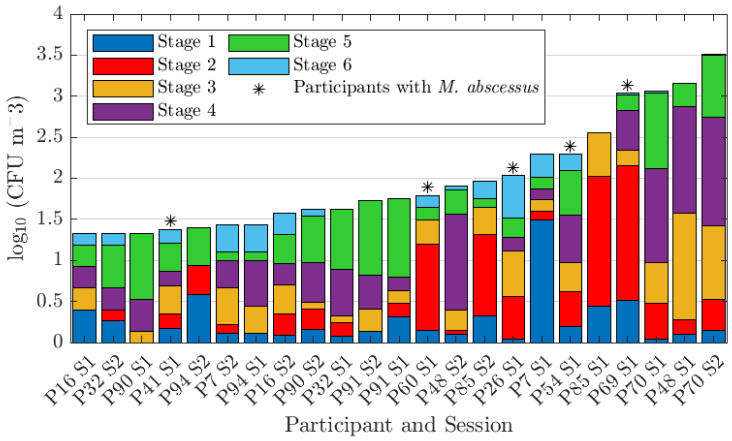

(a) Distribution of all aerobic colony counts (CFU m^{-3}).

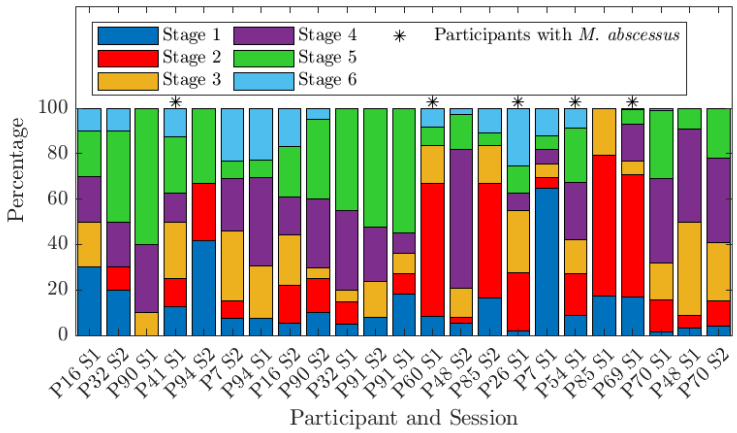

(b) Percentage of aerobic colony counts.

Figure 6.22: Comparison of aerobic colony counts (CFU m^{-3}) from Andersen Impactor CASS samples found at each Andersen Impactor stage.

The lower half of the bar chart indicates these sessions had a propensity towards stages 4 and 5. In the extreme outliers sessions (Table 6.6), the top four, stage 4 was a dominant stage which may explain why stage 4 had the greatest overall ACC (Figure 6.16a), but stage 5 had the largest median value (Figure 6.18). Furthermore, excluding the extreme outlier with *M. abscessus*, these participants heavily favoured smaller sized droplets. As a result demonstrating high probabilities of releasing large quantities of infectious aerosols through cough/exhaled breath in the respirable range. In addition, participants with *M. abscessus* had higher proportions of ACC on stage 2 than seen in participants from group A or B apart from participant 85.

Figure 6.23 displays the droplet size distributions produced by ACC of *P. aerugi-*

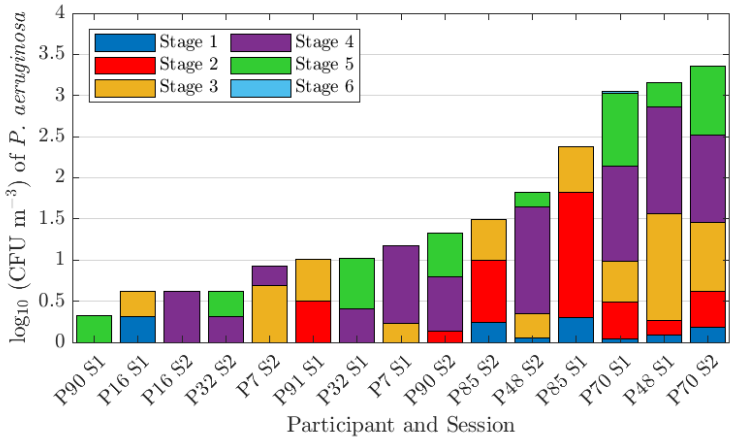

(a) Distribution of all aerobic colony counts (CFU m^{-3}).

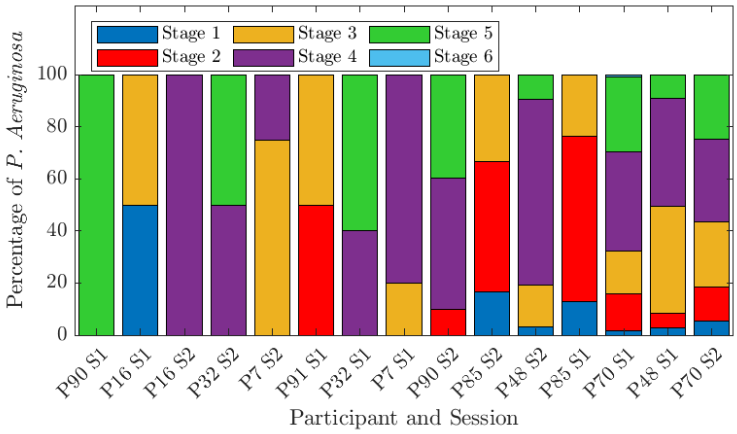

(b) Percentage of aerobic colony counts.

Figure 6.23: Comparison of aerobic colony counts of positive *P. aeruginosa* (CFU m^{-3}) from Andersen Impactor CASS samples found at each Andersen Impactor stage.

nosa, these data were displayed in ascending order of ACC of *P. aeruginosa*. Evaluating these data finds stage 4 to be the preferred droplet size correlating with the results in Figure 6.16a. Droplets of *P. aeruginosa* on stages 3, 4 and 5 appear throughout the sessions, but larger droplets, stages 1 and 2, and stage 6 appear more frequently in the latter half, increasing the range of stages with culturable *P. aeruginosa*. In conclusion, these data suggest that droplets of *P. aeruginosa* are more likely to appear in the respirable size range. However, as the number of droplets containing *P. aeruginosa* increase there is an increased likelihood of a varied droplet size distribution to also include larger droplets, stage 1 and 2, and very small droplets on stage 6.

6.4.3.4 Comparison between *P. aeruginosa* and *M. abscessus* droplet size distributions

Difference between droplet size distributions of participants with chronic *P. aeruginosa* and not *M. abscessus* (participants in group A and B) and participants with chronic *M. abscessus* (participants in group C) were evaluated. Assuming 1 droplet = 1 CFU the droplet size distribution for each group was calculated and the droplet diameter was represented by the lower limit of the Andersen Impactor size range (Table 2.1). The total number of droplets in each group was large (>500) and the mean number of droplets per m^3 for each group is presented in Figure 6.24 in the form of a histogram. Visually there are differences between the two distributions, participants chronically infected with *M. abscessus* favoured droplet diameters 4.7 µm–7 µm (stage 2) which is not seen in Figure 6.24a. Figure 6.25 presents a box plot of the logarithmically transformed aerobic colony counts at each Andersen Impactor stage. Stage 2 and 3 have distinctly higher medians from participants infected with *M. abscessus*. In addition, performing the Welch t-test found a significant difference between the two droplet size distributions ($p = 0.00$).

The distribution in Figure 6.24a from participants infected with *P. aeruginosa* only was a similar to what was observed in the overall distribution (Figure 6.16a). After converting droplet diameter to the representative Andersen Impactor stages the dominant stage was stage 4 which is the same as Figure 6.16a and the only difference in the order of the stages was that stage 2 and 5 had swapped. To determine if there was a difference in ACC between the stages from participants infected with chronic *P. aeruginosa* and not *M. abscessus* the Kruskal-Wallis test was performed, the null hypothesis was rejected H_0*:* There is no difference between the droplet size groups at the 5 % level ($p = 0.02$). Comparison between Andersen Impactor droplet size distributions of participants with *P. aeruginosa* can be compared to those measured

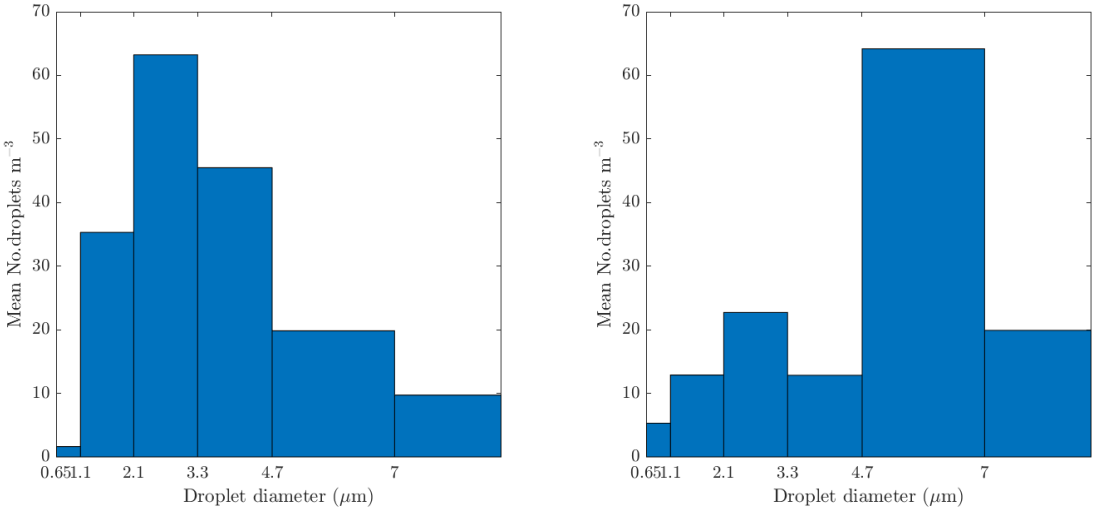

(a) Participants infected with chronic *P. aeruginosa* and not *M. abscessus*.

(b) Participants infected with chronic *M. abscessus*.

Figure 6.24: Histogram of the droplet size distribution of the mean number of droplets (CFU m^{-3}) from Andersen Impactor CASS samples found at each Andersen Impactor stage comparing participants with different microbiological infection status.

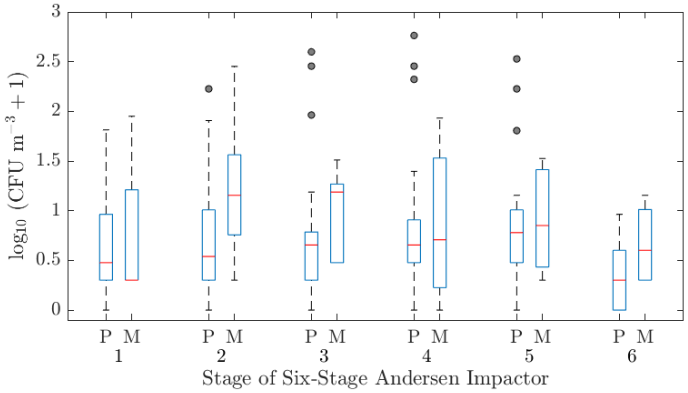

Figure 6.25: Grouped box plot of the logarithmic aerobic colony counts (CFU m^{-3}) split by participants microbiological status. P is participants infected with *P. aeruginosa* and not *M. abscessus*. M is participants infected with *M. abscessus*.

in the study conducted in Australia by Wainwright et al. (2009). Both studies found stages 3, 4 and 5 had the highest ACC, but Wainwright et al. (2009) found stage 5 to be the dominant stage. However, data on Table 6.8 showed that stage 5 has the greatest median. Another contrast in the studies was that ACC on stage 6 was greater than what was measured on stage 1 in the Australian study. Differences between these two similar studies highlight the variation seen in the droplet size distributions from people with CF, but their similarities inform us that the majority

Table 6.8: Summary of the mean, median and standard deviation aerobic colony counts (CFU m^{-3}) on each stage of the Andersen Impactor from participants in group A and B and participants in group C.

ACC (CFU m^{-3})	**Andersen Impactor Stage**					
	1	**2**	**3**	**4**	**5**	**6**
Group A and B*						
Mean	9.7	19.8	45.5	63.2	35.3	1.6
Median	2	2.5	3.6	3.6	5.1	1
SD	17.3	42.6	110.8	151.1	85.0	2.2
Group C†						
Mean	19.9	64.2	12.8	22.7	12.9	5.3
Median	1.0	13.3	14.4	4.1	6.1	3
SD	38.4	121.9	12.1	35.9	14.0	5.4

* Participants chronically infected with *P. aeruginosa* and not *M. abscessus*.
† Participants chronically infected with *M. abscessus*.

of droplets produced are within the range 1.1 µm–4.7 µm.

Examining Figure 6.24b a point of interest was that stage 2 was the dominant stage and there is larger ACC of stage 1 than seen in Figure 6.24a. Demonstrating participants infected with chronic *M. abscessus* had a preference towards smaller droplets in this study. However, data from Table 6.8 informs us that difference in medians is not as large as the mean. This fact compounded with the high standard deviation suggests the value mean of ACC on stage 2 was inflated by a high producer. In fact, data on the medians suggest that stage 2 and 3 are the dominant stages, which is still different to what was found for participants infected with *P. aeruginosa* only. To determine if there was a significant difference in ACC between the stages from participants infected with chronic *M. abscessus* the Kruskal-Wallis test was performed, the null hypothesis was accepted *H_0:* There is no difference between the droplet size groups at the 5 % level ($p = 0.77$). However, it must be remembered that this was a small sample size.

6.4.4 Room conditions and air sampling microbiology

Droplets containing microorganisms that people with CF produce are expelled into the indoor environment. Therefore, this section analyses the ambient air microbiology. By providing evidence of *P. aeruginosa* and *M. abscessus* in cough/exhaled breath and the air gives vital evidence towards airborne transmission of these two microorganisms. This section analyses data in relation to the second aim,

To characterise total bacterial load and the particle size distribution of cough and exhaled breath aerosols from adults with CF.

and the third aim of the study,

To compare the number of bacteria containing aerosols and detection of *Pseudomonas aeruginosa* and *Mycobacterium abscessus* with a CASS and mask sampling approach.

6.4.4.1 Room conditions

Air quality of a participants room was recorded for each sample day with a stand alone data logger (Airvisual). Recordings of the room conditions were taken from August to February. Data on the temperature in participants rooms is displayed in Figure 6.26. The median temperature is 22 °C and all data was close to this temperature with the a range of 18 °C–26 °C (excluding outliers). The outliers were from a sampling day for participant 91 during their first session, this was an extremely hot day and the participant was sampled in one of the south facing rooms (Figure 6.2) which gets direct sunlight.

Box plots on CO_2 data (Figure 6.27) showed a greater variability than the temper-

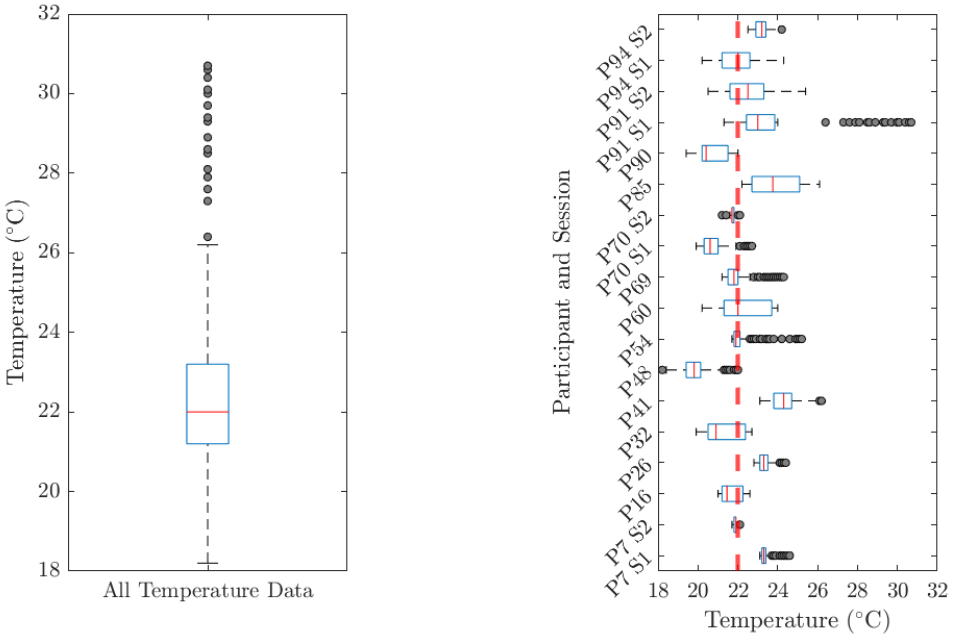

(a) All recorded temperature data during the study.

(b) Data from each day of sampling. Red dashed line indicates the median temperature.

Figure 6.26: Box plots of the background temperature recordings from the Airvisual.

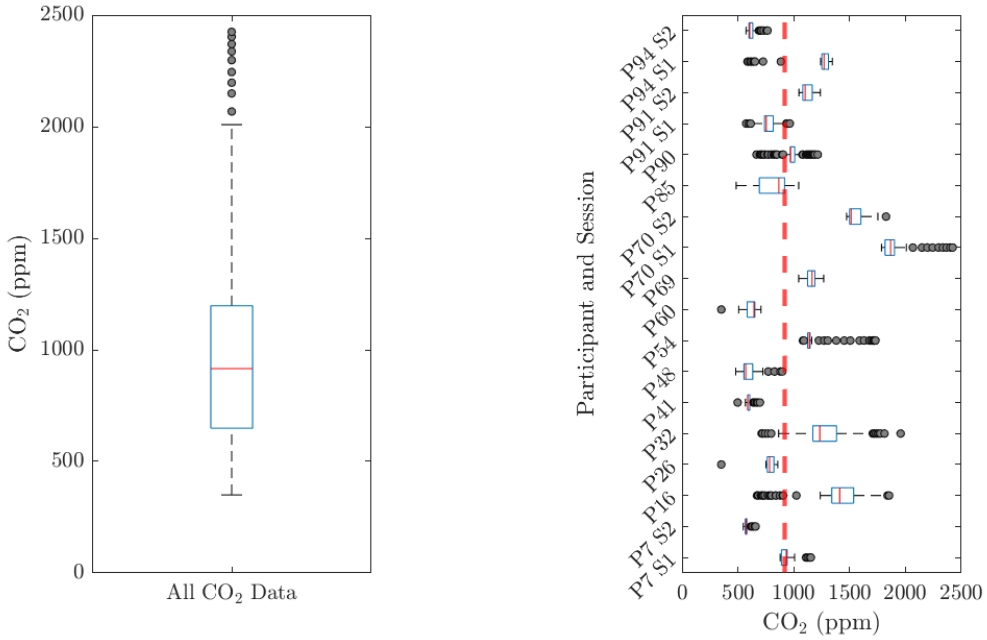

(a) All recorded CO_2 data during the study.

(b) Data from each day of sampling. Red dashed line indicates the median CO_2 recording.

Figure 6.27: Box plots of the background CO_2 recordings from the Airvisual.

ature data. Although, variability could have been a result of the number of people present in the participants room throughout the sampling time, but this data was not recorded. The median of the data was 916 ppm with IQR 650 ppm–1200 ppm. Ventilation rate is strong predictor of CO_2 level and indoor air quality and the importance has been recognised since the mid-nineteenth century when Max von Pettenkofer recommended a maximum CO_2 level of 1000 ppm (Locher, 2007). Over half of the recordings measured had CO_2 levels exceeding the threshold of 1000 ppm, but according to CIBSE guide A (CIBSE, 2015) the indoor air quality of the sampling rooms had an air quality standard of medium or moderate.

No exposure of $PM_{2.5}$ and PM_{10} has been described as safe but the World Health organisation has described an upper short term limit (24 h) of 25 $\mu g\,m^{-3}$ for $PM_{2.5}$ (WHO, 2006). All $PM_{2.5}$ levels measured were below this threshold and when compared with data from a naturally ventilated emergency room both $PM_{2.5}$ and PM_{10} levels (Figure 6.28) were lower than the 24.8 ppm and 30.8 ppm reported (Chamseddine et al., 2019). However, an emergency room has a higher occupancy and a more variables that could be sources of particulate matter. In naturally ventilated buildings with low indoor particle sources, indoor air particulate matter levels are closely related to outdoor air levels. Therefore, data from this study was compared to the DEFRA air quality index and all particulate matter levels were considered 'low'.

Participant 16 used their hairdryer during the day of measurements which resulted in resuspension of particles and explains the high $PM_{2.5}$ and PM_{10} levels compared to the other measurements.

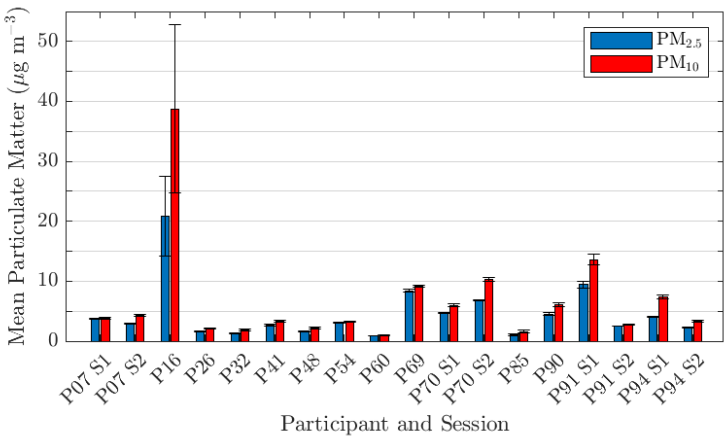

Figure 6.28: Mean mass per cubic metre of particulate matter less then 2.5 µm and 10 µm recorded with the Airvisual on each sampling day.

6.4.4.2 Ambient air bioaerosol samples

Table 6.9 displays the results from the ambient air samples. Air samples were only taken once per sampling day; hence, participants in group B and C only had one air sample taken. Highlighted rows indicate days which found positive colonies of *P. aeruginosa* or *M. abscessus* in ambient air bioaerosol samples and only four positive samples were recorded. Although *P. aeruginosa* was found in all but one cough/exhaled breath aerosols from participants chronically infected with *P. aeruginosa* only, a smaller incidence of *P. aeruginosa* was found in the air. These findings were analogous with Wainwright et al. (2009). Conversely, *M. abscessus* was found in the ambient air bioaerosol samples from one of the participants but not in cough/exhaled breath samples from the Andersen Impactor.

Finding *M. abscessus* in the ambient air samples was an important result. This data gave new evidence that *M. abscessus* can be found in the air in CF patient rooms. While there was only one finding during the study it still proved it was possible for *M. abscessus* to be aerosolised in droplets small enough to stay suspended and survive. Participant 60 was the first participant sampled, more ambient air bioaerosol samples were taken and sampling took place on the participants last day in hospital. Both of these factors could have increased the chances of finding *M. abscessus* in the

Table 6.9: Summary of ambient air microbiology data from the MicroBio MB2.

Participant	**Session**	**(In/Out)patient**	**Mean Ambient Air Colony Counts (CFU m^{-3})**
7	1	Outpatient	155.4
	2		113.5
16	1	Inpatient	118.6
26	1	Outpatient	76.2
32	1	Inpatient	311.7*
41	1	Outpatient	77.8
48	1	Inpatient	66.1
54	1	Outpatient	145.2
60	1	Inpatient	56.1
69	1	Outpatient	208.6
70	1	Outpatient	89.3
85	1	Inpatient	663.7*
90	1	Inpatient	134.3
91	1	Inpatient	208.3
	2		201.3
94	1	Outpatient	112.1
	2		154.7
Mean/Median			170.2/134.3
IQR			116.6

Blue highlight shows those which had positive isloates of *P. aeruginosa* in their aimbient air samples.
Red highlight shows those which had positive *M. abscessus* isolates in their ambient air samples.
* Outliers.

air. Figure 6.29 shows the positive sample taken from the ambient air bioaerosol samples in participant 60's room compared to a rough and smooth strain on the same RGM medium. The same distinctive fawn colour of *M. abscessus* on RGM can be seen on both, it produced a heavy growth on the agar and the participant had not been infected with any other non-tuberculosis mycobacteria in the last 6 months. Therefore, this was recorded as positive for *M. abscessus*.

Previous work within the literature in naturally ventilated hospital rooms measured ambient air bacterial load to be 125 CFU m^{-3} for single occupancy rooms and the range on the ward was 99 CFU m^{-3}–495 CFU m^{-3} with higher concentrations in the higher occupancy rooms (Verde et al., 2015). Similar results are seen in higher occupancy (10–20 patients) naturally ventilated wards with bacterial loads

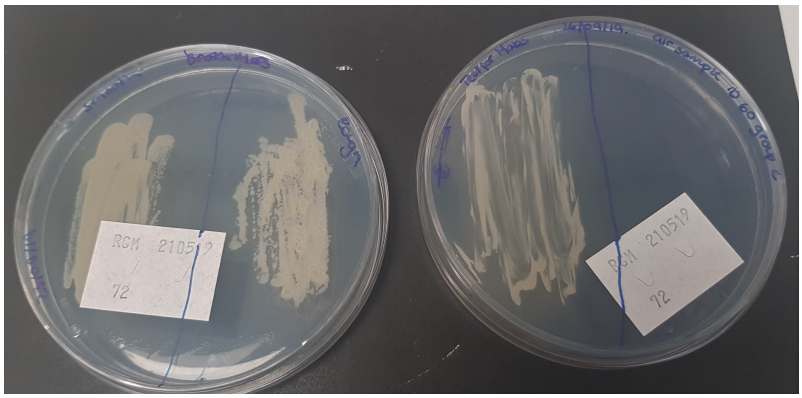

Figure 6.29: Positive isolate of *M. abscessus* from participants 60's ambient air samples compared to rough and smooth *M. abscessus* strains from the laboratory, both on RGM agar.

of 393.9 CFU m^{-3} and 383.9 CFU m^{-3} (Asif et al., 2018). Comparing these to results in this study it is found that the single occupancy room was similar to the mean/median measured, but some ambient air colony counts were similar to those recorded in the higher occupancy rooms.

Outliers who had higher mean ambient air colony counts were participants 32 and 85 and only participant 85 had *P. aeruginosa* colonies found in the air. Participant 85 was an outlier for ACC too (Table 6.6), albeit other outliers from Table 6.6 did not have positive air samples. In addition, performing the Mann-Whitney U test the null hypothesis was accepted ($p = 0.96$), *H_0:* there was no difference in the CFU in air samples with positive colonies for *P. aeruginosa* and *M. abscessus* and the CFU in air samples with no colonies of *P. aeruginosa* and *M. abscessus*. However, it must be considered that this is a small data set especially for data on positive room air samples.

Participant 41 was chronically infected with both *P. aeruginosa* and *M. abscessus* and was positive for neither in their cough/exhaled breath samples, but they had *P. aeruginosa* colonies found in their ambient air bioaerosols samples. This participant was an outpatient and the room was used by multiple patients so it is possible it came from another source. It is likely that the ambient air samples for outpatients will have been affected by factors such as how long the previous patients had been in the room and how often the windows had been opened (the only source of ventilation).

Theoretically, it seemed more likely to have *P. aeruginosa* or *M. abscessus* found in air samples from participants who were inpatients as they spent a significantly longer time in their room. However, for this small data set there was no relationship found between being an inpatient/outpatient and finding *P. aeruginosa* or *M. abscessus* in the air samples ($p = 0.29$ Fishers exact test). Additionally, there was no difference

found between the number of colony counts on the ambient air samples of inpatients and outpatients ($p = 0.48$ Mann-Whitney U test).

6.4.4.3 Factors associated with air sample microbiology

Continuous recorded variables were correlated with ambient air bioaerosol samples and the Spearman's rank correlation coefficient and p-value are included in Table 6.10. There was one variable found to be statistically significant at the 10 % level and that was CO_2 levels. The correlated variables are displayed in Figure 6.30 and a positive trend is observed which suggests that bioaerosols in the room are correlated with indoor sources. Previous studies have found similar results which concluded a moderate link between air total bacterial count and CO_2 levels (Hsu et al., 2012). The positive air samples are represented with a cross and these are not associated with high CO_2 levels comparatively to the other samples.

The correlation between $PM_{2.5}$ and ambient air bioaerosols samples is not significant but when inspecting at the data (Figure 6.31) it could be argued there was a slight positive trend. The significance of the correlation may be skewed by an outlier which has high bacterial load in the air samples but low $PM_{2.5}$. With more data points this trend may become significant and $PM_{2.5}$ has been previously correlated with colony counts in hospital indoor air (Ling and Hui, 2019). Again it was found that the positive isolates of *P. aeruginosa* and *M. abscessus* found in the air samples did not have higher levels of $PM_{2.5}$.

A hypothesis of a correlation between aerobic colony counts (ACC) from cough/exhaled breath and colony counts in the room air samples was made prior to analysis of the data. Yet, the results did not find a significant correlation. Figure 6.32 presents

Table 6.10: Spearman's rank correlation coefficients and p-values for continuous recorded variable vs mean logarithmic ambient air sample colony counts ($CFU\,m^{-3}$).

Factor	r_s	***P*-value**
CO_2	0.46	0.07
$PM_{2.5}$	0.15	0.59
PM_{10}	0.06	0.82
Aerobic colony counts	0.05	0.84
Inpatient CFU	-0.05	0.94
Outpatient CFU	0.37	0.34

Where highlighted represents a statistically significant value at the 10 % level.

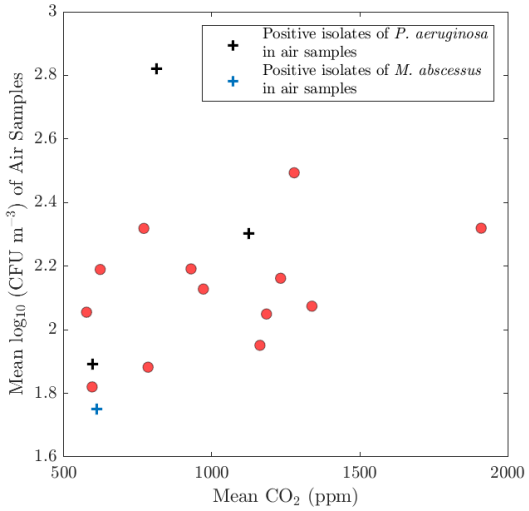

Figure 6.30: Correlation of mean CO_2 levels (ppm) with mean logarithmic ambient air sample colony counts (CFU m^{-3}) from each sampling day.

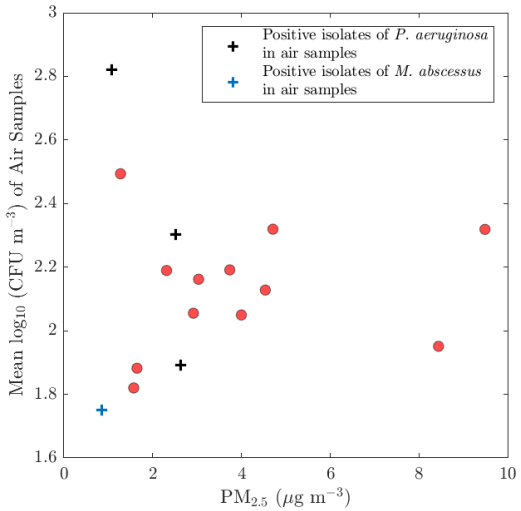

Figure 6.31: Correlation of mean $PM_{2.5}$ levels (µg m^{-3}) with mean logarithmic ambient air sample colony counts (CFU m^{-3}) from each sampling day.

this data and a positive trend could be argued. There are two data points in the bottom right corner of the figure that do not fit with the correlation. These data points are participants who produced high ACC and low bacterial load in air samples which had no positive isolated of *P. aeruginosa* and *M. abscessus*. However, adding more data points could reveal the potential trend is as this was a small study.

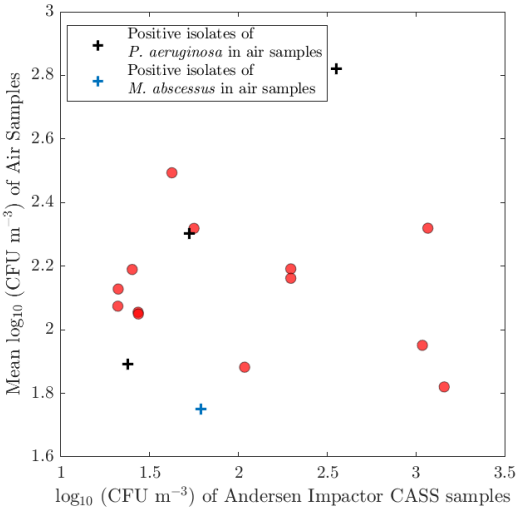

Figure 6.32: Correlation of mean logarithmic ambient air sample colony counts (CFU m^{-3}) from each sampling day with logarithmic aerobic colony counts (CFU m^{-3}).

6.4.5 Effects of study groups on cough/exhaled breath samples

Knowledge on changes in bacterial load or droplet size distributions over time and treatment could provide insight in how to best mitigate against airborne infection through understanding of when a host in most infectious. Consequently, this section analyses the data from the study groups and further investigates these data based off time of day, exacerbation, and medication taken, which encompasses the final aim of the study,

> To gain preliminary data to inform future studies on the influence of time and treatment on droplet size distributions and presence of *Pseudomonas aeruginosa* and *Mycobacterium abscessus* in cough/exhaled breath aerosols from adults with CF.

First, the data was examined for group A. These were participants chronically infected with *P. aeruginosa* and not *M. abscessus* and had their samples taken at the start and end of their two week IV treatment (Table 6.1). Figure 6.33a displays the aerobic colony counts (ACC) for all bacteria and for *P. aeruginosa* for each individual participant. A total of three out of the four participants had higher ACC at the start of their treatment than the end, apart from participant 70 who was one of the extreme outliers (Table 6.6). The effects of the high producer are seen in Figure 6.33b where for stages 2–5 the end of treatment ACC are higher than at the start of the treatment. In addition, the affect of this participant is presented in the data in Table 6.11 where total and mean end ACC are much greater than the start of

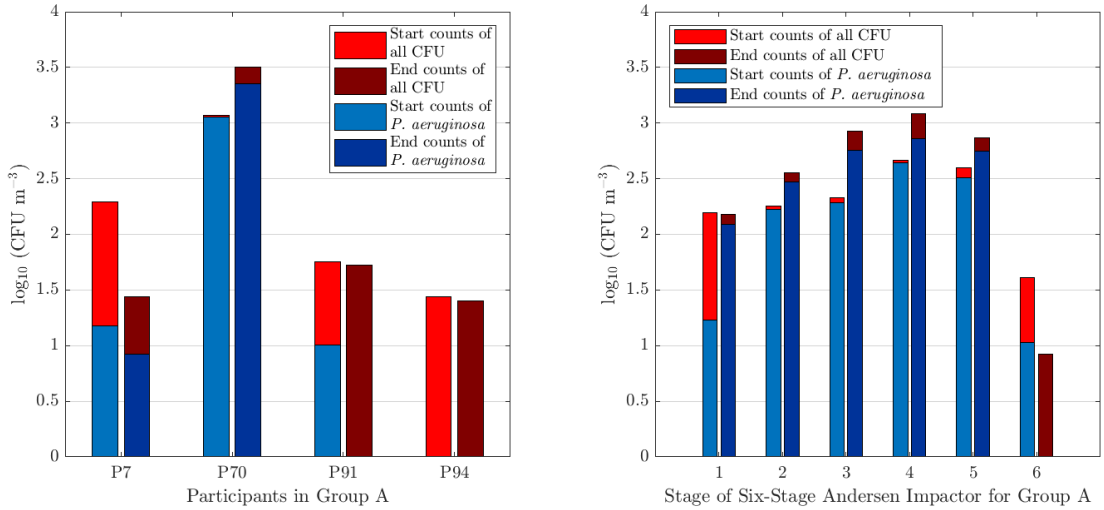

(a) Comparison of start and end for individual participants.

(b) Totalled distribution over each Andersen Impactor stage for all participants.

Figure 6.33: Comparison of logarithmic aerobic colony counts for all bacteria and *P. aeruginosa* (CFU m^{-3}) from Andersen Impactor CASS samples for participants in group A.

Table 6.11: Summary of the total, mean, median and standard deviation of the aerobic colony counts and positive colony counts from participants in group A and B.

	Group A: Start	**Group A: end**	**Group B: Morning**	**Group B: Afternoon**
ACC (CFU m^{-3})				
Total	1445	3314	1877	275
Mean	361	828	375	55
Median	127	40	42	42
Standard deviation	540	1587	611	30
PCC* (CFU m^{-3})				
Total	1150	2265	1685	127
Mean	383	1132	337	25
Meadian	15	1132	11	21
Standard deviation	642	1589	618	26

* Positive colony counts (PCC) was defined by positive colonies of *P. aeruginosa*.

treatment sessions.

A box plot of this data is given in Figure 6.34 which tells a slightly different story. While the majority of stages had higher tails and IQR at the end of treatment the median value of ACC for all stages is higher at the start of treatment. Conversely,

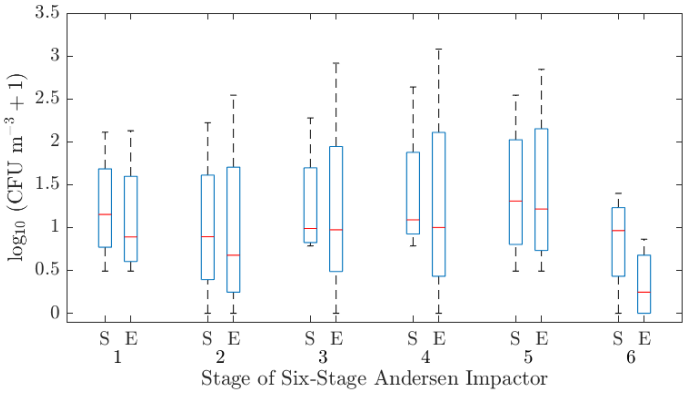

(a) All aerobic colony counts.

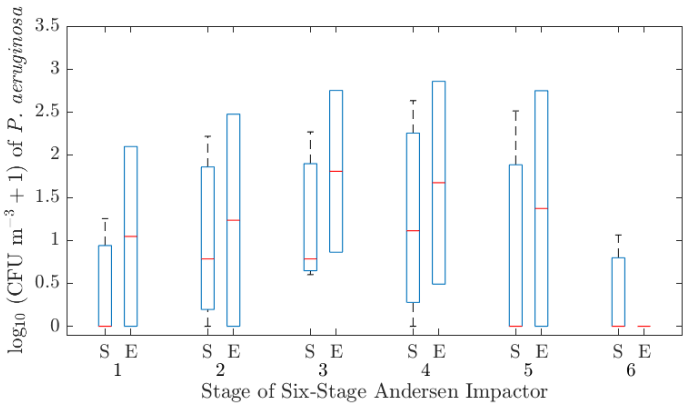

(b) Positive colony counts of *P. aeruginosa*.

Figure 6.34: Box plot of the aerobic colony counts ($\mathrm{CFU\,m^{-3}}$) from Andersen Impactor CASS samples found at each Andersen Impactor stage for participants in group A. S represents samples taken at the start and E represents samples taken at the end or a participants treatment.

the opposite is true for colonies of *P. aeruginosa*, the median value is lower at the start of treatment than the end. This is interesting because in Figure 6.33b on average the percentage of *P. aeruginosa* colonies in the overall ACC had a higher percentage of *P. aeruginosa* in start counts. Illustrated by the data in Table 6.11, start ACC were 80 % *P. aeruginosa* colonies vs 68 % *P. aeruginosa* colonies for end ACC. Therefore, the higher percentages of *P. aeruginosa* found at the start of treatment could be a consequence of participant 70 producing higher percentages of *P. aeruginosa* at the start of treatment vs the end. Additionally, there was no significant difference found between the ACC at the start of treatments compared to ACC found at the end of treatment ($p = 0.88$ Wilcoxon signed rank test). However, this is a small data set, but examining Table 6.11 the ACC at the end had a smaller median and a larger standard deviation, whereas the opposite is true for PCC. In conclusion, ACC were higher a the start of treatment (not significantly so), but

participants were still producing *P. aeruginosa* at the end of treatment and at higher percentages. Therefore, while people with CF may produce a smaller number of droplets containing microorganisms at the start of treatment the results did not provide evidence to suggest that the infection risk posed by a patient aerosolising *P. aeruginosa* reduced over the course of treatment.

Next, the data for group B were analysed. These were participants chronically infected with *P. aeruginosa* and not *M. abscessus* and had samples taken in the morning and afternoon of the same day (Table 6.1). Figure 6.35a displays the ACC for all bacteria and for *P. aeruginosa* for each participant in the group. A total of three out of five participants had higher ACC in the morning sessions than in the afternoon sessions. Those who were outliers in the study (Table 6.6) had higher ACC in morning sessions. At each stage of the Andersen Impactor (Figure 6.35b) there was larger ACC in the morning than in the afternoon apart from stage 6. Furthermore, Table 6.11 reports the same result, when comparing total and mean ACC over the two sessions higher ACC is found in the morning. However, the median for each session is equal. Therefore, it is possible that the data was skewed by participants 48 and 85 producing larger ACC in their morning sessions, but only their morning sessions were classed as outliers (Table 6.6). This begs the question, 'did these participants produce larger ACC in the morning because of the time of day or was it another factor?'

The results are less clear when comparing the data displayed in the box plots in

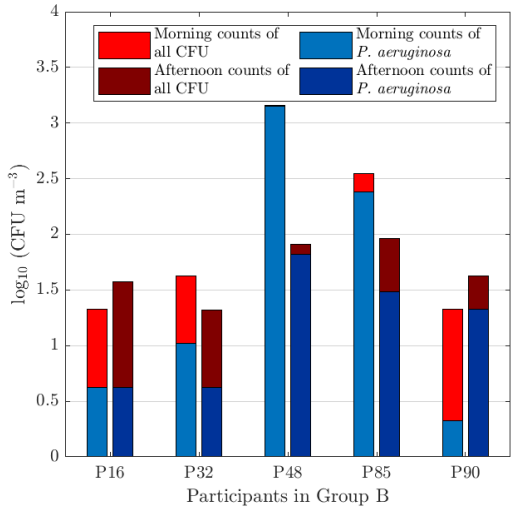

(a) Comparison of morning and afternoon for individual participants.

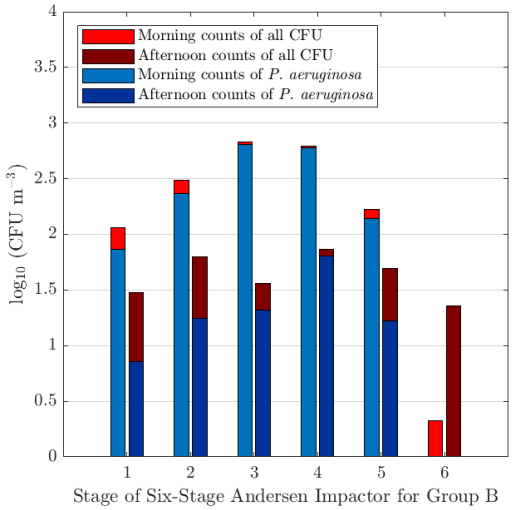

(b) Totalled distribution over each Andersen Impactor stage for all participants.

Figure 6.35: Comparison of logarithmic aerobic colony counts for all bacteria and *P. aeruginosa* (CFU m^{-3}) from Andersen Impactor CASS samples for participants in group B.

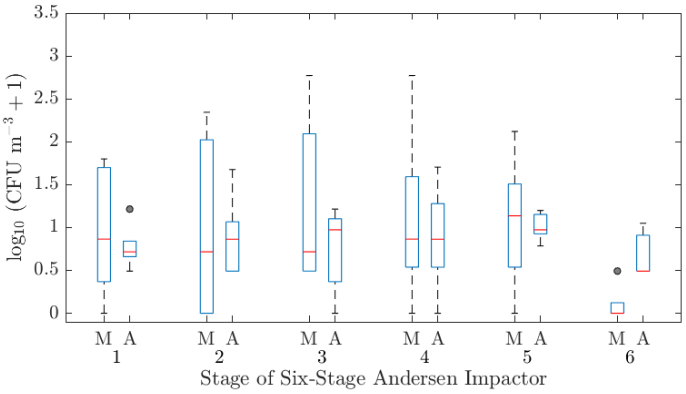

(a) All aerobic colony counts.

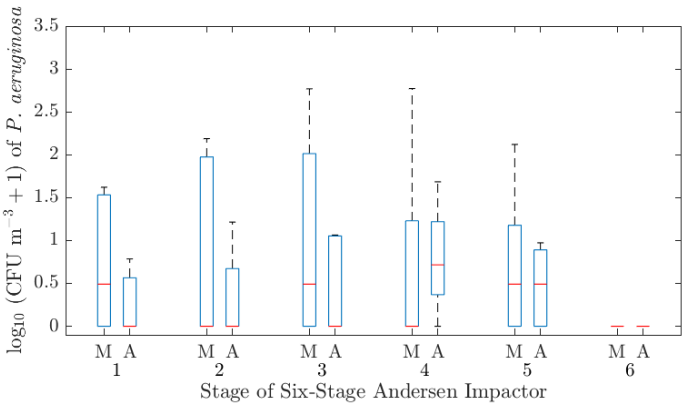

(b) Positive colony counts of *P. aeruginosa*.

Figure 6.36: Box plot of the aerobic colony counts ($\mathrm{CFU\,m^{-3}}$) from Andersen Impactor CASS samples found at each Andersen Impactor stage for participants in group B. M represents samples taken in the morning and A represents samples taken in the afternoon.

Figure 6.36. The IQR for morning results was larger, but the median is only greater in the morning 50 % of the time. Additionally, for ACC of *P. aeruginosa* the results are again varied, three stages (2, 5 and 6) are equal, two stages have higher ACC of *P. aeruginosa* in the morning (1 and 3) and the final stage has higher ACC of *P. aeruginosa* in the afternoon (4). As a general trend there was higher percentages of *P. aeruginosa* in the ACC in the morning than in the afternoon, overall this is 90 % and 46 % respectively (Table 6.11). The difference between the sessions from participants in group B is greater; however, there was no significant difference found between measured ACC in the morning and afternoon sampling sessions for participants ($p = 0.31$ Wilcoxon signed rank test).

6.4.5.1 Variation between measured factors

Further analysis was conducted on all participants in the study. First, all participants were grouped into two groups. Participants who were exacerbating at the time of sampling and those who were not (similar to the difference between sessions for group A). Mean ACC was used as the number of participants in the two groups were unequal. Figure 6.37 displays the data from these two groups, a greater mean ACC in participants that were exacerbating was observed than for those who were not. The box plot data mostly agrees with this, when a participant was exacerbating the median was greater on all stages apart from stage 2 and 6. A summary of the mean, median and standard deviation of the ACC from the grouped participants is given in Table 6.12. Both the mean and median are larger with a smaller standard deviation when a participant was exacerbating. However, there was not a statistically significant difference between the ACC produced by participants who were exacerbating and those who were not ($p = 0.31$ Mann-Whitney U test).

Subsequently, all participants were grouped into a further two groups. Participants sampled in the morning and participants sampled in the afternoon (the same conditions for group B). The mean ACC was used as the number of participants in each group was unequal. Figure 6.38 displays the data from these two groups. Differences between the data from the Andersen Impactor can be seen in Figure 6.38a. Stages 3, 4 and 5 have much larger values of ACC in the morning compared to the

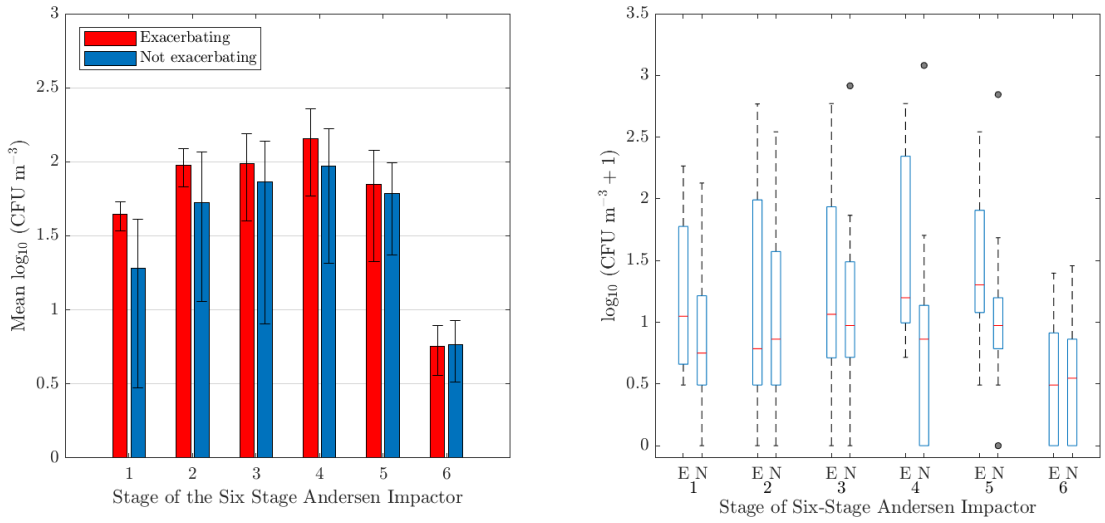

(a) Mean distribution.

(b) Box plot distribution.

Figure 6.37: Comparison of the distribution of logarithmic aerobic colony counts (CFU m^{-3}) from Andersen Impactor CASS samples found at each Andersen Impactor stage for participants that were exacerbating (E) and those that were not (N).

Table 6.12: Summary of the mean, median and standard deviation of the aerobic colony counts from all grouped participants.

ACC ($CFU\,m^{-3}$)	**All: Exacerbating**	**All: Not exacerbating**	**All: Morning**	**All: Afternoon**
Mean	457	305	478	188
Median	81	48	55	81
Standard deviation	589	841	907	341

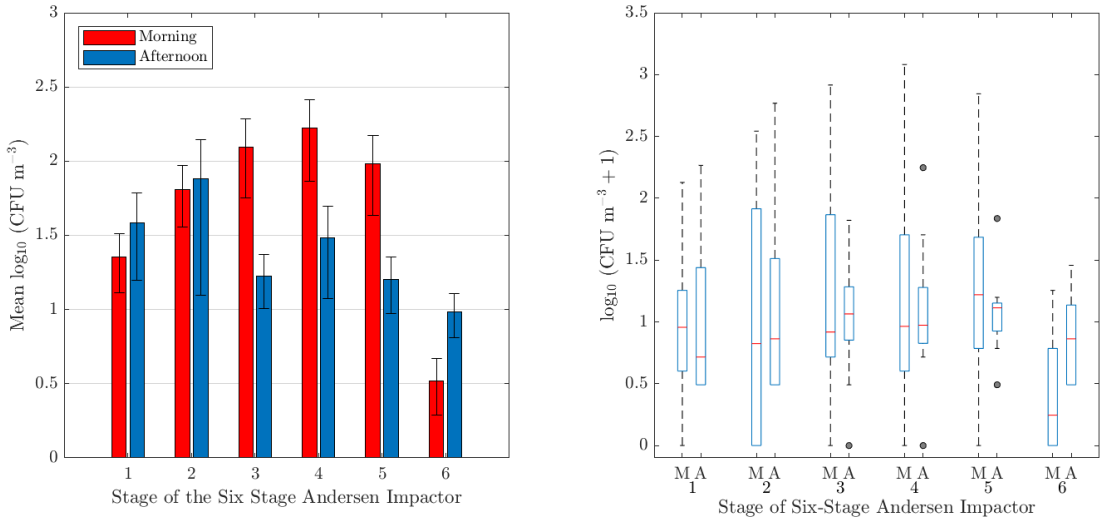

(a) Mean distribution.

(b) Box plot distribution.

Figure 6.38: Comparison of the distribution of logarithmic aerobic colony counts ($CFU\,m^{-3}$) from Andersen Impactor CASS samples found at each Andersen Impactor stage for participants that were sampled in the morning (M) and those sampled in the afternoon (A).

afternoon. Conversely, stages 1, 2 and 6 have higher ACC in the afternoon. The distribution from afternoon sessions was interesting, the distribution deviates from the bell curve observed in Figure 6.16a. Stages 3, 4 and 5 are lower than the norm and stages 1, 2 and 6 are higher. Overall, the mean is higher in the morning than in the afternoon (Table 6.12), but the median in the box plots (Figure 6.38b) is lower in the morning for 4 out of the 6 stages. Furthermore, the overall median is higher in the afternoon with a lower standard deviation. This suggests that the outliers who were only outliers in their morning session (Table 6.6) skewed the data. It cannot be said for certain that time of day is not the reason they are producing a higher bacterial load in the morning, because participants throughout the study mentioned a build up of mucus overnight and they felt they clear their lungs more in the morning and consequently produce more bacteria. Although, when comparing the ACC from both groups there was no significant difference found between the

morning and afternoon sessions ($p = 0.95$ Mann-Whitney U test).

Considering the affects of medication participants were taking and when was difficult to examine. People with CF take a wide range of medications and there was not sufficient data points to make solid conclusions. Mucolytic treatment decreases the viscosity and elasticity of mucus with the goal of improving mucus clearance from the airways (Henke and Ratjen, 2007). Therefore, investigation into this treatment was considered. Analysis established that all of the extreme outliers seen in Table 6.6 had mucolytic treatment before the session. Yet, participant 7 and participant 41 also had mucolytic treatment before their sessions and had low ACC in comparison. It could be possible that mucolytic treatment had an effect on ACC and maybe droplet size distributions considering its rheological changes to mucus but to conclude this with any certainty a study with a focus on this aim needs to be undertaken.

6.5 Summary

The primary objective of the study was achieved with regard to *P. aeruginosa* which was found to be present in the majority of cough/exhaled breath aerosols. *M. abscessus* was detected but only in mask samples and it cannot be confidently stated that the primary objective for *M. abscessus* was achieved. Hence, this study gives clear evidence that *P. aeruginosa* can be aerosolised by people with CF and it is likely that *M. abscessus* is too. When comparing the sampling methods, CASS sampling with an AGI-30 did not measure high enough bacterial load for presence of bacteria to be detected and this method is not recommended for the short sampling times in this study. Nevertheless, the CASS with an Andersen Impactor worked well for measuring *P. aeruginosa* in cough/exhaled breath samples, individual colonies could be tested and low total bacterial counts were still found to be positive for *P. aeruginosa*. Another advantage of this method was that droplet size distributions were measured and this sampling method is recommended for detecting *P. aeruginosa*. However, *M. abscessus* was not detected in any CASS samples but was found in mask samples. The sensitivity in the PCR method for detecting *M. abscessus* was apparent in these results and it was assumed mask samples would likely have found presence for *P. aeruginosa* if tested. The very straight forward testing method of the mask has advantages for widespread clinical use, but it was not able to provide information on droplet size distributions.

Total bacterial load was calculated for all participants in the study and aerobic colony counts were correlated with colony counts of *P. aeruginosa*. Participants

who had higher total bacterial load also had higher bacterial load of *P. aeruginosa*. However, participants who were infected with both *P. aeruginosa* and *M. abscessus* did not have *P. aeruginosa* detected in their cough/exhaled breath, which is notable since *P. aeruginosa* was isolated from all but one participant with *P. aeruginosa* only. A subset of participants who were named 'super producers' produced at least an order higher aerobic colony counts ($CFU\,m^{-3}$) than the majority of other participants. Super producers have been reported to produce as many as 80 % of infections (Endo et al., 2020) and this could impact infection control measures if these super producers are identified. A conflicting correlation between FEV_1 and aerobic colony counts was found with Wainwright et al. (2009) and in both cases it was the super producers driving the correlation. In the case of this study, high producers had low FEV_1 which gave a negative correlation and the opposite was true in the study conducted by Wainwright et al. (2009). In conclusion, it can be assumed FEV_1 does not correlate with aerobic colony counts and that producing a high bacterial load does not depend on FEV_1.

Examining the droplet size distributions found droplets containing culturable bacteria were dominated by sizes within the respirable range. After splitting the droplets into the traditional definitions of large ($\geq$5 µm) and small ($<$5 µm) droplets the result confirmed there was a preferential towards small droplets for *P. aeruginosa* and the other bacteria measured. This finding was significant as this study presents evidence that droplets small enough to stay suspended within the air and deposit in the lower respiratory tract where they are likely to cause infection were produced and at greater quantities than larger droplets. In addition, droplet size distributions of the bacteria from participants infected with *P. aeruginosa* and not *M. abscessus* were compared to those infected with *M. abscessus* and the distributions were found to be statistically significant. Participants infected with *M. abscessus* favoured Andersen Impactor stages 2 and 3 which was not seen by the other participants. This sample size was small so further investigation would be needed to draw accurate conclusions. Similarities were drawn between the droplet size distributions produced by those infected with *P. aeruginosa* and not *M. abscessus* to participants in the study conducted by Wainwright et al. (2009), the small differences demonstrated the variability within the droplet size distributions produced but the similarities established that participants infected with chronic *P. aeruginosa* will produce larger quantities of droplets containing bacteria on stages 3, 4 and 5 on the Andersen Impactor (1.1 µm–4.7 µm).

Bacterial load in the air was found to be related to indoor but not outdoor sources and mean ambient air colony counts were similar to those measured in studies on naturally ventilated hospital wards. Additionally, a relationship between aerobic

colony counts and ambient air colony counts was suggested, but further work and more data are needed to determine if this potential relationship is significant. Only a small subset of samples found positive isolates of *P. aeruginosa* or *M. abscessus*. Concluding ventilation or location of sampling may have been a key factor in detecting a positive colonies of *P. aeruginosa* or *M. abscessus*. Although, the method of detection did not test every colony and could have influenced this result. One of the most significant results in the study was that *M. abscessus* was found in an ambient air sample. Assuming there were no other sources of *M. abscessus* in the participants room this results proves that *M. abscessus* has the ability to be aerosolised in small enough droplets to stay suspended in the air and survive for long enough to be sampled.

Groupings of the participants did not show any statistically significant results and no significance was found when generalising these groups over all participants. Overall, participants recorded higher aerobic colony counts when exacerbating compared to participants not exacerbating, but the infection risk of a participant aerosolising *P. aeruginosa* did not reduce over the course of treatment. Exacerbation was not measured on a scale and droplet formation can depend on visocity and patient sputum will change with exacerbation. Morning aerobic colony counts were on averge greater than afternoon colony counts but the data was swayed by 'super producers'. Although time of day could have played an important role in these participants producing greater colony counts in the morning. Mucolytic treatment was found to have been taken before each of the high producing sessions, but it was also taken by other participants in lower producing sessions. There was great variability seen in the data between participants and more investigation is needed on influence of time of sampling and treatment as this study has present some interesting hypothesis finding work.

Chapter 7

Evaluation of factors influencing airborne transmission risk

Infection control guidelines are of paramount importance to stop the transmission of pathogens associated with CF. Although mitigation measures are in place on CF units and people with CF have been shown to produce viable pathogens in their cough/exhaled breath, quantitative risk to a person with CF from airborne pathogens has not been extensively studied. To address this gap the results from Chapters 5 and 6 are discussed and compared to determine input parameters to a mass-balance risk model which simulates bacteria concentrations in room air, exposure rates, and the risk to a susceptible person with CF. In addition, the model was used to explore different room sizes, patient interactions, and ventilation rates to determine how these factors influenced the risk of infection.

7.1 Comparison of laboratory experiments and the cross-sectional study

Comparisons can be made with the data from both the laboratory work in Chapter 5 and the cross-sectional hospital study in Chapter 6. In both of these studies bacterial aerosols were measured on all stages of the Andersen Impactor, but the majority of the bacteria was located in the small droplets (<5 µm), Figure 7.1. Data from the Spraytec particle sizer indicated large numbers of very small droplets (<1 µm) in the laboratory experiments. Several studies from the literature have measured the majority of droplets expelled from the mouth of healthy volunteers to be less than 1 µm (Papineni and Rosenthal, 1997; Morawska et al., 2009) and it is expected that in the cough/exhaled breath of people with CF there will also be a large number of very small droplets. However, this was not seen in the measurement data, but the bacteria of interest are typically 0.5 µm–2 µm and therefore would not be present in many of the droplets of this size to be measured up by the Andersen Impactor. In the laboratory experiments more culturable colonies of *P. aeruginosa* were found on stage 6 compared with the hospital data. This could be one of two reasons: the Collison nebuliser limiting the size range of the droplets and producing many more droplets in the size range for stage 6 on the Andersen Impactor; and the difference in the sputum rheology compared to the experimental studies - which was not able to be tested. Both factors could also explain why there was higher proportions of *P. aeruginosa* on stages 1, 2, and 3 from cough/exhaled breath aerosols from people with CF.

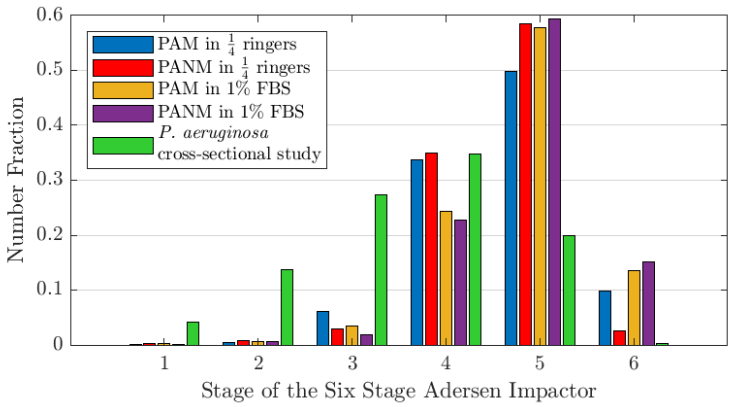

Figure 7.1: Comparison of Andersen Impactor measurement data for *P. aeruginosa* mucoid (PAM) and non-mucoid (PANM) strains in 1/4 ringers and 1 % FBS at 1 m in the BACA to *P. aeruginosa* measured in cough/exhaled breath samples from people with CF during the cross-sectional study.

Studies of cough/exhaled breath from people with various respiratory infections have shown similarities to the data collected in this thesis. The droplet size distributions measured had a predominance of pathogens reported in small droplets (<5 µm) (Fennelly et al., 2004; Wainwright et al., 2009; Lindsley et al., 2010; Fennelly et al., 2012; Lindsley et al., 2012; Bischoff et al., 2013; Gralton et al., 2013; Knibbs et al., 2014; Patterson et al., 2017; Theron et al., 2020). However, there are several factors that could be influencing the size of droplets suspending pathogens. Droplets can originate from different parts of the respiratory tract and are formed during many expiratory activities such as breathing, talking, shouting, coughing, sneezing, singing or laughing. The droplet produced can range in size from <1 µm to >100 µm, the size distribution is largely dependant on the expiratory activity and follows a complex distribution (Morawska et al., 2009; Johnson et al., 2011). Smaller droplets are created in the lungs whereas larger droplets are created in the oral cavity (Johnson et al., 2011). In the case of people with CF the infection occurs within the lungs and consequently the culturable aerosols measured had a preferential for droplets within the respirable range (<5 µm). Similarly, this is the case for *Mycobacterium Tuberculosis*, but for a virus that uses receptors on the surface of cells that are present within the respiratory tracts all droplet fractions (Table 1.2) containing virus are likely to be produced (Milton, 2020). In addition, when a pathogen can be detected in the oral cavity large ballistic behaving droplets are likely to contain pathogens.

Secondly, measuring a majority of smaller droplets could be an artefact of the sampling method used. In the literature cited for having a predominance for small droplets all but two studies used an Andersen Impactor for isolating pathogens in cough/exhaled breath. The Andersen Impactor sampling efficiency drops with increasing particle size (Upton et al., 1994) potentially leading to an under representation of larger particles. Finally, an important factor to consider is the evaporation of the droplet before being sampled and the following section analyses this further.

7.1.1 Droplet evaporation

Investigation into droplet evaporation is key to determine the original size of the droplets produced in the cross-sectional study and how the size of droplets affect deposition rates as a removal method of the bacteria in the room air for the subsequent risk model. A simple droplet evaporation model which assumes a pure water droplet is used to demonstrate the influence of evaporation. Here the model entailed computing the net flux of water vapour molecules by diffusion into the air

surrounding the droplet. A time-dependant equation for particle diameter (Nicas et al., 2005), d is expressed as:

$$d(t) = \sqrt{d_0^2 - \left(8 \times v_m \times D \times \left(\frac{P_{ws} - P_w}{k \times T}\right) \times t\right)} \tag{7.1}$$

where P_{ws} is water's saturation vapour pressure at ambient air temperature T (K), P_w is the partial pressure of water vapour in ambient air and is equal to ${}^{RH}/_{100} \times P_{ws}$. Time, t, is measured in seconds and at $t = 0$ droplet diameter is d_0 (m). The constant parameters in this expression are as follows, k is Boltzmann's constant ($1.38 \times 10^{-23}\,\mathrm{J\,K^{-1}}$), v_m is the condensed-phase volume occupied by a single water molecule ($2 \times 10^{-29}\,\mathrm{m^3}$), and D is the molecular diffusivity of water vapour in air ($1.8 \times 10^{-5}\,\mathrm{m^2\,s^{-1}}$).

Figure 7.2 displays the time taken for a water droplet to evaporate at 22 °C for varying initial diameters and relative humidities. A 20 µm droplet at 50 % relative humidity can completely evaporate in 0.29 s. However, Nicas et al. (2005) reported that a respiratory droplet will reach an equilibrium diameter which is half of its original size due to presence of non-volatile solids (protein, salts, surfactant and microorganisms), which was subsequently backed up by an experimental study (Vejerano and Marr, 2018). Hence, time taken for a 20 µm droplet at 50 % relative humidity to reach its equilibrium diameter was 0.21 s and for a 5 µm droplet at the same relative humidity it was 0.01 s. It was assumed that in the studies cited above the droplets had reached their equilibrium diameter before measurement and the original sizes would likely be double that reported. Concluding, that only some of the droplets will still be traditionally defined as small droplets (<5 µm) and some

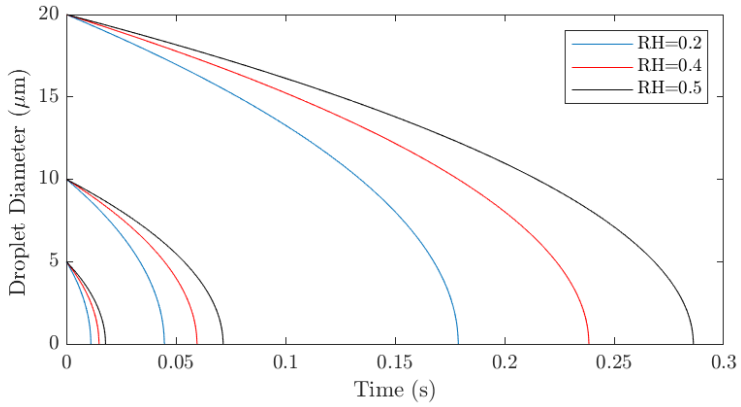

Figure 7.2: Evaporation of droplets according to (7.1) at 22 °C, varying relative humidities, and initial diameters of 5 µm, 10 µm and 20 µm.

of the droplets original size will be above that threshold.

7.1.1.1 Increasing relative humidity

Relative humidity (RH) plays a key role in the evaporation of droplets, in Figure 7.2 the greater the RH the slower the evaporation. It was possible that in the CASS chamber the relative humidity reached high enough levels that it slowed down evaporation enough so the measured size of the droplet was not its equilibrium diameter. To investigate this a changing RH was added to the droplet evaporation model. First, RH is defined as follows:

$$RH = \frac{\rho_w}{\rho_{ws}}, \tag{7.2}$$

where:
RH = relative humidity (as a decimal),
ρ_w = density of water vapour ($\mathrm{g\,m^{-3}}$),
ρ_{ws} = saturation density of water vapour ($\mathrm{g\,m^{-3}}$).

As a participant exhaled into the CASS they added moisture into the chamber increasing the RH. Using a mass-balance model the concentration of water vapour inside the CASS was calculated. This model takes into account that the flow rate of the Andersen Impactor (outflow from the CASS) was higher than the breathing rate of the participants; therefore, clean air from the room was drawn inside the CASS too. The density of water vapour inside the CASS, ρ_w ($\mathrm{g\,m^{-3}}$), can be described by:

$$V\frac{d\rho_w}{dt} = q + (Q - p)\rho_{air} - Q\rho_w, \tag{7.3}$$

where ρ_{air} is the density of water vapour in the room air, Q is the flow rate of the Andersen Impactor ($28.3\,\mathrm{L\,min^{-1}}$), V is the volume of the CASS ($50.9\,\mathrm{m^3}$), $q = p \times M$ and p is the respiratory/cough rate of the participant ($11.9\,\mathrm{L\,min^{-1}}$, section 7.2.2.4) and M is the water vapour content in expired air. Water per litre of expired air, M, was assumed to be $29.5\,\mathrm{mg\,L^{-1}}$ (Bruck, 1962; Ferrus et al., 1980). Solving gives

$$\rho_w(t) = \frac{q}{Q} + \frac{(Q - p)\rho_{air}}{Q} + \frac{(\rho_{w0}Q - q - (Q - p)\rho_{air})}{Q}e^{-Qt/V}, \tag{7.4}$$

at $t = 0$, $\rho_w = \rho_{w0}$ and $\rho_{w0} = \rho_{air}$ which assumes the air inside the CASS at t_0 is the same as the room air. After analysing data gathered in the cross-sectional study the average temperature was 22 °C (95 %CI 22.1–22.3 °C) and average RH was 49 % (95 %CI 48.4–49.2 %). For the purposes of the model the average values

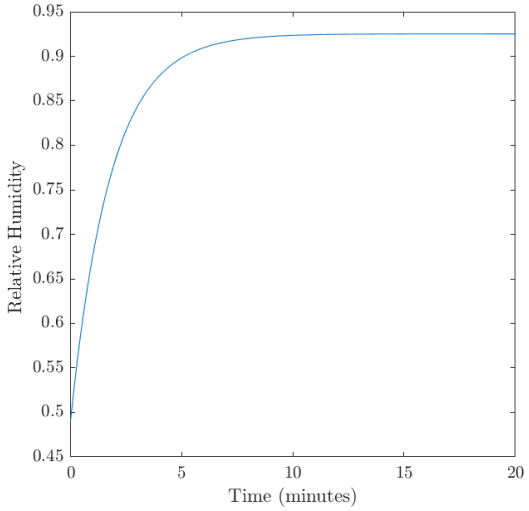

Figure 7.3: Change in relative humidity inside the CASS drum with time. Temperature was 22 °C and initial relative humidity was 49 %.

of temperature and RH were used. At 22 °C the saturated water density in air is $\rho_{ws} = 19.3\,\mathrm{g\,m^{-3}}$. Saturated water density and (7.4) allow the change in RH in the CASS over time to be calculated. Figure 7.3 displays how the RH in the CASS increases with time reaching a steady state concentration of 93 % after 18 minutes.

An investigation into how this change in RH would increase the time taken for a droplet to evaporate was undertaken and the results demonstrated that the increase in RH was not a rapid enough rate to significantly increase the time taken for a droplet to evaporate. A 20 µm droplet entering the CASS at the starting RH of 48 % did not increase the time taken to evaporate to its equilibrium diameter (0.21 s) to two significant figures. However, the increasing RH within the CASS does indicate that droplets expelled into the CASS towards the end of sampling when the RH had significantly increased would take longer to evaporate. Figure 7.4 gives an example of how a 20 µm droplet evaporates with increasing relative humidities from varying initial RH. The RH values were: 48 %, the lowest RH inside the CASS; 70 %; and 93 %, the steady state RH inside the CASS. Although the droplets take longer to evaporate at high values of RH they were still able to reach their equilibrium diameter before being measured by the Andersen Impactor. Therefore, it was assumed that all droplet measured by the Andersen Impactor in the cross-sectional study were fully evaporated.

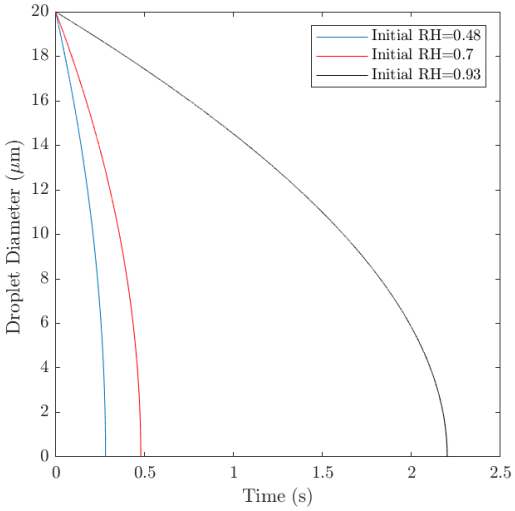

Figure 7.4: Evaporation of droplets according to (7.1) and an increasing RH at 22 °C, varying initial relative humidities, and initial diameter of 20 µm.

7.1.1.2 Droplet momentum

After their emission, droplets fall to the ground or are displaced by room air depending on their mass and initial momentum. Concurrently, smaller droplets (<100 µm) evaporate rapidly and can reduce to one half of their original size which decreases their mass and terminal velocity (Xie et al., 2007). It is possible for small aerosolised droplets to remain airborne for several hours and be dispersed by local currents. To determine how 'quickly' droplets fall the trajectory of a single droplet was calculated using the Lagrangian approach where the equations of momentum were solved for an individual droplet. The droplet modelled was assumed to be a spherical pure water droplet. Both the gravity and buoyancy forces were considered together with aerodynamic drag, all other forces (e.g Basset, Magnus and Saffman) were neglected. The governing equations that describe the droplet motion are as follows (de Oliveira et al., 2021):

$$\frac{d\mathbf{X_d}}{dt} = \mathbf{u_d}, \tag{7.5}$$

and

$$\frac{d\mathbf{u_d}}{dt} = \frac{3C_D}{d_d}\left(\frac{\rho_a}{\rho_d}\right) \mid \mathbf{u_a} - \mathbf{u_d} \mid (\mathbf{u_a} - \mathbf{u_d}) + \left(1 - \frac{\rho_a}{\rho_d}\right)\mathbf{g}, \tag{7.6}$$

where t indicates the time, d_d is the diameter of the droplet, $\mathbf{g}$ is the acceleration due to gravity, $\mathbf{X}$ and $\mathbf{u}$ are the position and velocity vectors, ρ is the density of the droplet, and the subscripts a and d refer to the continuous phase (air) and the dispersed phase (droplet) respectively. The parameter C_D is the aerodynamic drag term in (7.6) and is a function of the Reynolds number of the droplet, Re_d. The

Reynolds number is calculated based on the relative velocity between the dispersed and continuous phase:

$$Re_d = \frac{\rho_a d_d \mid \mathbf{u_a} - \mathbf{u_d} \mid}{\mu_a}, \tag{7.7}$$

where μ_a is the dynamic viscosity of the air. Here the Schiller (1933) correlation is used for aerodynamic drag:

$$C_D = \begin{cases} 0.424, & \text{for} Re_d > 10^3 \\ \frac{24}{Re_d}\left(1 + \frac{Re_k^{2/3}}{6}\right), & \text{for} Re_k < 10^3. \end{cases} \tag{7.8}$$

Assuming the maximum velocity of a droplet expelled during a cough is $11.7\,\mathrm{m\,s^{-1}}$ (Chao et al., 2009), the maximum Reynolds number will be of the order 10^2. Therefore, for all simulations $Re_d < 10^3$. The momentum equation (7.6) can be expressed in the form of its horizontal and vertical components:

$$\frac{du_d}{dt} = \frac{3C_D}{d_d}\left(\frac{\rho_a}{\rho_d}\right) \mid u_a - u_d \mid (u_a - u_d), \tag{7.9}$$

$$\frac{dv_d}{dt} = \frac{3C_D}{d_d}\left(\frac{\rho_a}{\rho_d}\right) \mid v_a - v_d \mid (v_a - v_d) + \left(1 - \frac{\rho_a}{\rho_d}\right) g, \tag{7.10}$$

where u is the horizontal velocity and v is the vertical velocity.

The settling of droplets in still air within the size range of the Andersen Impactor is shown in Figure 7.5. The droplet sizes modelled are the equilibrium diameters because the timescales of droplet evaporation are very short compared to the timescales observed for deposition. The deposition rates over 60 minutes for 5 µm and 10 µm droplets are very slow. As expected there was a greater deposition from the larger droplet and after 60 minutes it has fallen around 250 mm. Extrapolating the same falling rate for subsequent hours it would take around 7 hours for a 10 µm droplet to fall to the ground from a height of 1.8 m. In addition, droplets of this size lose momentum from the initial velocity they experienced from exhaled breath/cough and quickly move with the room air. But indoor air is not still and the upward velocity of air in a thermal plume from a human body was reported to be greater than the settling velocity of a 50 µm droplet (Gena et al., 2020). Deposition of small droplets (≤ 10 µm) is hard to predict as it depends significantly on the airflow patterns in a room but average deposition rates have been reported in the literature as $2.45 \times 10^{-4}\,\mathrm{s^{-1}}$ for 1 µm–2.5 µm, $4.48 \times 10^{-4}\,\mathrm{s^{-1}}$ for 2 µm–5 µm and $1.7 \times 10^{-3}\,\mathrm{s^{-1}}$

for 9 µm–10 µm (Lai, 2002; Howard-Reed et al., 2003; Tran et al., 2017).

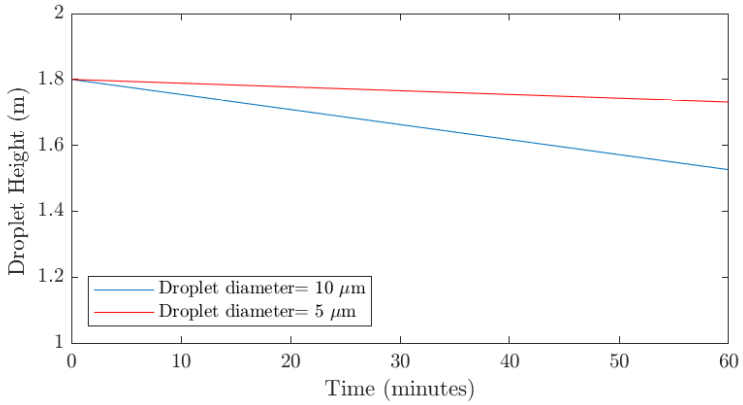

Figure 7.5: Deposition of droplets in still air according to (7.5) and (7.6) at constant diameters of 5 µm and 10 µm.

7.2 Modelling aerosol infection risk

Investigating the number of bacteria contained in aerosols produced by people with CF within an indoor space is crucial in determining the risk to a secondary susceptible individual. The time taken to remove the viable bacteria and how much of this bacteria is inhaled by a susceptible host will give quantitative data to inform airborne infection mitigation measures. Hence, on the basis of data gathered within this thesis, mathematical models were used to undertake the following aims:

1. Compare steady state calculations of concentration of bacteria within simulated hospital rooms to measurements of the room air taken in the cross-sectional study (Chapter 6).
2. Determine concentration of bacteria within the room, number of bacteria inhaled, and risk of an infection with *P. aeruginosa* to the susceptible individual for multiple scenarios. The scenarios modelled were as follows:
   i Outpatient clinic,
   ii Lift,
   iii Waiting room,
   iv Domestic setting.
3. Explore how a change in ventilation rates can alter concentration of bacteria within the room, number of bacteria inhaled, and risk of an infection with *P. aeruginosa*.

In an approach commonly used to model indoor contaminant concentrations, number of bacteria contained in droplets in an indoor space was modelled using a mass-balance approach as described below. In applying this approach, the following assumptions were made:

1. There was a single infectious individual who emitted aerosols containing bacteria at a constant rate, E (CFU s^{-1}) throughout the event.
2. The infectious respiratory aerosol quickly dispersed and was evenly distributed throughout the space with volume V (m^3), so that the change in concentration of bacteria, C (CFU m^{-3}), in the space with time, t (s), was approximately the same regardless of the sampling point.
3. There was no prior source of the pathogen in the space.
4. The latent period of the disease was longer than the timescale of the event.
5. Viable bacteria in the air of the space were removed by a combined single removal rate, λ (s^{-1}), which was the sum of ventilation, inactivation, and deposition.

Assumption 2, the well-mixed assumption, may be somewhat unphysical. In reality spaces are not well mixed and there will be a higher concentration of the bacteria close to the emission source and in some rooms there are also concentration gradients due to ventilation flows. This must be considered when assessing the implications of the model. However, the well-mixed assumption is reasonable in many rooms providing people are at least 1 m–2 m from the infectious person.

The aerosolised bacterial concentration increased with time from an initial value of zero and the rate of change in the concentration of bacteria was described by the mass-balance model:

$$\frac{dC}{dt} = \frac{E}{V} - \lambda C. \tag{7.11}$$

Solving (7.11) over a known period of time that starts at $t = 0$ where $C = C_0$, gives the concentration of bacteria in the space as a function of time,

$$C(t) = \frac{E}{\lambda V} + \left(\frac{C_0 \lambda V - E}{\lambda V} \right) e^{-\lambda t}. \tag{7.12}$$

The exposure to the susceptible individual was estimated from the total number of bacteria inhaled, $\sum n$ (CFU inhaled), over the exposure period, T (s),

$$\sum n = p \int_0^T C(t) dt, \tag{7.13}$$

so that

$$\sum n = p\left(\frac{E}{\lambda V}\left(T - \frac{1}{\lambda}\left(1 - e^{-\lambda T}\right)\right) + \frac{C_0}{\lambda}\left(1 - e^{-\lambda T}\right)\right), \tag{7.14}$$

where the total number of bacteria inhaled is dependant on the volumetric breathing rate of a person with CF, p ($\mathrm{m^3\,s^{-1}}$).

7.2.1 Dose-response for *P. aeruginosa*

A dose-response model can be used to assess whether exposure to a pathogen is likely to result in infection. Several statistical models based on empirical data have been proposed to describe dose-response with the most common being the exponential model:

$$\mathrm{P(response)} = 1 - \exp\left(-k \times \mathrm{dose}\right), \tag{7.15}$$

where k is a pathogen specific parameter.

There is a lack of data on dose-response for many respiratory pathogens but there is reported data for *P. aeruginosa* which uses the exponential model. Dose-response models are based on empirical data which involves trials where humans or animals are inoculated and their immune response is monitored for different infectious doses. Analysis of experiments conducted by Hazlett et al. (1978) found $k = 1.05 \times 10^{-4}$ for *P. aeruginosa*. However, the experiment measured for the response of death in mice after inoculation of *P. aeruginosa*, the possible inaccuracy of this model is considered when discussing the analysis. Figure 7.6 displays the published dose-response curves for *P. aeruginosa*, influenza, and rhinovirus. Dose for both influenza

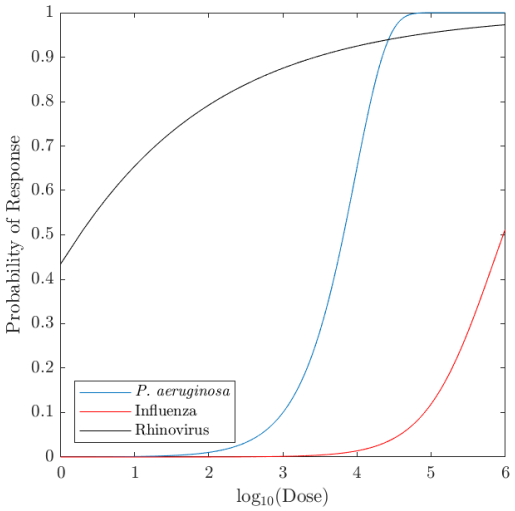

Figure 7.6: Dose-response curve for *P. aeruginosa* , influenza and rhinovirus

and rhinovirus was intranasal and the response was infection (Mitchell et al., 2021). The dose-response curve for *P. aeruginosa* sits in the middle of the two viruses. In a stochastic model the curve can be used to estimate the range of infection risk expected from a dose distribution.

7.2.2 Input parameters

7.2.2.1 Bacterial emission rate, E

Emission rates for the model were estimated from the cross-sectional study (Chapter 6). Logarithmic corrected colony counts were adjusted by the time of sampling and a log-normal distribution was fitted to the data. All sampling sessions were used to provide data points for the emission rates of all bacteria. Emission rate of all bacteria was probable over the range $\log_{10}(0-6)\,\mathrm{CFU\,h^{-1}}$ and was given by the log-normal distribution shown in Figure 7.7. The Kolmogorov-Smirnov test accepted null hypothesis that the data comes from a population with a log-normal distribution, $p = 0.41$. Sessions from participants in groups A and B (section 6.4.5) were used to calculate the emission rates for *P. aeruginosa*. The emission rate of *P. aeruginosa* was probable over the range $\log_{10}(0-6)\,\mathrm{CFU\,h^{-1}}$ and was given by the log-normal distribution shown in Figure 7.8. The Kolmogorov-Smirnov test accepted the null hypothesis that the data came from a population with a log-normal distribution, $p = 0.51$.

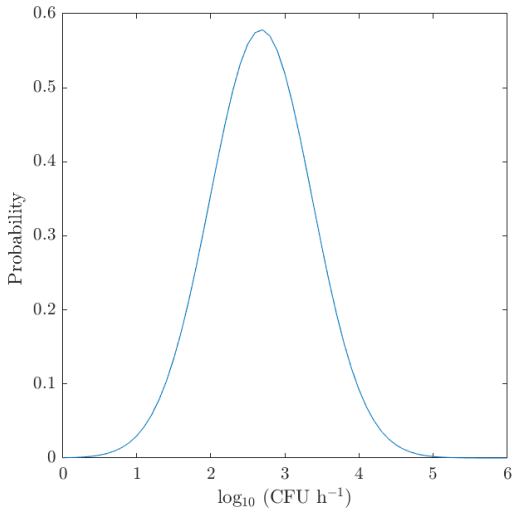

Figure 7.7: Log-normal distribution truncated on the range [0, 6) for the emission rates of all bacteria from people with CF, $\mu = 2.7$ and $\sigma = 0.7$

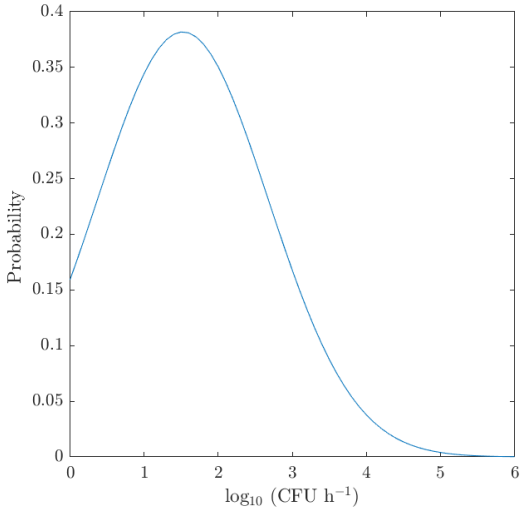

Figure 7.8: Log-normal distribution truncated on the range [0, 6) for the emission rates of *P. aeruginosa* from people with CF, $\mu = 1.5$ and $\sigma = 1.2$

Emission rates were calculated from cough/exhaled breath from people with CF which was measured by an Andersen Impactor. It was not assumed that emission rates were overestimated due to the participants coughing in their samples as no correlation was found between cough count and aerobic colony counts. Furthermore, similar studies for other pathogens found no correlation between cough count and aerobic colony counts and microorganism output was not affected during sleep (Williams et al., 2020). However, emission rates were based on culturable CFU from the Andersen Impactor and all bacteria present may not have been cultured. Therefore, emission rates could be an underestimation due to efficiency of the sampling method.

7.2.2.2 Space volume, V

The volume term in equation (7.11) describes the volume of the space modelled for each scenario and the values are given in Table 7.1. It is important to note that the volume term may be overestimated as the space volume can include people and objects where the aerosols containing bacteria cannot mix. The result of this is that the mixing volume and the space volume are not equal. However, in the scenarios considered the mixing volume and space volume were assumed to be equal. For the outpatient clinic scenario the volume was varied as a uniform distribution over the range of volumes for rooms on the CF unit where sampling took place during the cross-sectional study (Figure 6.2). The lift took a variable volume based off the difference in hospital lift sizes and the waiting room took a constant value. Domestic

settings were based of variable living room sizes.

Table 7.1: Aerosol infection risk model space volumes.

Space	**Floor Area, A_f (m^2)**	**Space Volume, V (m^3)**
Inpatient room 1	15.2	41.0
Inpatient room 2	15.1	40.1
Inpatient room 4	14.3	38.6
Inpatient room 6	15.6	42.1
Inpatient room 9	13.5	36.5
Inpatient room 12	13.5	36.5
Outpatient room 1	11.8	31.9
Outpatient room 2	11.8	31.9
Outpatient room 4	16.2	43.7
Lift	3.4–4.7	7.8–10.8
Waiting room	25	67.5
Domestic setting	16–22	36.8–50.6

7.2.2.3 Removal rate, λ

The concentration of bacteria within the air of the modelled space is reduced by a number of mechanisms: dilution and removal due to ventilation, λ_v; deposition onto surfaces, λ_d; and bacterial decay, k. Total removal rate is given by their sum:

$$\lambda = \lambda_v + \lambda_d + k \tag{7.16}$$

As the spaces are naturally ventilated or have full fresh-air ventilation systems, removal due to filtration was not included and re-suspension following deposition onto surfaces was not considered.

Loss rate due to ventilation, λ_v (s^{-1}) Occupant generated CO_2 has been widely used to estimate ventilation rates based on a fully mixed mass-balance model (Batterman, 2017):

$$V\frac{dC}{dt} = E + QC_R - QC, \tag{7.17}$$

where:

V = space volume (m^3),
C = CO_2 concentration in the space ($mg\,m^{-3}$),
C_R = CO_2 concentration in outdoor or replacement air ($mg\,m^{-3}$),
Q = removal rate of outdoor or replacement air ($m^3\,h^{-1}$),
E = CO_2 emission rate in the indoor space.

The CO_2 emission rate is generally attributed to the number of peopled in the space, n, and the average CO_2 generation rate per person, G_p. Hence, emission rate in the indoor space is calculated as $E = nG_p$. Ventilation rates are generally described as air change rates per hour, A (h^{-1}), and $A = Q/V$. Given the widespread practice of concentrations of CO_2 given in units of ppm a conversion factor (6×10^4) is included and under steady state conditions air changes per hour, A_s (h^{-1}), can be calculated as:

$$A_s = 6 \times 10^4 \cdot \frac{nG_p}{V(C_S - C_R)}, \tag{7.18}$$

where:
n = number of people in the space,
G_p = average CO_2 generation rate per person ($L\,min^{-1}$),
V = space volume (m^3),
C_s = steady state CO_2 concentration in the space (ppm),
C_R = CO_2 concentration in outdoor or replacement air (ppm).

Measurements of CO_2 were taken during the cross-sectional hospital study and were used to determine the average steady state CO_2 concentration for naturally ventilated hospital rooms. Calculation found C_S =789 ppm (95 %CI 773–806 ppm), this valued was determined using sessions where two people ($n = 2$) were always in the room and the CO_2 concentrations had reached a steady state. An average area of the rooms used in sampling was taken (Figure 6.2) and area = 14.1 m^2, using an average ceiling height (2.7 m) in hospitals then $V = 39.07\,m^3$. Persily and de Jonge (2017) measured carbon dioxide generation rates for building occupants and from the data presented generation rate for participants in the cross-sectional study was estimated to be in the range G_p = 0.246–0.324 $L\,min^{-1}$ and according to CIBSE (2015) outdoor CO_2 concentration is around 400 ppm. A Monte Carlo simulation was run (N = 1000 iterations) to estimate the loss rate due to ventilation, λ_v, on the CF unit at St James University Hospital Leeds Teaching Hospitals NHS Trust. The mean ($\pm$ SD) inferred loss rate due to ventilation was λ_v = 2.3 ($\pm$ 0.2) air changes per hour, which is equivalent to λ_v =$6.4 \times 10^{-4}\,s^{-1}$. In addition, ventilation rates were varied for the outpatient scenario of naturally ventilated hospital rooms. Two ventilation rates were chosen: 1 $ac\,h^{-1}$, for poor ventilation; and 6 $ac\,h^{-1}$, the hospital guidelines for the space modelled (Macintosh et al., 2007).

Loss rate due to deposition, λ_d (s^{-1}) The risk model does not include droplet sizes, but emission rates reported in Chapter 6 found the majority of droplets were less than 5 µm and according the reported droplet depositions rates in the literature (section 7.1.1.2) deposition rates are low. In addition, section 7.1.1.2 uses the governing equations to describe droplet motion and found slow deposition rates for droplets within the size range of the Andersen Impactor. Hence, for the risk model it was assumed that loss rates due to deposition is zero and that the droplet sizes considered in this model are able to stay in the room air indefinitely.

Loss rate due to biological decay, k (s^{-1}) Biological decay rate is a function of the half-life of bacteria, $t_{1/2}$ (s):

$$k = \frac{ln(2)}{t_{1/2}} \tag{7.19}$$

Knibbs et al. (2014) reported a decay for *P. aeruginosa* from cough aerosols from people with CF followed an exponential decay with half life of 50 minutes (95 %CI 30 to 151 minutes). Similar results were reported by Clifton (2009) who aerosolised several clinical strains of *P. aeruginosa* into the air in a controlled chamber and found the half life in the range 46–270 minutes. Both of these reuslts are similar and the risk model uses a uniform distributions over the confidence interval range proposed by Knibbs et al. (2014), 30 to 151 minutes. This equates to a loss rate due to biological decay per second to have the range of $7.65 \times 10^{-5}\,s^{-1}$ to $3.85 \times 10^{-4}\,s^{-1}$.

The laboratory work in this thesis (Chapter 5) obtained a high decay rate for *P. aeruginosa*, $k = 0.03\,s^{-1}$. However, the timescales to calculate this decay were short (80 s) and the bacteria experienced rapid initial die off possibly as a result of the experimental conditions. Clifton et al. (2008) conducted a similar experiment and the data suggested a similar rapid die off. The volume of the BACA system was a similar size to the CASS drum. Therefore, the emission rates measured by the CASS could be under represented due to a rapid decay rate of *P. aeruginosa* and further investigation into short timescale decay rates is needed.

7.2.2.4 Volumetric breathing rate, p $m^3\,s^{-1}$

Volumetric breathing rates of people with CF were used in the simulations. Bell et al. (1996) reported respiratory rates from people with CF to have an average of $10.5\,L\,min^{-1}$ with standard deviation $1.5\,L\,min^{-1}$. The respiratory rates measured during this study were compared to a control group (people who did not have CF)

and the control had a lower average respiratory rate of $7.0\,\mathrm{L\,min^{-1}}$ with standard deviation $1.2\,\mathrm{L\,min^{-1}}$. The higher respiratory rates in people with CF were attributed to a higher breathing rate (breaths per minute); this was confirmed in a second study (Hart et al., 2002). Subsequently, Thin et al. (2004) measured respiratory rates form people with CF at rest and during exercise. At rest respiratory rates had a slightly higher average of $13.6\,\mathrm{L\,min^{-1}}$ with standard deviation $2.7\,\mathrm{L\,min^{-1}}$. The measured data from both studies was pooled and gave a mean of $11.9\,\mathrm{L\,min^{-1}}$ (95 % CI 10.2–12.0). The confidence interval range was used in the model and was converted into volumetric breathing rates which gave a uniform distibution input for volumetric breathing rate to be in the range of $1.7 \times 10^{-4}\,\mathrm{m^3\,s^{-1}}$–$2.5 \times 10^{-3}\,\mathrm{m^3\,s^{-1}}$.

7.2.2.5 Infected occupancy, no occupancy, and exposure time, t (s).

Each scenario considered a range of timings which were appropriate to the event that was modelled. Each scenario modelled considered three timings:

1. Infected occupancy time is the time the infected host spent in the modelled space;
2. No occupancy time is when the modelled space had no occupancy, this was the time elapsed between the infected host leaving and the susceptible host entering the modelled space; and
3. Exposure time is the time the susceptible host was exposed to the concentration of bacteria in the modelled space.

Table 7.2: Aerosol infection risk model scenario timings.

Scenario	**Occupancy time (minutes)**	**No occupancy time (minutes)**	**Exposure time (minutes)**
Outpatient clinic	30 or 60 or 120 or 180	30	30 or 60 or 120 or 180
Waiting room	30	0	30
Lift	5	0	5
Domestic setting	30 or 60 or 120 or 180	0	30 or 60 or 120 or 180

Timings modelled in the outpatient clinic scenario were based off average times for standard outpatient visits:

30 minutes brief review, blood test, and port flush;

60 minutes full review;

120 minutes start IV antibiotic appointment;

180 minutes annual assessment including glucose tolerance test.

and the timings used in each of the scenarios are given in Table 7.2.

7.3 Risk modelling results

7.3.1 Comparison of steady state model to air sampling in the cross-sectional study

The following analysis considers the emission rate of all bacteria from people with CF and compares the predicted concentration of bacteria in the room to the ambient air samples measured in the cross-sectional study. The model assumes all bacteria contained in droplets were emitted from a single source. This addresses the first aim:

> Compare steady state calculations of concentration of bacteria within simulated hospital rooms to measurements of the room air taken in the cross-sectional study (Chapter 6).

Ambient air samples taken during the cross-sectional study were assumed to have come from rooms that had reached a steady state concentration of bacteria. Therefore, the data from the ambient air samples were compared to the calculated steady state concentrations from the simulation. When a long enough time has elapsed concentration of CFU in room air will reach steady state, that is $e^{-\lambda t} \to 0$ in (7.12) which gives steady state concentration as:

$$C(t) = \frac{E}{\lambda V}. \tag{7.20}$$

A Monte Carlo simulation was carried out for ($N = 10\,000$ iterations) to estimate C for the hospital rooms given a range of input values. The unknown parameters specified in Table 7.3 were given probabilistic distributions bounded by upper and lower limits. Only *P. aeruginosa* and *M. abscessus* were identified in the cross-sectional

Table 7.3: Parametric values used in the Monte Carlo simulation for estimation of the steady state concentration of CFU in room air.

Parameter	**Value(s)**	**Distribution**
Emission rate, E (CFU h^{-1})	$\log_{10}$(0–6)	Log normal (Figure 7.7)
Space volume, V (m^3)	31.9–43.7	Uniform
Loss rate due to ventilation, λ_v (ac h^{-1})	2.3	Constant
Loss rate due to deposition, λ_d (s^{-1})	0	Constant
Loss rate due to biological decay, k (min^{-1})	0	Uniform

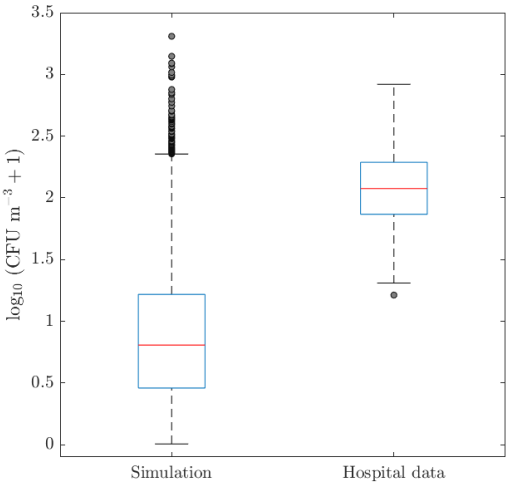

Figure 7.9: Comparison of the concentration of bacteria, C (CFU m^{-3}), in the steady state simulation and from the cross-sectional study.

study and all other bacterial colonies remained unknown. Hence, an accurate decay rate could not be deduced and loss rate due to biological decay was set to zero. However, this assumption could have resulted in an over estimation of the concentration of bacteria within the room air. In addition, deposition was also set to zero and may have resulted in on overestimation in the steady state concentration of bacteria in the room air.

The mean ($\pm$ standard deviation) of the concentration of bacteria (CFU m^{-3}) was 19.5 CFU m^{-3} ($\pm$ 53.9) and 163.8 CFU m^{-3} ($\pm$ 149.7) for the simulation and hospital data respectively. A graphical depiction of the comparison is given by boxplots and displayed in Figure 7.9. There is a clear difference between the two results but this difference is to be expected. The concentration of bacteria in the simulation is only from bacteria suspended in small airborne droplets that has been aerosolised by an

infectious individual. In comparison the results from the hospital study are a mixture of emissions from an infected individual, resuspended particles, environmental sources, and skin squame. Conclusions that were drawn from these results demonstrate that on average only a small percentage, just under 12 %, of the concentration of bacteria suspended in room air is emitted from an infectious individual, but for high emitters this percentage could be much larger as shown by the long tail on the distribution for the simulated results.

7.3.2 Modelling infection risk of *P. aeruginosa* in people with cystic fibrosis

This section analyses the outputs of the risk model simulations and discusses the possible risk to the susceptible individual, which covers the second aim:

> Determine concentration of bacteria within the room, number of bacteria inhaled, and risk of an infection with *P. aeruginosa* to the susceptible individual for multiple scenarios.

In addition, ventilation rates within the modelled space are varied to determine the effects on the model outputs in relation to the third aim:

> Explore how a change in ventilation rates can alter concentration of bacteria within the room, number of bacteria inhaled, and risk of an infection with *P. aeruginosa*.

7.3.2.1 Outpatient clinic scenario

This model examines the risk to a person with CF at an outpatient clinic following a visit from an infectious individual. The model encompasses three distinct phases and the timings of these are specified in Table 7.2.

Phase one Infectious individual enters the outpatient clinic room and remains in the room for a range of times, these are the occupancy times.

Phase two Infectious individual leaves the room and the room is left unoccupied, the time for this phase is the no occupancy time.

Phase three A susceptible host enters the room for their outpatient visit. The exposure time is the duration they stay in the room.

Figure 7.10 shows the predicted concentration of bacteria, C (CFU m^{-3}), in the space and the number of CFU inhaled, $\sum n$, when CFU were emitted at the highest

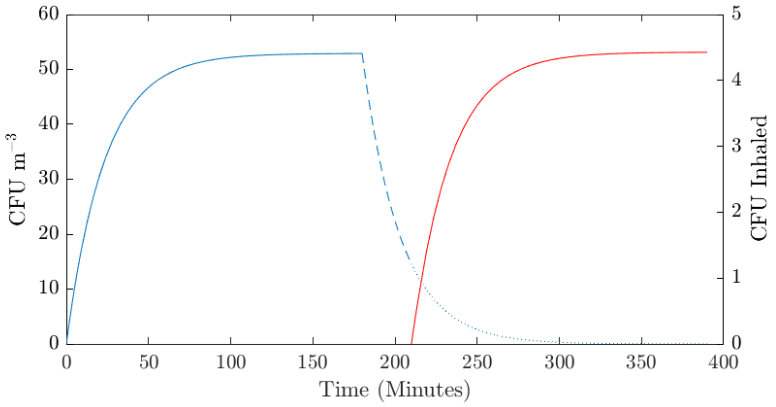

Figure 7.10: Concentration of bacteria, C ($\mathrm{CFU\,m^{-3}}$), in the space and the number of CFU inhaled, $\sum n$, for two 180 minute outpatient clinic visits. A single individual was emitting $4.3 \times 10^3\,\mathrm{CFU\,h^{-1}}$ in a space of volume $V = 31.9\,\mathrm{m^3}$, the susceptible host had a breathing rate of $12\,\mathrm{L\,min^{-1}}$, and the half life of *P. aeruginosa* was assumed to be 151 minutes. Blue line is concentration and the red line is CFU inhaled.

measured value in the cross-sectional study, $4.3 \times 10^3\,\mathrm{CFU\,h^{-1}}$, and the scenario was for two 180 minute outpatient visits. The space volume was taken to be the smallest room volume in the cross-sectional study, $V = 31.9\,\mathrm{m^3}$, the breathing rate of the susceptible host was $12\,\mathrm{L\,min^{-1}}$, and the half life of *P. aeruginosa* was assumed to be 151 minutes. These values were chosen to output data on the 'worst case' scenario.

The solid blue line shows the concentration in the room reaching a steady state of $52.9\,\mathrm{CFU\,m^{-3}}$ after 155 minutes. Once the infectious individual leaves the room, the beginning of phase two, the bacteria in the room air reduces. After 30 minutes of no occupancy time (phase two, dashed line) the susceptible individual enters the room with the concentration of bacteria in the air at $14.6\,\mathrm{CFU\,m^{-3}}$. During phase three the bacteria continued to decay (dotted blue line) to a 99.9 % reduction from the steady state concentration. Consequently, inhaled CFU increases sharply over a short period of time and plateaus when the concentration of bacteria in the room air decreased to a low enough level. In this scenario a susceptible host can expect to have inhaled over 4 CFU during their outpatient clinic visit. The infectious inoculum required to initiate an infection with *P. aeruginosa* is unknown for people with CF and may vary between patients. However, using the dose-response model described in section 7.2.1 this dose of CFU gives a risk of 0.05 % for developing an infection with *P. aeruginosa*.

Additionally, a Monte Carlo simulation was carried out (N = 10 000 iterations) to estimate the concentration of bacteria, C, the number of CFU inhaled, $\sum n$, and

Table 7.4: Parametric values used in the Monte Carlo simulation risk model for the outpatient scenario.

Parameter	**Value(s)**	**Distribution**
Emission rate, E ($\mathrm{CFU\,h^{-1}}$)	$\log_{10}(0–6)$	Log normal (Figure 7.8)
Space volume, V ($\mathrm{m^3}$)	31.9–43.7	Uniform
Loss rate due to ventilation, λ_v ($\mathrm{ac\,h^{-1}}$)	2.3	Constant
Loss rate due to deposition, λ_d ($\mathrm{s^{-1}}$)	0	Constant
Loss rate due to biological decay, k ($\mathrm{min^{-1}}$)	0.02–0.005	Uniform
Breathing rate, p ($\mathrm{L\,min^{-1}}$)	10.2–12.0	Uniform

the risk of initiating an infection with *P. aeruginosa*. The ranges of the parameters explored in the Monte Carlo simulations are summarised in Table 7.4.

A selection of timings were simulated to describe a series of outpatient clinic visits and the cases given for the simulated timings are described in Table 7.5. Results for each of these simulations are summarised in Table 7.6. It was found that an occupancy time of 30 minutes gave lower concentrations after phase one when compared to the longer occupancy times. This was because the average emission rate was relatively low and after 30 minutes the majority of concentrations had reached a steady state. In phase 3 it can be seen that increasing the exposure time and hence allowing a longer period of time for the bacteria to decay the concentration in phase three decreases with an increase in exposure time. However, number of CFU inhaled still increases with the low bacteria concentration in the air and longer exposure times. The number of CFU inhaled is mainly affected by the exposure time not the occupancy time. In conclusion, the average CFU inhaled for the simulations conducted is small which results in a small average risk of infection with *P. aeruginosa* for all scenarios. Although, the highest risks are observed for occupancy times greater than 30 minutes and exposure times 120 minutes or greater.

All data from the $\mathrm{N} = 10\,000$ iterations from the Monte Carlo simulation is presented as box plots in Figure 7.11 for the timings in case P (Table 7.5). As expected the final concentration at the end of each phase reduces over time and is driven by the emission rate. High emitters result in a large number of outliers at phase one and two and it is these outliers that create the large standard deviations found in Table 7.6. The final concentration in phase three has a much smaller number of outliers as after the total time the majority of the bacteria have been removed from the air via ventilation or they have decayed. Overall, concentrations are less than

Table 7.5: Case given to the range of occupancy and exposure times modelled in the Monte Carlo simulations for the outpatient clinic scenario.

Occupancy time (minutes)	**Exposure time (minutes)**			
	30	**60**	**120**	**180**
30	A	B	C	D
60	E	F	G	H
120	I	J	K	L
180	M	N	O	P

Table 7.6: Mean (standard deviation) outputs from the Monte Carlo model for the different timings simulated in the outpatient clinic scenario.

	Concentration (CFU $\mathbf{m^{-3}}$)				
Case	**Phase one**	**Phase two**	**Phase three**	**Inhaled**	**Risk (%)**
A	7.0 (60.0)	1.7 (15.0)	0.4 (3.8)	0.5 (4.4)	0.004 (0.0005)
B	7.6 (70.7)	1.9 (18.3)	0.1(1.3)	0.7 (7.2)	0.007 (0.0007)
C	8.2 (84.3)	2.0 (21.3)	0.008 (0.09)	0.7 (7.2)	0.008 (0.0008)
D	8.6 (114.4)	2.0 (26.9)	0.0005 (0.005)	0.8 (11.1)	0.008 (0.001)
E	10.3 (103.2)	2.5 (24.4)	0.6 (5.9)	0.7 (7.4)	0.007 (0.0008)
F	9.1 (84.9)	2.2 (20.5)	0.01 (1.3)	0.7 (6.7)	0.008 (0.0007)
G	9.2 (115.7)	2.2 (26.6)	0.009 (0.08)	0.8 (11.8)	0.009 (0.001)
H	12.0 (146.3)	2.9 (37.4)	0.0008 (0.01)	1.1 (12.2)	0.01 (0.001)
I	10.0 (88.8)	2.4 (20.0)	0.6 (4.6)	0.6 (5.3)	0.007 (0.0005)
J	8.4 (63.2)	2.0 (16.0)	0.1 (1.1)	0.7 (5.7)	0.007 (0.0006)
K	9.0 (67.2)	2.2 (16.6)	0.009 (0.07)	0.8 (6.3)	0.009 (0.0007)
L	10.1 (76.2)	2.5 (19.1)	0.0007 (0.006)	0.9 (7.7)	0.01 (0.0008)
M	8.1 (52.8)	2.0 (12.5)	0.5 (3.0)	0.5 (3.3)	0.006 (0.0003)
N	9.8 (100.8)	2.4 (25.4)	0.1 (1.7)	0.8 (10.1)	0.009 (0.001)
O	10.2 (127.8)	2.5 (34.3)	0.01 (0.2)	0.9 (9.9)	0.009 (0.001)
P	10.5 (87.8)	2.6 (21.8)	0.0007 (0.007)	1.0 (8.4)	0.01 (0.0009)

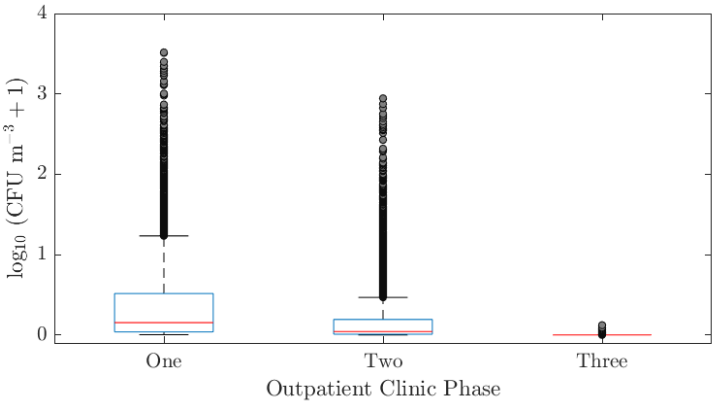

(a) Concentration of bacteria, C (CFU m^{-3}).

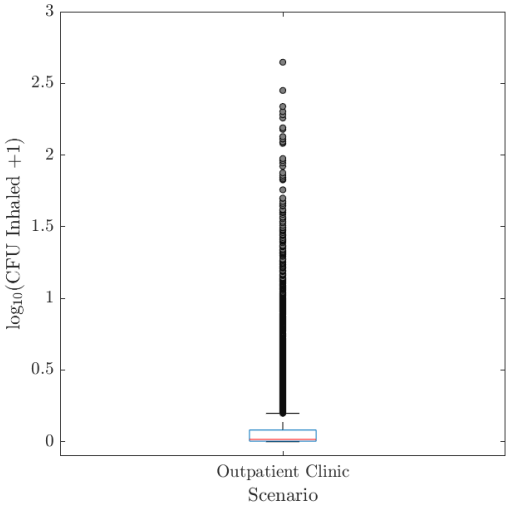

(b) Number of CFU inhaled, $\sum n$.

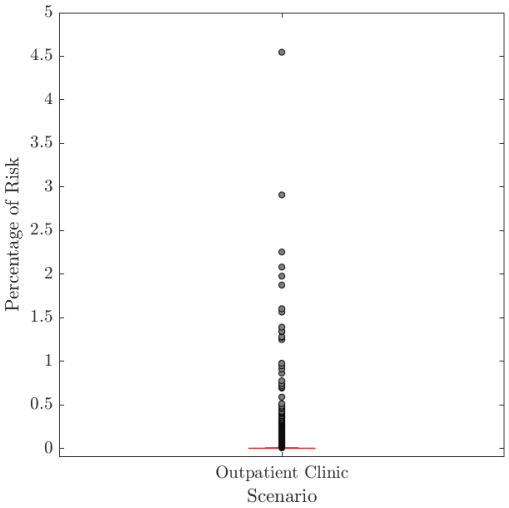

(c) Risk of infection with *P. aeruginosa*.

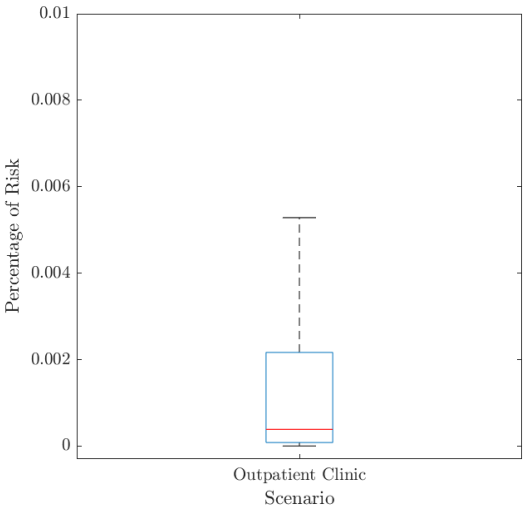

(d) Risk of infection with *P. aeruginosa* with outliers removed.

Figure 7.11: Outputs of the simulation from two 180 minute outpatient visits. All data from the N = 10 000 iterations from the Monte Carlo simulation is presented.

$10\,\mathrm{CFU\,m^{-3}}$; outliers affected the mean value reported in Table 7.6 and the median value of concentration after phase one for this simulation was $0.4\,\mathrm{CFU\,m^{-3}}$. The majority of simulations predict the number of CFU inhaled to be less than 1 CFU and it is the outliers which have a maximum of 443 CFU inhaled that present the greatest risk. These correlate to those outliers which show the greatest risk to the susceptible individual (Figure 7.11c) of up to 4.5 %. Removing outliers from the risk data shows that for the majority of iterations the simulation has a risk of less than 0.006 %.

Although the average risk in this scenario seems low it must be remembered that the consequence of this risk is high. Progressive lung disease, the primary cause of morbidity and mortality in people with CF, is a consequence of repeated pulmonary bacterial infections. Furthermore, this risk is only the risk to a susceptible patient for one event. Records from the CF unit at Leeds Teaching Hospitals NHS Trust (LTHT) estimate on average each patient attended 7 clinic visits per year based off the pre-SARS-CoV-2 2019/2020 cohort. Assuming at every visit the patient was susceptible (S) and their visit followed that of an infectious individual (I), and the risk per visit was the highest average risk of 0.01 %. Defining X = number of events where the patient pair was [I, S] = 7 and N = number of the X events where susceptible gets infected, then risk to the patient over the course of a year would be:

$$\begin{aligned} P(\mathrm{N} \geq 1) &= 1 - P(\mathrm{N} = 0)^{\mathrm{X}} \\ &= 1 - (1 - P(\text{infected}))^{\mathrm{X}} \\ &= 1 - (1 - 0.0001)^{7} \\ &= 0.0007. \end{aligned} \tag{7.21}$$

To calculate the percentage value (7.21) was multiplied by one hundred to give the risk of infection to be 0.07 %. This value gives a rough estimate of infection risk to a susceptible patient attending outpatient clinic over the course of the year, but if the infectious individual at any of the clinic visits prior to the patient was a high emitter this risk could be much higher.

It is not only individual patient risk that should be examined but risk to the whole cohort population. During 2019/2020 at the LTHT CF unit there were 2714 outpatient attendances. Assuming outpatient clinics run five days per week fifty weeks per year this averaged at 11 outpatient clinic visits a day. Another key assumption that was made was that on average concentration levels at the end of phase three were very low so only sequential patient pairs of [I, S] were considered. It was assumed

that only neighbouring outpatient visits had an effect on each other, i.e an infectious individual could not infect a susceptible individual two appointments later. To determine the average number of times an infectious individual was followed by a susceptible individual at an appointment a vector of length 11 was populated with I's and S's on the probability of being infected. The probability of a person with CF attending an outpatient clinic being infectious (I) was estimated from the percentage of the adult CF population in the UK that have chronic *P. aeruginosa*, these were assumed to always be infectious and was 39 % (Charman et al., 2019). The rest of the population (61 %) were assumed to be susceptible. It should be noted that this includes 17 % of the adult CF population who have an intermittent infection with *P. aeruginosa*. However, as per the definition of intermittent infection of *P. aeruginosa* (Lee et al., 2003) the person with CF is more likely to be susceptible than infectious. Hence, this 17 % of the population were also defined as susceptible. After running 10 000 iterations of populating the [I, S] vector the average patient pairs of [I, S] per day was 2.39. As a result the average risk of a outpatient with CF becoming infected with *P. aeruginosa* per clinic day was 0.0239 %, extrapolating this result to the to the cohort over the whole year gives a risk of 6.0 %. This percentage is not large, but is not insignificant and confirms the need for infection control guidelines for airborne transmission.

The methodologies described above to calculate both the individual risk and risk to the patient cohort over a year used the highest mean risk found in the outpatient scenarios, 0.01 %. However, potentially including the full probability distribution for emission rates, rather than the highest mean value for the scenarios measured, could more accurately account for the impacts of potential high emitters. In doing so may allow for additional understanding of uncertainty/variability in the risk predictions and the frequency with which you could expect to see very high risk scenarios that could lead to superspreading events.

It is not only emission rate that is a big factor in risk of initiating an infection with *P. aeruginosa* but so is the loss rate of the bacteria, and particularly the ventilation rate plays an important role. Figure 7.12 displays the results for concentration of bacteria, C ($\mathrm{CFU\,m^{-3}}$), in the space and the number of CFU inhaled, $\sum n$, when loss rates due to ventilation were $1\,\mathrm{ac\,h^{-1}}$ and $6\,\mathrm{ac\,h^{-1}}$. Bacteria were emitted into the air at the highest measured value in the cross-sectional study, $4.3 \times 10^3\,\mathrm{CFU\,h^{-1}}$, the scenario was for two 180 minute outpatient visits, space volume was taken to be the smallest room volume in the cross-sectional study, $V = 31.9\,\mathrm{m^3}$, the breathing rate of the susceptible host was $12\,\mathrm{L\,min^{-1}}$, and the half life of *P. aeruginosa* was assumed to be 151 minutes. It is clear from Figure 7.12 the impact ventilation has on the concentration and the number of CFU inhaled by the susceptible host. At

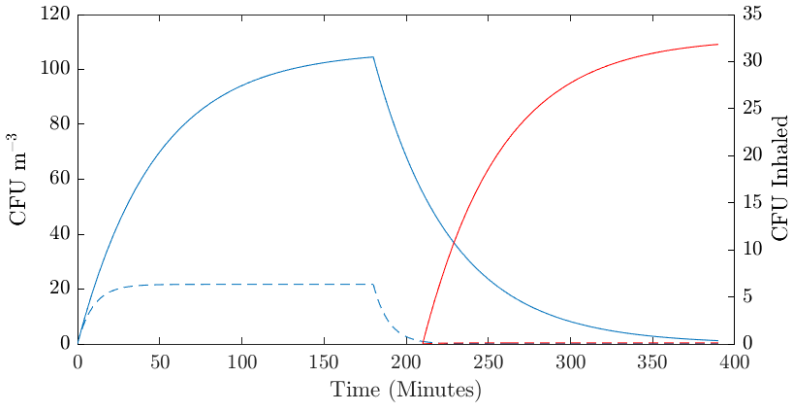

Figure 7.12: Concentration of bacteria, C (CFU m^{-3}), in the space and the number of CFU inhaled, $\sum n$, for two 180 minute outpatient clinic visits at different ventilation rates 1 ac h^{-1} (solid line) and 6 ac h^{-1} (dashed line). A single individual was emitting 4.3×10^3 CFU h^{-1} in a space of volume $V = 31.9$ m^3, the susceptible host had a breathing rate of 12 L min^{-1}, and the half life of *P. aeruginosa* was assumed to be 151 minutes. Blue line is concentration and the red line is CFU inhaled.

1 ac h^{-1} the concentration of bacteria in the room air does not reach steady state concentration and if the infectious individual remained in the room for longer the concentration within the room air would have continued to increase. Conversely, at 6 ac h^{-1} time taken to reach 99.9 % steady state concentration was 63 minutes, but this value was 22 CFU m^{-3} which was much lower than steady state concentrations seen at lower ventilation rates. In addition, the percentage reduction within the room air before the susceptible individual enters the room in phase three is 53 % for 1 ac h^{-1} compared to 96 % for 6 ac h^{-1}. Consequently, a much greater number of bacteria was inhaled at the lower ventilation rate of 32 CFU, whereas at the higher ventilation rate not a single CFU was expected to be inhaled. The measured 2.3 ac h^{-1} for the CF unit was representative of a typical ventilation rate for naturally ventilated rooms but it is likely that this ventilation rate could be lower. It is important to note that the measured ventilation rate was lower than the recommendation in current UK guidance of 6 ac h^{-1} (Macintosh et al., 2007). Therefore, this comparison of ventilation rates highlights the importance of good ventilation when considering the impacts of airborne infection.

Risk of infection with *P. aeruginosa* has been based on the dose-response described in section 7.2.1, but in reality the accuracy of the dose-response is unknown and there is no certainty on what 'dose' initiates infection. Therefore, if it was required to remove nearly all the *P. aeruginosa* in the air before starting the subsequent outpatient visit it could potentially take a long period of time dependant on the

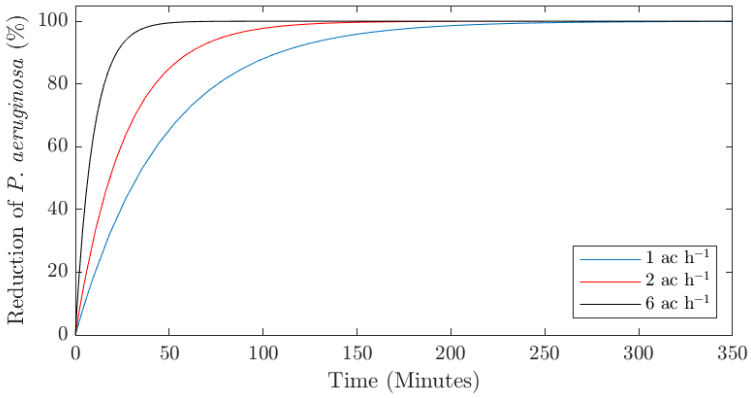

Figure 7.13: Time taken to achieve a percentage reduction in *P. aeruginosa* in the room air from a starting steady state concentration due to the combined effects of biological decay and ventilation. Steady state concentration had been reached from a single individual was emitting 4.3×10^3 CFU h^{-1} in a space of volume $V = 31.9\,m^3$, and the half life of *P. aeruginosa* was assumed to be 151 minutes.

Table 7.7: Time taken to achieve 10, 50, 90, 99 and 99.9 % reductions in airborne *P. aeruginosa* from a starting steady state concentration due to the combined effects of biological decay and room ventilation. Steady state concentration had been reached from a single individual was emitting 4.3×10^3 CFU h^{-1} in a space of volume $V = 31.9\,m^3$, and the half life of *P. aeruginosa* was assumed to be 151 minutes.

Ventilation rate (ac h^{-1})	**Reduction time (minutes)**				
	10 %	**50 %**	**90 %**	**99 %**	**99.9 %**
1	5	33	108	216	323
2	3	19	61	121	182
6	1	7	22	44	66

ventilation rate. Figure 7.13 displays the time taken to reduce *P. aeruginosa* concentration in the room at different ventilation rates from a steady state concentration when a single individual was emitting 4.3×10^3 CFU h^{-1} of *P. aeruginosa* in a space of volume $V = 31.9\,m^3$, and the half life of *P. aeruginosa* was assumed to be 151 minutes. Table 7.7 summarises the time taken at each ventilation rate to achieve 10, 50, 90, 99 and 99.9 % reductions in airborne *P. aeruginosa* for the same conditions. The recommended 6 ac h^{-1} (Macintosh et al., 2007) allows a near complete removal of *P. aeruginosa* in the air in just over 1 hour and it is reiterated this emission rate was the highest recorded; hence, this is one of the high emitters and most emission

rates are much lower and would have taken less time for removal of *P. aeruginosa*. When ventilation rates are lowered time taken to remove *P. aeruginosa* in the room air increased 5 fold for $1\,\mathrm{ac\,h^{-1}}$ and 3 fold for $2\,\mathrm{ac\,h^{-1}}$. However, in reality these times will be shorter due to deposition of the bacteria at these large timescales.

7.3.2.2 Single room scenario

The single room scenario simulates an infectious individual and a susceptible host entering and leaving a space at the same time. The two spaces considered are a lift and a waiting room. Entering and leaving a lift at the same time is appropriate but the timings may not be completely realistic for a waiting room. However, this scenario shows how size of the space, ventilation rates, and duration of the event can have an impact on the concentration of bacteria in the air, the number of CFU inhaled, and the risk of infection.

A single individual was modelled to emit CFU at the highest measured rate in the cross-sectional study, $4.3 \times 10^3\,\mathrm{CFU\,h^{-1}}$, and the scenario was two 180 minute outpatient visits. Figure 7.14 shows the predicted concentration of bacteria, C ($\mathrm{CFU\,m^{-3}}$), in the space and the number of CFU inhaled, $\sum n$. The space volume for the lift was taken to be $V = 7.8\,\mathrm{m^3}$ and the waiting room had a simulated volume of $V = 67.5\,\mathrm{m^3}$, the breathing rate of the susceptible host was $12\,\mathrm{L\,min^{-1}}$, and the half life of *P. aeruginosa* was assumed to be 151 minutes. These values were chosen to output data on a 'worst case' scenario for each of the single rooms.

The solid blue line shows the concentration in the lift increasing almost linearly to $44\,\mathrm{CFU\,m^{-3}}$ over the short time the infectious individual is in the space. The overall inhaled CFU during the event is 1.3, this value increases slowly initially before the concentration of bacteria in the room has built up. Once the bacterial concentration in the room has increased there is a sharp incline in the number of CFU inhaled and if this were to last longer this value would increase rapidly due to the high concentration within the space. During the 30 minutes simulated for the waiting room concentration of *P. aeruginosa* begins to plateau but does not reach steady state, the final concentration in the room is $18\,\mathrm{CFU\,m^{-3}}$ much less than that seen in the lift. The rate of CFU inhaled begins to increase after 10 minutes and after 30 minutes in the room the susceptible individual inhales just under 4 CFU of *P. aeruginosa*. As the lift is a much smaller room with a lower ventilation rate the concentration of bacteria in the room air is much higher. However, as the time of the scenario is less the susceptible individual inhales less bacterium. It is reiterated that the infectious inoculum required to initiate an infection with *P. aeruginosa*

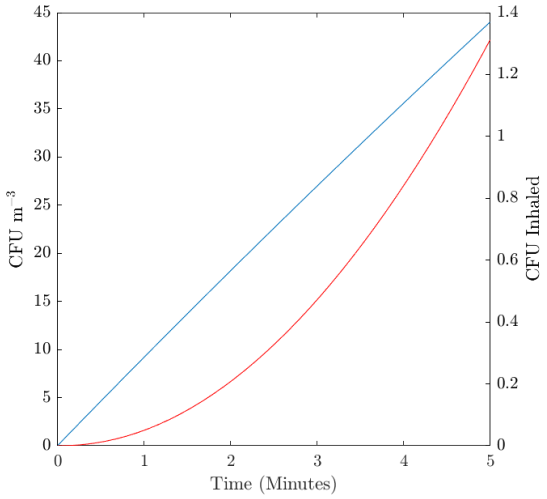

(a) Lift.

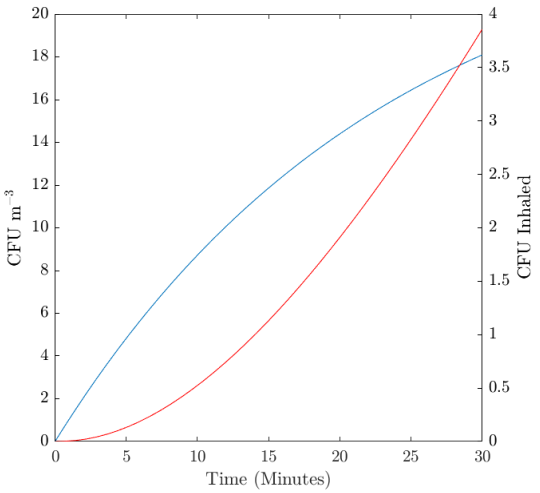

(b) Waiting room.

Figure 7.14: Comparison of the concentration of bacteria, C (CFU m^{-3}), in the space and the number of CFU inhaled, $\sum n$. A single individual was emitting 4.3×10^3 CFU h^{-1} in a lift of volume $V = 7.8\,\mathrm{m}^3$ and waiting room of volume $V = 67.5\,\mathrm{m}^3$, the susceptible host had a breathing rate of $12\,\mathrm{L\,min}^{-1}$, and the half life of *P. aeruginosa* was assumed to be 151 minutes. Blue line is concentration and the red line is CFU inhaled.

Table 7.8: Parametric values used in the Monte Carlo simulation risk model for the single room scenario.

Parameter	**Value(s)**	**Distribution**
Emission rate, E (CFU h^{-1})	$\log_{10}$(0–6)	Log normal (Figure 7.8)
Space volume, V (m^3)		
Lift	7.8–10.8	Uniform
Waiting room	67.5	Constant
Loss rate due to ventilation, λ_v (ac h^{-1})		
Lift	1	Constant
Waiting room	2.3	Constant
Loss rate due to deposition, λ_d (s^{-1})	0	Constant
Loss rate due to biological decay, k (min^{-1})	0.02–0.005	Uniform
Breathing rate, p (L min^{-1})	10.2–12.0	Uniform

is unknown for people with CF, but using the dose-response model described in section 7.2.1 the risk in each event is 0.01 % and 0.04 % for the lift and waiting room respectively.

A Monte Carlo simulation was carried out (N = 10 000 iterations) to estimate the

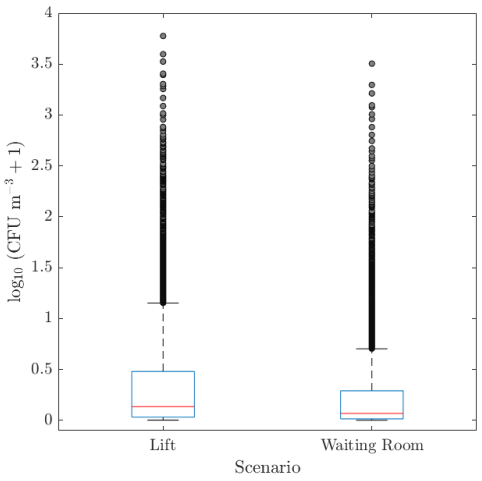

(a) Concentration.

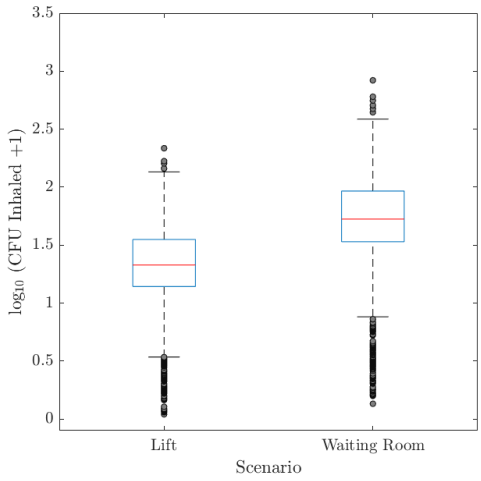

(b) Inhaled CFU.

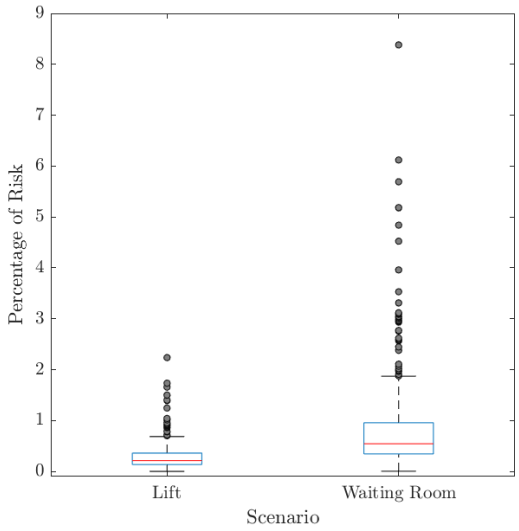

(c) Risk.

Figure 7.15: Concentration of bacteria, C (CFU m^{-3}), in the space, the number of CFU inhaled, $\sum n$, and the risk of infection with *P. aeruginosa* for the susceptible host. All data from the N = 10 000 iterations from the Monte Carlo simulation is presented.

concentration of bacteria, C, the number of CFU inhaled, $\sum n$, and the risk of initiating an infection with *P. aeruginosa* in the single room scenarios. The ranges of the parameters explored in these Monte Carlo simulations are summarised in Table 7.8.

Results from the Monte Carlo simulations are displayed in Figure 7.15. Similar to the results seen in the outpatient clinic scenario the majority of the iterations have low concentrations but some outliers in these events recorded concentrations over 5000 CFU m^{-3} in the lift scenario. These outliers are driven by high emitters and while not common is possible. As the two individuals, the infected and the

susceptible, remain in the room together the concentration of bacteria continually increases and as a consequence the number of CFU inhaled is much greater with a smaller proportion of outliers. As a result the risk of infection with *P. aeruginosa* is higher than the outpatient clinic reaching 8.3 % in the waiting room scenario.

These results demonstrate why shared waiting rooms are not used in CF units and the importance of adherence to mitigation measures which are put in place so people with CF are unlikely to share an enclosed space. An assumption made in the risk model is the well mixed assumption, this is when the concentration of bacteria is evenly distributed throughout the space. In reality this means that close to the source the risk model will not hold true as the concentration of bacteria will be higher. Therefore, the model will break down when the two individuals are close to each other which may be true in the case of the lift. In addition, this model only considers 'small' droplets that remain airborne and does not include larger droplets which would impact the risk of infection in small space. As people entering a lift could be facing one another in a small space the number of CFU inhaled and the risk of infection are likely an underestimation of reality. The same would apply to patients in a waiting room sat close to each other. This reinforces the narrative that people with CF must practice social distancing and measures must be in place to mitigate against people with CF meeting in enclosed spaces such as lifts and waiting rooms.

7.3.2.3 Domestic setting

People with CF are advised to maintain strict social distancing from one another due to the heightened risk of infection through the transmission of pathogens. Yet, CF is hereditary and there are many siblings with CF who potentially visit each other in the indoor environment. The domestic setting scenario considered a visit in a house where a person with CF lives and the concentration of bacteria in the room air had reached steady state. In the simulation the infected individual stays in the room with the susceptible host for the duration of the visit. Two instances are considered, simulating windows closed which has a ventialtion of $0.5\,\mathrm{ac\,h^{-1}}$ and simulating windows open which increases the ventilation to 2–$3\,\mathrm{ac\,h^{-1}}$.

Figure 7.16 displays the number of CFU inhaled, $\sum n$, and the risk of an infection with *P. aeruginosa* when CFU were emitted at the highest measured value in the cross-sectional study, $4.3 \times 10^3\,\mathrm{CFU\,h^{-1}}$, and the scenario was simulated for 180 minutes at different ventilation rates $0.5\,\mathrm{ac\,h^{-1}}$ and $3\,\mathrm{ac\,h^{-1}}$. The space volume was taken to be $V = 36.8\,\mathrm{m^3}$, the breathing rate of the susceptible host was $12\,\mathrm{L\,min^{-1}}$,

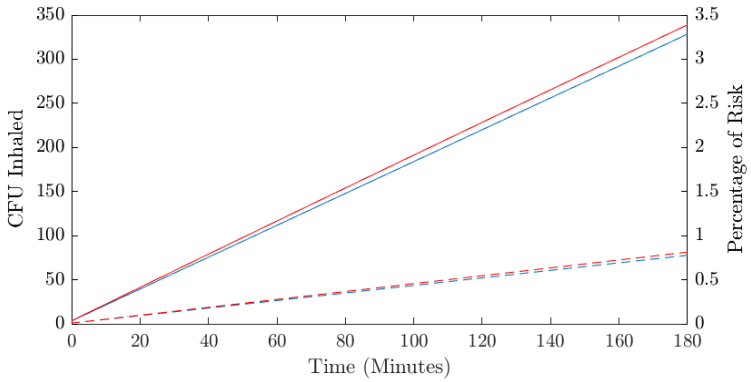

Figure 7.16: Number of CFU inhaled, $\sum n$, and the risk of infection with *P. aeruginosa* for the susceptible host. A single individual was emitting 4.3×10^3 CFU h^{-1} in a domestic space of volume $V = 36.8\,m^3$ at different ventilation rates $0.5\,ac\,h^{-1}$ (solid line) and $3\,ac\,h^{-1}$ (dashed line). The susceptible host had a breathing rate of $12\,L\,min^{-1}$, and the half life of *P. aeruginosa* was assumed to be 151 minutes. Blue line is CFU inhaled and the red line is risk of infection with *P. aeruginosa*.

and the half life of *P. aeruginosa* was assumed to be 151 minutes. Concetration of bacteria within the space air had reached steady state, this was 152.2 CFU m^{-3} and 36.0 CFU m^{-3} for $0.5\,ac\,h^{-1}$ and $3\,ac\,h^{-1}$ respectively. The steady state values reported immediately show the difference a higher ventilation rate can have on the number of bacteria suspended in the room air. Consequently, by opening the windows and thus increasing ventilation the number of CFU inhaled dramatically reduced and in turn the risk of infection. Both the infectious and the susceptible individual remained in the room during the simulation; therefore the CFU inhaled and risk of infection increased linearly over time. After one hour with closed windows there was 111.6 CFU m^{-3} of *P. aeruginosa* in the room air increasing to 328.5 CFU m^{-3} by the end of the simulation. Opening the windows reduced these values and after one hour there was 26.4 CFU m^{-3} of *P. aeruginosa* in the room air increasing to 77.8 CFU m^{-3} by the end of the simulation.

A Monte Carlo simulation was conducted (N = 10 000 iterations) to estimate the number of CFU inhaled, $\sum n$, and the risk of initiating an infection with *P. aeruginosa* in the domestic setting scenario. Concentration of bacteria suspended in the room air remained at steady state for the duration of the simulation. The ranges of the parameters explored in the Monte Carlo simulation are summarised in Table 7.9.

Table 7.10 displays the results from the Monte Carlo simulations for different times

Table 7.9: Parametric values used in the Monte Carlo simulation risk model for the domestic setting scenario.

Parameter	**Value(s)**	**Distribution**
Emission rate, E (CFU h^{-1})	$\log_{10}$(0–6)	Log normal
Space volume, V (m^3)	36.8–50.6	Uniform
Loss rate due to ventilation, λ_v (ac h^{-1})		
Windows closed	0.5	Constant
Windows open	2–3	Uniform
Loss rate due to deposition, λ_d (s^{-1})	0	Constant
Loss rate due to biological decay, k (min^{-1})	0.02–0.005	Uniform
Breathing rate, p (L min^{-1})	10.2–12.0	Uniform

Table 7.10: Mean (standard deviation) outputs from the Monte Carlo simulation risk model for the domestic setting scenario at different timings and ventilation rates at N = 10 000 iterations.

	Inhaled CFU		**Risk (%)**	
Time (minutes)	**0.5 ac h^{-1}**	**2–3 ac h^{-1}**	**0.5 ac h^{-1}**	**2–3 ac h^{-1}**
30	10.7 (78.4)	3.9 (39.9)	0.1 (0.8)	0.04 (0.4)
60	24.2 (267.6)	7.5 (71.0)	0.2 (1.8)	0.08 (0.7)
120	54.6 (758.9)	15.7 (144.0)	0.4 (3.1)	0.2 (1.3)
180	71.1 (541.1)	28.2 (293.7)	0.6 (3.5)	0.3 (2.2)

and ventilation rates simulated. The concentration of bacteria remained at steady state as the infectious individual remained within the space. As a consequence the number of inhaled CFU did not plateau but increased with time. Through opening the windows and increasing the ventilation the inhaled CFU after 180 minutes is similar to that after a 60 minute visit with the windows closed. If the dose-response model is accurate the risk of infection with *P. aeruginosa* is double after 180 minutes when the windows are closed vs the windows being open. Therefore, opening the windows should be advised if people with CF were to meet indoors in addition to shortening the visit to reduce the risk.

Data from the Monte Carlo simulations for a 180 minute visit is presented in Figure 7.17. The steady state concentrations are driven by the emission rates and it can be seen how high emitters affect the overall concentration in the room air. However, the results for both windows open and closed show a skewed distribution to the lower concentrations and the median concentration of bacteria in the room air was

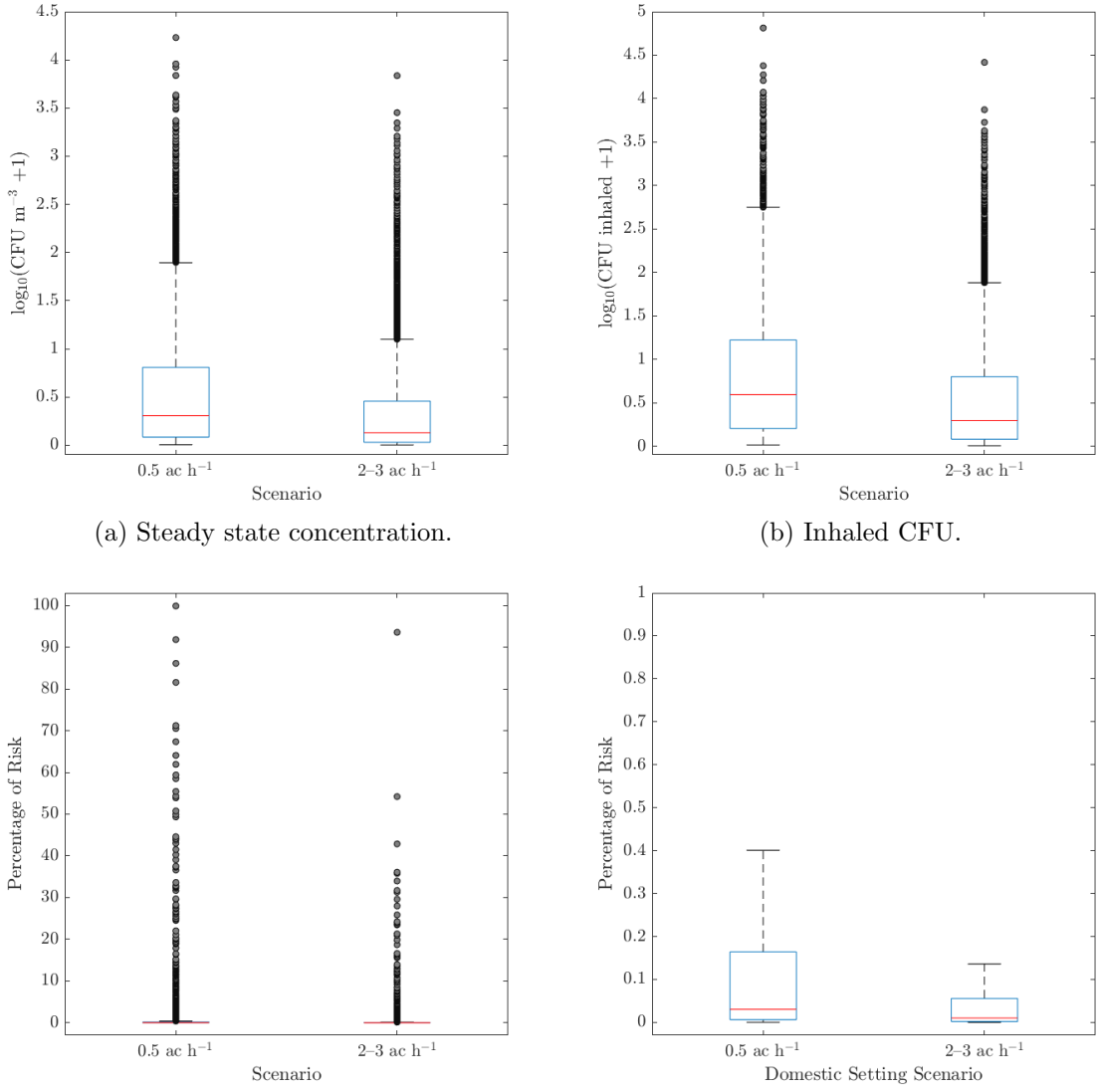

(a) Steady state concentration.

(b) Inhaled CFU.

(c) Risk.

(d) Risk with no outliers.

Figure 7.17: Concentration of bacteria, C (CFU m^{-3}), in the space, the number of CFU inhaled, $\sum n$, and the risk of infection with *P. aeruginosa* for the susceptible host during a 180 minute domestic setting visit. All data from the N = 10 000 iterations from the Monte Carlo simulation is presented.

2.9 CFU m^{-3} and 1.0 CFU m^{-3} for windows closed and open respectively. The concentration in the room air directly correlates to the number of CFU the susceptible individual is expected to inhale. The values are less for windows open overall, but in the case of high emitters there was recorded cases where up to 26 000 CFU were inhaled. Assuming the dose-response model described in section 7.2.1 is correct, when the windows are closed the risk of infection with *P. aeruginosa* could reach 100 %. Open windows did record some high outliers but the risk never reached 100 %. Although risk of infection remained low with the majority less than 1 % the data was skewed, median values were 0.03 % and 0.01 % for windows closed and

open respectively. However, this is the risk for just one event and if the individuals met once a week over the course of a year, following the method described in (7.21), the risk over the year (X = 52) for the susceptible individual was 14 % and 5 % for windows closed and open respectively. Considering the consequences of the risk of infection this value is likely too high for people with CF.

It must be acknowledged that for these simulations it was assumed the infectious and susceptible individuals were not in close contact with each other due to the well mixed assumption. If the two individuals were sat next to each other the model would not hold true as emission close to the source is much higher and the effects of large droplets are not considered in this model; therefore, the results presented would be an underestimation.

7.4 Summary

Comparing the experiments completed in the laboratory and the cross-sectional study found both droplet size distributions had a predominance for droplets less than 5 µm. In addition, data from the Spraytec particle sizer indicated large numbers of very small droplets (<1 µm). Several studies from the literature measured droplets expelled from the mouth to be less than 1 µm and it is expected that in the cough/exhaled breath of people with CF there will be large number of very small droplets. It was concluded that although there is a preferential for smaller droplets this could be an artefact of three factors: where the infection resides, the sampling efficiency of larger droplets on the Andersen Impactor, and that the droplets will have evaporated to their equilibrium diameter by the time they were measured.

The results from the steady state risk model were evaluated and compared to the results from the room air samples measured in the cross-sectional study. These data determined that the only a small percentage of bacteria present in the room air is attributed to the emissions of an infectious individual. However, for high emitters it is likely that this percentage could be much higher.

In the outpatient clinic, highest risks were observed for occupancy times greater than 30 minutes and exposure times 120 minutes or greater. Therefore, it was the exposure time that has the greatest impact on risk. The highest average risk was low 0.01 %, but the consequence of this risk is high due to the mortality and morbidity associated with recurrent pulmonary infections in people with CF; therefore, infection control measures are important. Furthermore, when the infectious individual is

a high emitter the risk to the susceptible individual increased substantially to over 4 %. The risk for the whole CF unit population over the course of a year rose to 6 %. While this percentage was not large it still provides evidence for the implementation of mitigation measures against airborne infection.

Modelling two people in the room together, the susceptible and infectious individuals, was completed for lift and waiting room scenarios. This resulted in greater numbers of bacteria expected to be inhaled by the susceptible individual than in the outpatient clinic and in turn the risk was higher, over 8 % in the modelled waiting room in the case of a high emitter. Consequently, these modelled scenarios provided evidence to support the need for CF units to abandon the use of waiting rooms at clinics and for people with CF to not encounter each other in enclosed spaces for extended periods of time.

Two people with CF who visit each other in a domestic setting was modelled with bacteria concentration at steady state for the event duration. As a result, this scenario presented the highest risk to the susceptible individual. However, for the average emitter the risk was still relatively low, less than 1 %. Extrapolating this event to once a week per year increased to the risk to 14 %, which would likely be perceived as too much of a risk for people with CF.

Increasing airflow rates to control diseases is not a new approach. A quote from Florence Nightingale's notes on nursing was to "keep the air a person breathes as pure as the external air, without chilling them" (Nightingale, 1992). These modelled scenarios demonstrate the importance of ventilation on reducing the concentration levels of bacteria within the room air and ultimately the risk of infection. Comparing the recommended $6\,\mathrm{ac\,h^{-1}}$ to a likely scenario of $1\,\mathrm{ac\,h^{-1}}$ for naturally ventilated rooms, the time taken to remove *P. aeruginosa* from the room air increased 5 fold. The lift that was modelled was much smaller with poorer ventilation rates than the waiting room and hence had much higher levels of bacteria within the space. In addition, when windows were closed in the domestic setting, representing $0.5\,\mathrm{ac\,h^{-1}}$, a Monte Carlo simulation recorded a risk of infection to be 100 % which was not seen if the windows were modelled to be open. Reiterating the importance of opening windows if this situation is unavoidable.

In conclusion, this chapter finds that high emitters are the main cause for concern when considering risk to a susceptible individual. This correlated with the literature which has reported an estimation of 80 % of infections occur from 10 % of people (Endo et al., 2020). As a consequence of these findings a recommended hierarchy of risk controls can be adopted to mitigate against airborne infection. These are:

engineering, such as ventilation; admin, this can include how outpatient clinics are organised; and personal protective equipment, the use of masks have been reported to be effective in reducing the dispersal of viable aerosols (Wood et al., 2018) and hence reduce bacteria concentrations in the room.

Chapter 8

Conclusions, future work, and implications of the research

Cystic fibrosis is a condition characterised by repeated pulmonary infections and progressive lung function decline. Many of the pathogens responsible for pulmonary infections in people with CF, including *P. aeruginosa* and *M. abscessus*, are ubiquitous in the environment. The environment is considered one source of acquisition but more recently evidence suggests that cross-infection via the airborne route is an important pathway of infection transmission. The research presented in this thesis aimed to provide a deeper insight into the potential for airborne transmission of two pathogens which cause infection in people with CF, *P. aeruginosa* and *M. abscessus*. This was achieved by forging a multidisciplinary analysis in experimental techniques coupled with clinical cross-sectional studies and mathematical modelling.

The key findings of these three main elements of this research are summarised below. Possible areas for future work are identified and discussed, and considerations are given to the implications of the findings from this thesis. It is noted that several aspects of the laboratory studies and the cough aerosol sampling were significantly impacted by the COVID-19 pandemic restrictions and in some areas this has limited the ability to draw firm conclusions.

8.1 Key Findings

A number of specific observations and conclusions have been made in each of the results chapters and the key conclusions of this thesis are arranged under these three themes and are presented below.

8.1.1 Bioaerosol characterisation experiments

This series of laboratory based experiments presented in Chapter 5 was designed to quantify the combined effects of suspension fluid and bacterial strain on droplet size distributions and survival of *P. aeruginosa* and *M. abscessus* in a controlled environment and to determine the effectiveness of the methodology used to measure these effects. From these experiments it was concluded that:

1. The presence of *P. aeruginosa* did not have a significant impact on the properties of the suspension fluid at the concentrations measured. Key non-dimensional numbers such as the Weber and Ohnesorge number did not change with the small changes measured and it was assumed droplet size distributions were not affected by a change in surface tension caused by *P. aeruginosa*.
2. There was a difference in survival between strains of *P. aeruginosa* and *M. abscessus*. The *P. aeruginosa* environmental strain had the best survivability and the patient mucoid strain showed an enhanced survivability over the patient non-mucoid strain. Hence, people with CF chronically infected with *P. aeruginosa* expressing a mucoid phenotype may be more likely to disseminate potentially infectious aerosols. *M. abscessus* appeared to have a slower decay than *P. aeruginosa* and the smooth morphotype of *M. abscessus* had higher colony counts in 1 % FBS than the rough morphotype. All bacteria were easily able to survive for up to 4 m without much decay and the majority of droplets were of the size 1.1 µm–2.1 µm.
3. There was a rapid decay of bacteria observed when using the BACA for residency times of 80 s. The half life of *P. aeruginosa* was less than 1 minute and for *M. abscessus* it was just over 1 minute. Comparable studies which were conducted over longer periods of time ($\geq$ 1 h) recorded the half life of *P. aeruginosa* to be greater than 30 minutes. This rapid decay could potentially be the stress of the nebuliser but it is more likely that in room air sampling decay is not measured on these timescales and is therefore not observed. Additionally, room air that has been sampled is generally considered well mixed

and these same conditions were not observed in the BACA.

4. The 1 % FBS suspension improved the survivability of *P. aeruginosa*, particularly for small droplets on stages 5 and 6 of the Andersen Impactor (0.65 µm–2.1 µm). However, this was not the case for *M. abscessus* and 1 % FBS resulted in lower colony counts on all stages. The artificial mucus sample that was tested had comparable colony counts at 1 m to the ¼ ringers suspension. A difference in the suspension fluids droplet size distribution measured by Spraytec was observed at the short range and over the Andersen Impactor size range when using the BACA. It could be possible suspension fluid has an impact on droplet size distributions but this was a small sample size.
5. Correlations were made between the Andersen Impactor samples and the Spryatec data. The majority of the volume frequency plots over the Andersen Impactor range demonstrated a clear peak at stage 5, the dominant stage for culturable colony counts. However, when measuring microorganisms Spraytec and optical particle counters cannot be relied on to pick up the difference in distributions between bacterial strains and be representative of the culturable distribution. Therefore, the Spraytec device is not recommended for use alone when measuring droplet size distributions of bioaerosols.

8.1.2 Cough aerosol sampling

This element of the research presented in Chapter 6 aimed to measure the presence of *P. aeruginosa* and *M. abscessus*, characterise emission rates of these bacteria in cough/exhaled breath aerosols from adults with CF, and evaluate the sampling methods used through design and completion of a cross-sectional study. The COVID-19 pandemic had impacts on the study size and the statistical significance of the findings were limited by the number of participants, in particular participants with *M. abscessus* and the participant groups. The key findings from the cough aerosol sampling study were:

1. *P. aeruginosa* was found in the majority of cough/exhaled breath samples using the CASS. *M. abscessus* was found in mask samples and in an air sample. Hence, this study gave clear evidence that *P. aeruginosa* can be aerosolised by people with CF and it is likely that *M. abscessus* is too.
2. The AGI-30 sampler was not effective for sampling with the CASS, but the Andersen 6-stage Impactor worked well especially for *P. aeruginosa* and was able to yield droplet size distribution data. However, the CASS may result in under representation of emission rates due to sampling efficiency for larger

droplets and losses in the tubing.

3. *M. abscessus* was only detected in mask samples from cough/exhaled breath and not in the CASS samples. This was possibly due to the greater sensitivity of PCR method and mask sampling is recommended for determining if a person with CF is emitting *M. abscessus* aerosols. Although the COVID-19 restrictions meant that participant recruitment was very limited for people infected with *M. abscessus*.

4. A subset of participants were considered 'super producers' and produced at least an order of magnitude higher aerobic colony counts than the majority of other participants. Super producers have been reported to produce as many as 80 % of infections for a number of diseases which has broader implications for infection control guidelines beyond CF.

5. Measured droplets from people with CF had a predominance for small droplets less than 5 µm, but this could have been a consequence of where the infection exists, sampling efficiency, and droplet evaporation.

6. The droplet size distributions of cough/exhaled breath from people with CF with a chronic infection of *P. aeruginosa* and people with CF with a chronic infection of *M. abscessus* were statistically different. Participants infected with *M. abscessus* favoured Andersen Impactor stages 2 and 3 which was not seen in the participants infected with *P. aeruginosa*. Additionally, participants chronically infected with both *P. aeruginosa* and *M. abscessus* did not have *P. aeruginosa* detected in their cough aerosols.

7. Time of sampling or exacerbation did not have a statistically significant effect on the droplet size distributions. Although, participants had higher aerobic colony counts when exacerbating compared to when not exacerbating, but aerobic colony counts with *P. aeruginosa* did not reduce over course of treatment. Morning aerobic colony counts were on average greater but may have been influenced by the 'super producers'. Mucolytic treatment was found to have been taken before each of the high producing sessions and is known to change the rheological porperties of sputum. However, it was also taken by other participants in lower producing sessions.

8.1.3 Evaluation of factors influencing airborne transmission risk

The aim of the model presented in Chapter 7 was to bring together findings from the laboratory and clinical studies to provide quantitative data on concentration of bacteria, number of bacteria inhaled, and risk of infection with *P. aeruginosa* in multiple simulated indoor scenarios using the measured emission rates from the cross-sectional study. Results from this model concluded that:

1. A steady state model was compared to the air samples taken in the cross sectional study and suggested that only a small percentage of bacteria in the room air came from emission by an infectious individual. However, this percentage was likely to increase if the person was a high emitter.
2. In the outpatient scenario, highest risks were observed for occupancy times greater than 30 minutes and exposure times 120 minutes or greater. Therefore, it was the exposure time that had the greatest impact on risk. The average highest risk was low 0.01 %, but this increased dramatically to over 4 % for high emitters. Extrapolating the risk to the whole population over the course of a year saw a risk of 6.0 %. This percentage was not large, but was not insignificant and confirms the need for infection control guidelines for airborne transmission. However, the risk to the whole population was based of the mean risk of 0.01 % and using the probability distribution for emission rates could have helped account for the impact of potential high emitters.
3. In the lift and waiting room scenarios the risks were higher as two people, the susceptible and infectious, were modelled in the room together and risks rose as high as 8 % for the waiting room. These models provided evidence to support the need for CF units to abandon the use of waiting rooms at clinics and for people with CF to not encounter each other in enclosed spaces for extended periods of time.
4. In the domestic setting, as expected, the risks to the susceptible individual were highest as this was ultimately the 'worst case' scenario. However, for the average emitter the risk was still relatively low. Extrapolating this event to once a week per year increased to 14 % risk of infection over the course of the year, which would likely be perceived as too much of a risk for people with CF.
5. For all the scenarios the importance of ventilation on reducing the concentration levels of bacteria in the room and ultimately the risk of infection was observed. Comparing the recommended $6\,\mathrm{ac\,h^{-1}}$ to a likely scenario of $1\,\mathrm{ac\,h^{-1}}$

for naturally ventilated rooms, the time taken to remove *P. aeruginosa* from the room air increased 5 fold. In addition, when windows were closed in the domestic setting, representing $0.5\,\mathrm{ac\,h^{-1}}$, a Monte Carlo simulation recorded a risk of infection to be 100 % which was not seen if the windows were modelled to be open.

8.2 Future work

This research has produced some important conclusions which have contributed to the current knowledge on the potential for airborne transport of CF pathogens and has also generated valuable quantitative data on risk of infection to people with CF. Nonetheless, some knowledge gaps have been identified and these areas will benefit from further investigations. Some of the most important are summarised in this section.

Droplet size distributions The Collison nebuliser limited the size range of droplets generated during laboratory scale experimental studies. Further investigation using a series of aerosolisation techniques, mimicking the size distributions for coughing/breathing, will allow a more detailed exploration into how rheology of the suspension fluid may affect the resulting size distributions of aerosolised bacterial suspensions. Evaporation of droplets of this size ($<10\,\mu\mathrm{m}$) occur on extremely short timescales and it would therefore be beneficial for these further investigations to measure droplet size distributions over short distances.

Rapid decay of bacteria Data obtained in the experimental work suggested that *P. aeruginosa* and *M. abscessus* experienced a rapid decay at short timescales that was not seen in decay experiments of artificially generated aerosols and cough generated aerosols of *P. aeruginosa* into a controlled room environment over longer periods of time. In comparison, the half lives of *P. aeruginosa* was found to be less than 1 minute for the residency time of 80 s compared to greater than 30 minutes found in previous research for *P. aeruginosa* (Clifton et al., 2010; Knibbs et al., 2014). Thus, further research is required to assess this phenomenon and deduce if this rapid decay is apparent for other pathogens and whether it is a feature of the pathogen, the suspension fluid or the aerosolisation technique (Brouwer et al., 2017).

Cross-sectional study The COVID-19 pandemic halted the cross-sectional study and while this thesis was still able to present some valuable conclusions it would be beneficial to resume the study to gather more data as a key challenge of this

study was the limited sample size. The resumed study should focus on gathering data from *M. abscessus* patients to determine if *M. abscessus* can be detected in cough/exhaled breath using the CASS and analyse data from the mask samples using quantitative polymerase chain reaction (qPCR). Additionally, further study would allow for more data to be collected on how time and treatment affects number of culturable bacteria measured. In particular, investigation into mucolytics and hypertonic saline that alter airway surface tension or sputum viscosity.

Super producers A subset of people with CF were identified as high emitters or 'super producers' and these people had culturable bacteria an order of magnitude higher detected in their cough/exhaled breath than the majority of other participants. Since it is these high emitters that are the most likely to cause a cross-infection event between people with CF it becomes imperative that a more extensive study is conducted into investigating this subset of people with CF. Key areas to identify are what proportion of people with CF are high emitters, are they always high emitters, and what clinical/demographic characteristics, if any, are associated with being a high emitter. In addition, it may be of relevance to include experiments that measure the droplet size distribution and not the bacteria to conclude if this is likely to hold regardless of pathogen.

Risk framework The proposed risk model in Chapter 7 has the potential to be expanded for other pathogens and put into a risk framework with variable parameters that can easily be used by clinicians. This will be of great relevance for other pathogens and diseases and this aspect of future research is already being undertaken. Furthermore, there are a number of uncertainties for *P. aeruginosa* and other pathogens including dose-response, distribution of droplet sizes, and short range transmission. Future models could incorporate the short range transmission and there is a recommendation for improvement of dose-response models.

8.3 Implications of the research and final remarks

The findings of this thesis have implications for infection control guidelines for people with CF with an active infection with *P. aeruginosa* and/or *M. abscessus*. Firstly, this research has verified the ability for *P. aeruginosa* and *M. abscessus* to survive and travel up to 4 m in artificially generated aerosols and that survival is similar for a range of different strains. In addition, the cross-sectional study provided clear evidence that *P. aeruginosa* can be aerosolised within particles of the respirable size range. It is likely that this is the case for *M. abscessus* too based on the limited

mask samples and one room air sample. Concluding the laboratory data and clinical measurements suggest that airborne transmission of both pathogens may be possible. The 'super producers' which demonstrated some people chronically infected with *P. aeruginosa* can produce substantially higher amounts of the microorganism in aerosols suggests that this risk may not be heterogeneous. Although the infection risks predicted through the mathematical model in Chapter 7 were on average low, high emitters or 'super producers' were shown to be responsible for the highest risk cases. In addition, the consequence of these risks are high due to the increased morbidity and mortality associated with recurrent pulmonary infections with pathogens associated with CF. Therefore, these data presented confirms the need for continued vigilant infection control measures and assures clinicians the mitigation measures currently in place are vital. Based on these findings, it is paramount that airborne precautions to limit infection risk are implemented in CF units, in both the inpatient and outpatient setting, if not already. These data suggest that:

- People with CF should not meet indoors in any clinical circumstance, but if they must for personal reasons, they should keep a safe distance and increase ventilation where possible. In between clinic visits windows should be opened and people with CF should be accommodated within hospital rooms with negative pressure and/or adequate air exchange;
- Clinics should be organised by microbiological status and if future research is conducted to identify 'super producers' it may be advisable for these people to be seen at the end of the day or last on the ward rounds;
- As highlighted by the recent COVID-19 pandemic and recent studies on people with CF, Wood et al. (2018) reported that masks were effective in reducing the dispersal of viable aerosols. This supports infection control guidelines suggesting wearing a mask in communal areas to reduce the risk of transmission.

This research has been devoted to providing novel data on the generation and survival of aerosolised *P. aeruginosa* and *M. abscessus*, two bacteria affecting those with CF, and using these data to infer risk to people with CF through the use of a mathematical model. Not only is the model applicable for CF pathogens, it also offers the possibility of simulating risk for a broader range of airborne microorganisms. The importance of this has been demonstrated with the need for rapid results on infection control measures for SARS-CoV-2. Finally, it is hoped that this newly acquired knowledge will assist in guiding infection control measures, allow people with CF and healthcare professionals to understand the risk of infection, and further protect people with CF from recurrent pulmonary infection and lung function decline as a consequence of acquisition and transmission of airborne pathogens.

Appendix A

Bioaerosol characterisation apparatus design

A.1 Refining rig deign

A steady state computational fluid dynamics (CFD) model was used to model a 2D geometry of the experimental apparatus in ANSYS Fluent (v 17.2). The Reynolds Average Navier-Stokes (RANS) approach was used to simulate the flow with a COUPLED pressure-velocity coupling algorithm. Second order upwind discretisation was used for all the equations, and simulations were said to be converged when residuals for all variables dropped below 10^{-8} and stayed there for at least 100 iterations.

The standard k-ϵ model was chosen due to the models robustness and its ability to be reasonably accurate for a wide range of flows. This two-equation model was used with the wall functions turned on and has been used before for separating flows (Ratha and Sarkar, 2015). Initially, a two-dimensional model was created of the 'laminar flow model' (Clifton et al., 2008) to determine if there was any large recirculation zones that could be to reduced by a different inlet. Subsequently, new inlet designs were explored using a 2D model.

Both the geometry and mesh for all 2D models were created using ICEM (ANSYS v17.2). The geometry used for modelling the original pipe is given in Figure 4.10. The mesh was structured and mesh refinements were carried out in the corners of the geometry. Several simulations of this model were conducted to compare the air flow in 1 m, 2 m, 3 m, and 4 m lengths and it was deemed that the length of the pipe made no difference to the recirculation zones in the flow. Final cell count of the 1 m

model was in the region of 6000 cells.

Boundary conditions for the original model were as follows. The nebuliser inlet was a velocity inlet at $1.57\,\mathrm{m\,s^{-1}}$ with hydraulic diameter 0.009 m. The air inlet was set as a default pressure inlet with hydraulic diameter 0.009 m. The outlet was set as a velocity inlet with $-7.34\,\mathrm{m\,s^{-1}}$, large negative gauge pressure of $-25\,\mathrm{Pa}$ and hydraulic diameter 0.009 m. All other boundaries were set to no slip walls. The boundary conditions were chosen to match reality, the volume flow rates were set by the equipment used and were $6\,\mathrm{L\,min^{-1}}$ for the nebuliser and $28\,\mathrm{L\,min^{-1}}$ for the pump. Velocity was calculated using the equation $v = Q/A$ where v is velocity, Q is flow rate and A is area.

Figure A.1 shows streamlines of the 2D laminar flow model at the inlet and the outlet and it can be seen that there are larger disturbance at the inlet of the pipe. The difference in velocity of the air coming through both of the inlets and the 'T' shape of the pipe causes these disturbances. Removing these recirculation zones was necessary to potentially reduce the number of droplets carrying viable microorganisms entrained into recirculation zones and hence not being measured at the end of the bioaerosol characterisation apparatus (BACA).

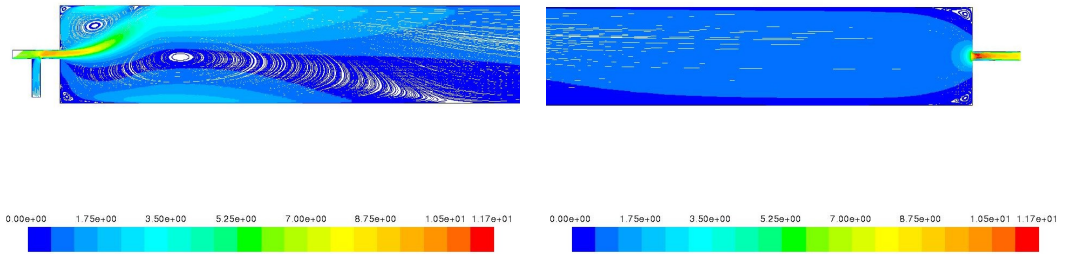

(a) Inlet of the pipe from 0 m-0.4 m (b) Outlet of the pipe from 0.6 m-1 m

Figure A.1: Streamlines of velocity ($\mathrm{m\,s^{-1}}$) of the 2D 'laminar flow' geometry for CFD simulation.

A.1.0.1 Modelling new inlets

Two inlets were considered based on the availability of standard pipe fittings, these fittings had 'Y' geometry at different angles, 45° and 60°. However, after simulations of these geometries the streamlines of velocity demonstrated no reduction in the recirculation when compared with the 'T' inlet from the original laminar flow geometry. Therefore, due to the physical limitations of standard double inlet pipes it was decided to consider a customised inlet. The velocities through each inlet were matched to reduce the recirculation seen in the flow field. This new geometry

represented a 'pipe within a pipe' inlet where the velocities were matched by the difference in pipe sizes. The resulting streamlines of velocity for the simulation are shown in Figure A.2. The streamlines appear to show a reduction in recirculation and the velocity is more consistent. Velocities in the x-direction along the pipe at $y = -0.4\,\mathrm{m}$ and $y = 0.4\,\mathrm{m}$ were found to be consistent with no extreme changes as seen in the streamlines of velocity in both the 'Y' and 'T' inlets. In conclusion, the 'pipe within a pipe' geometry was found to reduce the recirculation at the inlet and this design was chosen for the BACA.

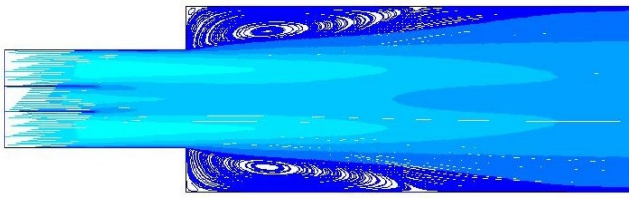

Figure A.2: Streamlines of velocity ($\mathrm{m\,s^{-1}}$) using the 'pipe within a pipe' 2D geometry for CFD simulation.

Appendix B

Additional aerosol characterisation figures

B.1 Nebuliser aerosol size distribution: Droplets on glass slides

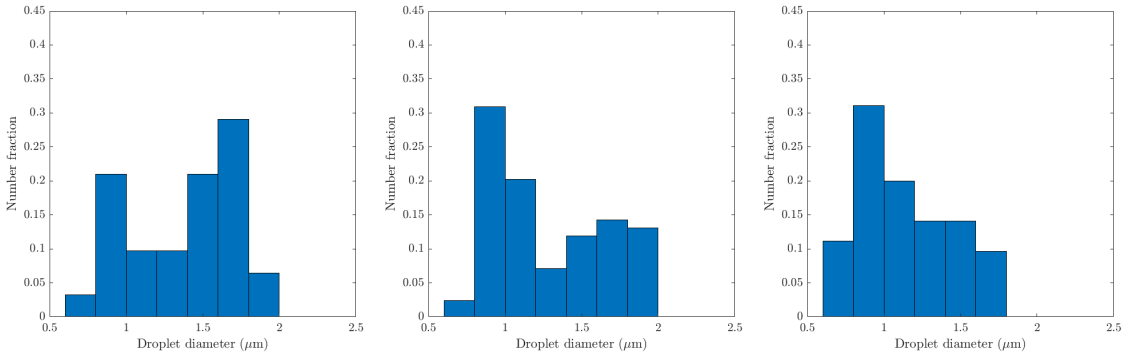

(a) 0 mm. (b) 50 mm. (c) 100 mm.

Figure B.1: Number fraction droplet size distributions from aerosolising *P. aeruginosa* environmental strain in 1/4 ringers onto microscope slides in the class II microbiology cabinet.

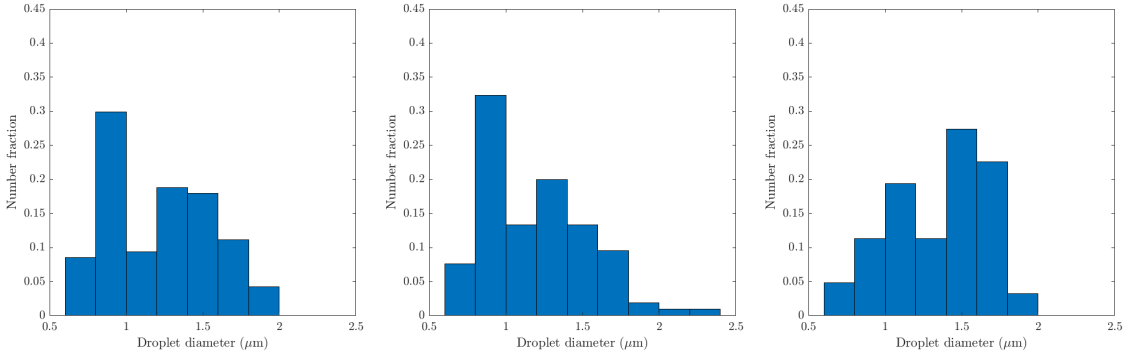

(a) 0 mm. (b) 50 mm. (c) 100 mm.

Figure B.2: Number fraction droplet size distributions from aerosolising *P. aeruginosa* Manchester strain in 1/4 ringers onto microscope slides in the class II microbiology cabinet.

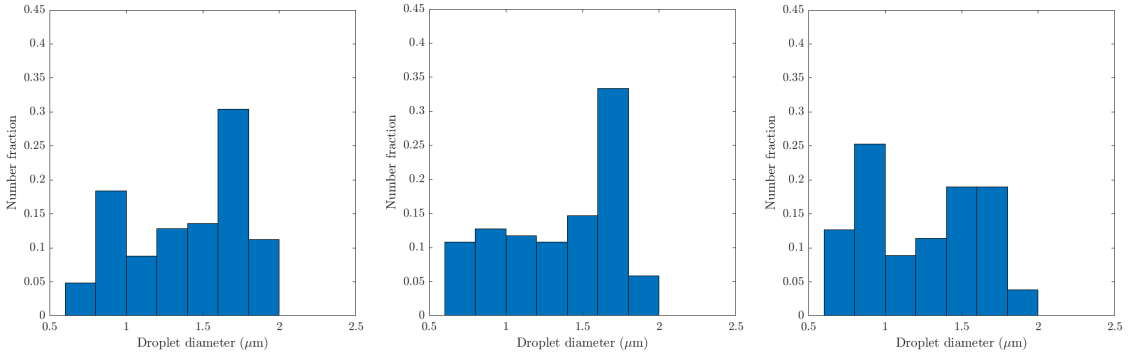

(a) 0 mm. (b) 50 mm. (c) 100 mm.

Figure B.3: Number fraction droplet size distributions from aerosolising *P. aeruginosa* Newcastle strain in 1/4 ringers onto microscope slides in the class II microbiology cabinet.

B.2 Nebuliser aerosol size distribution: Spraytec short range measurements

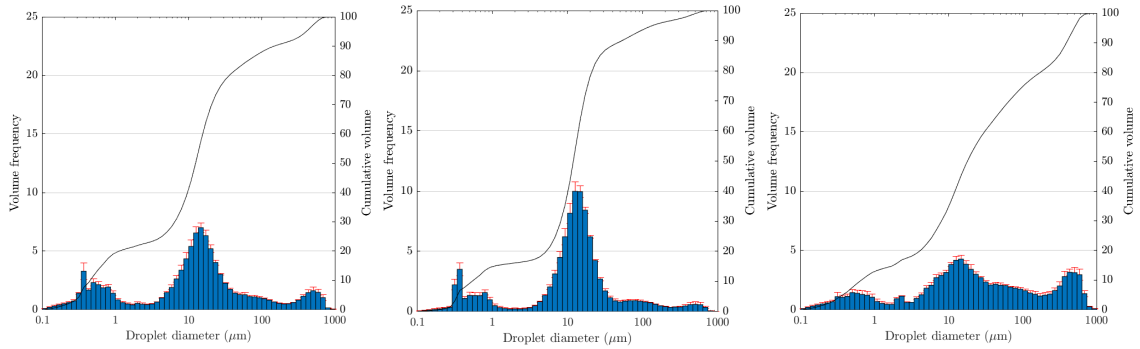

(a) 0 mm. (b) 50 mm. (c) 100 mm.

Figure B.4: Cumulative volume and volume frequency of aerosolised *P. aeruginosa* environmental in 1/4 ringers into room air at a distance of 0 mm–100 mm from the Spraytec device.

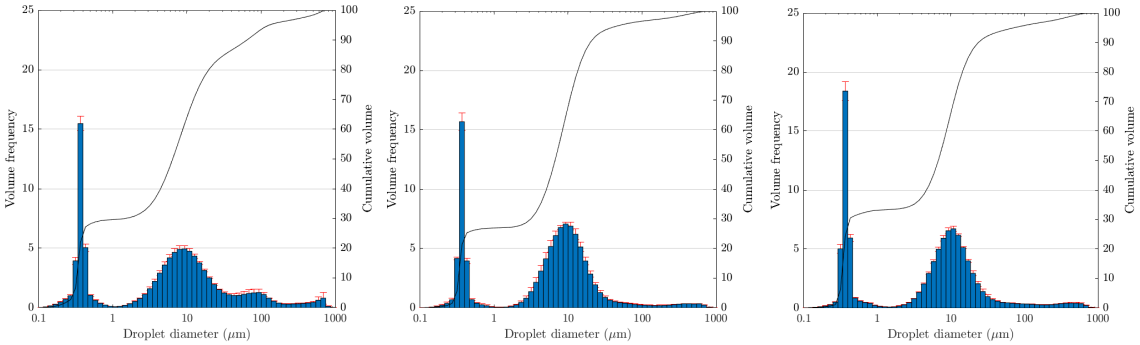

(a) 0 mm. (b) 50 mm. (c) 100 mm.

Figure B.5: Cumulative volume and volume frequency of aerosolised *P. aeruginosa* Manchester in 1/4 ringers into room air at a distance of 0 mm–100 mm from the Spraytec device.

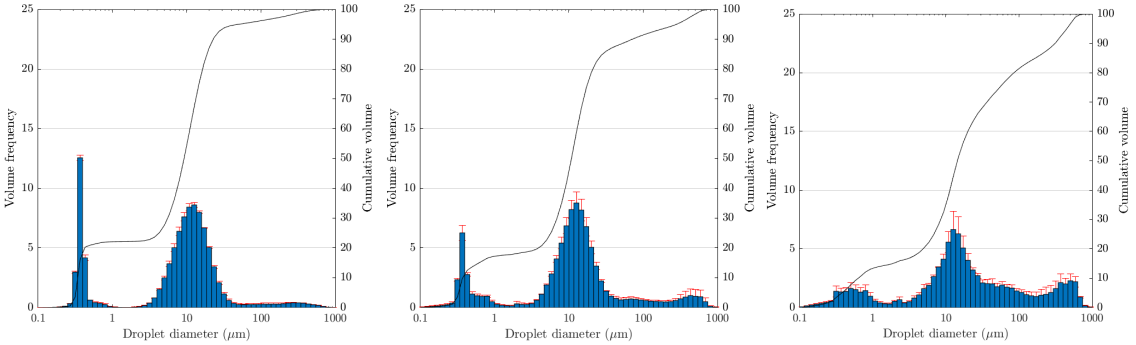

(a) 0 mm. (b) 50 mm. (c) 100 mm.

Figure B.6: Cumulative volume and volume frequency of aerosolised *P. aeruginosa* Newcastle in 1/4 ringers into room air at a distance of 0 mm–100 mm from the Spraytec device.

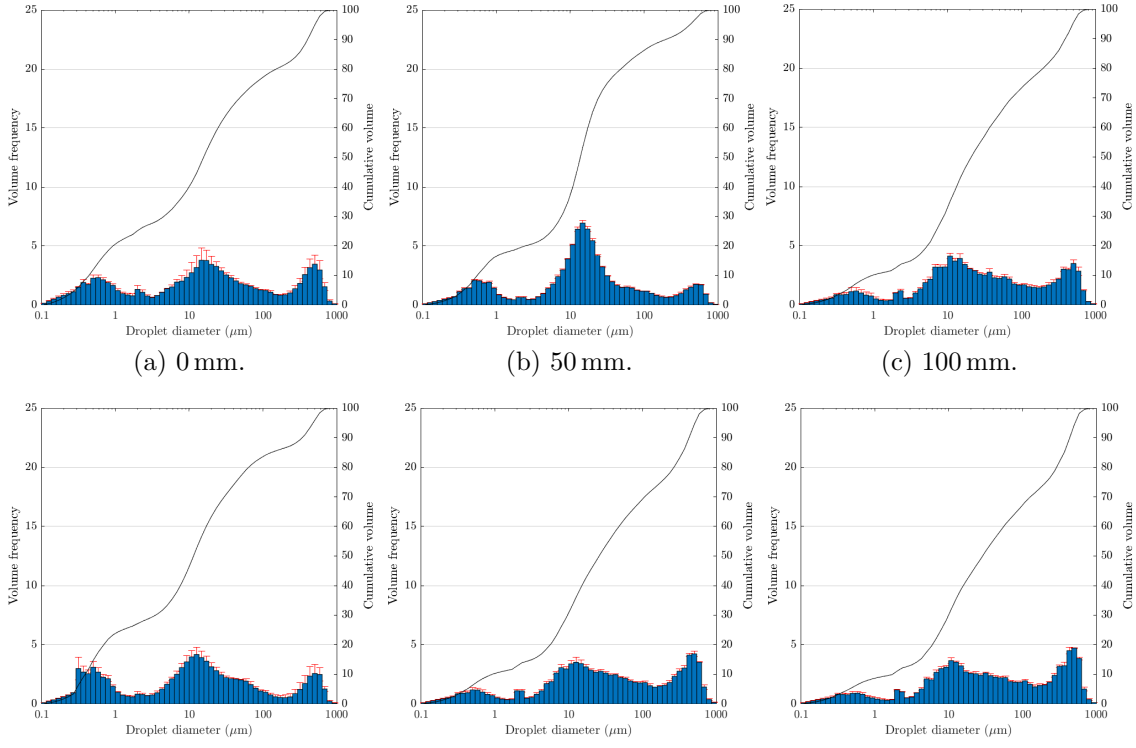

(a) 0 mm. (b) 50 mm. (c) 100 mm.

(d) 0 mm. (e) 50 mm. (f) 100 mm.

Figure B.7: Cumulative volume and volume frequency of aerosolised *P. aeruginosa* patient non-mucoid in 1/4 ringers ((a)–(c)) and 1 % FBS ((d)–(f)) into room air at a distance of 0 mm–100 mm from the Spraytec device.

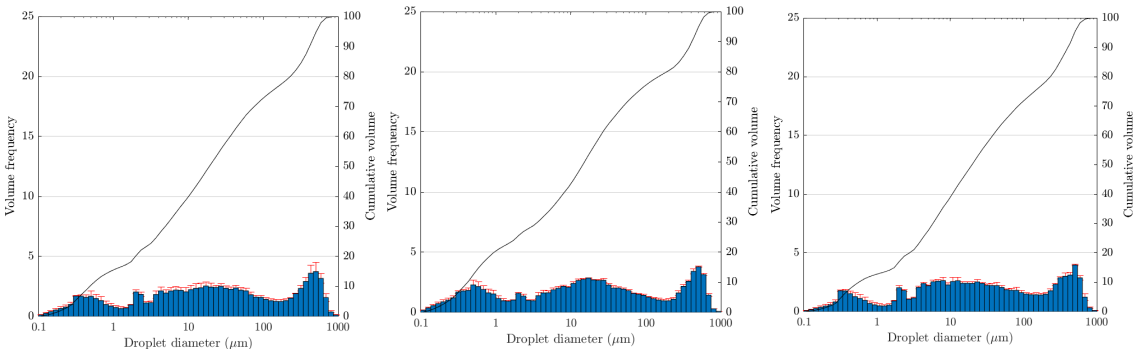

(a) 0 mm. (b) 50 mm. (c) 100 mm.

Figure B.8: Cumulative volume and volume frequency of aerosolised *M. abscessus* rough in 1 % FBS ((d)–(f)) into room air at a distance of 0 mm–100 mm from the Spraytec device.

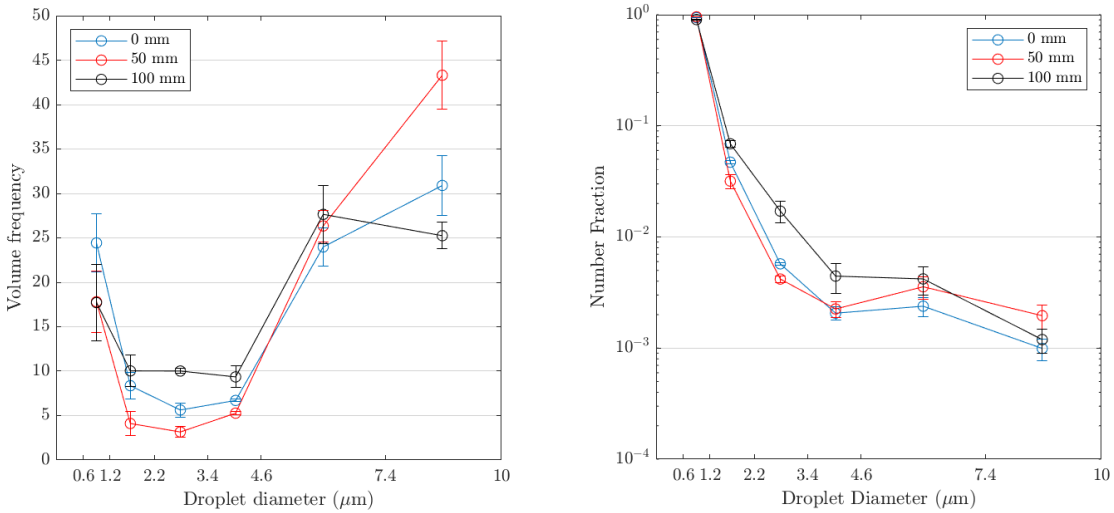

(a) Volume frequency. (b) Number fraction.

Figure B.9: Volume frequency and number fraction droplet size distribution truncated for the Andersen Impactor size range produced by aerosolising *P. aeruginosa* environmental in 1/4 ringers into room air at a distance of 0 mm–100 mm from the Spraytec device.

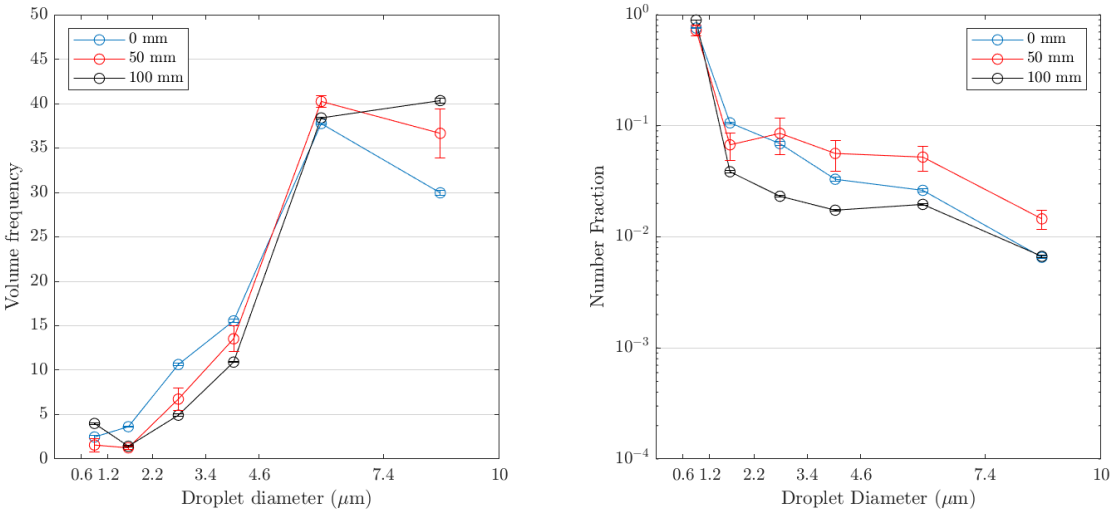

(a) Volume frequency. (b) Number fraction.

Figure B.10: Volume frequency and number fraction droplet size distribution truncated for the Andersen Impactor size range produced by aerosolising *P. aeruginosa* Manchester in 1/4 ringers into room air at a distance of 0 mm–100 mm from the Spraytec device.

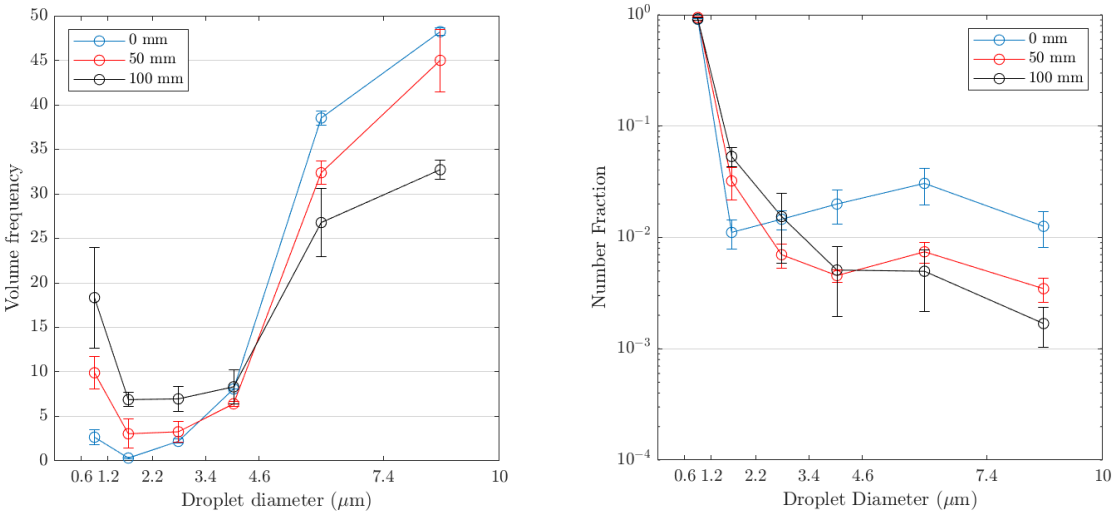

(a) Volume frequency. (b) Number fraction.

Figure B.11: Volume frequency and number fraction droplet size distribution truncated for the Andersen Impactor size range produced by aerosolising *P. aeruginosa* Newcastle in 1/4 ringers into room air at a distance of 0 mm–100 mm from the Spraytec device.

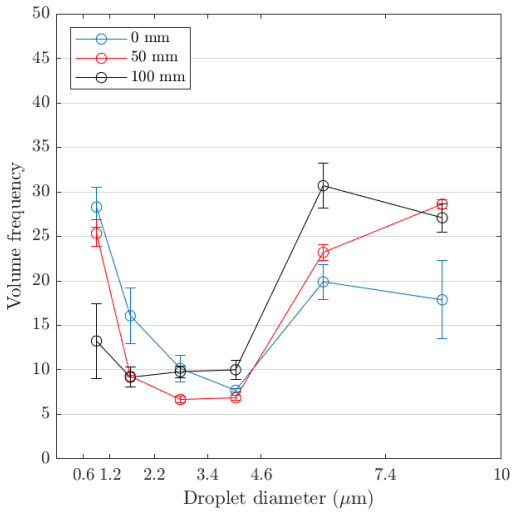

(a) 1/4 ringers.

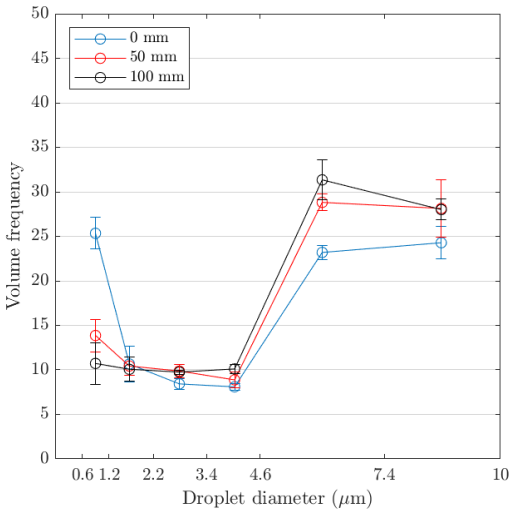

(b) 1 % FBS.

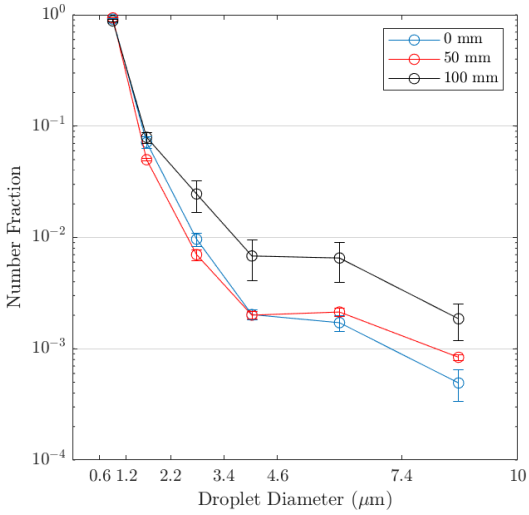

(c) 1/4 ringers.

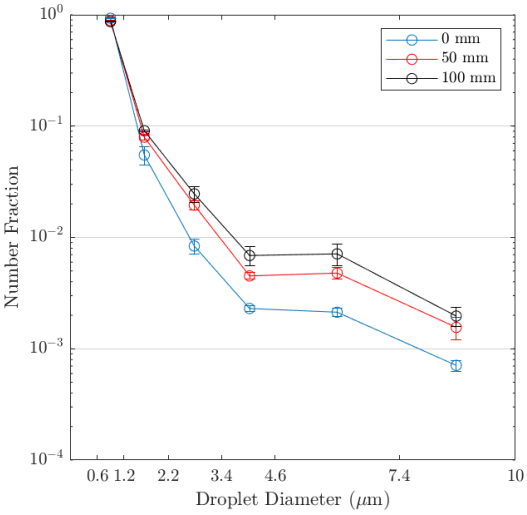

(d) 1 % FBS.

Figure B.12: Volume frequency ((a)–(b)) and number fraction ((c)–(d)) droplet size distribution truncated for the Andersen Impactor size range produced by aerosolising *P. aeruginosa* patient mucoid strain in different suspensions into room air at a distance of 0 mm–100 mm from the Spraytec device.

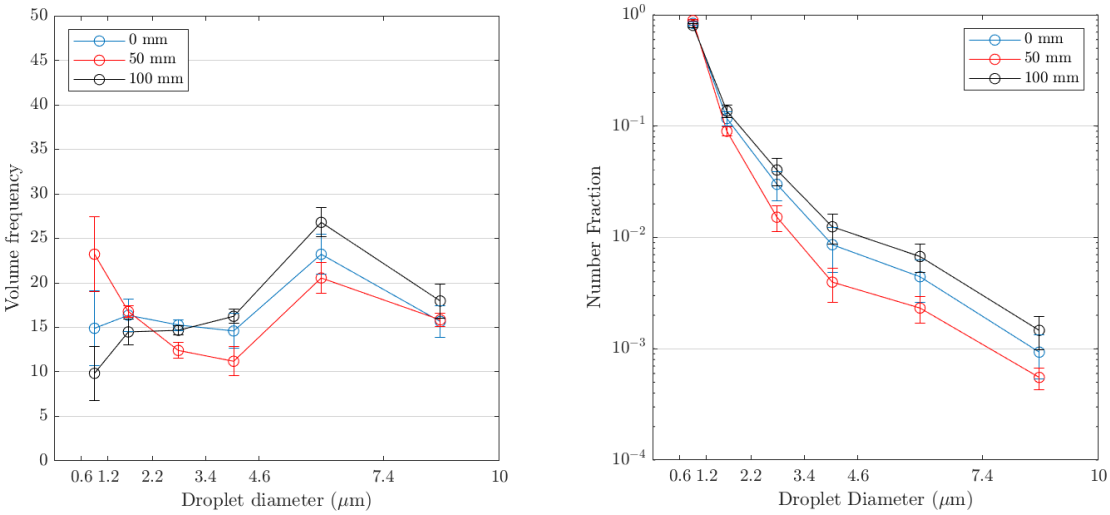

(a) Volume frequency.

(b) Number fraction.

Figure B.13: Volume frequency and number fraction droplet size distribution truncated for the Andersen Impactor size range produced by aerosolising *M. abscessus* rough in 1 % FBS into room air at a distance of 0 mm–100 mm from the Spraytec device.

B.3 Controlled flow: Effect of bacterial strain

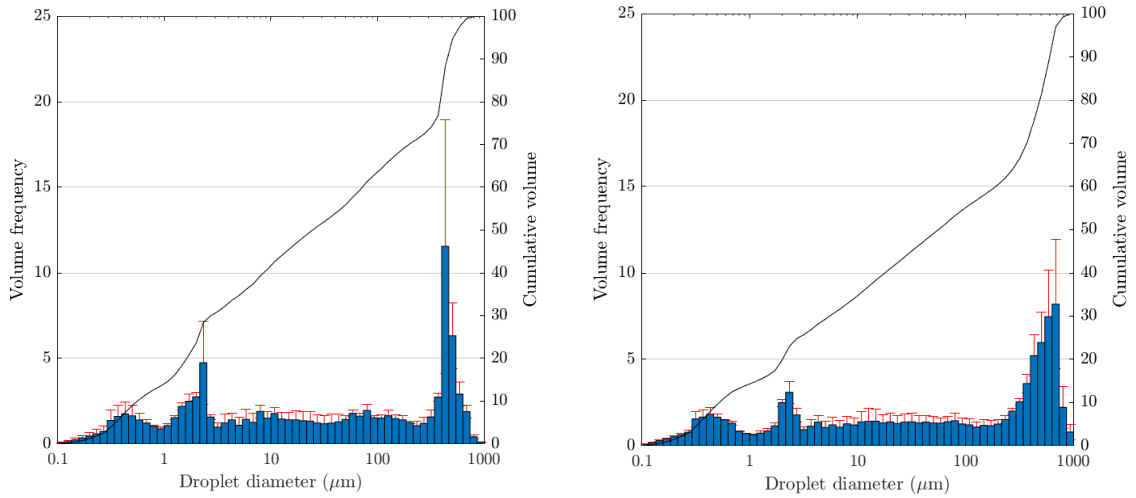

(a) 1 m.

(b) 2 m.

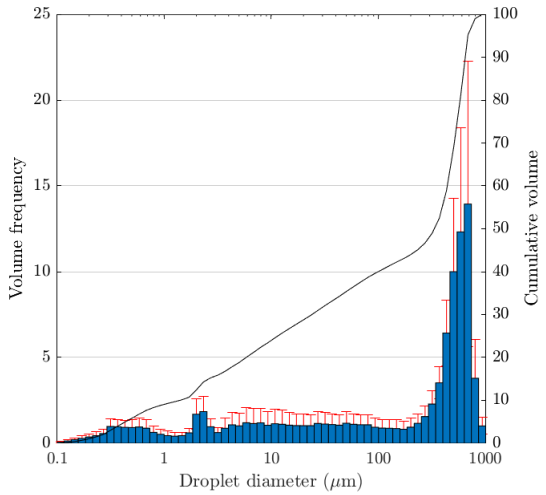

(c) 3 m.

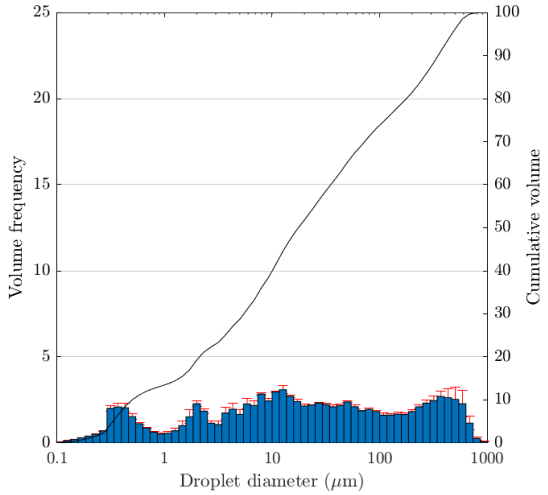

(d) 4 m.

Figure B.14: Cumulative volume and volume frequency of aerosolised *P. aeruginosa* Manchester in 1/4 ringers solution using the BACA over 1 m–4 m.

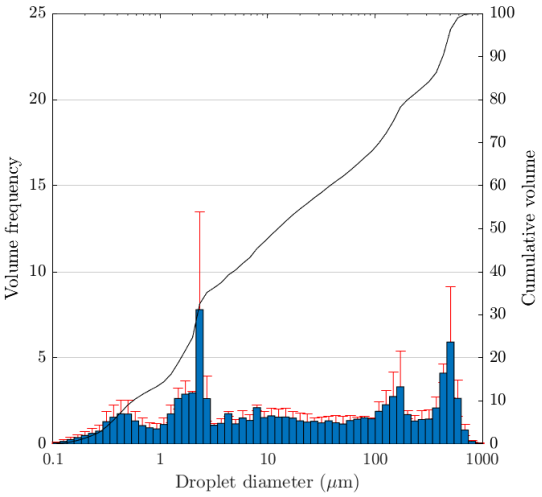

(a) 1 m.

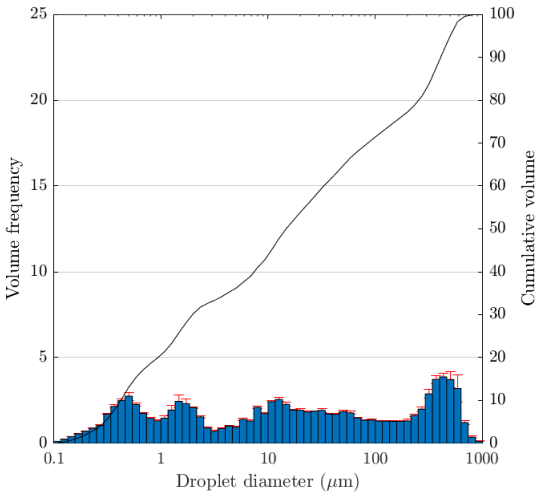

(b) 2 m.

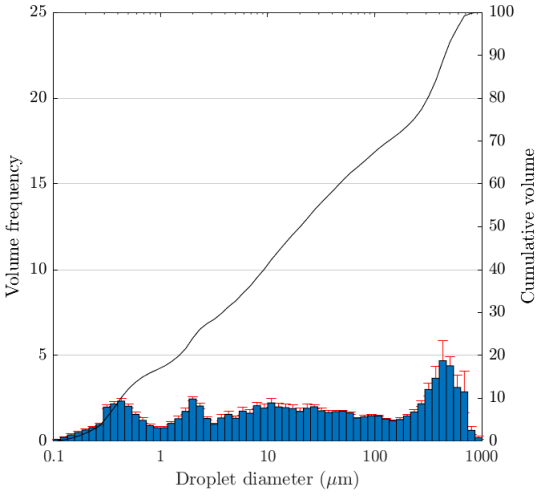

(c) 3 m.

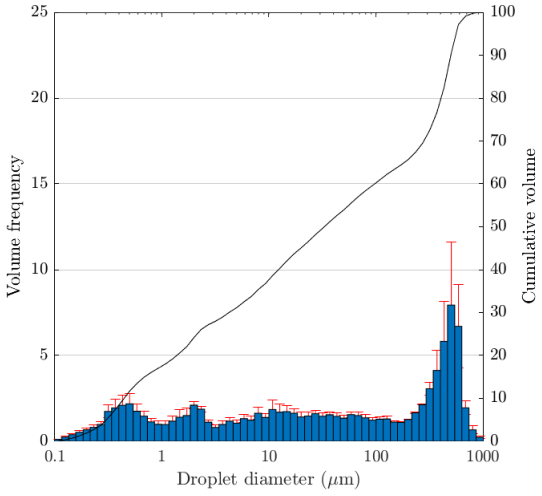

(d) 4 m.

Figure B.15: Cumulative volume and volume frequency of aerosolised *P. aeruginosa* Newcastle in 1/4 ringers solution using the BACA over 1 m–4 m.

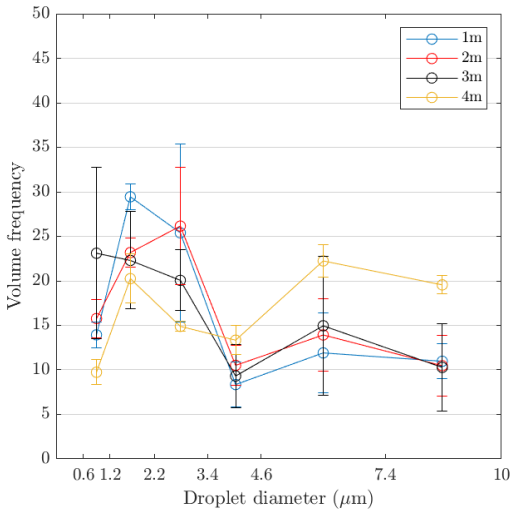

(a) *P. aeruginosa* Manchester volume frequency.

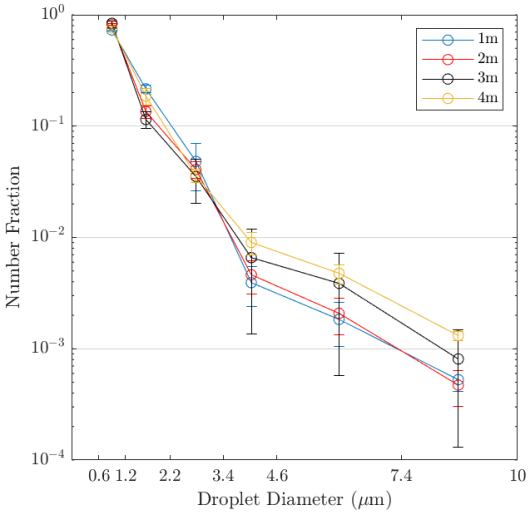

(b) *P. aeruginosa* Manchester number fraction.

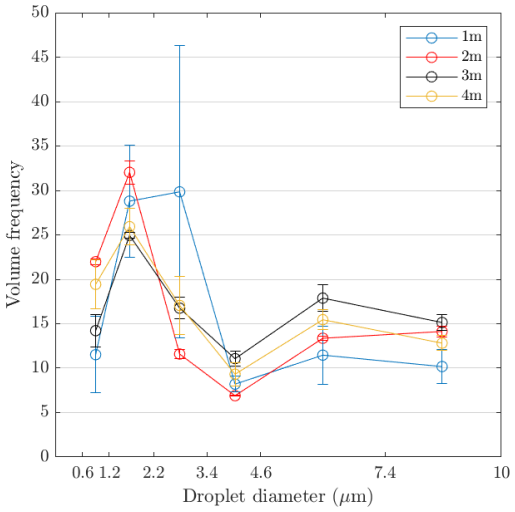

(c) *P. aeruginosa* Newcastle volume frequency.

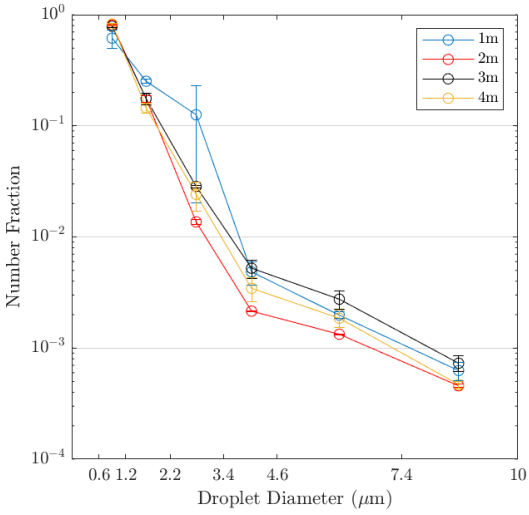

(d) *P. aeruginosa* Newcastle number fraction.

Figure B.16: Volume frequency droplet size distribution truncated for the Andersen Impactor size range produced by aerosolising *P. aeruginosa* strains in 1/4 ringers using the BACA over 1 m–4 m.

B.4 Controlled flow: Effect of suspension fluid

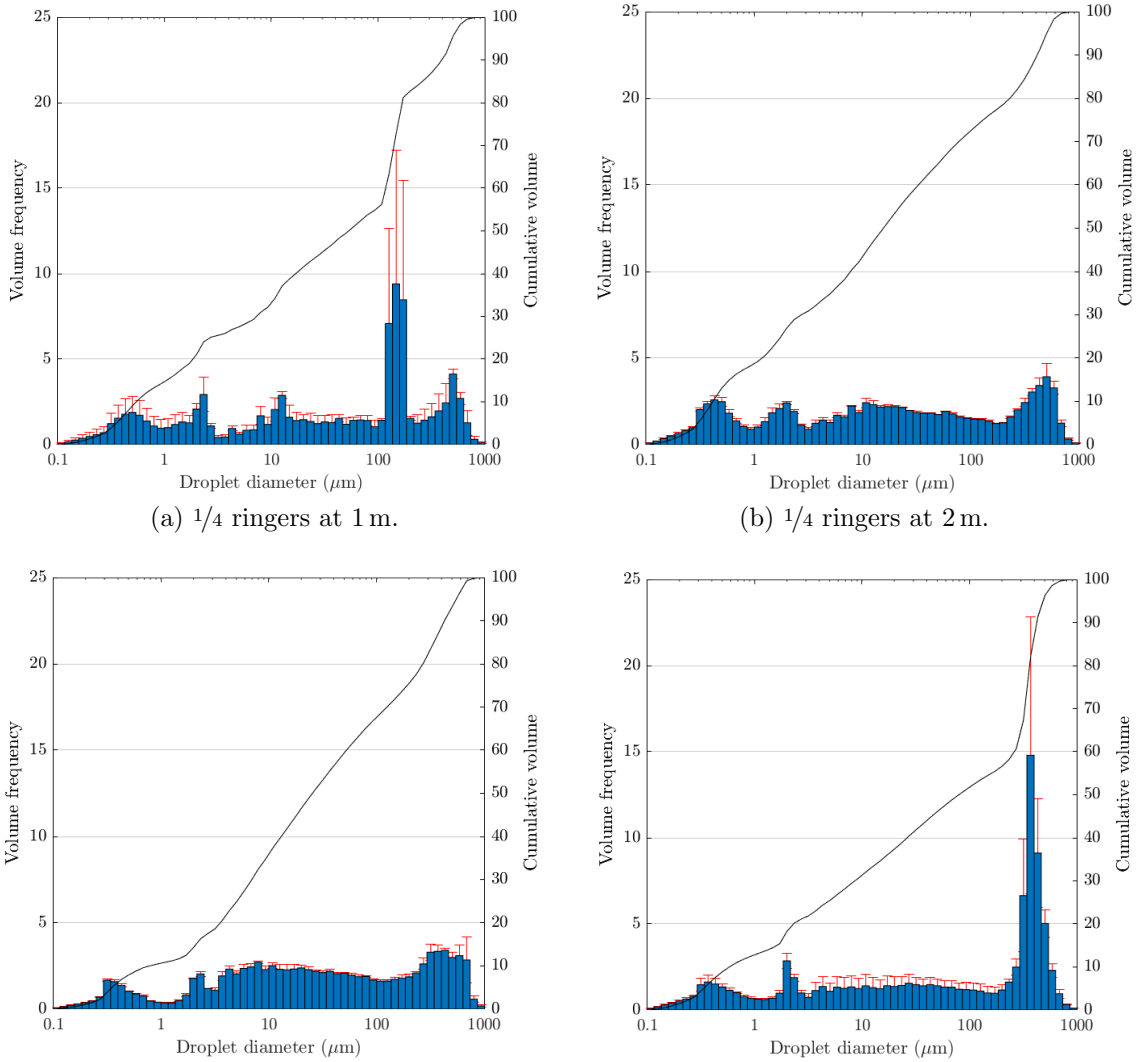

(a) 1/4 ringers at 1 m.

(b) 1/4 ringers at 2 m.

(c) 1 % FBS at 1 m.

(d) 1 % FBS at 2 m.

Figure B.17: Cumulative volume and volume frequency of aerosolised *P. aeruginosa* patient non-mucoid in two suspensions using the BACA at 1 m and 2 m.

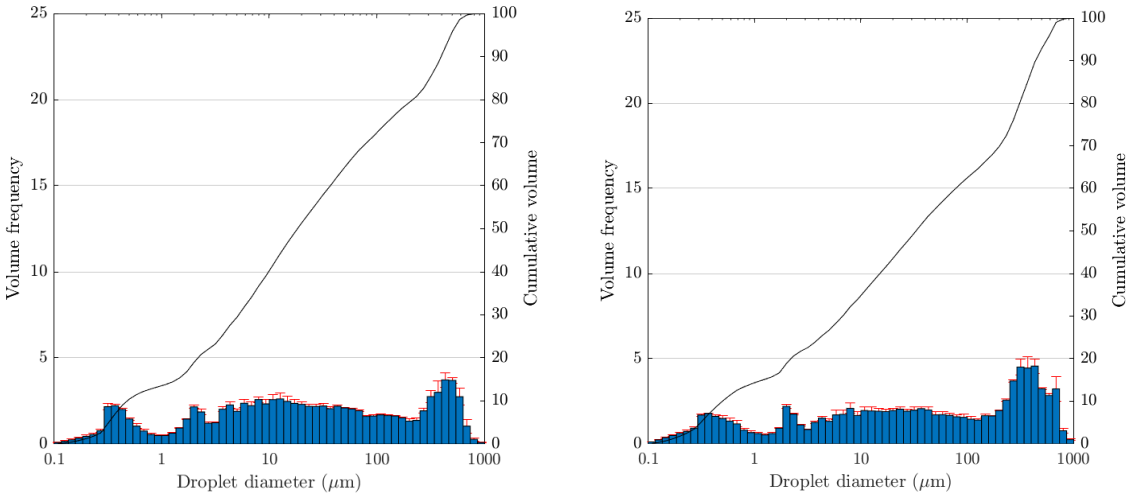

(a) 1 m. (b) 2 m.

Figure B.18: Cumulative volume and volume frequency of aerosolised *M. abscessus* rough in 1 % FBS using the BACA over at 1 m and 2 m.

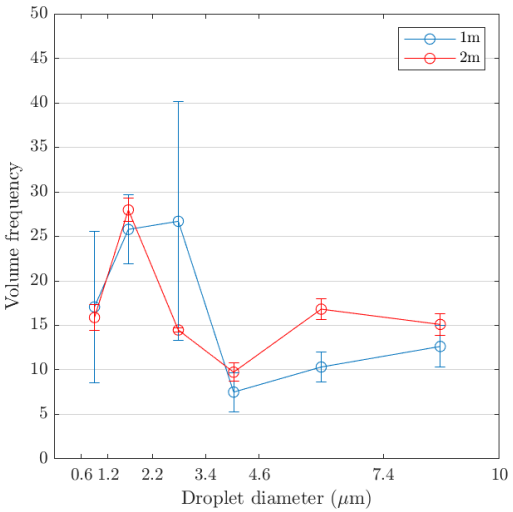

(a) 1/4 ringers.

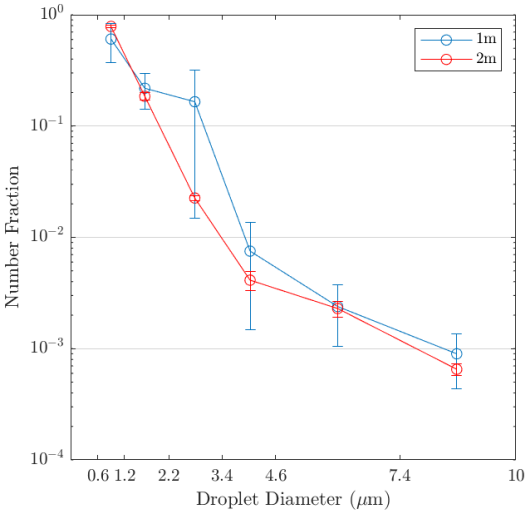

(b) 1/4 ringers number fraction.

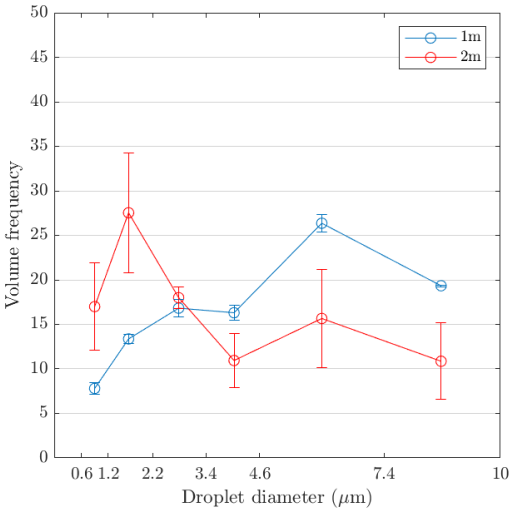

(c) 1 % FBS.

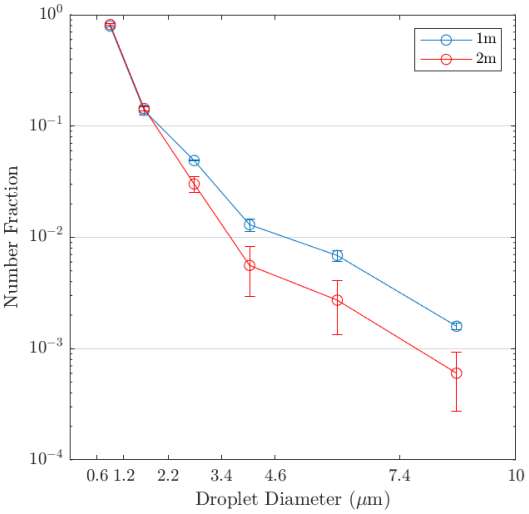

(d) 1 % FBS ringers number fraction.

Figure B.19: Droplet size distribution truncated for the Andersen Impactor size range produced by aerosolising *P. aeruginosa* patient non-mucoid in two suspensions using the BACA at 1 m and 2 m.

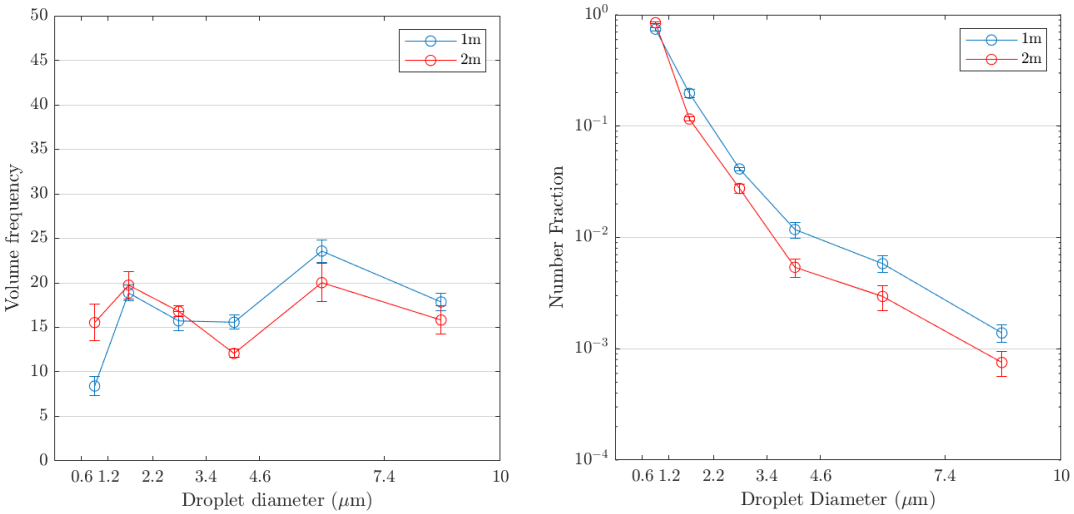

(a) 1 % FBS volume frequency.

(b) 1 % FBS ringers number fraction.

Figure B.20: Droplet size distribution truncated for the Andersen Impactor size range produced by aerosolising *M. abscessus* rough in 1 % FBS using the BACA at 1 m and 2 m.

B.5 Evaporation analysis

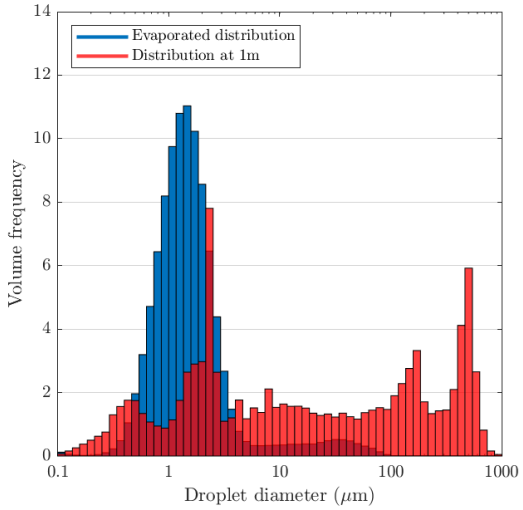

Figure B.21: Comparison of predicted evaporated volume frequency droplet size distribution and droplet size distribution of *P. aeruginosa* Newcastle in 1/4 ringers at 1 m in the BACA.

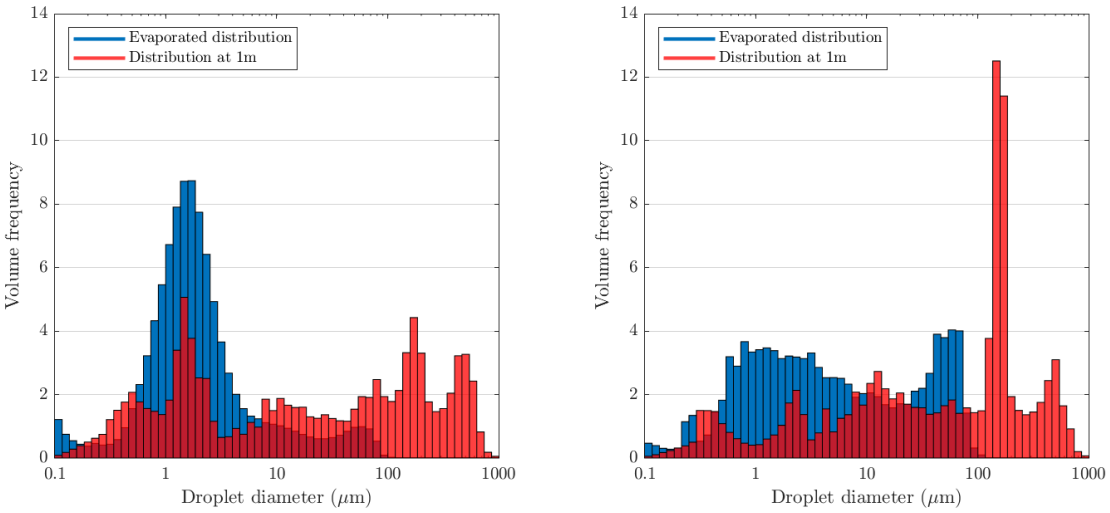

(a) 1/4 ringers.

(b) 1 % FBS.

Figure B.22: Comparison of predicted evaporated volume frequency droplet size distribution and droplet size distribution of aerosolised *P. aeruginosa* patient mucoid in two suspensions at 1 m in the BACA.

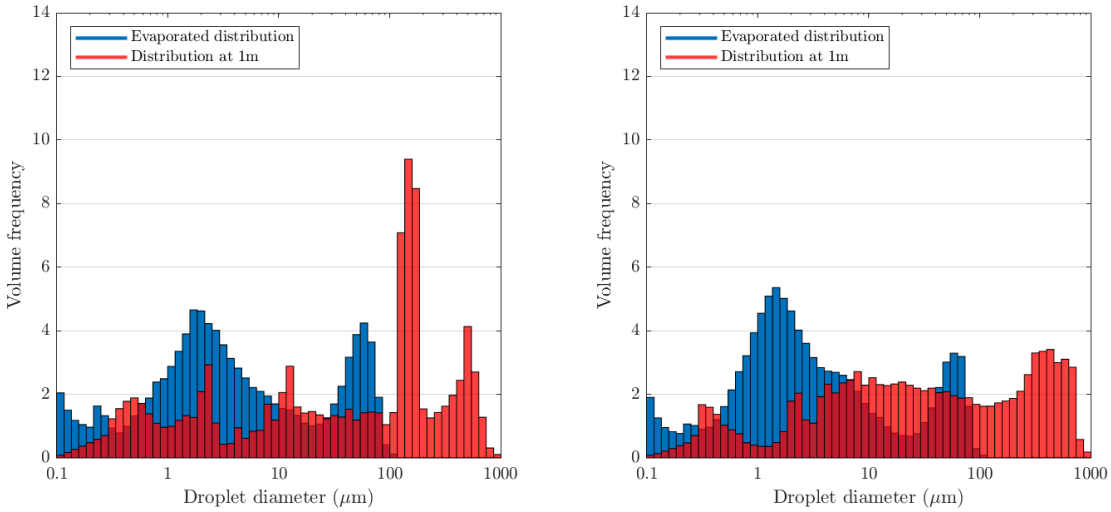

(a) 1/4 ringers. (b) 1 % FBS.

Figure B.23: Comparison of predicted evaporated volume frequency droplet size distribution and droplet size distribution of aerosolised *P. aeruginosa* patient non-mucoid in two suspensions at 1 m in the BACA.

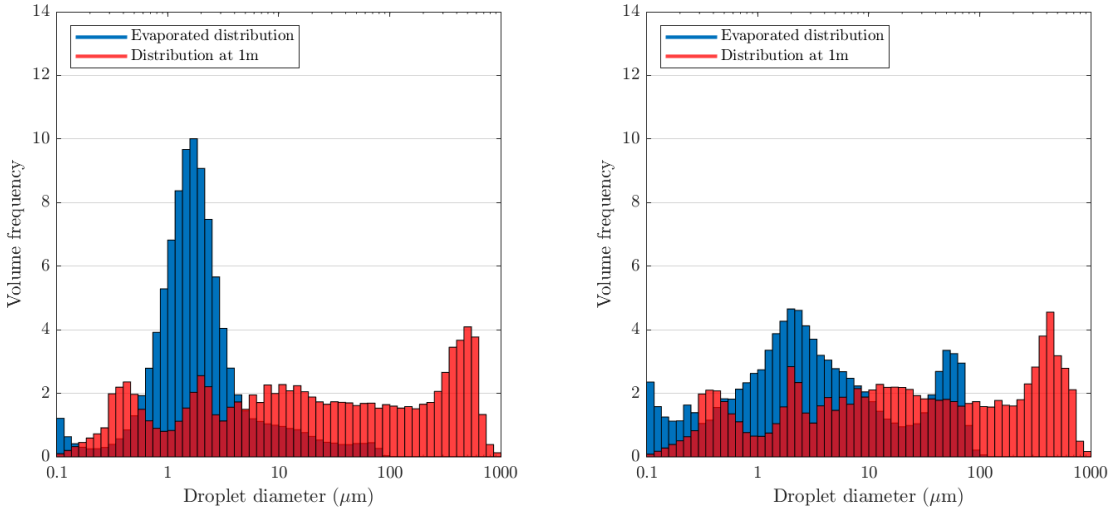

(a) 1/4 ringers. (b) 1 % FBS.

Figure B.24: Comparison of predicted evaporated volume frequency droplet size distribution and droplet size distribution of aerosolised *M. abscessus* smooth in two suspensions at 1 m in the BACA.

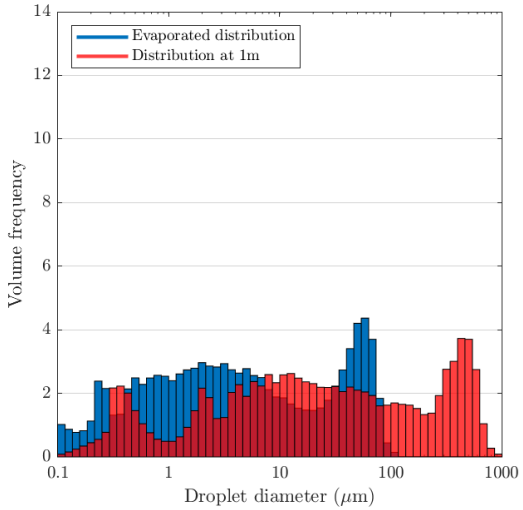

Figure B.25: Comparison of predicted evaporated volume frequency droplet size distribution and droplet size distribution of *M. abscessus* rough in 1 % FBS at 1 m in the BACA.

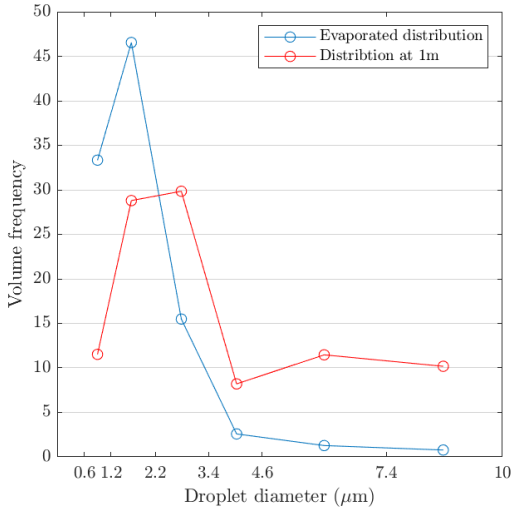

Figure B.26: Comparison of predicted evaporated volume frequency droplet size distribution and droplet size distribution of aerosolised *P. aeruginosa* Newcastle in 1/4 ringers at 1 m in the BACA truncated to the Andersen Impactor size range.

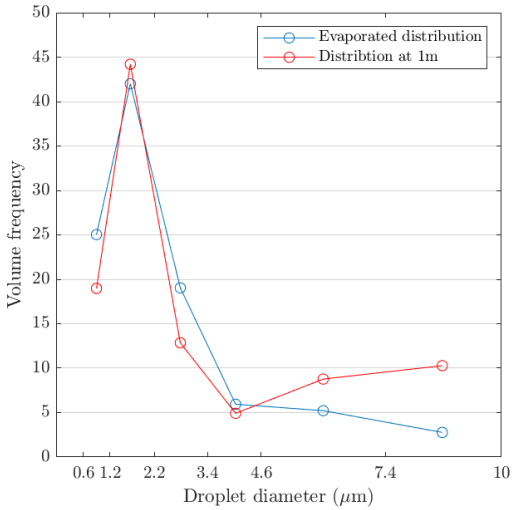

(a) 1/4 ringers.

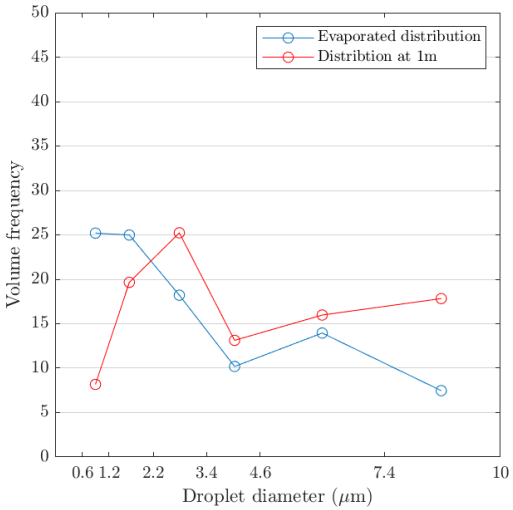

(b) 1 % FBS.

Figure B.27: Comparison of predicted evaporated volume frequency droplet size distribution and droplet size distribution of aerosolised *P. aeruginosa* patient mucoid in two suspensions at 1 m in the BACA truncated to the Andersen Impactor size range.

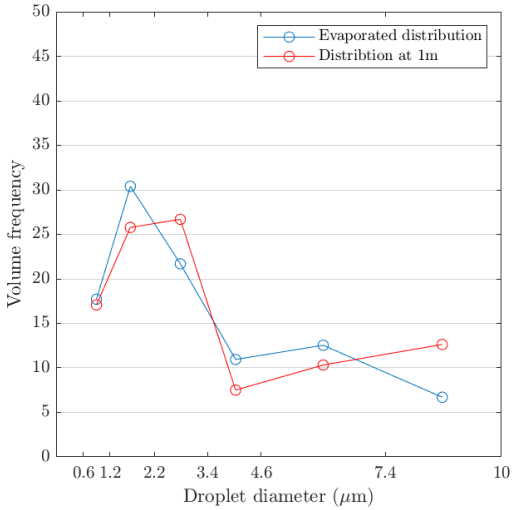

(a) 1/4 ringers.

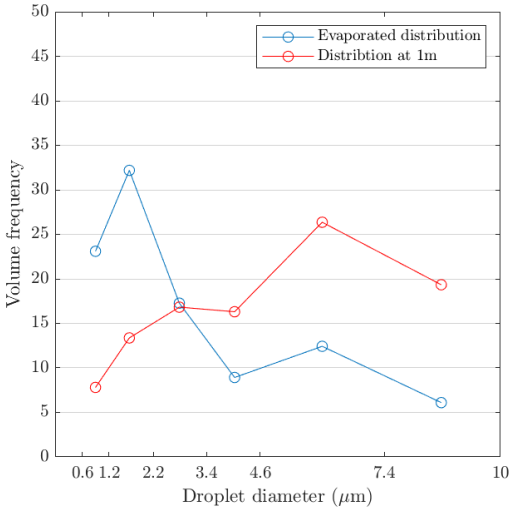

(b) 1 % FBS.

Figure B.28: Comparison of predicted evaporated volume frequency droplet size distribution and droplet size distribution of aerosolised *P. aeruginosa* patient non-mucoid in two suspensions at 1 m in the BACA truncated to the Andersen Impactor size range.

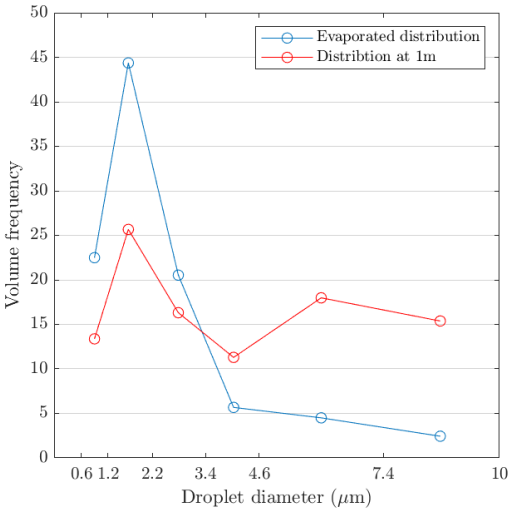

(a) 1/4 ringers.

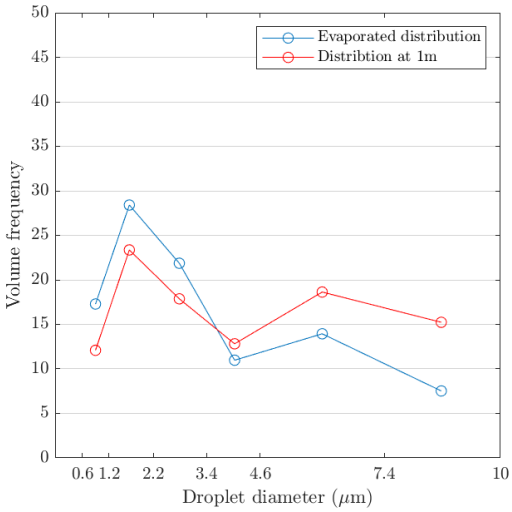

(b) 1 % FBS.

Figure B.29: Comparison of predicted evaporated volume frequency droplet size distribution and droplet size distribution of aerosolised *M. abscessus* smooth in two suspensions at 1 m in the BACA truncated to the Andersen Impactor size range.

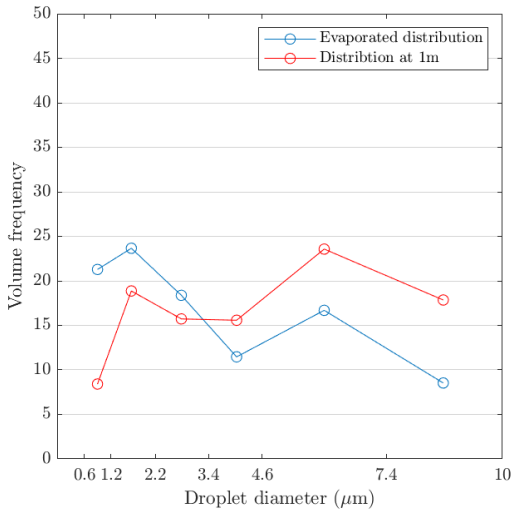

Figure B.30: Comparison of predicted evaporated volume frequency droplet size distribution and droplet size distribution of aerosolised *M. abscessus* rough in 1 % FBS at 1 m in the BACA truncated to the Andersen Impactor size range.

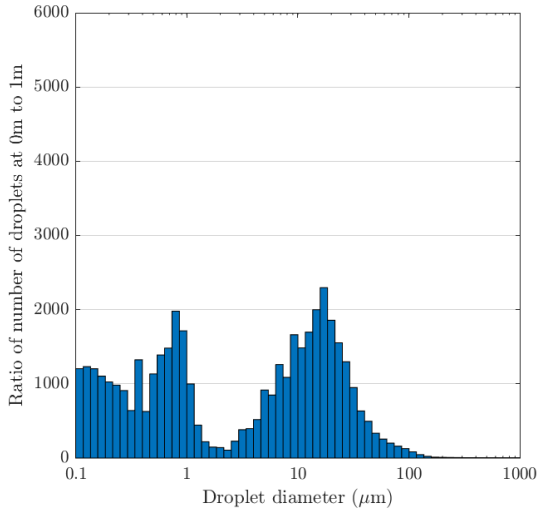

(a) Environmental

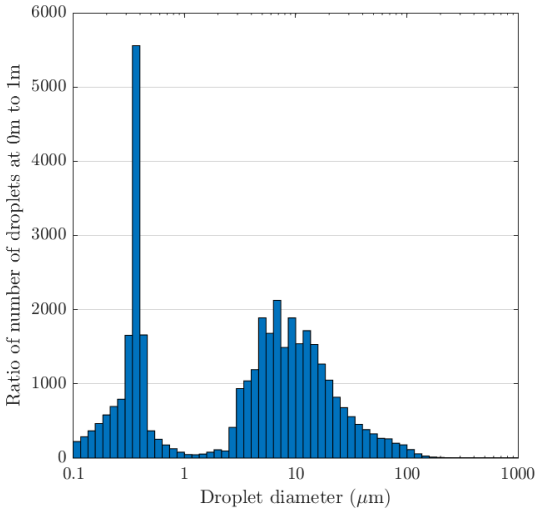

(b) Manchester

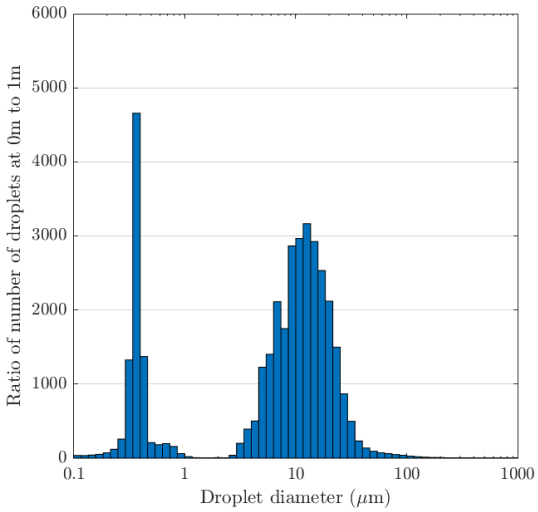

(c) Newcastle

Figure B.31: Ratio of one droplet at 1 m using the BACA to number of droplets at 0 m in air after aerosolisation of *P. aeruginosa* strains in 1/4 ringers.

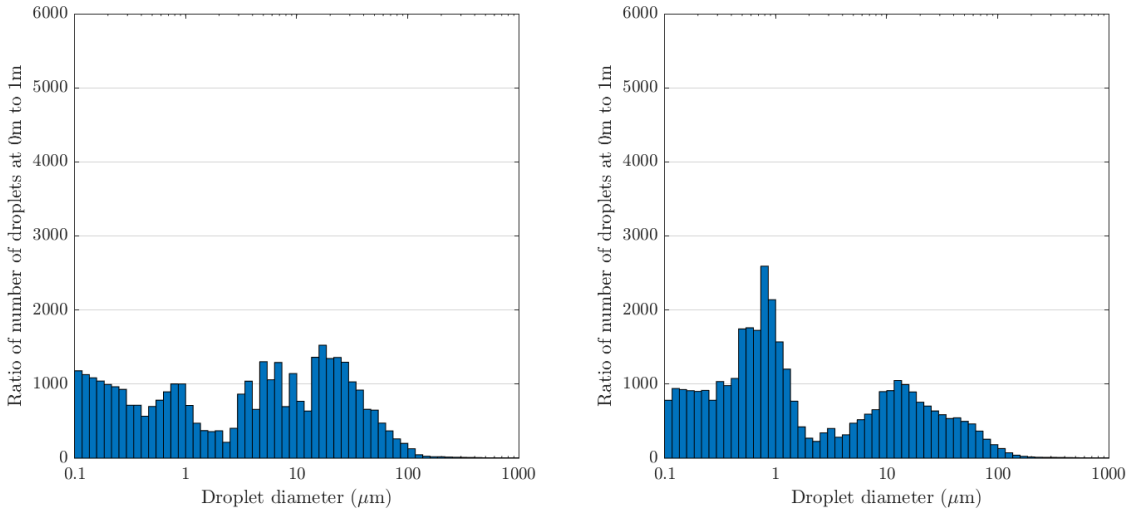

(a) 1/4 ringers. (b) 1 % FBS.

Figure B.32: Ratio of one droplet at 1 m using the BACA to number of droplets at 0 m in air after aerosolisation of *P. aeruginosa* patient non-mucoid in two suspensions.

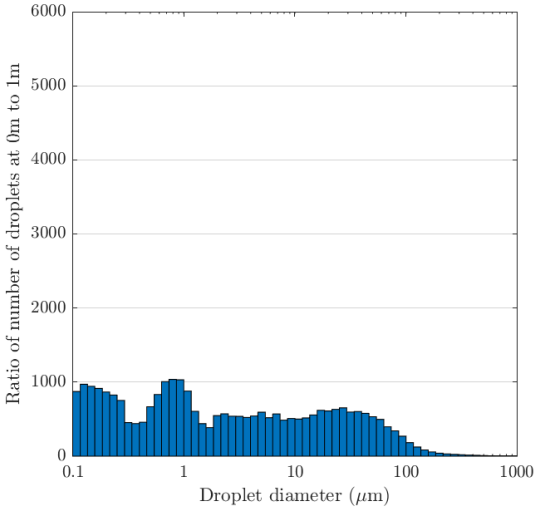

Figure B.33: Ratio of one droplet at 1 m using the BACA to number of droplets at 0 m in air after aerosolisation of *M. abscessus* rough in 1 % FBS.

Appendix C

Cross-sectional study approvals and key documents

C.1 Ethical approval

Prof Catherine Noakes
Professor of Environmental Engineering for Buildings,
Director of Research and Innovation
University of Leeds
Leeds
4.14 School of Civil Engineering
LS2 9JT

Email: hra.approval@nhs.net
Research-permissions@wales.nhs.uk

28 February 2019

Dear Prof Noakes

HRA and Health and Care Research Wales (HCRW) Approval Letter

Study title:	**Study characterising the aerosolisation of microbial particles from people with cystic fibrosis and determining if Pseudomonas aeruginosa and Mycobacterium abscessus are present in patient cough/exhaled breath aerosols in the inpatient setting.**
IRAS project ID:	**229122**
Protocol number:	**N/A**
REC reference:	**18/SC/0654**
Sponsor	**University of Leeds**

I am pleased to confirm that **HRA and Health and Care Research Wales (HCRW) Approval** has been given for the above referenced study, on the basis described in the application form, protocol, supporting documentation and any clarifications received. You should not expect to receive anything further relating to this application.

How should I continue to work with participating NHS organisations in England and Wales?
You should now provide a copy of this letter to all participating NHS organisations in England and Wales, as well as any documentation that has been updated as a result of the assessment.

Following the arranging of capacity and capability, participating NHS organisations should **formally confirm** their capacity and capability to undertake the study. How this will be confirmed is detailed in the "*summary of assessment*" section towards the end of this letter.

You should provide, if you have not already done so, detailed instructions to each organisation as to how you will notify them that research activities may commence at site following their confirmation of capacity and capability (e.g. provision by you of a 'green light' email, formal notification following a site

initiation visit, activities may commence immediately following confirmation by participating organisation, etc.).

It is important that you involve both the research management function (e.g. R&D office) supporting each organisation and the local research team (where there is one) in setting up your study. Contact details of the research management function for each organisation can be accessed here.

How should I work with participating NHS/HSC organisations in Northern Ireland and Scotland?
HRA and HCRW Approval does not apply to NHS/HSC organisations within the devolved administrations of Northern Ireland and Scotland.

If you indicated in your IRAS form that you do have participating organisations in either of these devolved administrations, the final document set and the study wide governance report (including this letter) has been sent to the coordinating centre of each participating nation. You should work with the relevant national coordinating functions to ensure any nation specific checks are complete, and with each site so that they are able to give management permission for the study to begin.

Please see IRAS Help for information on working with NHS/HSC organisations in Northern Ireland and Scotland.

How should I work with participating non-NHS organisations?
HRA and HCRW Approval does not apply to non-NHS organisations. You should work with your non-NHS organisations to obtain local agreement in accordance with their procedures.

What are my notification responsibilities during the study?
The document "*After Ethical Review – guidance for sponsors and investigators*", issued with your REC favourable opinion, gives detailed guidance on reporting expectations for studies, including:

- Registration of research
- Notifying amendments
- Notifying the end of the study

The HRA website also provides guidance on these topics, and is updated in the light of changes in reporting expectations or procedures.

I am a participating NHS organisation in England or Wales. What should I do once I receive this letter?
You should work with the applicant and sponsor to complete any outstanding arrangements so you are able to confirm capacity and capability in line with the information provided in this letter.

The sponsor contact for this application is as follows:

Name: Ms Claire Skinner
Tel: 0113 343 7587
Email: governance-ethics@leeds.ac.uk

Who should I contact for further information?
Please do not hesitate to contact me for assistance with this application. My contact details are below.

IRAS project ID	229122

Your IRAS project ID is **229122**. Please quote this on all correspondence.

Yours sincerely

Aliki Sifostratoudaki
Assessor

Email: hra.approval@nhs.net

Copy to: *Ms Claire Skinner, University of Leeds, Sponsor Contact*
R&I Team N/A, Leeds Teaching Hospitals NHS Trust, R&D contacts

Figure C.1: Health research authority ethical approval.

C.2 Participant Information

(FORM TO BE ON NHS LETTERHEAD)

PARTICIPANT INFORMATION SHEET

IRAS ID: 229122
V1.2 19/02/2019

UNIVERSITY OF LEEDS

Cough aerosol sampling from people with cystic fibrosis

We would like to invite you to take part in a study which is being carried out by researchers in the Faculty of Engineering at the University of Leeds in collaboration with the Regional Adult Cystic Fibrosis Centre at the Leeds Teaching Hospitals NHS trust.

We are carrying out a study to determine the size of the droplets people with cystic fibrosis (CF) release into the air during breathing and coughing - we call this a bioaerosol. We also want to know whether these droplets contain *Pseudomonas aeruginosa* or *Mycobacterium abscessus* microorganisms. *P. aeruginosa and M. abscessus* are two bacteria that are particularly harmful to you and others with CF as they can cause chronic infections. We think they can present in small droplets produced when people infected with them are coughing/ breathing, which can travel through the air and potentially infect another person. The study's findings could help understand how these infections are spread, and so would help to improve infection control measures for people with CF. This study is research being carried out for the purposes of a PhD.

Before you decide whether to take part, it is important for you to understand why the research is being done and what it will involve.

- Please take the time to read the following information carefully. If you wish you can discuss it with friends and relatives.
- It is your choice to take part in this study. If you choose not to take part this will not affect the care you receive from your healthcare team.
- If anything is unclear, or you would like more information please ask Dr. Clifton or a research nurse.

Why is this study needed?

We know that airborne infection is a concern for those of you with cystic fibrosis and we want to help improve infection control measures by understanding more about the droplets you and others with CF produce.

- By knowing the size of the droplets you release into the air while coughing, we can determine if these droplets are likely stay in the air and transmit harmful bacteria.
- If we detect *P. aeruginosa* or *M. abscessus* in the droplets you produce either by coughing or breathing we will know that these bacteria can become airborne and could travel through the air in small droplets.
- If we can detect *P. aeruginosa* or *M. abscessus* using a simple face mask we will be able to start investigating its use for diagnosis of infection in people with CF.

Full study title: Study characterising the aerosolisation of microbial particles from people with cystic fibrosis and determining if *Pseudomonas aeruginosa* and *Mycobacterium abscessus* are present in patient cough/exhaled breath aerosols in the in patient hospital setting.

What does taking part involve?

You have been invited to take part because you are a patient of the Regional Adult Cystic Fibrosis Centre at the Leeds Teaching Hospitals NHS trust. Once you have read this document you will have time to decide if you want to take part in the study. If that's a yes a research nurse will assess to determine if you are eligible for the study by looking at your medical records. If you are eligible you will be asked to sign a consent form.

A nurse will check your medical records to determine if you are infected with *P. aeruginosa* or *M. abscessus* . If you are infected with chronic *P. aeruginosa* and not *M. abscessus,* you will be randomly allocated to group 1 or 2. This means you will give your samples over 1 or 2 days. If you are infected with chronic *M. absessus,* you will automatically be allocated into group 3. All sampling will be conducted by Jessica Proctor a PhD student who is co-ordinating this study.

Sampling in this study would involve you:

- Being asked to cough into a mouthpiece connected to a device called a cough aerosol sampling system (CASS) for 5 minutes.
    - If you are in group 1 you will give four samples. This will be two in a morning session and two in the afternoon on the same day.
    - If you are in group 2 you will give four samples. This will be two in a session at the beginning of your hospital stay and two at the end.
    - If you are in group 3 you will give two samples. This will be in one session.
- Being asked to wear a face mask for up to 1 hour.
    - If you are in group 1 this will be once in the morning and once in the afternoon on the same day
    - If you are in group 2 this will be once at the start of your hospital stay and once at the end of your hospital stay.
    - If you are in group 3 this will be once during one session.
- Being asked to produce a sputum sample at the time of sampling.
- Have air samples taken from your room and data loggers recording temperature, humidity and C02 levels.
- Agreeing to have your cough, mask and sputum samples taken during the study to be tested for *P. aeruginosa* and *M. abscessus*.
- Consenting to your GP being informed.

What are the benefits of the study?

There is no immediate benefit to you and you may not benefit personally from joining the study. However, as this study could result in improved and more focused infection control and potentially improved diagnostic measures, it is hoped it will result in better treatment for CF in the future. Reduction in cross-infection and increase in prompt diagnosis would have a specific benefit to all people with CF in terms of enhanced infection control.

Are there any risks for me in joining the study?

There is a small risk of discomfort during coughing into the CASS sampler. However, we will not make you continue to cough during the 5 minute sampling time if it is uncomfortable. You are also

allowed to breathe into the mouthpiece during this 5 minutes. If coughing becomes too uncomfortable we will halt sampling and continue at a later time only if you wish to do so.

Wearing the face mask may be warm and slightly uncomfortable for some people. You will be given the opportunity to try the face mask prior to starting the study and if you do not wish to go ahead with this type of sampling then this can be easily accommodated. If during the sampling you find the mask uncomfortable, the mask can be lifted for short periods or sampling halted as you wish.

Many of you with CF are concerned about cross-infection. During this study we believe there is no more risk to you than you would experience during a normal day at the hospital. All items being used to sample with are either disposable after each use or they can be autoclaved. This means they are sterilised and no bacteria survives.

Further information

What if something does go wrong?: The risk of participants suffering harm as a result of taking part is minimal and the University of Leeds/NHS has insurance in place to deal with any negligent harm caused by participation

What will happen if I don't want to continue with the study? You are free to withdraw from the study at any time, without giving a reason. This decision will have no influence on the care you receive from your healthcare team. Once withdrawn from the study we will ask for your consent on whether we can use the data we collect up to the point you withdrew from the study.

How will my information be kept confidential? Only the clinical members of the research team will have access to your medical records. You will be given a study ID number and all data stored about you will not include any personal identifying details. Researchers working with your samples and data will, therefore, never know your identity.

What will happen to the samples I give? These will stored and analysed at the Infection Control Laboratory, Leeds General Infirmary, the University of Leeds or the University of Leicester. All samples will be destroyed at the end of the study.

Who is organising and funding this study? This study is part of a PhD project which is funded by the Engineering and Physical Sciences Research Council (EPSRC). The study has been organised by the student with help from academic supervisors.

How will the results from the study be shared? As a publicly funded research project, the results will be made freely available. The study findings will be published in a PhD thesis and in papers that will be published in academic journals and conferences. The data in these papers will be in a fully anonymised form that will not identify you. Results will also be available to you via a newsletter distributed at the hospital and we may also share the study results through social media, newspapers and TV/radio outlets if the findings are felt to be of wide public interest. Again your data will be completely anonymous.

Contact information

If you have any questions, please talk to Dr Ian Clifton or contact Jessica Proctor the student who will be co-ordinating this study via email on mm11jp@leeds.ac.uk

Full study title: Study characterising the aerosolisation of microbial particles from people with cystic fibrosis and determining if *Pseudomonas aeruginosa* and *Mycobacterium abscessus* are present in patient cough/exhaled breath aerosols in the in patient hospital setting.

If you have any complaints about this study please contact the PALS team via email patientexperience.leedsth@nhs.net or Tel: (0113) 2066261 (09:00-16:30 Mon-Fri) (0113) 2067168 (out of normal working hours).

GDPR compliance

The University of Leeds is the sponsor for this study based in United Kingdom. We will be using information from your medical records in order to undertake this study and will act as the data controller for this study. This means that we are responsible for looking after your information and using it properly. The University of Leeds will keep identifiable information about you for 10 years after the study has finished. This information will be held by the Leeds Teaching Hospitals NHS trust.

Your rights to access, change or move your information are limited, as we need to manage your information in specific ways in order for the research to be reliable and accurate. If you withdraw from the study, we will keep the information about you that we have already obtained. To safeguard your rights, we will use the minimum personally-identifiable information possible.

You can find out more about how we use your information by contacting the University of Leeds data controller on DOP@leeds.ac.uk.

Leeds Teaching Hospitals Trust will collect information from your medical records for this research study in accordance with our instructions. Leeds Teaching Hospitals Trust will keep your name, NHS number and contact details confidential and will not pass this information to the University of Leeds. Leeds Teaching Hospitals Trust will use this information as needed, to contact you about the research study, and make sure that relevant information about the study is recorded for your care, and to oversee the quality of the study. Certain individuals from the University of Leeds and regulatory organisations may look at your medical and research records to check the accuracy of the research study. The University of Leeds will only receive information without any identifying information. The people who analyse the information will not be able to identify you and will not be able to find out your name, NHS number or contact details. Leeds Teaching Hospitals Trust will keep identifiable information about you from this study for 10 years after the study has finished.

When you agree to take part in a research study, the information about your health and care may be provided to researchers running other research studies in this organisation and in other organisations. These organisations may be universities, NHS organisations or companies involved in health and care research in this country or abroad. Your information will only be used by organisations and researchers to conduct research in accordance with the UK Policy Framework for Health and Social Care Research. This information will not identify you and will not be combined with other information in a way that could identify you. The information will only be used for the purpose of health and care research, and cannot be used to contact you or to affect your care. It will not be used to make decisions about future services available to you, such as insurance.

Full study title: Study characterising the aerosolisation of microbial particles from people with cystic fibrosis and determining if *Pseudomonas aeruginosa* and *Mycobacterium abscessus* are present in patient cough/exhaled breath aerosols in the in patient hospital setting.

Figure C.2: Participant Information Sheet.

C.3 Source data

Source data for clincical team

Study ID number: _ _
Group number: _ _

Date of admission: _ _ / _ _ / _ _ (in form of d d / m m / y y)

Home IV's	Y/N	If yes, time and date of appointments	Start	_ _ / _ _ /_ _ _ _ : _ _
			End	_ _ / _ _/ _ _ _ _ : _ _

Participant willing to continue to session 2: Y / N

Brief description of participants relative health:

Presence of chronic Pseudomonas Aeruginosa: Y / N

Presence of chronic Myscobacterium Abscessus: Y / N

If yes have any other NTM been present in participants sputum? If yes which and when:

Positive for any other pathogens in last 6 months? Y/N

If yes which?:

Antibiotic treatment:

IV antibiotics, (Y/N) plus which:

Nebulised antibiotics, (Y/N) plus which:

Long term oral antibiotics, (Y/N) plus which:

Mucolytic treatment:

Hypertonic saline	Y / N
DNAase	Y / N
Modulated treatment	Y/N

Source data for clincical team

	Sampling session 1	Sampling session 2
FEV 1% (with date)		
Antibiotic treatment taken today until start of session		
Mucolytic treatment taken today until start of session (incl modulated treatment)		
Physiotherapy treatment today until start of session		

Extra notes (Sputum taken?):

Sign off when completed: Signature: Date:
Print name:

PI signature: Date:
Print name:

Figure C.3: Source data for the clinical team.

Souce data for cheif investigat

Study ID number (to be filled out by clinical team only): _ _
Group number: _ _

Leave blank or write n/a if there was no second room data sample
Room dimensions:

Room layout and number:

Ventilation:

	Sampling session 1	Sampling session 2
Start and end time of loggers		
Total time room air sampler on		

Date and time of sampling session 1: _ _ / _ _ / _ _ (in form of d d / m m / y y) _ _: _ _ (in form of h h:m m 24h clock)
Date and time of sampling session 2: _ _ / _ _ / _ _ (in form of d d / m m / y y) _ _: _ _ (in form of h h:m m 24h clock)
Leave blank or write n/a if participant did not take part in second sampling session

	Sampling session 1	Sampling session 2
Sampling sequence		
Cough count sample 1 (Impinger)		
Cough count sample 2 (Andersen)		
Total time wearing mask (minutes)		

Extra notes (e.g on sputum taken):

Sign off when complete: PI signature: Date:
Print name:

Page 1

Figure C.4: Source data for the principal investigator.

C.4 CASS CAD drawings

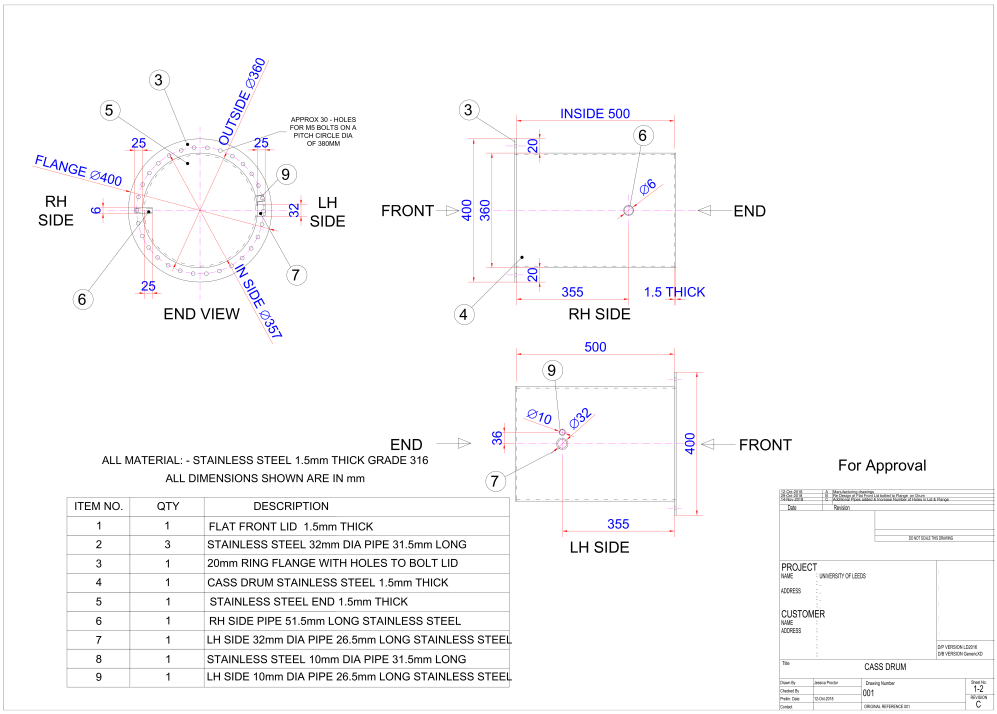

ITEM NO.	QTY	DESCRIPTION
1	1	FLAT FRONT LID 1.5mm THICK
2	3	STAINLESS STEEL 32mm DIA PIPE 31.5mm LONG
3	1	20mm RING FLANGE WITH HOLES TO BOLT LID
4	1	CASS DRUM STAINLESS STEEL 1.5mm THICK
5	1	STAINLESS STEEL END 1.5mm THICK
6	1	RH SIDE PIPE 51.5mm LONG STAINLESS STEEL
7	1	LH SIDE 32mm DIA PIPE 26.5mm LONG STAINLESS STEEL
8	1	STAINLESS STEEL 10mm DIA PIPE 31.5mm LONG
9	1	LH SIDE 10mm DIA PIPE 26.5mm LONG STAINLESS STEEL

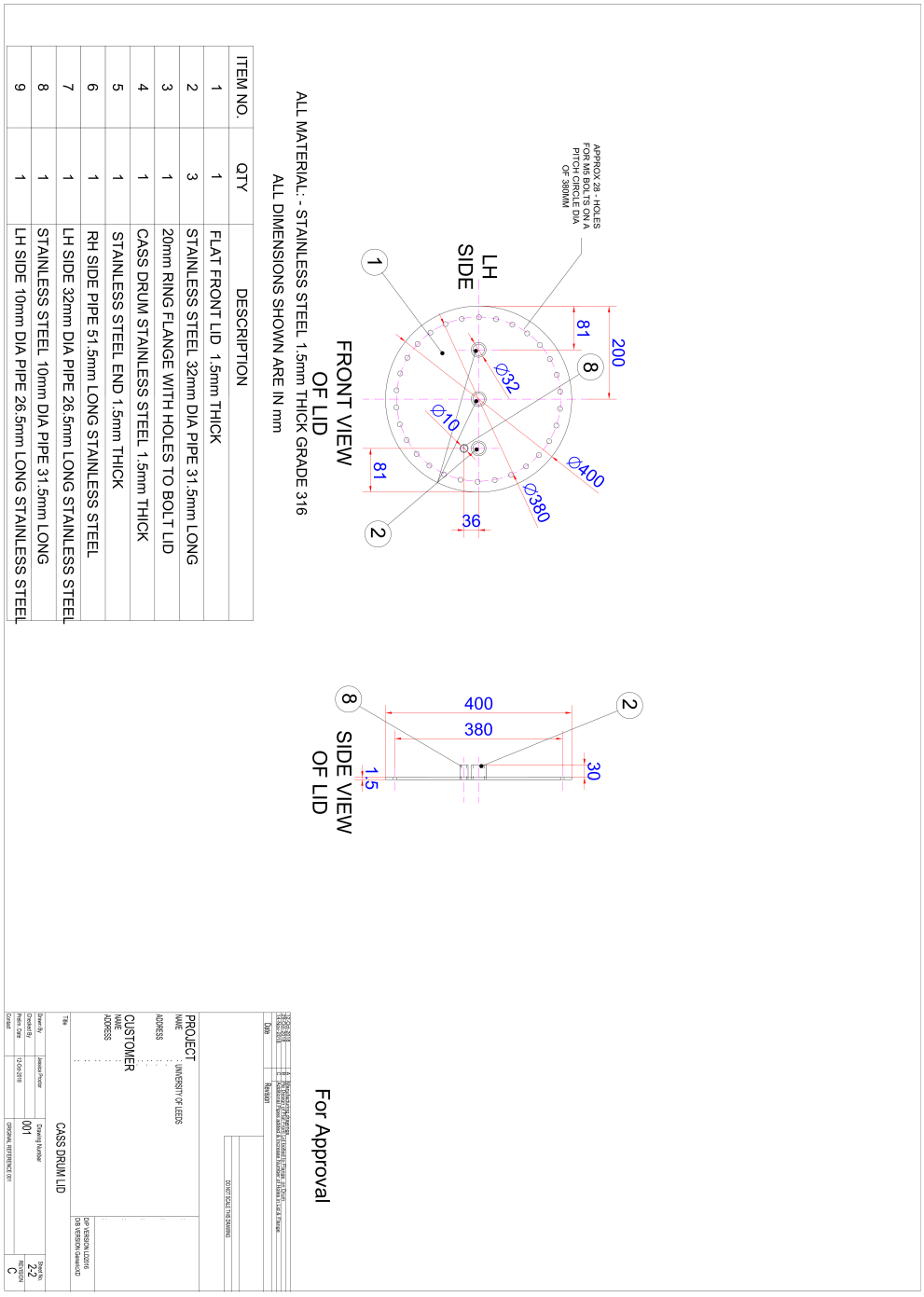

ITEM NO.	QTY	DESCRIPTION
1	1	FLAT FRONT LID 1.5mm THICK
2	3	STAINLESS STEEL 32mm DIA PIPE 31.5mm LONG
3	1	20mm RING FLANGE WITH HOLES TO BOLT LID
4	1	CASS DRUM STAINLESS STEEL 1.5mm THICK
5	1	STAINLESS STEEL END 1.5mm THICK
6	1	RH SIDE PIPE 51.5mm LONG STAINLESS STEEL
7	1	LH SIDE 32mm DIA PIPE 26.5mm LONG STAINLESS STEEL
8	1	STAINLESS STEEL 10mm DIA PIPE 31.5mm LONG
9	1	LH SIDE 10mm DIA PIPE 26.5mm LONG STAINLESS STEEL

Figure C.5: CAD drawing of the cough aerosol sampling system.

References

Citing pages are listed after each entry.

Aaron, S. D., Vandemheen, K. L., Ramotar, K., et al. 2010. Infection with transmissible strains of pseudomonas aeruginosa and clinical outcomes in adults with cystic fibrosis. *Jama*. **304**(19), pp. 2145–2153. Cited on p. 36.

Abraham, J., Plourde, B., and Vallez, L. 2017. Comprehensive review and study of the buoyant air flow within positive-pressure hospital operating rooms. *Numerical Heat Transfer, Part A: Applications*. **72**(1), pp. 1–20. Cited on p. 34.

Ai, Z., Hashimoto, K., and Melikov, A. K. 2019. Airborne transmission between room occupants during short-term events: Measurement and evaluation. *Indoor air*. **29**(4), pp. 563–576. Cited on p. 17.

Aitken, M. L., Limaye, A., Pottinger, P., et al. 2012. Respiratory outbreak of mycobacterium abscessus subspecies massiliense in a lung transplant and cystic fibrosis center. *American journal of respiratory and critical care medicine*. **185** (2), pp. 231–232. Cited on pp. 35 and 36.

Al-Aloul, M., Crawley, J., Winstanley, C., et al. 2004. Increased morbidity associated with chronic infection by an epidemic pseudomonas aeruginosa strain in cf patients. *Thorax*. **59**(4), pp. 334–336. Cited on p. 6.

Andersen, A. A. 1958. New sampler for the collection, sizing, and enumeration of viable airborne particles. *Journal of Bacteriology*. **76**(5), pp. 471. Cited on pp. xxviii, 26, 76, and 131.

Anderson, D. H. 1938. Cystic fibrosis of the pancreas and its relation to celiac disease. *Am J Dis Child*. **56**(2), pp. 344–399. Cited on p. 3.

Armstrong, D. S., Nixon, G. M., Carzino, R., et al. 2002. Detection of a widespread clone of pseudomonas aeruginosa in a pediatric cystic fibrosis clinic. *American*

journal of respiratory and critical care medicine. **166**(7), pp. 983–987. Cited on pp. 35 and 36.

Asadi, S., Wexler, A. S., Cappa, C. D., et al. 2019. Aerosol emission and superemission during human speech increase with voice loudness. *Scientific reports*. **9** (1), pp. 1–10. Cited on p. 49.

Ashish, A., Shaw, M., Winstanley, C., Ledson, M. J., and Walshaw, M. J. 2012. Increasing resistance of the liverpool epidemic strain (les) of pseudomonas aeruginosa (psa) to antibiotics in cystic fibrosis (cf)—a cause for concern? *Journal of Cystic Fibrosis*. **11**(3), pp. 173–179. Cited on p. 6.

Asif, A., Zeeshan, M., Hashmi, I., Zahid, U., and Bhatti, M. F. 2018. Microbial quality assessment of indoor air in a large hospital building during winter and spring seasons. *Building and environment*. **135**, pp. 68–73. Cited on p. 197.

Atkinson, M. P. and Wein, L. M. 2008. Quantifying the routes of transmission for pandemic influenza. *Bulletin of mathematical biology*. **70**(3), pp. 820–867. Cited on pp. 15 and 33.

Atwood, J. L. 2017. *Comprehensive supramolecular chemistry II*. Elsevier. Cited on p. 44.

Aulicino, A., Dinan, A. M., Miranda-CasoLuengo, A. A., et al. 2015. High-throughput transcriptomics reveals common and strain-specific responses of human macrophages to infection with mycobacterium abscessus smooth and rough variants. *BMC genomics*. **16**(1), pp. 1046. Cited on p. 8.

Bange, F.-C., Brown, B. A., Smaczny, C., Wallace, R. J., and Böttger, E. C. 2001. Lack of transmission of mycobacterium abscessus among patients with cystic fibrosis attending a single clinic. *Clinical infectious diseases*. **32**(11), pp. 1648–1650. Cited on pp. 7 and 36.

Basser, P., McMahon, T., and Griffith, P. 1989. The mechanism of mucus clearance in cough. Cited on p. 41.

Batterman, S. 2017. Review and extension of co2-based methods to determine ventilation rates with application to school classrooms. *International journal of environmental research and public health*. **14**(2), pp. 145. Cited on p. 224.

Beggs, C. B., Noakes, C. J., Shepherd, S. J., et al. 2006. The influence of nurse cohorting on hand hygiene effectiveness. *American journal of infection control*. **34**(10), pp. 621–626. Cited on p. 11.

Beggs, C. B., Kerr, K. G., Noakes, C. J., Hathway, E. A., and Sleigh, P. A. 2008. The ventilation of multiple-bed hospital wards: review and analysis. *American journal of infection control*. **36**(4), pp. 250–259. Cited on pp. 28 and 34.

Bell, S., Saunders, M., Elborn, J., and Shale, D. 1996. Resting energy expenditure and oxygen cost of breathing in patients with cystic fibrosis. *Thorax*. **51**(2), pp. 126–131. Cited on p. 226.

Bernards, A. T., Frénay, H. M., Lim, B. T., et al. 1998. Methicillin-resistant staphylococcus aureus and acinetobacter baumannii: an unexpected difference in epidemiologic behavior. *American journal of infection control*. **26**(6), pp. 544–551. Cited on p. 27.

Bischoff, W. E., Swett, K., Leng, I., and Peters, T. R. 2013. Exposure to influenza virus aerosols during routine patient care. *The Journal of infectious diseases*. **207** (7), pp. 1037–1046. Cited on p. 213.

Bjørn, E. and Nielsen, P. V. 2002. Dispersal of exhaled air and personal exposure in displacement ventilated rooms. *Indoor air*. **12**(3), pp. 147–164. Cited on pp. xv and 17.

Blachere, F. M., Lindsley, W. G., Pearce, T. A., et al. 2009. Measurement of airborne influenza virus in a hospital emergency department. *Clinical Infectious Diseases*. **48**(4), pp. 438–440. Cited on p. 28.

Bodey, G. P., Bolivar, R., Fainstein, V., and Jadeja, L. 1983. Infections caused by pseudomonas aeruginosa. *Review of Infectious Diseases*. **5**(2), pp. 279–313. Cited on p. 4.

Bolister, N., Johnson, H., and Wathes, C. 1992. The ability of airborne klebsiella pneumoniae to colonize mouse lungs. *Epidemiology and infection*. **109**(1), pp. 121. Cited on p. 56.

Booth, T. F., Kournikakis, B., Bastien, N., et al. 2005. Detection of airborne severe acute respiratory syndrome (sars) coronavirus and environmental contamination in sars outbreak units. *The Journal of infectious diseases*. **191**(9), pp. 1472–1477. Cited on pp. 24 and 28.

Bourouiba, L. 2020. Turbulent gas clouds and respiratory pathogen emissions: potential implications for reducing transmission of covid-19. *Jama*. **323**(18), pp. 1837–1838. Cited on p. 51.

Boyes, W. 2009. *Instrumentation reference book*. Butterworth-Heinemann. Cited on p. 42.

Brenière, S. F., Aznar, C., and Hontebeyrie, M. 2010. Vector transmission. In: *American Trypanosomiasis*. Elsevier, pp. 525–538. Cited on p. 11.

Brohus, H., Balling, K., and Jeppesen, D. 2006. Influence of movements on contaminant transport in an operating room. *Indoor air*. **16**(5), pp. 356–372. Cited on p. 34.

Brouwer, A. F., Eisenberg, M. C., Remais, J. V., et al. 2017. Modeling biphasic environmental decay of pathogens and implications for risk analysis. *Environmental science & technology*. **51**(4), pp. 2186–2196. Cited on pp. 116 and 254.

Brown, S. M. 2010. Multiple strains of non-tuberculous mycobacteria in a patient with cystic fibrosis. *Journal of the Royal Society of Medicine*. **103**(Supplement 1), pp. S34–S43. Cited on p. 8.

Brown, V. and Lowbury, E. 1965. Use of an improved cetrimide agar medium and other culture methods for pseudomonas aeruginosa. *Journal of Clinical Pathology*. **18**(6), pp. 752–756. Cited on p. 162.

Bruck, E. 1962. Water in expired air: physiology and measurement. *The Journal of pediatrics*. **60**(6), pp. 869–881. Cited on p. 215.

Bryant, J. M., Grogono, D. M., Greaves, D., et al. 2013. Whole-genome sequencing to identify transmission of mycobacterium abscessus between patients with cystic fibrosis: a retrospective cohort study. *The Lancet*. **381**(9877), pp. 1551–1560. Cited on pp. 2, 7, and 37.

Bueno de Mesquita, P. J., Noakes, C. J., and Milton, D. K. 2020. Quantitative aerobiologic analysis of an influenza human challenge-transmission trial. *Indoor air*. **30**(6), pp. 1189–1198. Cited on p. 33.

Buonanno, G., Stabile, L., and Morawska, L. 2020. Estimation of airborne viral emission: quanta emission rate of sars-cov-2 for infection risk assessment. *Environment International*. pp. 105794. Cited on p. 33.

Byrd, T. F. and Lyons, C. R. 1999. Preliminary characterization of a mycobacterium abscessus mutant in human and murine models of infection. *Infection and immunity*. **67**(9), pp. 4700–4707. Cited on pp. 8 and 9.

Capurro, M. and Barberis, F. 2014. Evaluating the mechanical properties of biomaterials. In: *Biomaterials for Bone Regeneration*. Elsevier, pp. 270–323. Cited on p. 43.

Carter, K. C. 1977. The germ theory, beriberi, and the deficiency theory of disease. *Medical History*. **21**(2), pp. 119–136. Cited on p. 10.

Carvalho, F. K., Antuniassi, U. R., Chechetto, R. G., et al. 2017. Viscosity, surface tension and droplet size of sprays of different formulations of insecticides and fungicides. *Crop Protection*. **101**, pp. 19–23. Cited on p. 44.

Caverly, L. J., Caceres, S. M., Fratelli, C., et al. 2015. Mycobacterium abscessus morphotype comparison in a murine model. *PloS one*. **10**(2), pp. e0117657. Cited on p. 8.

CDC. 1977. *Tuberculosis, TB.*. Number 33. Department of Health, Education, and Welfare, Public Health Service, Center for Disease Control. Cited on p. 24.

Chadwick, P. and McCann, R. 1994. Transmission of a small round structured virus by vomiting during a hospital outbreak of gastroenteritis. *Journal of Hospital Infection*. **26**(4), pp. 251–259. Cited on p. 28.

Chalermskulrat, W., Sood, N., Neuringer, I. P., et al. 2006. Non-tuberculous mycobacteria in end stage cystic fibrosis: implications for lung transplantation. *Thorax*. **61**(6), pp. 507–513. Cited on pp. 7, 9, and 10.

Chambers, D., Scott, F., Bangur, R., et al. 2005. Factors associated with infection by pseudomonas aeruginosa in adult cystic fibrosis. *European Respiratory Journal*. **26**(4), pp. 651–656. Cited on p. 6.

Chamseddine, A., Alameddine, I., Hatzopoulou, M., and El-Fadel, M. 2019. Seasonal variation of air quality in hospitals with indoor–outdoor correlations. *Building and Environment*. **148**, pp. 689–700. Cited on p. 194.

Changyong, F., Hongyue, W., Naiji, L., et al. 2014. Log-transformation and its implications for data analysis. *Shanghai archives of psychiatry*. **26**(2), pp. 105. Cited on p. 164.

Chao, C. Y. H., Wan, M. P., Morawska, L., et al. 2009. Characterization of expiration air jets and droplet size distributions immediately at the mouth opening. *Journal of Aerosol Science*. **40**(2), pp. 122–133. Cited on pp. 46, 47, 48, 49, 50, and 218.

Charan, J. and Biswas, T. 2013. How to calculate sample size for different study designs in medical research? *Indian journal of psychological medicine*. **35**(2), pp. 121. Cited on p. 151.

Charman, S., McClenaghan, E., Cosgriff, R., Lee, A., and Carr, S. 2019. *UK Cystic Fibrosis Registry 2018 Annual Data Report*. Technical report, Cystic Fibrosis Trust. Cited on pp. 3, 5, 8, 35, and 236.

Chen, P.-S. and Li, C.-S. 2008. Concentration profiles of airborne mycobacterium tuberculosis in a hospital. *Aerosol Science and Technology*. **42**(3), pp. 194–200. Cited on p. 27.

Chen, W., Zhang, N., Wei, J., Yen, H.-L., and Li, Y. 2020. Short-range airborne route dominates exposure of respiratory infection during close contact. *Building and Environment*. pp. 106859. Cited on pp. 15, 16, and 55.

Cheng, K., Smyth, R. L., Govan, J. R., et al. 1996. Spread of β-lactam-resistant pseudomonas aeruginosa in a cystic fibrosis clinic. *The Lancet*. **348**(9028), pp. 639–642. Cited on pp. 6 and 35.

Cheng, Y.-H., Wang, C.-H., You, S.-H., et al. 2016. Assessing coughing-induced influenza droplet transmission and implications for infection risk control. *Epidemiology & Infection*. **144**(2), pp. 333–345. Cited on p. 33.

Cho, J. 2019. Investigation on the contaminant distribution with improved ventilation system in hospital isolation rooms: Effect of supply and exhaust air diffuser configurations. *Applied Thermal Engineering*. **148**, pp. 208–218. Cited on pp. 16 and 34.

CIBSE. 2015. *Environmental design: CIBSE guide A*. Chartered Institution of Building Services Engineers. Cited on pp. 194 and 225.

Clarke, R., Katstra, J., Man, J., et al. 2005. Pulmonary delivery of anti-contagion aerosol to diminish exhaled bioaerosols and airborne infectious disease. *American Journal of Infection Control*. **33**(5), pp. e85. Cited on p. 45.

Clifton, I., Fletcher, L., Beggs, C., et al. 2010. An aerobiological model of aerosol survival of different strains of pseudomonas aeruginosa isolated from people with cystic fibrosis. *Journal of Cystic Fibrosis*. **9**(1), pp. 64–68. Cited on pp. 37, 115, 140, and 254.

Clifton, I. J. 2009. *Environmental survival of Pseudomonas aeruginosa strains in people with cystic fibrosis*. PhD thesis, University of Leeds. Cited on pp. 3, 61, 151, and 226.

Clifton, I. J., Fletcher, L. A., Beggs, C. B., Denton, M., and Peckham, D. G. 2008. A laminar flow model of aerosol survival of epidemic and non-epidemic strains of pseudomonas aeruginosa isolated from people with cystic fibrosis. *BMC microbiology*. **8**(1), pp. 105. Cited on pp. xvi, 17, 37, 59, 72, 76, 82, 83, 85, 115, 121, 140, 151, 226, and 259.

Consortium, C. F. G. A. et al. 2005. Cystic fibrosis mutation database. *See http://www. genet. sickkids. on. ca/cftr*. Cited on p. 3.

Constantini, D., Russo, M., Cariani, L., et al. 2005. Nontuberculous mycobacteria in sputum of cystic fibrosis patients. *J Cyst Fibros.* **4**(Suppl 1), pp. S39. Cited on p. 7.

Cortes, M. A., Nessar, R., and Singh, A. K. 2010. Laboratory maintenance of mycobacterium abscessus. *Current Protocols in Microbiology.* **18**(1), pp. 10D–1. Cited on pp. xv, 61, 65, 67, 91, and 122.

Cowling, P., Siddiqui, R., Aramouni, M., et al. 2015. *UK Standards for Microbiology Investigations ID 17: identification of Pseudomonas species and other non glucose fermenters.* Technical report, Public Health England, UK Standards for Microbiology Investigations. Cited on pp. 162 and 164.

Cox, C. S. *Bioaerosols handbook*, chapter Physical aspects of bioaerosol particles. In Cox and Wathes (1995)., 1995. Cited on p. 12.

Cox, C. S. and Wathes, C. M. 1995. *Bioaerosols handbook*. crc press. Cited on pp. 12, 24, 25, 56, and 305.

Creamer, E., Shore, A. C., Deasy, E. C., et al. 2014. Air and surface contamination patterns of meticillin-resistant staphylococcus aureus on eight acute hospital wards. *Journal of Hospital Infection.* **86**(3), pp. 201–208. Cited on p. 27.

Crone, S., Vives-Flórez, M., Kvich, L., et al. 2020. The environmental occurrence of pseudomonas aeruginosa. *Apmis.* **128**(3), pp. 220–231. Cited on p. 5.

Cullen, A. R., Cannon, C. L., Mark, E. J., and Colin, A. A. 2000. Mycobacterium abscessus infection in cystic fibrosis: colonization or infection? *American journal of respiratory and critical care medicine.* **161**(2), pp. 641–645. Cited on p. 9.

Dalgaard, P., Ross, T., Kamperman, L., Neumeyer, K., and McMeekin, T. A. 1994. Estimation of bacterial growth rates from turbidimetric and viable count data. *International journal of food microbiology.* **23**(3-4), pp. 391–404. Cited on p. 69.

Davis, P. B. 2006. Cystic fibrosis since 1938. *American journal of respiratory and critical care medicine.* **173**(5), pp. 475–482. Cited on p. 3.

Dayal, P., Shaik, M. S., and Singh, M. 2004. Evaluation of different parameters that affect droplet-size distribution from nasal sprays using the malvern spraytec®. *Journal of pharmaceutical sciences.* **93**(7), pp. 1725–1742. Cited on p. 44.

de Oliveira, P. M., Mesquita, L. C., Gkantonas, S., Giusti, A., and Mastorakos, E. 2021. Evolution of spray and aerosol from respiratory releases: theoretical estimates for insight on viral transmission. *Proceedings of the Royal Society A*. **477**(2245), pp. 20200584. Cited on pp. 55 and 217.

Deligianni, E., Pattison, S., Berrar, D., et al. 2010. Pseudomonas aeruginosa cystic fibrosis isolates of similar rapd genotype exhibit diversity in biofilm forming ability in vitro. *BMC microbiology*. **10**(1), pp. 38. Cited on pp. xv and 4.

Dinter, P. and Müller, W. 1984. Tenacity of bacteria in the airborne state. iii. model studies on the epidemiology of pasteurella multocida influenced by a tropical climate. *Zentralblatt fur Bakteriologie, Mikrobiologie und Hygiene. 1. Abt. Originale B, Hygiene*. **179**(2), pp. 139–150. Cited on p. 56.

Doggett, R. G., Harrison, G. M., and Wallis, E. S. 1964. Comparison of some properties of pseudomonas aeruginosa isolated from infections in persons with and without cystic fibrosis. *Journal of bacteriology*. **87**(2), pp. 427–431. Cited on p. 5.

Dravid, V., Songsermpong, S., Xue, Z., Corvalan, C. M., and Sojka, P. E. 2006. Two-dimensional modeling of the effects of insoluble surfactant on the breakup of a liquid filament. *Chemical engineering science*. **61**(11), pp. 3577–3585. Cited on p. 44.

Duan, M., Liu, L., Da, G., et al. 2020. Measuring the administered dose of particles on the facial mucosa of a realistic human model. *Indoor air*. **30**(1), pp. 108–116. Cited on p. 29.

Duguid, J. 1946. The size and the duration of air-carriage of respiratory droplets and droplet-nuclei. *Epidemiology & Infection*. **44**(6), pp. 471–479. Cited on pp. 45, 46, 47, 48, 55, and 96.

Eames, I., Tang, J., Li, Y., and Wilson, P. Airborne transmission of disease in hospitals, 2009. Cited on p. 29.

Ebnesajjad, S. 2010. *Handbook of adhesives and surface preparation: technology, applications and manufacturing*. William Andrew. Cited on p. 44.

Edwards, D. A., Man, J. C., Brand, P., et al. 2004. Inhaling to mitigate exhaled bioaerosols. *Proceedings of the National Academy of Sciences*. **101**(50), pp. 17383–17388. Cited on pp. 45, 49, and 174.

Eggers, J. and Villermaux, E. 2008. Physics of liquid jets. *Reports on progress in physics*. **71**(3), pp. 036601. Cited on p. 43.

Emerson, J., Rosenfeld, M., McNamara, S., Ramsey, B., and Gibson, R. L. 2002. Pseudomonas aeruginosa and other predictors of mortality and morbidity in young children with cystic fibrosis. *Pediatric pulmonology.* **34**(2), pp. 91–100. Cited on p. 2.

Endo, A. et al. 2020. Estimating the overdispersion in covid-19 transmission using outbreak sizes outside china. *Wellcome Open Research.* **5**. Cited on pp. 49, 208, and 247.

Ensor, E., Humphreys, H., Peckham, D., Webster, C., and Knox, A. 1996. Is burkholderia (pseudomonas) cepacia disseminated from cystic fibrosis patients during physiotherapy? *Journal of Hospital Infection.* **32**(1), pp. 9–15. Cited on p. 35.

Escombe, A. R., Moore, D. A., Gilman, R. H., et al. 2008. The infectiousness of tuberculosis patients coinfected with hiv. *PLoS Med.* **5**(9), pp. e188. Cited on p. 49.

Esther, C. R., Henry, M. M., Molina, P. L., and Leigh, M. W. 2005. Nontuberculous mycobacterial infection in young children with cystic fibrosis. *Pediatric pulmonology.* **40**(1), pp. 39–44. Cited on p. 7.

Esther, C. R., Esserman, D. A., Gilligan, P., Kerr, A., and Noone, P. G. 2010. Chronic mycobacterium abscessus infection and lung function decline in cystic fibrosis. *Journal of Cystic Fibrosis.* **9**(2), pp. 117–123. Cited on pp. 2 and 8.

Fabian, P., McDevitt, J. J., DeHaan, W. H., et al. 2008. Influenza virus in human exhaled breath: an observational study. *PloS one.* **3**(7), pp. e2691. Cited on pp. 51 and 52.

Farrington, M., Ling, J., Ling, T., and French, G. 1990. Outbreaks of infection with methicillin-resistant staphylococcus aureus on neonatal and burns units of a new hospital. *Epidemiology & Infection.* **105**(2), pp. 215–228. Cited on p. 27.

Faulkner, W. B., Memarzadeh, F., Riskowski, G., Kalbasi, A., and Ching-Zu Chang, A. 2015. Effects of air exchange rate, particle size and injection place on particle concentrations within a reduced-scale room. *Building and Environment.* **92**, pp. 246–255. Cited on p. 30.

Fauroux, B., Delaisi, B., Clement, A., et al. 1997. Mycobacterial lung disease in cystic fibrosis: a prospective study. *The Pediatric infectious disease journal.* **16** (4), pp. 354–358. Cited on p. 7.

Fedorenko, A., Grinberg, M., Orevi, T., and Kashtan, N. 2020. Virus survival in evaporated saliva microdroplets deposited on inanimate surfaces. *bioRxiv*. Cited on p. 57.

Fennelly, K. P., Martyny, J. W., Fulton, K. E., et al. 2004. Cough-generated aerosols of mycobacterium tuberculosis: a new method to study infectiousness. *American journal of respiratory and critical care medicine*. **169**(5), pp. 604–609. Cited on pp. 49, 52, 53, 144, 155, and 213.

Fennelly, K. P., Jones-López, E. C., Ayakaka, I., et al. 2012. Variability of infectious aerosols produced during coughing by patients with pulmonary tuberculosis. *American journal of respiratory and critical care medicine*. **186**(5), pp. 450–457. Cited on pp. 49, 52, and 213.

Fernandez, M. O., Thomas, R. J., Garton, N. J., et al. 2019. Assessing the airborne survival of bacteria in populations of aerosol droplets with a novel technology. *Journal of the Royal Society Interface*. **16**(150), pp. 20180779. Cited on p. 56.

Ferrus, L., Guenard, H., Vardon, G., and Varene, P. 1980. Respiratory water loss. *Respiration physiology*. **39**(3), pp. 367–381. Cited on p. 215.

Fiegel, J., Clarke, R., and Edwards, D. A. 2006. Airborne infectious disease and the suppression of pulmonary bioaerosols. *Drug discovery today*. **11**(1-2), pp. 51–57. Cited on p. 41.

Fletcher, L. A., Chen, Y., Whitaker, P., et al. 2016. Survival of mycobacterium abscessus isolated from people with cystic fibrosis in artificially generated aerosols. *European Respiratory Journal*. **48**(6), pp. 1789–1791. Cited on pp. 17, 37, and 151.

Floto, R. A., Olivier, K. N., Saiman, L., et al. 2016. Us cystic fibrosis foundation and european cystic fibrosis society consensus recommendations for the management of non-tuberculous mycobacteria in individuals with cystic fibrosis. *Thorax*. **71** (Suppl 1), pp. i1–i22. Cited on p. 38.

Fothergill, J. L., Walshaw, M. J., and Winstanley, C. 2012. Transmissible strains of pseudomonas aeruginosa in cystic fibrosis lung infections. *European Respiratory Journal*. **40**(1), pp. 227–238. Cited on p. 35.

Friedlander, S. and Serre, D. 2002. *Handbook of mathematical fluid dynamics*. Elsevier. Cited on p. 42.

Galvani, A. P. and May, R. M. 2005. Dimensions of superspreading. *Nature*. **438** (7066), pp. 293–295. Cited on p. 50.

Gammaitoni, L. and Nucci, M. C. 1997. Using a mathematical model to evaluate the efficacy of tb control measures. *Emerging infectious diseases.* **3**(3), pp. 335. Cited on p. 32.

Gena, A. W., Voelker, C., and Settles, G. S. 2020. Qualitative and quantitative schlieren optical measurement of the human thermal plume. *Indoor air.* **30**(4), pp. 757–766. Cited on p. 218.

Gerone, P. J., Couch, R. B., Keefer, G. V., et al. 1966. Assessment of experimental and natural viral aerosols. *Bacteriological reviews.* **30**(3), pp. 576. Cited on pp. 51 and 52.

Ghasemi, A. and Zahediasl, S. 2012. Normality tests for statistical analysis: a guide for non-statisticians. *International journal of endocrinology and metabolism.* **10** (2), pp. 486. Cited on p. 164.

Gilkeson, C., Camargo-Valero, M., Pickin, L., and Noakes, C. 2013. Measurement of ventilation and airborne infection risk in large naturally ventilated hospital wards. *Building and environment.* **65**, pp. 35–48. Cited on p. 31.

Girod, S., Zahm, J., Plotkowski, C., Beck, G., and Puchelle, E. 1992. Role of the physiochemical properties of mucus in the protection of the respiratory epithelium. *European Respiratory Journal.* **5**(4), pp. 477–487. Cited on p. 129.

Goldberg, L., Watkins, H., Boerke, E., Chatigny, M., et al. 1958. The use of a rotating drum for the. study of aerosols over extended periods of time. *American journal of hygiene.* **68**(1), pp. 85–93. Cited on p. 30.

Gralton, J., Tovey, E. R., McLaws, M.-L., and Rawlinson, W. D. 2013. Respiratory virus rna is detectable in airborne and droplet particles. *Journal of medical virology.* **85**(12), pp. 2151–2159. Cited on pp. 52 and 213.

Green, S. K., Schroth, M. N., Cho, J. J., Kominos, S. D., and Vitanza-Jack, V. B. 1974. Agricultural plants and soil as a reservoir for pseudomonas aeruginosa. *Applied microbiology.* **28**(6), pp. 987–991. Cited on p. 4.

Grothues, D., Koopmann, U., Von Der Hardt, H., and Tümmler, B. 1988. Genome fingerprinting of pseudomonas aeruginosa indicates colonization of cystic fibrosis siblings with closely related strains. *Journal of clinical microbiology.* **26**(10), pp. 1973–1977. Cited on pp. 34 and 35.

Gstraunthaler, G. and Lindl, T. 2013. Zell-und gewebekultur. Cited on pp. 61 and 94.

Guedes, R. M. 2019. *Creep and fatigue in polymer matrix composites*. Woodhead Publishing. Cited on p. 43.

Han, Z., Weng, W., and Huang, Q. 2013. Characterizations of particle size distribution of the droplets exhaled by sneeze. *Journal of the Royal Society Interface*. **10**(88), pp. 20130560. Cited on pp. 46 and 47.

Hansen, C. R., Pressler, T., Ridderberg, W., Johansen, H., and Skov, M. 2013. Achromobacter species in cystic fibrosis: cross-infection caused by indirect patient-to-patient contact. *Journal of Cystic Fibrosis*. **12**(6), pp. 609–615. Cited on p. 35.

Harris, K. A., Kenna, D. T., Blauwendraat, C., et al. 2012. Molecular fingerprinting of mycobacterium abscessus strains in a cohort of paediatric cystic fibrosis patients. *Journal of clinical microbiology*. pp. JCM–00155. Cited on p. 36.

Harris, K. A., Underwood, A., Kenna, D. T., et al. 2015. Whole-genome sequencing and epidemiological analysis do not provide evidence for cross-transmission of mycobacterium abscessus in a cohort of pediatric cystic fibrosis patients. *Clinical Infectious Diseases*. **60**(7), pp. 1007–1016. Cited on p. 37.

Harrison, F. 2007. Microbial ecology of the cystic fibrosis lung. *Microbiology*. **153** (4), pp. 917–923. Cited on p. 4.

Hart, N., Polkey, M. I., Clément, A., et al. 2002. Changes in pulmonary mechanics with increasing disease severity in children and young adults with cystic fibrosis. *American journal of respiratory and critical care medicine*. **166**(1), pp. 61–66. Cited on p. 227.

Hasan, M. A., Lange, C. F., and King, M. L. 2010. Effect of artificial mucus properties on the characteristics of airborne bioaerosol droplets generated during simulated coughing. *Journal of non-newtonian fluid mechanics*. **165**(21-22), pp. 1431–1441. Cited on pp. 45, 129, and 146.

Hathway, E., Noakes, C., Sleigh, P., and Fletcher, L. 2011. Cfd simulation of airborne pathogen transport due to human activities. *Building and Environment*. **46**(12), pp. 2500–2511. Cited on pp. 16 and 29.

Hathway, E., Noakes, C., Fletcher, L., et al. 2013. The role of nursing activities on the bioaerosol production in hospital wards. *Indoor and Built Environment*. **22** (2), pp. 410–421. Cited on p. 28.

Haworth, C. S., Banks, J., Capstick, T., et al. 2017. British thoracic society guideline for the management of non-tuberculous mycobacterial pulmonary disease (ntm-pd). *BMJ Open Respiratory Research*. **4**(1). Cited on pp. 9, 147, 159, and 170.

Hazlett, L., Rosen, D., and Berk, R. 1978. Age-related susceptibility to pseudomonas aeruginosa ocular infections in mice. *Infection and immunity*. **20**(1), pp. 25–29. Cited on p. 221.

Henke, M. O. and Ratjen, F. 2007. Mucolytics in cystic fibrosis. *Paediatric respiratory reviews*. **8**(1), pp. 24–29. Cited on p. 207.

Henry, R. L., Mellis, C. M., and Petrovic, L. 1992. Mucoid pseudomonas aeruginosa is a marker of poor survival in cystic fibrosis. *Pediatric pulmonology*. **12**(3), pp. 158–161. Cited on p. 6.

Hersen, G., Moularat, S., Robine, E., et al. 2008. Impact of health on particle size of exhaled respiratory aerosols: Case-control study. *CLEAN–Soil, Air, Water*. **36** (7), pp. 572–577. Cited on p. 47.

Hess, G. E. 1965. Effects of oxygen on aerosolized serratia marcescens. *Applied microbiology*. **13**(5), pp. 781–787. Cited on p. 56.

Hoffmann, N., Rasmussen, T. B., Jensen, P., et al. 2005. Novel mouse model of chronic pseudomonas aeruginosa lung infection mimicking cystic fibrosis. *Infection and immunity*. **73**(4), pp. 2504–2514. Cited on pp. 5 and 111.

Høiby, N., Bjarnsholt, T., Givskov, M., Molin, S., and Ciofu, O. 2010. Antibiotic resistance of bacterial biofilms. *International journal of antimicrobial agents*. **35** (4), pp. 322–332. Cited on pp. 5 and 111.

Howard, S. T., Rhoades, E., Recht, J., et al. 2006. Spontaneous reversion of mycobacterium abscessus from a smooth to a rough morphotype is associated with reduced expression of glycopeptidolipid and reacquisition of an invasive phenotype. *Microbiology*. **152**(6), pp. 1581–1590. Cited on pp. 8 and 9.

Howard-Reed, C., Wallace, L., and Emmerich, S. 2003. Deposition rates of fine and coarse particles in residential buildings: literature review and measurements in an occupied townhouse. *National Institute of Standards and Technology*. Cited on p. 219.

Hsu, Y.-C., Kung, P.-Y., Wu, T.-N., Shen, Y.-H., et al. 2012. Characterization of indoor-air bioaerosols in southern taiwan. *Aerosol and Air Quality Research*. **12** (4), pp. 651–661. Cited on p. 198.

Huang, W.-C., Chiou, C.-S., Chen, J.-H., and Shen, G.-H. 2010. Molecular epidemiology of mycobacterium abscessus infections in a subtropical chronic ventilatory setting. *Journal of medical microbiology*. **59**(10), pp. 1203–1211. Cited on p. 36.

Hubad, B. and Lapanje, A. 2012. Inadequate hospital ventilation system increases the risk of nosocomial mycobacterium tuberculosis. *Journal of Hospital Infection*. **80**(1), pp. 88–91. Cited on p. 27.

Hubert, D., Réglier-Poupet, H., Sermet-Gaudelus, I., et al. 2013. Association between staphylococcus aureus alone or combined with pseudomonas aeruginosa and the clinical condition of patients with cystic fibrosis. *Journal of Cystic Fibrosis*. **12**(5), pp. 497–503. Cited on p. 178.

Hunfeld, K., Schmidt, C., Krackhardt, B., et al. 2000. Risk of pseudomonas aeruginosa cross-colonisation in patients with cystic fibrosis within a holiday camp–a molecular-epidemiological study. *Wiener klinische Wochenschrift*. **112**(7), pp. 329–333. Cited on p. 35.

Ijaz, M. K., Zargar, B., Wright, K. E., Rubino, J. R., and Sattar, S. A. 2016. Generic aspects of the airborne spread of human pathogens indoors and emerging air decontamination technologies. *American journal of infection control*. **44**(9), pp. S109–S120. Cited on p. 56.

Isaacs, A. 1996. *Oxford dictionary of physics*. Cited on p. 42.

Jensen, P. A., Todd, W. F., Davis, G. N., and Scarpino, P. V. 1992. Evaluation of eight bioaerosol samplers challenged with aerosols of free bacteria. *The American Industrial Hygiene Association Journal*. **53**(10), pp. 660–667. Cited on p. 25.

John, W. The characteristics of environmental and laboratory-generated aerosols, 1993. Cited on p. 77.

Johnson, G., Morawska, L., Ristovski, Z., et al. 2011. Modality of human expired aerosol size distributions. *Journal of Aerosol Science*. **42**(12), pp. 839–851. Cited on p. 213.

Johnson, G. R., Knibbs, L. D., Kidd, T. J., et al. 2016. A novel method and its application to measuring pathogen decay in bioaerosols from patients with respiratory disease. *PloS one*. **11**(7), pp. e0158763. Cited on p. 53.

Jones, A., Govan, J., Doherty, C., et al. 2003. Identification of airborne dissemination of epidemic multiresistant strains of pseudomonas aeruginosa at a cf centre during a cross infection outbreak. *Thorax*. **58**(6), pp. 525–527. Cited on pp. 2, 4, and 36.

Jones, A., Alexander, E., Allen, O., et al. 2017. *Mycobacterium abscessus. Recommendations for infection prevention and control.* Technical report, Cystic Fibrosis Trust, Infection Control Working Group. Cited on p. 38.

Jones, A. M. 2014. Airborne dissemination of transmissible bacterial species in cystic fibrosis. *Thorax.* pp. thoraxjnl–2014. Cited on p. 38.

Jones, A. M., Govan, J. R., Doherty, C. J., et al. 2001. Spread of a multiresistant strain of pseudomonas aeruginosa in an adult cystic fibrosis clinic. *The Lancet.* **358**(9281), pp. 557–558. Cited on pp. 6 and 35.

Jones, B., Sharpe, P., Iddon, C., et al. 2021. Modelling uncertainty in the relative risk of exposure to the sars-cov-2 virus by airborne aerosol transmission in well mixed indoor air. *Building and environment.* pp. 107617. Cited on p. 32.

Jones-López, E. C., Namugga, O., Mumbowa, F., et al. 2013. Cough aerosols of mycobacterium tuberculosis predict new infection. a household contact study. *American journal of respiratory and critical care medicine.* **187**(9), pp. 1007–1015. Cited on pp. 49 and 52.

Jönsson, B. E., Gilljam, M., Lindblad, A., et al. 2007. Molecular epidemiology of mycobacterium abscessus, with focus on cystic fibrosis. *Journal of clinical microbiology.* **45**(5), pp. 1497–1504. Cited on p. 10.

Jordan, P., Stanley, T., Donnelly, F., et al. 2007. Atypical mycobacterial infection in patients with cystic fibrosis: update on clinical microbiology methods. *Letters in applied microbiology.* **44**(5), pp. 459–466. Cited on p. 7.

Kennedy, M., Ramsheh, M. Y., Williams, C. M., et al. 2018. Face mask sampling reveals antimicrobial resistance genes in exhaled aerosols from patients with chronic obstructive pulmonary disease and healthy volunteers. *BMJ open respiratory research.* **5**(1). Cited on p. 157.

Kerem, B.-s. 1989. Identification of the cystic fibrosis gene: genetic analysis. *Trends in Genetics.* **5**, pp. 363. Cited on p. 3.

Kidd, T. J., Ramsay, K. A., Hu, H., et al. 2013. Shared pseudomonas aeruginosa genotypes are common in australian cystic fibrosis centres. *European Respiratory Journal.* **41**(5), pp. 1091–1100. Cited on pp. 35 and 36.

King, M.-F., Noakes, C., Sleigh, P., and Camargo-Valero, M. 2013. Bioaerosol deposition in single and two-bed hospital rooms: A numerical and experimental study. *Building and Environment.* **59**, pp. 436–447. Cited on pp. 16, 17, 29, and 34.

Knibbs, L. D., Johnson, G. R., Kidd, T. J., et al. 2014. Viability of pseudomonas aeruginosa in cough aerosols generated by persons with cystic fibrosis. *Thorax*. **69**(8), pp. 740–745. Cited on pp. 53, 115, 140, 213, 226, and 254.

Koch, C., Cuppens, H., Rainisio, M., et al. 2001. European epidemiologic registry of cystic fibrosis (ercf): comparison of major disease manifestations between patients with different classes of mutations. *Pediatric pulmonology*. **31**(1), pp. 1–12. Cited on p. 3.

Kohn, W. G., Collins, A. S., Cleveland, J. L., et al. 2003. Guidelines for infection control in dental health-care settings-2003. Cited on pp. xv, 10, and 11.

Kreger, B. E., Craven, D. E., Carling, P. C., and McCabe, W. R. 1980. Gram-negative bacteremia: Iii. reassessment of etiology, epidemiology and ecology in 612 patients. *The American journal of medicine*. **68**(3), pp. 332–343. Cited on p. 4.

Kwon, S.-B., Park, J., Jang, J., et al. 2012. Study on the initial velocity distribution of exhaled air from coughing and speaking. *Chemosphere*. **87**(11), pp. 1260–1264. Cited on pp. 17 and 50.

Ladhani, L., Pardon, G., Meeuws, H., et al. 2017. Sampling and detection of airborne influenza virus towards point-of-care applications. *PloS one*. **12**(3), pp. e0174314. Cited on p. 27.

Lai, A. 2002. Particle deposition indoors: a review. *Indoor air*. **12**(4), pp. 211–214. Cited on p. 219.

Lai, A., Wong, L., Mui, K., Chan, W., and Yu, H. 2012. An experimental study of bioaerosol (1–10 μm) deposition in a ventilated chamber. *Building and environment*. **56**, pp. 118–126. Cited on p. 30.

Lai, C.-C., Tan, C.-K., Chou, C.-H., et al. 2010. Increasing incidence of nontuberculous mycobacteria, taiwan, 2000–2008. *Emerg Infect Dis*. **16**(2), pp. 294–296. Cited on p. 8.

Lam, J., Chan, R., Lam, K., and Costerton, J. 1980. Production of mucoid microcolonies by pseudomonas aeruginosa within infected lungs in cystic fibrosis. *Infection and immunity*. **28**(2), pp. 546–556. Cited on p. 5.

Lederberg, J., Alexander, M., Bloom, B. R., et al. 2000. *Encyclopedia of Microbiology, Four-Volume Set*. Academic Press. Cited on pp. 4 and 183.

Lednicky, J. A., Lauzard, M., Fan, Z. H., et al. 2020. Viable sars-cov-2 in the air of a hospital room with covid-19 patients. *International Journal of Infectious Diseases*. **100**, pp. 476–482. Cited on p. 28.

Lednicky, J. A., Lauzardo, M., Alam, M. M., et al. 2021. Isolation of sars-cov-2 from the air in a car driven by a covid patient with mild illness. *International Journal of Infectious Diseases*. Cited on p. 28.

Lee, T. W., Brownlee, K. G., Conway, S. P., Denton, M., and Littlewood, J. M. 2003. Evaluation of a new definition for chronic pseudomonas aeruginosa infection in cystic fibrosis patients. *Journal of Cystic Fibrosis*. **2**(1), pp. 29–34. Cited on pp. xxviii, 5, 147, 159, 167, 170, and 236.

Levy, I., Grisaru-Soen, G., Lerner-Geva, L., et al. 2008. Multicenter cross-sectional study of nontuberculous mycobacterial infections among cystic fibrosis patients, israel. *Emerg Infect Dis*. **14**(3), pp. 378–384. Cited on p. 10.

Li, D. 2008. *Encyclopedia of microfluidics and nanofluidics*. Springer Science & Business Media. Cited on p. 43.

Li, X., Shang, Y., Yan, Y., Yang, L., and Tu, J. 2018. Modelling of evaporation of cough droplets in inhomogeneous humidity fields using the multi-component eulerian-lagrangian approach. *Building and Environment*. **128**, pp. 68–76. Cited on pp. 16 and 55.

Li, Y., Huang, X., Yu, I., Wong, T., and Qian, H. 2005. Role of air distribution in sars transmission during the largest nosocomial outbreak in hong kong. *Indoor air*. **15**(2), pp. 83–95. Cited on pp. 24, 31, and 34.

Li, Y., Leung, G. M., Tang, J., et al. 2007. Role of ventilation in airborne transmission of infectious agents in the built environment-a multidisciplinary systematic review. *Indoor air*. **17**(1), pp. 2–18. Cited on p. 31.

Lighthart, B. and Shaffer, B. T. 1997. Increased airborne bacterial survival as a function of particle content and size. *Aerosol Science and Technology*. **27**(3), pp. 439–446. Cited on p. 56.

Lin, K. and Marr, L. C. 2019. Humidity-dependent decay of viruses, but not bacteria, in aerosols and droplets follows disinfection kinetics. *Environmental Science & Technology*. **54**(2), pp. 1024–1032. Cited on pp. 56 and 57.

Lindsley, W. G., Blachere, F. M., Thewlis, R. E., et al. 2010. Measurements of airborne influenza virus in aerosol particles from human coughs. *PloS one*. **5**(11), pp. e15100. Cited on pp. 51 and 213.

Lindsley, W. G., Pearce, T. A., Hudnall, J. B., et al. 2012. Quantity and size distribution of cough-generated aerosol particles produced by influenza patients during and after illness. *Journal of occupational and environmental hygiene*. **9** (7), pp. 443–449. Cited on pp. 48, 49, and 213.

Lindsley, W. G., Reynolds, J. S., Szalajda, J. V., Noti, J. D., and Beezhold, D. H. 2013. A cough aerosol simulator for the study of disease transmission by human cough-generated aerosols. *Aerosol Science and Technology*. **47**(8), pp. 937–944. Cited on p. 17.

Lindsley, W. G., Blachere, F. M., Beezhold, D. H., et al. 2016. Viable influenza a virus in airborne particles expelled during coughs versus exhalations. *Influenza and other respiratory viruses*. **10**(5), pp. 404–413. Cited on pp. 51 and 52.

Lindsley, W. G., Green, B. J., Blachere, F. M., et al. 2017. Sampling and characterization of bioaerosols. *NIOSH manual of analytical methods. 5th ed. Cincinnati (OH): National Institute for Occupational Safety and Health*. Cited on pp. xv, 25, 26, and 27.

Ling, S. and Hui, L. 2019. Evaluation of the complexity of indoor air in hospital wards based on pm2. 5, real-time pcr, adenosine triphosphate bioluminescence assay, microbial culture and mass spectrometry. *BMC infectious diseases*. **19**(1), pp. 1–10. Cited on p. 198.

LiPuma, J. J. 2010. The changing microbial epidemiology in cystic fibrosis. *Clinical microbiology reviews*. **23**(2), pp. 299–323. Cited on p. 35.

Littlewood, J., Dodd, M., Elborn, S., et al. 2004. *Pseudomonas aeruginosa infection in people with cystic fibrosis. Suggestions for Prevention and Infection Control*. Technical report, Cystic Fibrosis Trust, Infection Control Working Group. Cited on pp. 2 and 38.

Liu, L., Li, Y., Nielsen, P. V., Wei, J., and Jensen, R. L. 2017a. Short-range airborne transmission of expiratory droplets between two people. *Indoor Air*. **27**(2), pp. 452–462. Cited on pp. 15, 17, and 55.

Liu, L., Wei, J., Li, Y., and Ooi, A. 2017b. Evaporation and dispersion of respiratory droplets from coughing. *Indoor Air*. **27**(1), pp. 179–190. Cited on pp. 16 and 55.

Liu, Y., Ning, Z., Chen, Y., et al. 2020. Aerodynamic characteristics and rna concentration of sars-cov-2 aerosol in wuhan hospitals during covid-19 outbreak. *BioRxiv*. Cited on p. 28.

Locher, W. G. 2007. Max von pettenkofer (1818–1901) as a pioneer of modern hygiene and preventive medicine. *Environmental health and preventive medicine*. **12**(6), pp. 238–245. Cited on p. 194.

Lodish, H., Berk, A., Zipursky, S. L., et al. 2000. Molecular cell biology 4th edition. *National Center for Biotechnology Information, Bookshelf*. **9**. Cited on p. 61.

Loudon, R. and Roberts, R. 1967a. Relation between the airborne diameters of respiratory droplets and the diameter of the stains left after recovery. *Nature*. **213**(5071), pp. 95–96. Cited on pp. 46 and 96.

Loudon, R. G. and Roberts, R. M. 1967b. Droplet expulsion from the respiratory tract. *American Review of Respiratory Disease*. **95**(3), pp. 435–442. Cited on pp. 45, 46, 47, 48, and 96.

Loveday, H., Wilson, J., Pratt, R., et al. 2014. epic3: national evidence-based guidelines for preventing healthcare-associated infections in nhs hospitals in england. *Journal of Hospital Infection*. **86**, pp. S1–S70. Cited on p. 12.

Lyczak, J. B., Cannon, C. L., and Pier, G. B. 2002. Lung infections associated with cystic fibrosis. *Clinical microbiology reviews*. **15**(2), pp. 194–222. Cited on p. 5.

Ma, J. T., Tang, C., Kang, L., Voynow, J. A., and Rubin, B. K. 2018. Cystic fibrosis sputum rheology correlates with both acute and longitudinal changes in lung function. *Chest*. **154**(2), pp. 370–377. Cited on pp. 129 and 181.

Macher, J. M. 1989. Positive-hole correction of multiple-jet impactors for collecting viable microorganisms. *The American Industrial Hygiene Association Journal*. **50**(11), pp. 561–568. Cited on pp. 26, 78, 162, and 174.

Macintosh, C., McGrath, A., Sturdy, P., et al. 2007. *Health technical memorandum A 03-01: Specialised Ventilation for Healthcare Premises*. Technical report, Department of health. Cited on pp. 31, 225, 237, and 238.

Malani, P. N. 2010. Mandell, douglas, and bennett's principles and practice of infectious diseases. *JAMA*. **304**(18), pp. 2067–2071. Cited on p. 7.

Mangili, A. and Gendreau, M. A. 2005. Transmission of infectious diseases during commercial air travel. *The Lancet*. **365**(9463), pp. 989–996. Cited on p. 11.

Maselli, J. H., Sontag, M. K., Norris, J. M., et al. 2003. Risk factors for initial acquisition of pseudomonas aeruginosa in children with cystic fibrosis identified by newborn screening. *Pediatric pulmonology*. **35**(4), pp. 257–262. Cited on p. 6.

Masterson, T., Wildman, B. G., Newberry, B., et al. 2008. Compliance in cystic fibrosis: an examination of infection control guidelines. *Pediatric pulmonology*. **43**(5), pp. 435–442. Cited on p. 39.

Mateu, E., Calafell, F., Ramos, M. D., Casals, T., and Bertranpetit, J. 2002. Can a place of origin of the main cystic fibrosis mutations be identified? *The American Journal of Human Genetics*. **70**(1), pp. 257–264. Cited on p. 3.

May, K. 1973. The collison nebulizer: description, performance and application. *Journal of Aerosol Science*. **4**(3), pp. 235–243. Cited on p. 77.

McDonagh, A., Noakes, C. J., and Fletcher, L. Experimentally evaluating the effectivness of an upper-room uvgi system. Leeds, 2013. Cited on p. 66.

Medjahed, H., Gaillard, J.-L., and Reyrat, J.-M. 2010. Mycobacterium abscessus: a new player in the mycobacterial field. *Trends in microbiology*. **18**(3), pp. 117–123. Cited on p. 7.

Menzies, D., Fanning, A., Yuan, L., and FitzGerald, J. M. 2000. Hospital ventilation and risk for tuberculous infection in canadian health care workers. *Annals of Internal Medicine*. **133**(10), pp. 779–789. Cited on p. 31.

Miller, M. R., Hankinson, J., Brusasco, V., et al. 2005. Standardisation of spirometry. *European respiratory journal*. **26**(2), pp. 319–338. Cited on p. 159.

Miller, S. L., Nazaroff, W. W., Jimenez, J. L., et al. 2020. Transmission of sars-cov-2 by inhalation of respiratory aerosol in the skagit valley chorale superspreading event. *Indoor air*. Cited on pp. 32 and 49.

Milton, D. K. A rosetta stone for understanding infectious drops and aerosols, 2020. Cited on pp. xxviii, 2, 12, 13, and 213.

Milton, D. K., Fabian, M. P., Cowling, B. J., Grantham, M. L., and McDevitt, J. J. 2013. Influenza virus aerosols in human exhaled breath: particle size, culturability, and effect of surgical masks. *PLoS Pathog*. **9**(3), pp. e1003205. Cited on pp. 49 and 52.

Miroballi, Y., Garber, E., Jia, H., et al. 2012. Infection control knowledge, attitudes, and practices among cystic fibrosis patients and their families. *Pediatric pulmonology*. **47**(2), pp. 144–152. Cited on p. 39.

Mitchell, J., Weir, M., and Rose, J. Quantitative microbial risk assessment wiki, 2021. `http://qmrawiki.org/`, Last accessed on 2021-04-06. Cited on p. 222.

Moloney, E., Deasy, E., Swan, J., et al. 2019. Whole-genome sequencing identifies highly related pseudomonas aeruginosa strains in multiple washbasin u-bends at several locations in one hospital: evidence for trafficking of potential pathogens via wastewater pipes. *Journal of Hospital Infection*. Cited on p. 4.

Moore, M. and Frerichs, J. B. 1953. An unusual acid-fast infection of the knee with subcutaneous, abscess-like lesions of the gluteal region: Report of a case with a study of the organism, mycobacterium abscessus, n. sp. 1. *Journal of Investigative Dermatology*. **20**(2), pp. 133–169. Cited on p. 7.

Morales, P., Ros, J., Blanes, M., et al. Successful recovery after disseminated infection due to mycobacterium abscessus in a lung transplant patient: subcutaneous nodule as first manifestation—a case report. In: *Transplantation proceedings*, volume 39, pp. 2413–2415. Elsevier, 2007. Cited on p. 10.

Morawska, L. and Cao, J. 2020. Airborne transmission of sars-cov-2: The world should face the reality. *Environment International*. pp. 105730. Cited on p. 24.

Morawska, L., Johnson, G., Ristovski, Z., et al. 2009. Size distribution and sites of origin of droplets expelled from the human respiratory tract during expiratory activities. *Journal of Aerosol Science*. **40**(3), pp. 256–269. Cited on pp. 46, 48, 49, 212, and 213.

Moriarty, J. and Grotberg, J. 1999. Flow-induced instabilities of a mucus–serous bilayer. *Journal of Fluid Mechanics*. **397**, pp. 1–22. Cited on p. 41.

Mozes, N. and Rouxhet, P. 1987. Methods for measuring hydrophobicity of microorganisms. *Journal of Microbiological Methods*. **6**(2), pp. 99–112. Cited on p. 44.

Mussaffi, H., Rivlin, J., Shalit, I., Ephros, M., and Blau, H. 2005. Nontuberculous mycobacteria in cystic fibrosis associated with allergic bronchopulmonary aspergillosis and steroid therapy. *European Respiratory Journal*. **25**(2), pp. 324–328. Cited on pp. 7 and 10.

Nessar, R., Cambau, E., Reyrat, J. M., Murray, A., and Gicquel, B. 2012. Mycobacterium abscessus: a new antibiotic nightmare. *Journal of antimicrobial chemotherapy*. pp. dkr578. Cited on p. 8.

Nicas, M. and Jones, R. M. 2009. Relative contributions of four exposure pathways to influenza infection risk. *Risk Analysis: An International Journal*. **29**(9), pp. 1292–1303. Cited on p. 15.

Nicas, M. and Sun, G. 2006. An integrated model of infection risk in a health-care environment. *Risk Analysis.* **26**(4), pp. 1085–1096. Cited on p. 10.

Nicas, M., Nazaroff, W. W., and Hubbard, A. 2005. Toward understanding the risk of secondary airborne infection: emission of respirable pathogens. *Journal of occupational and environmental hygiene.* **2**(3), pp. 143–154. Cited on pp. xvi, 14, 15, 55, 61, 94, 95, 99, and 214.

Nightingale, F. 1992. *Notes on nursing: What it is, and what it is not.* Lippincott Williams & Wilkins. Cited on p. 247.

Noakes, C., Beggs, C., Sleigh, P., and Kerr, K. 2006. Modelling the transmission of airborne infections in enclosed spaces. *Epidemiology & Infection.* **134**(5), pp. 1082–1091. Cited on pp. 15 and 32.

Noakes, C. J. and Sleigh, P. A. 2009. Mathematical models for assessing the role of airflow on the risk of airborne infection in hospital wards. *Journal of the Royal Society Interface.* **6**(suppl_6), pp. S791–S800. Cited on pp. 30 and 32.

Oh, M.-d., Choe, P. G., Oh, H. S., et al. 2015. Middle east respiratory syndrome coronavirus superspreading event involving 81 persons, korea 2015. *Journal of Korean medical science.* **30**(11), pp. 1701. Cited on p. 50.

Ojeniyi, B., Frederiksen, B., and Høiby, N. 2000. Pseudomonas aeruginosa cross-infection among patients with cystic fibrosis during a winter camp. *Pediatric pulmonology.* **29**(3), pp. 177–181. Cited on p. 35.

Olivier, K. N., Weber, D. J., Wallace Jr, R. J., et al. 2003. Nontuberculous mycobacteria: I: multicenter prevalence study in cystic fibrosis. *American journal of respiratory and critical care medicine.* **167**(6), pp. 828–834. Cited on pp. 7, 8, 10, and 36.

Orazi, G. and O'Toole, G. A. 2017. Pseudomonas aeruginosa alters staphylococcus aureus sensitivity to vancomycin in a biofilm model of cystic fibrosis infection. *MBio.* **8**(4). Cited on p. 178.

O'Sullivan, B. P. and Freedman, S. D. 2009. Cystic fibrosis. *The Lancet.* **373**(9678), pp. 1891 – 1904. Cited on p. 3.

Owen, M., Ensor, D., and Sparks, L. 1992. Airborne particle sizes and sources found in indoor air. *Atmospheric Environment. Part A. General Topics.* **26**(12), pp. 2149–2162. Cited on pp. xv and 13.

Pacek, A., Man, C., and Nienow, A. 1998. On the sauter mean diameter and size distributions in turbulent liquid/liquid dispersions in a stirred vessel. *Chemical Engineering Science*. **53**(11), pp. 2005–2011. Cited on p. 109.

Panagea, S., Winstanley, C., Walshaw, M., Ledson, M., and Hart, C. 2005. Environmental contamination with an epidemic strain of pseudomonas aeruginosa in a liverpool cystic fibrosis centre, and study of its survival on dry surfaces. *Journal of Hospital Infection*. **59**(2), pp. 102–107. Cited on pp. 4 and 36.

Papineni, R. S. and Rosenthal, F. S. 1997. The size distribution of droplets in the exhaled breath of healthy human subjects. *Journal of Aerosol Medicine*. **10**(2), pp. 105–116. Cited on pp. 46, 47, 48, 49, and 212.

Parad, R. B., Gerard, C. J., Zurakowski, D., Nichols, D. P., and Pier, G. B. 1999. Pulmonary outcome in cystic fibrosis is influenced primarily by mucoid pseudomonas aeruginosa infection and immune status and only modestly by genotype. *Infection and immunity*. **67**(9), pp. 4744–4750. Cited on p. 6.

Parienta, D., Morawska, L., Johnson, G. R., et al. 2011. Theoretical analysis of the motion and evaporation of exhaled respiratory droplets of mixed composition. *Journal of aerosol science*. **42**(1), pp. 1–10. Cited on pp. 55 and 56.

Patterson, B., Morrow, C., Singh, V., et al. 2017. Detection of mycobacterium tuberculosis bacilli in bio-aerosols from untreated tb patients. *Gates open research*. **1**. Cited on p. 213.

Persily, A. and de Jonge, L. 2017. Carbon dioxide generation rates for building occupants. *Indoor air*. **27**(5), pp. 868–879. Cited on p. 225.

Pier, G. B., Saunders, J. M., Ames, P., et al. 1987. Opsonophagocytic killing antibody to pseudomonas aeruginosa mucoid exopolysaccharide in older noncolonized patients with cystic fibrosis. *New England Journal of Medicine*. **317**(13), pp. 793–798. Cited on p. 6.

Pirnay, J.-P., Matthijs, S., Colak, H., et al. 2005. Global pseudomonas aeruginosa biodiversity as reflected in a belgian river. *Environmental microbiology*. **7**(7), pp. 969–980. Cited on p. 4.

Preece, C. L., Perry, A., Gray, B., et al. 2016. A novel culture medium for isolation of rapidly-growing mycobacteria from the sputum of patients with cystic fibrosis. *Journal of Cystic Fibrosis*. **15**(2), pp. 186–191. Cited on p. 163.

Prevots, D. R., Shaw, P. A., Strickland, D., et al. 2010. Nontuberculous mycobacterial lung disease prevalence at four integrated health care delivery systems.

American journal of respiratory and critical care medicine. **182**(7), pp. 970–976. Cited on pp. 7 and 8.

Purdy-Gibson, M., France, M., Hundley, T., Eid, N., and Remold, S. 2015. Pseudomonas aeruginosa in cf and non-cf homes is found predominantly in drains. *Journal of Cystic Fibrosis*. **14**(3), pp. 341–346. Cited on p. 4.

Qian, H. and Zheng, X. 2018. Ventilation control for airborne transmission of human exhaled bio-aerosols in buildings. *Journal of thoracic disease*. **10**(Suppl 19), pp. S2295. Cited on p. 31.

Qian, H., Li, Y., Nielsen, P. V., and Huang, X. 2009. Spatial distribution of infection risk of sars transmission in a hospital ward. *Building and Environment*. **44**(8), pp. 1651–1658. Cited on p. 34.

Quittell, L. M. 2004. Management of non-tuberculous mycobacteria in patients with cystic fibrosis. *Paediatric respiratory reviews*. **5**, pp. S217–S219. Cited on pp. 8 and 10.

Ratha, D. and Sarkar, A. 2015. Analysis of flow over backward facing step with transition. *Frontiers of Structural and Civil Engineering*. **9**(1), pp. 71–81. Cited on p. 259.

Reddy, C., Beveridge, T. J., Breznak, J. A., and Marzluf, G. 2007. *Methods for general and molecular microbiology*. American Society for Microbiology Press. Cited on p. 164.

Redrow, J., Mao, S., Celik, I., Posada, J. A., and Feng, Z.-g. 2011. Modeling the evaporation and dispersion of airborne sputum droplets expelled from a human cough. *Building and Environment*. **46**(10), pp. 2042–2051. Cited on pp. xv, 16, and 56.

Renders, N., Sijmons, M., van Belkum, A., et al. 1997. Exchange of pseudomonas aeruginosa strains among cystic fibrosis siblings. *Research in microbiology*. **148** (5), pp. 447–454. Cited on p. 35.

Riley, E., Murphy, G., and Riley, R. 1978. Airborne spread of measles in a suburban elementary school. *American journal of epidemiology*. **107**(5), pp. 421–432. Cited on p. 32.

Riordan, J. R. 1989. Identification of the cystic fibrosis gene: cloning and characterization of complementary dna. *Trends in Genetics*. **5**, pp. 363. Cited on p. 3.

Roberts, K., Smith, C. F., Snelling, A. M., et al. 2008. Aerial dissemination of clostridium difficile spores. *BMC infectious diseases*. **8**(1), pp. 7. Cited on p. 29.

Römling, U., Wingender, J., Müller, H., and Tümmler, B. 1994. A major pseudomonas aeruginosa clone common to patients and aquatic habitats. *Applied and Environmental Microbiology*. **60**(6), pp. 1734–1738. Cited on p. 34.

Rommens, J. M., Iannuzzi, M. C., Kerem, B.-s., et al. 1989. Identification of the cystic fibrosis gene: chromosome walking and jumping. *Science*. **245**(4922), pp. 1059–1065. Cited on p. 3.

Rotcheewaphan, S., Odusanya, O. E., Henderson, C. M., et al. 2019. Performance of rgm medium for isolation of nontuberculous mycobacteria from respiratory specimens from non-cystic fibrosis patients. *Journal of clinical microbiology*. **57** (2). Cited on p. 163.

Roux, A.-L., Catherinot, E., Ripoll, F., et al. 2009. Multicenter study of prevalence of nontuberculous mycobacteria in patients with cystic fibrosis in france. *Journal of clinical microbiology*. **47**(12), pp. 4124–4128. Cited on pp. 7 and 8.

Rudnick, S. and Milton, D. 2003. Risk of indoor airborne infection transmission estimated from carbon dioxide concentration. *Indoor air*. **13**(3), pp. 237–245. Cited on p. 32.

Rüger, K., Hampel, A., Billig, S., et al. 2014. Characterization of rough and smooth morphotypes of mycobacterium abscessus isolates from clinical specimens. *Journal of clinical microbiology*. **52**(1), pp. 244–250. Cited on pp. xv, 7, 8, and 10.

Saiman, L., Siegel, J. D., LiPuma, J. J., et al. 2014. Infection prevention and control guideline for cystic fibrosis: 2013 update. *Infection Control & Hospital Epidemiology*. **35**(S1), pp. S1–S67. Cited on p. 38.

Salmela, A., Kokkonen, E., Kulmala, I., et al. 2018. Production and characterization of bioaerosols for model validation in spacecraft environment. *Journal of Environmental Sciences*. **69**, pp. 227–238. Cited on p. 16.

Sanguinetti, M., Ardito, F., Fiscarelli, E., et al. 2001. Fatal pulmonary infection due to multidrug-resistant mycobacterium abscessus in a patient with cystic fibrosis. *Journal of clinical microbiology*. **39**(2), pp. 816–819. Cited on pp. 7, 8, 9, and 10.

Scharfman, B., Techet, A., Bush, J., and Bourouiba, L. 2016. Visualization of sneeze ejecta: steps of fluid fragmentation leading to respiratory droplets. *Experiments in Fluids*. **57**(2), pp. 24. Cited on p. 45.

Schelstraete, P., De Boeck, K., Proesmans, M., et al. 2008. Pseudomonas aeruginosa in the home environment of newly infected cystic fibrosis patients. *European Respiratory Journal*. **31**(4), pp. 822–829. Cited on p. 4.

Schiller, L. 1933. Über die grundlegenden berechnungen bei der schwerkraftaufbereitung. *Z. Vereines Deutscher Inge.* **77**, pp. 318–321. Cited on p. 218.

Scott, F. W. and Pitt, T. L. 2004. Identification and characterization of transmissible pseudomonas aeruginosa strains in cystic fibrosis patients in england and wales. *Journal of medical microbiology*. **53**(7), pp. 609–615. Cited on p. 6.

Sergent, A.-P., Slekovec, C., Pauchot, J., et al. 2012. Bacterial contamination of the hospital environment during wound dressing change. *Orthopaedics & Traumatology: Surgery & Research*. **98**(4), pp. 441–445. Cited on p. 29.

Sermet-Gaudelus, I., Le Bourgeois, M., Pierre-Audigier, C., et al. 2003. Mycobacterium abscessus and children with cystic fibrosis. *Emerging infectious diseases*. **9**(12), pp. 1587–1591. Cited on pp. 7, 10, and 36.

Shah, S., Fung, K., Brim, S., and Rubin, B. K. 2005. Anin vitro evaluation of the effectiveness of endotracheal suction catheters. *Chest*. **128**(5), pp. 3699–3704. Cited on pp. xix and 129.

Shen, Z., Ning, F., Zhou, W., et al. 2004. Superspreading sars events, beijing, 2003. *Emerging infectious diseases*. **10**(2), pp. 256. Cited on p. 50.

Shiomori, T., Miyamoto, H., Makishima, K., et al. 2002. Evaluation of bedmaking-related airborne and surface methicillin-resistant staphylococcus aureus contamination. *Journal of Hospital Infection*. **50**(1), pp. 30–35. Cited on pp. 23 and 29.

Shirozu, K., Kai, T., Setoguchi, H., Ayagaki, N., and Hoka, S. 2018. Effects of forced air warming on airflow around the operating table. *Anesthesiology: The Journal of the American Society of Anesthesiologists*. **128**(1), pp. 79–84. Cited on p. 34.

Somayaji, R., Waddell, B., Workentine, M., et al. 2015. Infection control knowledge, beliefs and behaviours amongst cystic fibrosis patients with epidemic pseudomonas aeruginosa. *BMC pulmonary medicine*. **15**(1), pp. 1. Cited on p. 39.

Sornboot, J., Aekplakorn, W., Ramasoota, P., et al. 2019. Detection of airborne mycobacterium tuberculosis complex in high-risk areas of health care facilities in thailand. *The International Journal of Tuberculosis and Lung Disease*. **23**(4), pp. 465–473. Cited on p. 27.

Stelzer-Braid, S., Oliver, B. G., Blazey, A. J., et al. 2009. Exhalation of respiratory viruses by breathing, coughing, and talking. *Journal of medical virology*. **81**(9), pp. 1674–1679. Cited on p. 51.

Strausbaugh, S. D. and Davis, P. B. 2007. Cystic fibrosis: a review of epidemiology and pathobiology. *Clinics in chest medicine*. **28**(2), pp. 279–288. Cited on p. 35.

Streeck, H., Schulte, B., Kuemmerer, B., et al. 2020. Infection fatality rate of sars-cov-2 infection in a german community with a super-spreading event. *medrxiv*. Cited on p. 50.

Tan, M., Shen, F., Yao, M., and Zhu, T. 2011. Development of an automated electrostatic sampler (aes) for bioaerosol detection. *Aerosol Science and Technology*. **45**(9), pp. 1154–1160. Cited on p. 27.

Tang, J., Li, Y., Eames, I., Chan, P., and Ridgway, G. 2006. Factors involved in the aerosol transmission of infection and control of ventilation in healthcare premises. *Journal of Hospital Infection*. **64**(2), pp. 100–114. Cited on pp. 10, 15, and 28.

Tang, J. W., Liebner, T. J., Craven, B. A., and Settles, G. S. 2009. A schlieren optical study of the human cough with and without wearing masks for aerosol infection control. *Journal of the Royal Society Interface*. **6**(suppl_6), pp. S727–S736. Cited on p. 17.

Tang, J. W., Nicolle, A., Pantelic, J., et al. 2012. Airflow dynamics of coughing in healthy human volunteers by shadowgraph imaging: an aid to aerosol infection control. *PLoS One*. **7**(4), pp. e34818. Cited on p. 50.

Tang, J. W., Gao, C. X., Cowling, B. J., et al. 2014. Absence of detectable influenza rna transmitted via aerosol during various human respiratory activities–experiments from singapore and hong kong. *PLoS One*. **9**(9), pp. e107338. Cited on p. 30.

Tarran, R., Button, B., Picher, M., et al. 2005. Normal and cystic fibrosis airway surface liquid homeostasis: the effects of phasic shear stress and viral infections. *Journal of Biological Chemistry*. **280**(42), pp. 35751–35759. Cited on p. 130.

Taylor, J. L. and Palmer, S. M. 2006. Mycobacterium abscessus chest wall and pulmonary infection in a cystic fibrosis lung transplant recipient. *The Journal of heart and lung transplantation*. **25**(8), pp. 985–988. Cited on pp. 7 and 9.

Taylor, S. Airborne and surface survival rate of mycobacterium abscessus and their potential to cause or worsen respiratory infection in people with cystic fibrosis, 2016. Cited on pp. 37 and 151.

Teunis, P. and Havelaar, A. 2000. The beta poisson dose-response model is not a single-hit model. *Risk Analysis.* **20**(4), pp. 513–520. Cited on p. 33.

Theron, G., Limberis, J., Venter, R., et al. 2020. Bacterial and host determinants of cough aerosol culture positivity in patients with drug-resistant versus drug-susceptible tuberculosis. *Nature Medicine.* **26**(9), pp. 1435–1443. Cited on p. 213.

Thin, A., Dodd, J., Gallagher, C., Fitzgerald, M., and Mcloughlin, P. 2004. Effect of respiratory rate on airway deadspace ventilation during exercise in cystic fibrosis. *Respiratory medicine.* **98**(11), pp. 1063–1070. Cited on p. 227.

Thomas, J. C. and Van den Ende, M. 1941. Reduction of dust-borne bacteria in the air of hospital wards by liquid paraffin treatment of bedclothes. *British medical journal.* **1**(4199), pp. 953. Cited on p. 29.

Thompson, K.-A., Bennett, A., and Walker, J. 2011. Aerosol survival of staphylococcus epidermidis. *Journal of Hospital Infection.* **78**(3), pp. 216–220. Cited on p. 30.

Thompson, K.-A., Pappachan, J. V., Bennett, A. M., et al. 2013. Influenza aerosols in uk hospitals during the h1n1 (2009) pandemic–the risk of aerosol generation during medical procedures. *PloS one.* **8**(2), pp. e56278. Cited on pp. 23 and 28.

Thomson, R., Tolson, C., Carter, R., et al. 2013a. Isolation of nontuberculous mycobacteria (ntm) from household water and shower aerosols in patients with pulmonary disease caused by ntm. *Journal of clinical microbiology.* **51**(9), pp. 3006–3011. Cited on p. 7.

Thomson, R., Tolson, C., Sidjabat, H., Huygens, F., and Hargreaves, M. 2013b. Mycobacterium abscessus isolated from municipal water-a potential source of human infection. *BMC infectious diseases.* **13**(1), pp. 1. Cited on p. 7.

Tran, D. T., Alleman, L. Y., Coddeville, P., and Galloo, J.-C. 2017. Indoor particle dynamics in schools: Determination of air exchange rate, size-resolved particle deposition rate and penetration factor in real-life conditions. *Indoor and Built Environment.* **26**(10), pp. 1335–1350. Cited on p. 219.

Tung, Y.-C., Shih, Y.-C., and Hu, S.-C. 2009. Numerical study on the dispersion of airborne contaminants from an isolation room in the case of door opening. *Applied Thermal Engineering.* **29**(8-9), pp. 1544–1551. Cited on p. 34.

Upton, S., Mark, D., Douglass, E., Hall, D., and Griffiths, W. 1994. A wind tunnel evaluation of the physical sampling efficiencies of three bioaerosol samplers. *Journal of aerosol science.* **25**(8), pp. 1493–1501. Cited on p. 213.

Valerius, N. H., Koch, C., and Hoiby, N. 1991. Prevention of chronic pseudomonas aeruginosa colonisation in cystic fibrosis by early treatment. *The Lancet*. **338** (8769), pp. 725–726. Cited on p. 5.

Van Doremalen, N., Bushmaker, T., Morris, D. H., et al. 2020. Aerosol and surface stability of sars-cov-2 as compared with sars-cov-1. *New England Journal of Medicine*. **382**(16), pp. 1564–1567. Cited on p. 30.

Van Loosdrecht, M., Lyklema, J., Norde, W., Schraa, G., and Zehnder, A. 1987. The role of bacterial cell wall hydrophobicity in adhesion. *Applied and environmental microbiology*. **53**(8), pp. 1893–1897. Cited on pp. 91 and 122.

VanSciver, M., Miller, S., and Hertzberg, J. 2011. Particle image velocimetry of human cough. *Aerosol Science and Technology*. **45**(3), pp. 415–422. Cited on p. 50.

Vasudevan, M. and Lange, C. F. 2005. Property dependence of onset of instability in viscoelastic respiratory fluids. *International journal of engineering science*. **43** (15-16), pp. 1292–1298. Cited on p. 44.

Vasudevan, M. and Lange, C. F. 2007. Surface tension effects on instability in viscoelastic respiratory fluids. *Mathematical biosciences*. **205**(2), pp. 180–194. Cited on pp. 44 and 91.

Vejerano, E. P. and Marr, L. C. 2018. Physico-chemical characteristics of evaporating respiratory fluid droplets. *Journal of The Royal Society Interface*. **15**(139), pp. 20170939. Cited on pp. 14, 57, 121, and 214.

Verde, S. C., Almeida, S. M., Matos, J., et al. 2015. Microbiological assessment of indoor air quality at different hospital sites. *Research in Microbiology*. **166**(7), pp. 557–563. Cited on p. 196.

Verkman, A., Song, Y., and Thiagarajah, J. R. 2003. Role of airway surface liquid and submucosal glands in cystic fibrosis lung disease. *American Journal of Physiology-Cell Physiology*. **284**(1), pp. C2–C15. Cited on p. 3.

Villafruela, J., Olmedo, I., and San José, J. F. 2016. Influence of human breathing modes on airborne cross infection risk. *Building and Environment*. **106**, pp. 340–351. Cited on pp. 16 and 17.

Waine, D. J., Whitehouse, J., and Honeybourne, D. 2007. Cross-infection in cystic fibrosis: the knowledge and behaviour of adult patients. *Journal of Cystic Fibrosis*. **6**(4), pp. 262–266. Cited on p. 39.

Wainwright, C. E., France, M. W., O'Rourke, P., et al. 2009. Cough-generated aerosols of pseudomonas aeruginosa and other gram-negative bacteria from patients with cystic fibrosis. *Thorax*. **64**(11), pp. 926–931. Cited on pp. 49, 53, 145, 151, 157, 174, 176, 181, 191, 195, 208, and 213.

Wallace Jr, R. J., Brown, B. A., and Griffith, D. E. 1998. Nosocomial outbreaks/pseudo outbreaks caused by nontuberculous mycobacteria. *Annual Reviews in Microbiology*. **52**(1), pp. 453–490. Cited on p. 37.

Wang, B., Zhang, A., Sun, J., et al. 2005. Study of sars transmission via liquid droplets in air. *Transactions of the ASME-K-Journal of Biomechanical Engineering*. **127**(1), pp. 32–38. Cited on p. 55.

Weber, D. J., Rutala, W. A., Miller, M. B., Huslage, K., and Sickbert-Bennett, E. 2010. Role of hospital surfaces in the transmission of emerging health care-associated pathogens: norovirus, clostridium difficile, and acinetobacter species. *American journal of infection control*. **38**(5), pp. S25–S33. Cited on p. 12.

Wei, J. and Li, Y. 2015. Enhanced spread of expiratory droplets by turbulence in a cough jet. *Building and Environment*. **93**, pp. 86–96. Cited on pp. 16 and 55.

Wei, J. and Li, Y. 2016. Airborne spread of infectious agents in the indoor environment. *American Journal of Infection Control*. **44**(9), pp. S102–S108. Cited on p. 42.

Wei, J. and Li, Y. 2017. Human cough as a two-stage jet and its role in particle transport. *PloS one*. **12**(1), pp. e0169235. Cited on p. 17.

Wells, W. F. et al. 1934. On air-borne infection. study ii. droplets and droplet nuclei. *American Journal of Hygiene*. **20**, pp. 611–18. Cited on p. 13.

Wells, W. F. et al. 1955. Airborne contagion and air hygiene. an ecological study of droplet infections. *Airborne Contagion and Air Hygiene. An Ecological Study of Droplet Infections.* Cited on p. 32.

WHO. 2006. *Air quality guidelines: global update 2005: particulate matter, ozone, nitrogen dioxide, and sulfur dioxide*. World Health Organization. Cited on p. 194.

Williams, C. M., Cheah, E. S., Malkin, J., et al. 2014. Face mask sampling for the detection of mycobacterium tuberculosis in expelled aerosols. *PLoS One*. **9**(8), pp. e104921. Cited on pp. 52, 144, and 157.

Williams, C. M., Abdulwhhab, M., Birring, S. S., et al. 2020. Exhaled mycobacterium tuberculosis output and detection of subclinical disease by face-mask sampling: prospective observational studies. *The Lancet Infectious Diseases*. Cited on pp. 49, 52, 157, 181, and 223.

Wilson, R., Huang, S., and McLean, A. 2004. The correlation between airborne methicillin-resistant staphylococcus aureus with the presence of mrsa colonized patients in a general intensive care unit. *Anaesthesia and intensive care*. **32**(2), pp. 202–209. Cited on p. 27.

Wolkers, W. F. and Oldenhof, H. 2015. *Cryopreservation and freeze-drying protocols*. Springer. Cited on p. 160.

Wood, M. E. 2019. Infectious airborne transport in individuals with cystic fibrosis and mitigation strategies to reduce aerosol dispersal. Cited on pp. 53 and 54.

Wood, M. E., Stockwell, R. E., Johnson, G. R., et al. 2018. Face masks and cough etiquette reduce the cough aerosol concentration of pseudomonas aeruginosa in people with cystic fibrosis. *American journal of respiratory and critical care medicine*. **197**(3), pp. 348–355. Cited on pp. 53, 248, and 256.

Wood, M. E., Stockwell, R. E., Johnson, G. R., et al. 2019. Cystic fibrosis pathogens survive for extended periods within cough-generated droplet nuclei. *Thorax*. **74** (1), pp. 87–90. Cited on p. 53.

Wurie, F. B., Lawn, S. D., Booth, H., Sonnenberg, P., and Hayward, A. C. 2016. Bioaerosol production by patients with tuberculosis during normal tidal breathing: implications for transmission risk. *Thorax*. **71**(6), pp. 549–554. Cited on p. 48.

Xiao, S., Li, Y., Wong, T.-w., and Hui, D. S. 2017. Role of fomites in sars transmission during the largest hospital outbreak in hong kong. *PloS one*. **12**(7), pp. e0181558. Cited on pp. 24 and 33.

Xie, X., Li, Y., Chwang, A., Ho, P., and Seto, W. 2007. How far droplets can move in indoor environments–revisiting the wells evaporation-falling curve. *Indoor air*. **17**(3), pp. 211–225. Cited on pp. xv, 14, 15, 23, 54, and 217.

Yan, J., Grantham, M., Pantelic, J., et al. 2018. Infectious virus in exhaled breath of symptomatic seasonal influenza cases from a college community. *Proceedings of the National Academy of Sciences*. **115**(5), pp. 1081–1086. Cited on p. 51.

Yan, Y., Li, X., Shang, Y., and Tu, J. 2017. Evaluation of airborne disease infection risks in an airliner cabin using the lagrangian-based wells-riley approach. *Building and Environment*. **121**, pp. 79–92. Cited on p. 34.

Yang, S., Lee, G. W., Chen, C.-M., Wu, C.-C., and Yu, K.-P. 2007. The size and concentration of droplets generated by coughing in human subjects. *Journal of Aerosol Medicine*. **20**(4), pp. 484–494. Cited on pp. 46, 47, 48, and 49.

Yang, W., Elankumaran, S., and Marr, L. C. 2012. Relationship between humidity and influenza a viability in droplets and implications for influenza's seasonality. *PloS one*. **7**(10), pp. e46789. Cited on p. 56.

Yu, I. T., Wong, T. W., Chiu, Y. L., Lee, N., and Li, Y. 2005. Temporal-spatial analysis of severe acute respiratory syndrome among hospital inpatients. *Clinical Infectious Diseases*. **40**(9), pp. 1237–1243. Cited on p. 34.

Zayas, G., Chiang, M. C., Wong, E., et al. 2012. Cough aerosol in healthy participants: fundamental knowledge to optimize droplet-spread infectious respiratory disease management. *BMC pulmonary medicine*. **12**(1), pp. 1–12. Cited on pp. 46 and 47.

Zhang, T. and Chen, Q. Y. 2007. Novel air distribution systems for commercial aircraft cabins. *Building and Environment*. **42**(4), pp. 1675–1684. Cited on p. 16.

Zhen, H., Han, T., Fennell, D. E., and Mainelis, G. 2014. A systematic comparison of four bioaerosol generators: Affect on culturability and cell membrane integrity when aerosolizing escherichia coli bacteria. *Journal of Aerosol Science*. **70**, pp. 67–79. Cited on p. 130.

Zheng, Y. and Yao, M. 2017. Liquid impinger biosampler's performance for size-resolved viable bioaerosol particles. *Journal of Aerosol Science*. **106**, pp. 34–42. Cited on p. 25.

Zheng, Y., Chen, H., Yao, M., and Li, X. 2018. Bacterial pathogens were detected from human exhaled breath using a novel protocol. *Journal of aerosol science*. **117**, pp. 224–234. Cited on pp. 52 and 53.

Zhu, S., Kato, S., and Yang, J.-H. 2006. Study on transport characteristics of saliva droplets produced by coughing in a calm indoor environment. *Building and environment*. **41**(12), pp. 1691–1702. Cited on pp. 48, 50, and 51.

Zielenski, J. and Tsui, L.-C. 1995. Cystic fibrosis: genotypic and phenotypic variations. *Annual review of genetics*. **29**(1), pp. 777–807. Cited on p. 3.

Zuckerman, J. B., Zuaro, D. E., Prato, B. S., et al. 2009. Bacterial contamination of cystic fibrosis clinics. *Journal of Cystic Fibrosis*. **8**(3), pp. 186–192. Cited on p. 35.